

AD695719

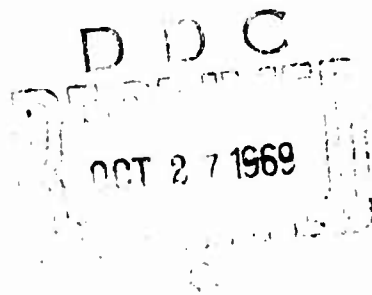
TECHNICAL REPORT M-1

CRITICAL NORMAL FRACTURE STRAIN OF PLAIN AND STEEL WIRE
FIBROUS-REINFORCED CONCRETE

by

Donald L. Birkimer

October 1969



Department of the Army
CONSTRUCTION ENGINEERING RESEARCH LABORATORY
Champaign, Illinois 61820

This document has been approved for public release and sale; its distribution is unlimited.

Reproduced by the
CLEARINGHOUSE
for Federal Scientific & Technical
Information Springfield Va 22151

212

SUBMISSION FOR	
CESTI	WHITE SECTION <input checked="" type="checkbox"/>
DOC	BUFF SECTION <input type="checkbox"/>
UNANNOUNCED	<input type="checkbox"/>
SPECIFIC TION	
Y	
DEATH BOTION AVAILABILITY CODES	
DIST.	AVAIL. AND or SPECIAL
/	

The findings of this report are not to be construed as an official Department of the Army position unless so designated by other authorized documents

DESTROY THIS REPORT WHEN IT IS NO LONGER NEEDED
DO NOT RETURN IT TO THE ORIGINATOR

TECHNICAL REPORT M-1

**CRITICAL NORMAL FRACTURE STRAIN OF PLAIN AND STEEL WIRE
FIBROUS-REINFORCED CONCRETE**

by

Donald L. Birkimer



October 1969

Department of the Army
CONSTRUCTION ENGINEERING RESEARCH LABORATORY
Champaign, Illinois 61820

This document has been approved for public release and sale; its distribution is unlimited.

ABSTRACT

This report presents the results of a series of eighty-one impact tests performed on 5.1 x 88.9-cm (2.0 x 35.0-in.) cylindrical test specimens. The cylinders consisted of either plain or steel wire fibrous-reinforced concrete.

Basic properties relating to the concrete test specimens used were quantitatively evaluated: static ultimate tensile strength and the corresponding ultimate tensile strain; static initial Young's modulus of elasticity; static ultimate unconfined compressive strength, specific gravity, mass density; seismic velocity; dynamic Young's modulus of elasticity. Histograms for the frequency distributions of basic material properties show variations of these properties within the experiment.

The results revealed that the critical normal fracture strain (critical value of tensile strain which causes fracture of the material) of the materials tested is functionally dependent on the rise times of the straining pulse. The results also showed that the critical normal fracture strain of plain concrete can be increased by the inclusion of the randomly placed steel wire fibre of the type tested.

Consideration of the variation of the critical normal fracture strain (or the corresponding calculated dynamic tensile strength) with rise times reveals that a minimum dynamic tensile strength should be used for design. Standard testing procedures should be developed based on this consideration.

FOREWORD

Under the auspices of the Office of the Chief of Engineers, the study of the behavior of fibrous-reinforced concrete described in this report was initially supported by the Defense Atomic Support Agency (DASA). Continuing support was provided by the Office of the Chief of Research and Development, DA, via the Project, "Military Engineering Applications of Nuclear Weapons Effects Research." This investigation was funded under Subtask R13B193 (Miscellaneous Reinforcements for Portland Cement Concrete). Research was performed by the Protective Construction Branch of the Construction Engineering Laboratory (CEL)*. Ohio River Division Laboratories (ORDL). Supporting work was received from the Instrumentation and Special Studies Branch, and the Concrete Laboratory.

The ORDL personnel actively engaged with the planning, testing, analysis and report phases of the work were Messrs. S. J. Hubbard, B. H. Gray, and D. L. Birkimer. This report was prepared by Mr. D. L. Birkimer.

Mr. F. M. Mellinger and Mr. R. L. Hutchinson were Director and Assistant Director, respectively, during this investigation. Mr. E. A. Lotz was Chief of the Construction Engineering Laboratory.

This report has been reviewed by, and revised based upon comments received from, the Office of the Chief of Engineers.

*In October, 1968 the CEL became the U. S. Army Construction Engineering Research Laboratory located in Champaign, Illinois since 1 July 1969.

CONTENTS

	<u>Page</u>
ABSTRACT.	iii
FOREWORD	v
LIST OF: TEXT ILLUSTRATIONS	ix
TEXT FIGURES	ix
TABLES	x
PLATES	x
FIGURES	xi
PART I: INTRODUCTION	1
Background	1
Objectives	3
Scope	3
PART II: THEORETICAL AND CONCEPTUAL PRINCIPLES	5
General	5
Theoretical Considerations	5
Conceptual Model	6
Measurements	11
PART III: FIBRE DESCRIPTION, COMPOSITION, AND PHYSICAL PROPERTIES OF TEST SPECIMENS	12
Crimped Steel Wire	12
Concrete Mixes	12
Casting Technique	15
Physical Properties	15
Discussion	16
PART IV: IMPACT TESTS OF PLAIN CONCRETE	17
General	17
Test Results	17
Discussion	23
PART V: IMPACT TESTS OF STEEL WIRE FIBROUS-REINFORCED CONCRETE	24
General	24
Test Results	24
Discussion	24

CONTENTS (Cont.)

	<u>Page</u>
PART VI: SUMMARY AND DISCUSSION	25
Comparison of Fracture Strain of Plain and Steel Wire	
Fibrous-Reinforced Concrete	25
Size Effect	25
Weakest Link Testing	25
Design Considerations	28
Limitations	28
PART VII: CONCLUSIONS	30
PART VIII: RECOMMENDATIONS	31
REFERENCES	33
TABLES 1-20	35-54
PLATES 1-2	55-56
FIGURES 1-120	57-176
APPENDIX A - IMPACT LOADING DEVICE	177
APPENDIX B - STRAIN MEASURING APPARATUS	195
DISTRIBUTION	
DD FORM 1473	

TEXT ILLUSTRATIONS

<u>Figure</u>		<u>Page</u>
A	Schematic of Strain Pulse after Reflection from Distal End	7
B	Schematic of Remaining Portion of Strain Pulse After Fracture	8
C	Schematic of Straining Pulses with Various Rise Times	9
D	Strain Time Trace: Specimen G	18
E	Data Projection for Strain Time Trace: Specimen G	19
F	Fracture Graph: Specimen G	20
G	Strain Time Trace: Specimen A	21
H	Data Projection for Strain Time Trace: Specimen A	21
I	Fracture Graph: Specimen A	22

T A B L E S

<u>Number</u>		<u>Page</u>
1	Fine Aggregate Gradation	35
2	Average Physical Properties of Concrete Test Specimens	36
3-6	Plain Concrete: Specific Gravity and Mass Density Specimens A-K, 1-11, I-XII, PG4-1--PG4-12	37-40
7-9	Steel Wire Fibrous-Reinforced Concrete: Specific Gravity and Mass Density Specimens PG6-1--PG6-11, PG7-1--PG7-12, PG8-1--PG8-12	41-43
10-13	Plain Concrete: Seismic Velocity and Dynamic Young's Modulus of Elasticity Specimens A-K, 1-11, I-XII, PG4-1--PG4-12	44-47
14-16	Steel Wire Fibrous-Reinforced Concrete: Seismic Velocity and Dynamic Young's Modulus of Elasticity Specimens PG6-1--PG6-11, PG7-1--PG7-12, PG8-1--PG8-12	48-50
17-18	Plain Concrete: Summary of Critical Normal Fracture Strain Data	51-52
19-20	Steel Wire Fibrous-Reinforced Concrete: Summary of Critical Normal Fracture Strain Data	53-54

P L A T E S

1	a. Specimen Casting Apparatus b. Specimen Support System	55
2	a. Typical Plain Concrete Fractured Specimen b. Typical Fibrous Concrete Fractured Specimen	56

FIGURES

<u>Number</u>		<u>Page</u>
1-2	Histogram for Distribution of Specific Gravity	57-58
3-4	Histogram for Distribution of Seismic Velocity	59-60
5-6	Critical Normal Fracture Strain vs Rise Time of Straining Pulse to Fracture Strain	61-62
7-69	Projected Data and Fracture Graphs for Plain Concrete Specimens	63-125
70-120	Projected Data and Fracture Graphs for Fibrous-Reinforced Specimens	126-176

BLANK PAGE

CRITICAL NORMAL FRACTURE STRAIN OF PLAIN AND STEEL WIRE FIBROUS-REINFORCED CONCRETE

PART I: INTRODUCTION

Background

1. The work reported herein is a part of a continuing research project investigating the technical feasibility, the physical properties, the static and dynamic response to load, and the application to protective construction of portland cement concretes reinforced with randomly placed, fibrous type materials. The investigation of fibrous-reinforced concrete was initiated at the Ohio River Division Laboratories (ORDL) in FY 1963. In general, the addition of steel wire fibres to concrete mixes increases the final strength of the concrete and imparts a post-fracture resistance to load to the fibrous concrete system. The addition of nylon fibres, however, imparts only the post-fracture resistance to load to the fibrous concrete system. Hence, the majority of the work has been elevated to steel wire fibrous-reinforced concrete.

2. The earliest studies were concerned with developing an inexpensive technique and apparatus with which to evaluate the critical normal fracture stress (minimum dynamic tensile stress) required to rupture concrete materials (1)*. Rinehart has defined the critical normal fracture stress as the maximum tensile stress which a material will tolerate (2). "Normal" implies that the direction of the maximum principal stress is perpendicular to the fracture plane. Rinehart further pointed out that a more exact definition would be the minimum dynamic tensile stress required to rupture the material. This report demonstrates that the more exact definition is necessary for the materials tested. From these early studies, the ORDL Impact Loader was initially designed. The initial apparatus was modified by the design of a direct reading strain gage system (3). Using this equipment, experimental support was provided to a theoretical development of the response of fibrous concrete to dynamic tension resulting from impact loadings (4). These early studies pointed out that fibrous concretes possessed a spall resistance (resistance to a separation of a portion of a material from the parent material by a transient tensional strain pulse) far superior to plain concrete.

* Parenthetic numerals indicate references.

3. Concurrent with this developmental work, the technical feasibility and static material properties of various fibrous-reinforced concretes were studied (5). This work demonstrated that not only could the strength of plain concrete be enhanced by the inclusion of some fibrous type materials, but also that the fibrous concrete system possessed a post-fracture resistance to flexural loads.

4. Field testing of simply supported slabs indicated that the addition of steel and nylon fibres to concrete mixes, used for construction of the slabs, increased their resistance to explosive loadings (6, 7). The fibres not only decreased the spall velocities but also decreased the amount of fragmentation of the slabs. This work also pointed out the technical feasibility of fibrous-reinforced concrete members with conventional steel reinforcement.

5. In furthering the understanding of the behavior of fibrous-reinforced concrete subjected to transient loadings, the dynamic tensile strength of fibrous-reinforced concrete was qualitatively compared to that of plain concrete (8). This comparison was based upon tests involving tensile strain pulses having rise times of approximately 30 micro-seconds. These studies pointed out the need not only for an understanding of the fracture strains associated with transient tensile loadings, but also a need for a quantitative comparison of the fracture strain of plain and fibrous-reinforced concrete.

6. The static and dynamic compressive behavior of plain and fibrous-reinforced concrete test cylinders was next evaluated (9). This work also examined the post-fracture resistance to load of the fibrous-reinforced concrete system loaded in compression. This study was a basic step towards designing and predicting the ultimate strength of fibrous-reinforced concrete members with conventional reinforcing subjected to static and dynamic flexural loading.

7. Recent tests to determine bond strength between concrete and various fibres indicated that steel fibres, crimped in one plane, provided the best bond strength of the fibres thus far tested. The final objective is to produce a fibre which will fail in tension and bond at the same time while supporting a significant load. Most nearly meeting this objective is the crimped steel wire fibre which was selected for use in this study.

8. The need for an understanding of the fracture strains associated with transient tensional strain pulses suggested studies of the variation of the critical normal fracture strain of portland cement concrete with regard to the rise time of the straining pulse up to that critical normal fracture strain (10). This work resulted in the development of a conceptual model of the fracture strain. This previous development, with a comparison to the critical normal fracture strain of steel wire fibrous-reinforced concrete specimens, is presented herein.

9. Extensions of basic studies to other structural members, such as prestressed fibrous-reinforced concrete members, are planned. Based upon fundamental studies of the behavior of these fibrous-reinforced concrete materials, which demonstrated desirable properties for use in protective construction, reasonable design techniques should be developed. The ultimate objective of such studies should be realized in the design and use of fibrous-reinforced concretes in situations where protective construction will benefit through application.

10. Concrete, useful in both military and civilian applications, has an extremely low tensile strength. Although concrete is not designed to accept tensile stresses under static loading conditions, it must be relied upon to accept tensile stresses resulting from transient loadings. The source of these transient loadings may be thermonuclear detonations, explosive detonations, earthquakes, impacting projectiles, turbulent water flow, machine vibrations, pile driving mechanisms, or any other source of rapidly applied loads. If the concrete does not accept transient tensile stresses, produced indirectly by these rapidly applied loads, it tends to fracture. These fractures, which may impair the adequacy of structural members, could result in complete loss or significant damage to the usefulness of these members after subsidence of the dynamic loadings (11). The development of an understanding of the behavior, as well as a comparison to plain concrete, of fibrous-reinforced concrete specimens subjected to transient tensile strain pulses treated in this report.

Objectives

11. The objectives of the research reported herein are:

- a. To examine the relationship between the rise time of the straining pulse and the critical normal fracture strain.
- b. To compare the critical normal fracture strain of steel wire fibrous-reinforced concrete test specimens to that of plain concrete test specimens.

Scope

12. The following tests were conducted during this investigation:

- a. Two direct tension tests of plain concrete
- b. Two direct tension tests of steel wire fibrous-reinforced concrete
- c. Specific gravity determinations for all impact test specimens

d. Fundamental longitudinal frequency determinations on all impact test specimens

e. Impact tests, employing straining pulses varying in rise times from 20 to 200 microseconds, of forty-six cylindrical test specimens composed of plain concrete

f. Impact tests of thirty-five cylindrical test specimens composed of steel wire fibrous-reinforced concrete employing similar straining pulses.

13. Reported herein is a description of the steel wire fibre used as reinforcement, the concrete mix proportions, and the mixing procedures used to fabricate the concrete test cylinders. Test equipment, test procedures, and test results along with conclusions and recommendations are presented.

PART II: THEORETICAL AND CONCEPTUAL PRINCIPLES

General

14. In rigid body dynamics, it is assumed that when a force is applied to a point in a rigid body the resulting stresses set every other point in motion instantaneously. The underlying assumption is that the time between the application of the load and the setting up of effective equilibrium is short with respect to the time in which observations are made. However, when one considers the application of a rapidly applied load, the resulting effects must be viewed from the standpoint of the propagation of stress waves.

15. If a material is stressed with a suddenly applied load, then the deformations are not immediately transmitted to all parts of the body. Parts of the body which are remote from the loading remain unstressed for some time. Deformations, in the form of transient strain pulses, travel through the body from the point of the applied load.

16. Several techniques can be used to introduce transient strain pulses in the laboratory. Typical of such devices are projectile impact loaders, shock tubes, explosive detonations, and electro-hydraulic discharges. The technique employed for this experiment was to use an air-fired projectile impact loader as described in Appendix A.

Theoretical Considerations

17. Upon impact by a projectile on one end of a cylindrical test specimen, a transient longitudinal compressional strain pulse travels down the test specimen towards the distal end. Upon reaching the distal end, provided the end of the specimen is plane and perpendicular to the direction of travel, the wave is reflected with the same shape but opposite in direction and sense. Based on the difference between the magnitude of the reflected tensile pulse and the tail of the longitudinal compressional pulse, at some point, the resultant net tensile strain may have a magnitude greater than the strain limit of the material. If this is the case, a fracture is formed and a portion of the material is propelled from the parent material. The critical value of tensile strain which causes fracture of the material is defined as the critical normal fracture strain. "Normal" implies that the direction of the fracture plane is perpendicular to the direction of the maximum principle strain.

18. If it is assumed that the test material is linearly elastic and isotropic, that the stress disturbance is a plane wave, and that the stress in the transverse direction is not of sufficient magnitude to affect the results, then the longitudinal strain caused by a plane wave traveling along a cylindrical bar can be computed from the following formula:

$$\xi_x = \frac{\nu}{c_x} \quad [\text{Eq.(1)}]$$

where

ν = particle velocity

c_x = seismic velocity of the material

19. Using the same basic assumptions, the longitudinal stress can be calculated by the following relationship:

$$\sigma_x = \rho c_x \nu \quad [\text{Eq.(2)}]$$

where

σ_x = longitudinal stress

ρ = mass density

Conceptual Model

20. A conceptual model of the relationship of the critical normal fracture strain to the rise time of the straining pulse up to that value of fracture strain was developed in another publication (10). The basic idea underlying the model is that the critical normal fracture strain (ξ_{CR}) is composed of two components. The first component (ξ_c) is defined as that magnitude of strain associated with initiating fracture of the cross section of the cylindrical test specimen. The second component (ξ_f) is that magnitude of strain which is transmitted across the incipient fracture during the time associated with macroscopic fracture of the cross section (t_f).

21. This relationship may then be expressed as:

$$\xi_{CR} = \xi_c + \xi_f \quad [\text{Eq.(3)}]$$

22. Now consider the leading edge of a tensile strain pulse traveling down a cylindrical test specimen.

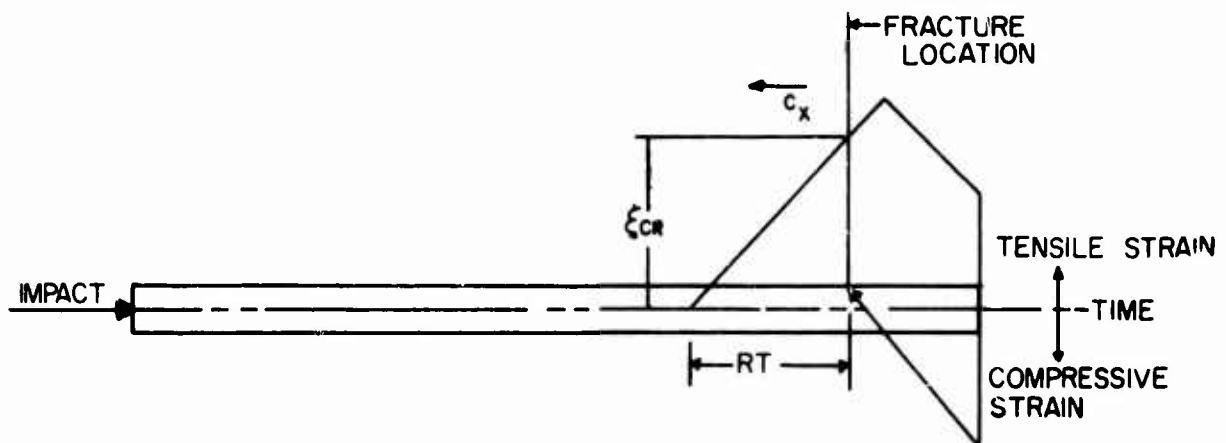


Fig A: Schematic of Strain Pulse Being Reflected from Distal End

23. If the magnitude of the net tensile strain reaches some critical value (ξ_{cr}), the material will fracture and a portion of the material, a spall, will be separated from the parent material.

24. Now consider some maximum value of strain which will not cause fracture of the cross section. The value (ξ_c) is obviously less than (ξ_{cr}). Consider further an additional amount of strain transmitted across the fracture during the time t_f .

This can be shown as follows:

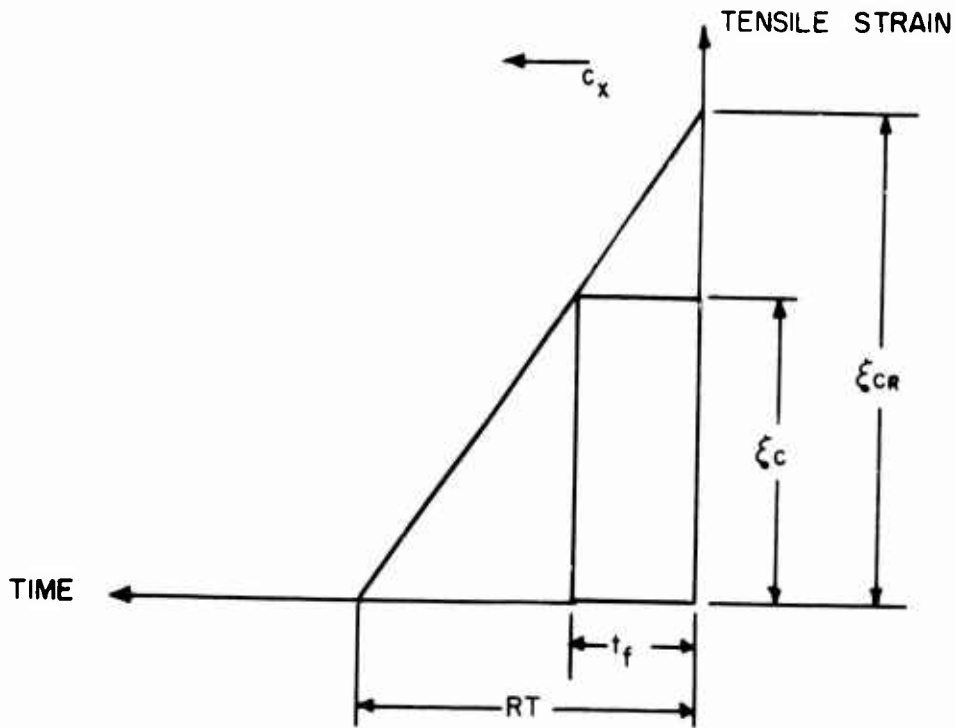


Fig. B: Schematic of Remaining Portion of Strain Pulse After Fracture

Let RT stand for the rise time of the straining pulse to the critical normal fracture strain ξ_{CR} . The following relationship can now be written:

$$\xi_{CR} = \xi_c + \left(\frac{\xi_c}{RT - t_f} \right) t_f \quad [Eq.(4)]$$

Now if ξ_c and t_f are both considered constants for a given material and cross section, then the formula represents the relationship of the critical normal fracture strain to the rise time up to the fracture strain. This relationship shall be referred to as the conceptual model.

25. Consider what the model shows by examining the following figure:

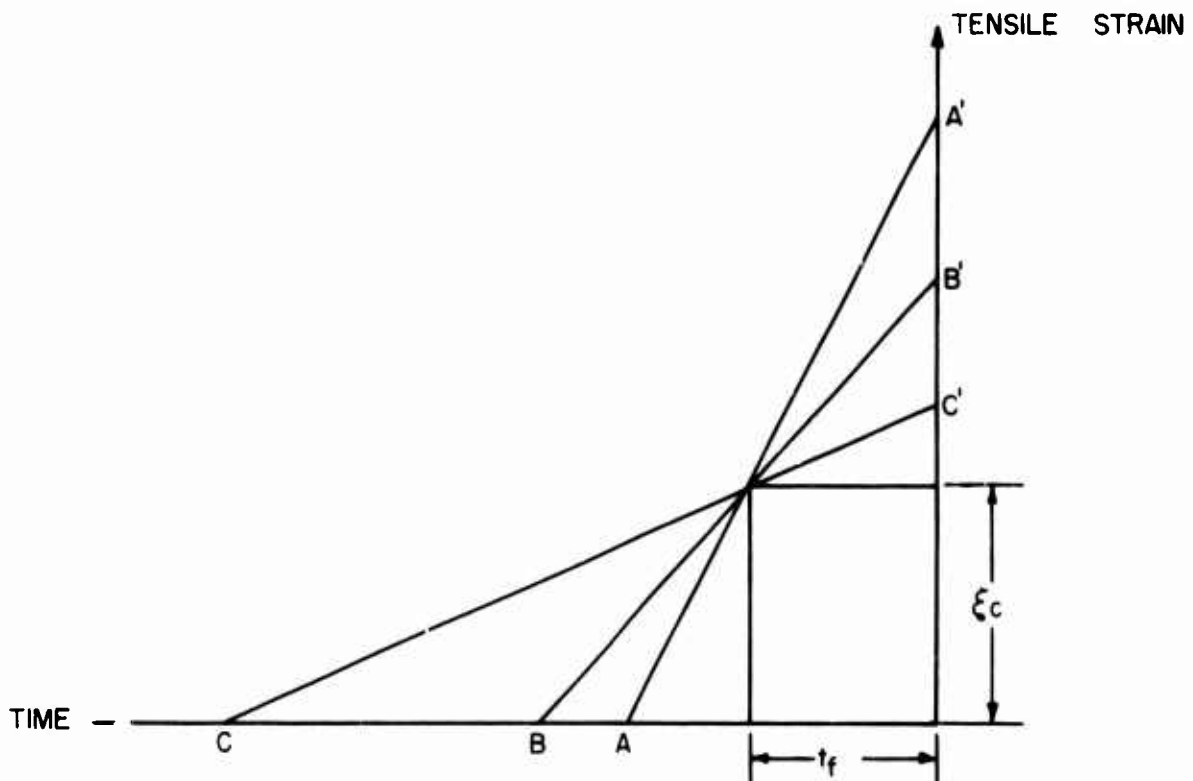


Fig. C: Schematic of Straining Pulses with Various Rise Times

For very short rise times (AA') the amount of strain associated with the fracturing time t_f is greater than the amount ξ_c . For very long rise times (CC') the larger amount is ξ_c with only a small amount associated with fracturing. Hence, as the rise time becomes very small, the critical normal fracture strain should increase over that fracture strain associated with long rise times.

26. Rearranging this equation, it can be shown that, in the limit, ξ_{CR} approaches ξ_c .

$$\xi_{CR} = \xi_c \left(\frac{RT - t_f + t_f}{RT - t_f} \right) = \xi_c \left(\frac{RT}{RT - t_f} \right) \quad [\text{Eq.(5)}]$$

Now if $RT \gg t_f$

$$\frac{RT}{RT - t_f} \rightarrow 1$$

Hence $\xi_{CR} \rightarrow \xi_c$ as RT becomes large.

Also, it can be shown that as RT approaches t_f , ξ_{CR} becomes large.

As $RT \rightarrow t_f$

$$\frac{RT}{RT - t_f} \rightarrow \infty$$

Hence

$$\xi_{CR} \rightarrow \infty$$

This mathematical treatment merely exemplifies what was shown geometrically above. The physical argument lies in the postulation that any material will support any load if the load is applied over an infinitely short period of time. On the other hand, from the physical behavior of flaw sensitive materials, it should be expected that there is some level of strain below which no macroscopic fracture occurs.

Measurements

27. The measurements of longitudinal strain were made using an external strain gage system. The strain measuring apparatus is described in Appendix B. Three surface strain gages were located symmetrically at 120° around the circumference of the test specimens at each of two gaging locations along the longitudinal axis. The gage locations were chosen according to the expected fracture location in an attempt to insure that the fracture locations were between gaging locations. Each strain gage was horizontally aligned to a corresponding gage at the other gaging location. Continuous records of strain versus time were then obtained using the system described in Appendix B.

PART III: FIBRE DESCRIPTION, COMPOSITION, AND PHYSICAL
PROPERTIES OF TEST SPECIMENS

Crimped Steel Wire

28. The crimped steel wire used as fibrous-reinforcement in the concrete test cylinders was supplied by Manufacturer A. The steel wire was a carbon steel that was crimped in one plane with a distance of 0.33 cm (0.13 in.) from crest to crest and a distance of 0.10 cm (0.04 in.) from crest to trough. The wire had a length of 2.5 cm (1.0 in.) after crimping and a diameter of 0.043 cm (0.017 in.). The crimped steel wire had a brass plating which was quickly dissolved by the alkali in the plastic concrete (5). This plating did not affect the bond strength of the wire to the concrete. This wire had a static ultimate tensile strength of 8820 kg/cm² (125,000 psi) and a direct bond pull out strength to concrete sufficient to fail the fibre in a one-inch pull out test (9).

Concrete Mixes

29. The proportioning of the concrete mixes used in the preparation of the test cylinders was as follows:

a. Plain Concrete: This mix consisted of the following absolute volumes and weights:

	m ³	ft ³	kg	lb
Cement	0.1412	.99	444.5	980
Water	0.2046	.23	204.6	451
Fine Aggregate	0.4183	14.78	1100.0	2425
	0.7641	27.00	1749.1	3856

The fine aggregate was a Camp Dennison natural sand having a specific gravity of 2.63. The specifications for the sieves used and the fine aggregate gradation are given in Table 1. No coarse aggregate or entrained air were used in the concrete in this experiment. The water-cement ratio was 0.46 by weight and the mix proportions were 1:2.47 by weight. Akcello, High Early Strength, Type III cement was used which produces in nine days a strength equivalent to the 28-day strength of standard portland cement concrete. The recorded slump, measured according to Corps of Engineers Method CRD-C5-63, "Method of Test for Slump of Portland

Cement Concrete, " was 14.6 cm (5.75 in.). The batch weights were for 0.354 m³ (1.25 ft³) of concrete and corrections were made for surface moisture on the fine aggregate. A summary of the strength properties of this plain concrete, taken from Table 2, is given below:

Table A

Plain Concrete
Summary of Strength Properties

Ultimate Tensile Strength	34.4 kg/cm ²	490 psi
Ultimate Tensile Strain	100 μ cm/cm	100 μ in./in.
Initial Modulus of Elasticity in Tension	3.240 x 10 ⁵ kg/cm ²	4.61 x 10 ⁶ psi
Ultimate Unconfined Com- pressive Strength	480.0 kg/cm ²	6830 psi
Dynamic Young's Modulus of Elasticity	3.44 x 10 ⁵ kg/cm ²	4.90 x 10 ⁶ psi

Consideration of these strength properties points out that these tests were conducted on a reasonably strong concrete, $f_c' > 350$ kg/cm² ($f_c' > 5000$ psi). The ultimate tensile strain, that strain corresponding to the ultimate tensile strength, was used for comparison to the critical normal fracture strain of this concrete.

b. Crimped Steel Wire Fibrous-Reinforced Concrete: The same basic materials were used in the design of the crimped steel wire fibrous-reinforced concrete mix. However, due to difficulties in the placement of the fibrous-reinforced concrete in the 5.1-cm (2.0-in.) diameter molds, the water-cement ratio was

increased to 0.49 by weight. The final fibrous-reinforced concrete mix design had the following absolute volumes and weights:

	m ³	ft ³	kg	lb
Cement	0.1409	4.98	443.6	978
Water	0.2173	7.68	217.3	479
Fine Aggregate	0.4058	14.34	1063.2	2344
Crimped Steel				
Wire Fibre	<u>0.0096</u>	<u>0.34</u>	<u>74.4</u>	<u>164</u>
	0.7736	27.34	1798.5	3965

30. The proportioning of the fibres is usually expressed as 1.25%. This percentage is the ratio of the volume of the fibre to the volume of the mortar phase (fine aggregate, cement, water) multiplied by 100. Since no coarse aggregate was used in this work, this percentage corresponds to the percentage of total volume made up of fibre. A summary of the strength properties of this fibrous concrete, taken from Table 2, is given below:

Table B
Steel Wire Fibrous-Reinforced Concrete
Summary of Strength Properties

Ultimate Tensile Strength	40.30 kg/cm ²	573 psi
Ultimate Tensile Strain	150 μm/cm	150 μin./in.
Initial Modulus of Elasticity in Tension	2.640 x 10 ⁵ kg/cm ²	3.75 x 10 ⁶ psi
Ultimate Unconfined Compressive Strength	421.0 kg/cm ²	5990 psi
Dynamic Young's Modulus of Elasticity	3.340 x 10 ⁵ kg/cm ²	4.75 x 10 ⁶ psi

Comparison of Tables A and B shows a considerable difference in the strains corresponding to the ultimate tensile strengths of the plain and fibrous-reinforced concrete. It should be remembered that the water-cement ratio was increased for the fibrous-reinforced concrete and hence it should be expected that there would be a decrease in the unconfined compressive strength. This decrease should be offset somewhat by the increase due to the fibres.

Casting Technique

31. The plastic concrete was placed in plexiglass casting tubes by using an extended funnel. A light vibrator was attached to the funnel in order to minimize surface honeycombs. The concrete was then placed through the funnel into the tubes as the funnel was slowly removed from the tubes. The apparatus used for this casting technique is shown by Plate 1a.

32. The cylinders were held in a vertical position in a moist room for one day. The molds were then removed and the cylinders were immersed in water and water cured for eight days in a horizontal position. The cylinders were then removed and remained at room conditions until tested on the tenth day.

Physical Properties

33. Average physical properties of the plain and steel wire fibrous-reinforced concrete test specimens are given in Table 2.

34. The static ultimate tensile strength and corresponding strain were determined as the arithmetic average of two tests performed on 5.1 x 25.4-cm (2.0 x 10.0-in.) cylindrical test specimens. The tests were direct tension tests and the failures were perpendicular to the longitudinal axis of the test specimens and approximately 2.5 cm (1.0 in.) from the grips. The initial modulus of elasticity was taken as the average of the linear slopes of the stress-strain curves from no stress to ultimate stress.

35. The static ultimate unconfined compressive strength of each concrete type was determined as the average of six tests performed on standard 15 x 30-cm (6 x 12-in.) concrete cylinders according to Corps of Engineers Method CRD-C 14-65, "Method of Test for Compressive Strength of Molded Concrete Cylinders."

36. The specific gravities of all test specimens were determined on small test pieces taken from the top end of each specimen. The specific gravities were determined on the air-dried test pieces at the same age and condition as the specimens.

The weights in air were determined in grams on a Torsion Balance. The weights in water were determined in grams using a Dunnigan Bucket Scale.

37. The fundamental frequency of each cylinder was determined using a laboratory Sonometer. The Sonometer determines the natural frequency of a bar in longitudinal vibrations.

38. All other material properties listed in Table 2 were calculated from the basic properties discussed above. The mass density of each bar was calculated from the specific gravity, and the seismic velocity was calculated from the fundamental frequency. The dynamic Young's modulus of elasticity was then calculated as $E_d = \rho c_x^2$.

Discussion

39. Part II of this report demonstrates that the most crucial physical properties, related to this type of loading, are mass density and seismic velocity. Since the mass density is calculated directly from specific gravity, the variation of this property should be examined. Histograms for the frequency distribution of the specific gravity of the plain and steel wire fibrous-reinforced concrete test specimens are given in Figures 1 and 2, respectively. Histograms for the frequency distributions of the seismic velocity of the plain and fibrous-reinforced concrete test specimens are given in Figures 3 and 4, respectively. The recorded values for specific gravity, mass density, seismic velocity, and dynamic Young's modulus of elasticity are given for all test specimens in Tables 3 through 16. The histograms for the specific gravities point out that the variations in this property are quite small. The histograms for the seismic velocities show the variations in this property to be considerable, but still less than 300 m/sec (1000 ft/sec).

PART IV: IMPACT TESTS OF PLAIN CONCRETE

General

40. Forty-six plain concrete test cylinders 5.1 cm in diameter by 88.9 cm in length (2.0 x 35.0 in.) were cast using the technique previously described (paras. 29a, 31 ff). All of the test cylinders which had surface irregularities were discarded. All of the cylinders suitable for testing were tested only once. If the test specimen did not fracture under the first impact, it was not tested again.

41. The specimen support system consisted of simple supports placed 20.4 cm (8.0 in.) on center in a longitudinal line (Plate 1b). The specimens rested on felt pads placed between the specimen and the supports. The longitudinal centerline of the tube of the impact loader was leveled and lined with respect to the longitudinal centerline of the specimen. The gages were placed at 120° around the circumference of the specimen at each of two gaging locations. The gage locations were chosen based on the expected fracture location for each test.

Test Results

42. In the design of this experiment it was easily seen that the most definitive test would be one in which the fracture location was directly between the two gaging locations and had a direction normal to the longitudinal axis of the specimen. If the wave was plane, then the gages located at a specific gaging location should have recorded identical strain time traces. In this case, the fracture location as well as the magnitude of the tensile strain transmitted across the fracture was known.

43. This type of data can be examined by interpreting the test results for Specimen G. The strain time trace as obtained by the oscilloscope is shown below. The top two traces are readouts of strain (vertical) versus time (horizontal) for two of the gages closest to the impact end. The third gage malfunctioned. The final three traces are readouts of strain versus time for the gages closest to the distal end. Each large grid represents one square centimeter. The vertical calibration is such that one centimeter equals 500 micrometers/inch of strain and the horizontal calibration is such that one centimeter equals 100 microseconds in time. The initial horizontal section of each trace represents the base line. Compressional strains record below the base line and tensile strains record above the base line.



Fig. D: Strain Time Trace / Specimen G

By use of an opaque projector the data, useful in interpretation, can be given a more definitive form. This projection of original data is shown on the following page by Figure E in which only the initial compressive pulse and the reflected tensile pulse are considered.

44. Using the projection of data, or the original data, a pictorial representation of the fracture situation may be constructed. This representation, termed a fracture graph (Figure F, page 20) was obtained in the following manner for Specimen G:

- a. Read the strain time curves of the compressional pulse at the gaging location closest to the impact end (Figure E, Gages A-1 and A-2). Use the average of these curves as the shape of the straining pulse (average of Gages A-1 and A-2).
- b. Record the location of the fracture with respect to the distal end of the test specimens (See schematic of Figure E).
- c. Read the magnitude of the tensile strain transmitted across the fracture on the strain time traces of the gages closest to the impact end (Figure E, Maximum Tensile Strain, Gages A-1 and A-2). Use the average of these readings as the amount of tensile strain transmitted.

d. Position the straining pulse about the fracture location such that the correct amount of tensile strain will be transmitted (Figure F) across that incipient fracture plane.

e. Record the critical normal fracture strain (ϵ_{CR}) and the rise time to that strain (RT).

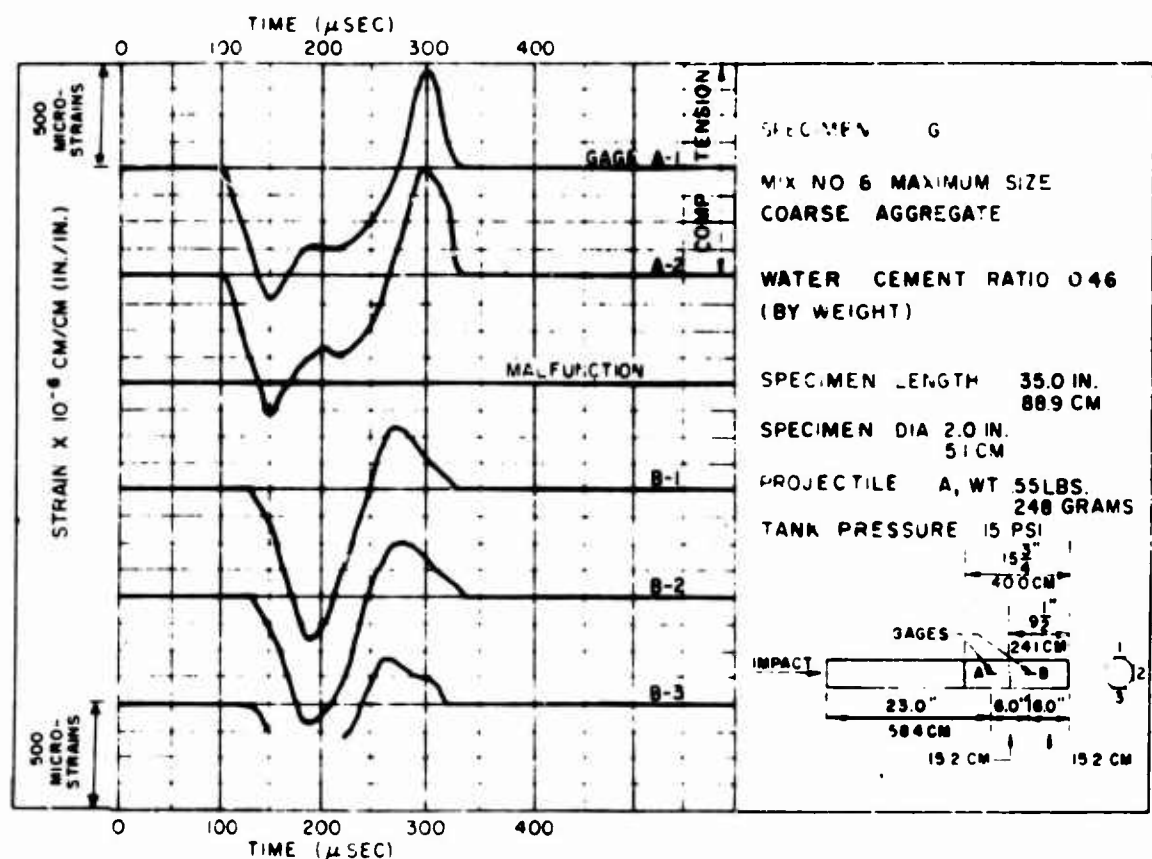


Fig. E: Data Projection for Strain Time Trace / Specimen G

The value of the critical normal fracture strain (ϵ_{CR}) taken from the fracture graph, Figure F, on the following page is 500 microinches/inch and the rise time to this fracture strain (RT) is 34 microseconds. This value is plotted in its respective position on Figure 5.

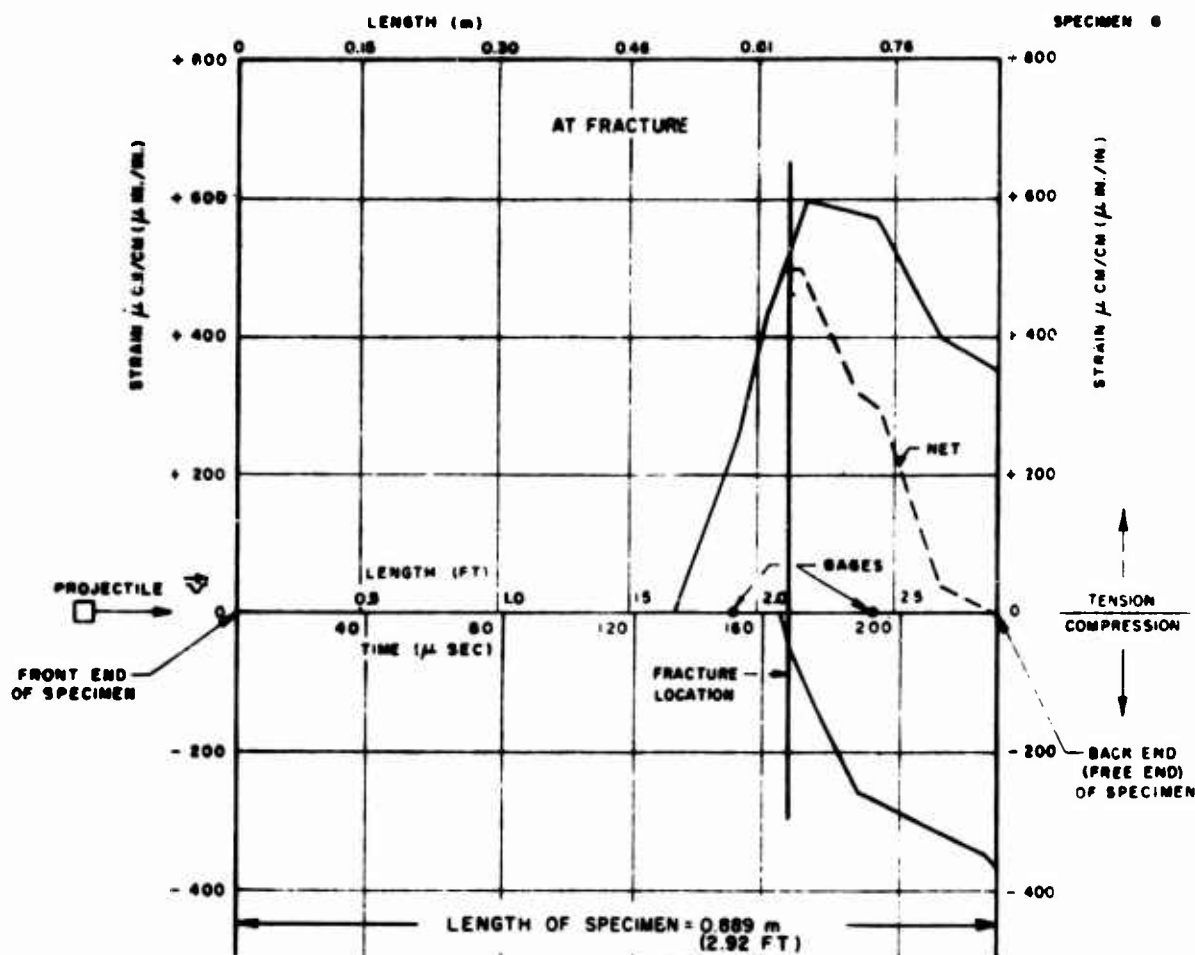


Fig. F: Fracture Graph / Specimen G

45. Another unique type of data is provided when the fracture location is between the gage location farthest from the impact end and the distal end of the test specimen. This type of data is provided by Specimen A. The strain time trace as obtained by the oscilloscope camera is shown on the next page. This strain time has the same calibration as the one shown previously except that one horizontal centimeter represents 200 microseconds. The projected data and the constructed fracture graph are given as Figures H and I.

46. The recorded value of the critical normal fracture strain in this case is 425 microcentimeter/centimeter ($\mu\text{in./in.}$) and the rise time to that strain is 162 microseconds. This value is plotted in its respective location on Figure 5. Notice that in this case the critical normal fracture strain is recorded as the average of the readings of the gages nearest the distal end of the test specimen. In this particular instance a very weak location was found by the pulse and the material was fractured again.



Fig. G: Strain Time Trace / Specimen A

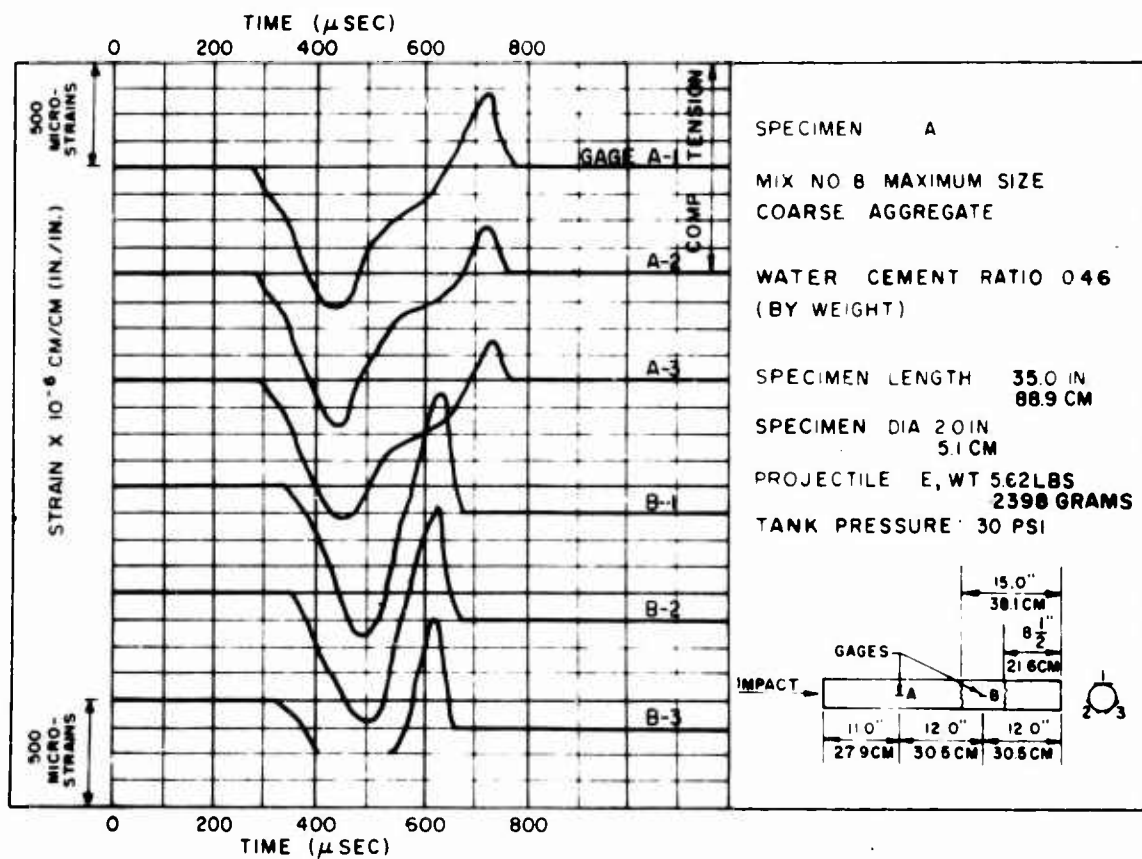


Fig. H: Data Projection for Strain Time Trace / Specimen A

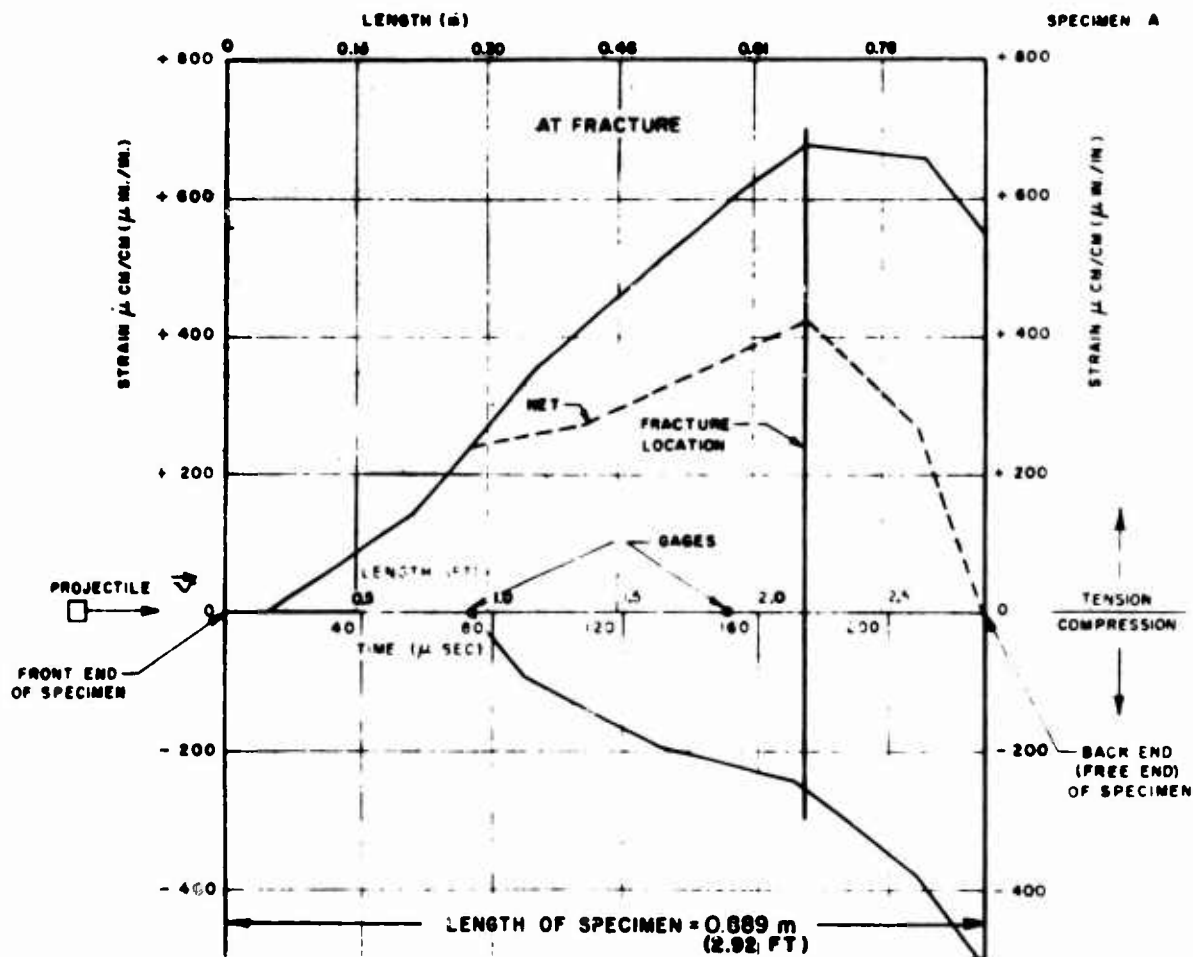


Fig. I: Fracture Graph / Specimen A

47. In the case where the fracture location is closer to the impact end than either gaging location, little interpretation can be given. There are, however, two exceptions. First, when no fracture occurs, it is known that the critical normal fracture strain is greater than the magnitude of strain which was introduced. Second, the fracture occurs very close to a gaging location. Upon examination of the gaging location a sudden relaxation is noted in the strain time traces. It can then be argued that the critical normal fracture strain is just below this value in magnitude.

48. The projected data and the constructed fracture graphs for the plain concrete specimens are given in Figures 7 through 69.

49. Using the ideas of interpretation given above, it is informative to consider the types of fractures common to each of the five projectile configurations. The type most common to each projectile is shown by the fracture graph for the specimens indicated in the following table. (See Appendix A for projectile description.)

<u>Projectile</u>	<u>Specimen</u>	<u>Figure</u>
A	11	36
B	PG4-10	69
C	8	30
D	1	22
E	J	18

50. Using the interpretations outlined above and the fracture graphs, the final data for the plain concrete test specimens can be collected by recording the fracture strain and the rise time to that fracture strain for each specimen. The values recorded are shown in Tables 17 and 18.

51. A graphical interpretation of the data is shown by Figure 5. The scatter of data is shown by cross-hatching and the values of strain which did not cause fracture are shown as arrow-headed points inferring that the critical normal fracture strain for that specimen is greater in magnitude than the value recorded.

Discussion

52. Based upon the tests performed, the critical normal fracture strain of portland cement concrete is functionally dependent on the rise time of the straining pulse up to that magnitude of critical normal fracture strain. An experimental determination of that function is shown by Figure 5. Instead of attempting to present a best fit curve to this data, a fit based upon the conceptual model is presented (See paragraph 24, Equation 4). This fit is shown by a dashed line on Figure 5. This curve is based upon an average value of ξ_c equal to $400 \mu\text{cm/cm}$ ($\mu\text{in./in.}$) and a value of t_f equal to 10microseconds. These values, at best, are only approximations based on the experimental data. However, it does point out that the conceptual model fits the data obtained experimentally.

53. The reason for no specimens being tested more than once is that after one test, if the value of the seismic velocity for that specimen is compared to a value obtained before the test, the value obtained after impact is smaller in magnitude. This would indicate some internal damage.

PART V: IMPACT TESTS OF STEEL WIRE FIBROUS-REINFORCED CONCRETE

General

54. Thirty-five steel wire fibrous-reinforced concrete cylinders of the same dimensions as the plain concrete cylinders were cast using the technique previously described (paras. 29b - 35). The same care in specimen selection and testing was exercised in these tests. The experimental setup was the same as that used for the plain concrete cylinders.

Test Results

55. The projected data and the fracture graphs for the steel wire fibrous-reinforced concrete test cylinders are shown by Figures 70 through 120. The recorded values of critical normal fracture strain and rise time to that fracture strain are given in Tables 19 and 20. A graphical interpretation of the data is given by Figure 6.

Discussion

56. The failure of the plain concrete test cylinders was due to the formation of a spall which was propelled from the parent material. The failure in the fibrous-reinforced concrete cylinders, however, was different. In the fibrous-reinforced concrete cylinders, a fracture would form a spall but was not propelled from the parent material. The fractures on the fibrous-reinforced concrete appeared only as a hair-line crack.

57. Based upon the tests performed, the critical normal fracture strain of steel wire fibrous-reinforced concrete appears to be functionally dependent on the rise time of the straining pulse. The experimental determination of that function is presented by Figure 6. The function was not examined above rise times of approximately 105 microseconds. The pulse length associated with the longer projectiles was extremely long for the fibrous-reinforced concrete. The long pulse lengths made significant interference of the incident compressional pulse and the reflected tensile pulse and hence the data for the long rise times could not be obtained. Instead of attempting to present a best fit curve to this data, a fit based upon the conceptual model is presented (See paragraph 24, Equation 4). This curve is based upon an average value of ξ_c equal to 450 $\mu\text{cm/cm}$ ($\mu\text{in./in.}$) and a value of t_c equal to 10 microseconds. These values, at best, are only approximations based on the experimental data. However, it does point out that the conceptual model fits the fibrous-reinforced concrete data obtained experimentally. Since the values of ξ_{CR} could not be obtained over a considerable range of rise times, the model fit to the data was not and cannot be refined. For a better fit, data in the ranges not tested herein should be examined.

PART VI: SUMMARY AND DISCUSSION

Comparison of Fracture Strain of Plain and Steel Wire Fibrous-Reinforced Concrete

58. Figures 5 and 6 present the fracture data obtained for plain and steel wire fibrous-reinforced concrete test cylinders, respectively. Over the range of rise times investigated, it appears that the fracture strain of the fibrous-reinforced concrete was greater than the fracture strain of the plain concrete. It should be remembered that the water-cement ratio was greater for the steel wire fibrous-reinforced concrete mix than the plain concrete mix. If anything, this should reduce the tensile strength obtained with the fibrous-reinforced concrete samples from that which would have been obtained if the water-cement ratio had not been increased.

59. The failure obtained with the plain concrete cylinders was by either single or multiple spalling. The failure obtained with the steel wire fibrous-reinforced concrete cylinders was by hairline fracturing. In no case were the fibrous-reinforced concrete cylinders actually spalled. Thus, not only do the fibres enhance the strength of the concrete, but they also provide a load-carrying capacity after the fracture of the concrete matrix.

Size Effect

60. The conceptual model is based upon ξ_c and t_f being constants. For a particular size specimen, the time associated with macroscopic fracture of the cross section should be a constant. However, for specimens with large diameters, the value of that time should be greater than the value associated with a small diameter. The obvious extension of the work presented herein is to establish the variation of the critical normal fracture strain with regard to the cross sectional size effects. The value of strain necessary to initiate fracture is probably close to a constant for a given volume of the material. However, the tension failure is a first crack fracture. If the volume of the specimen is increased, the probability of finding a crack sufficiently large to initiate fracture for a given strain level is greater. Hence, the volume size effect should be considered in future work.

Weakest Link Testing

61. The scatter of the data may be considered using Figures 5 and 6. One contributing factor to this scatter is the fact that once a strain pulse is produced at a given strain magnitude then the strain pulse will travel down the specimen. The pulse,

in effect, may be supported for a portion of this travel but then a weakest link section may be found. A fracture forms and the lower magnitude of strain is called the critical normal fracture strain for that specimen. However, a section of the specimen had actually supported that strain. If limitations were placed upon the allowable location of the first fracture then the scatter of the data would be reduced. This weakest link testing should manifest itself in the fracture locations. The fracture locations produced in plain concrete by Projectile A are given in Table C. This data may be collected from the projected data or the fracture graphs already presented.

Table C

Plain Concrete Fracture Locations

Specimen No.	Tank Pressure		Distance from Distal End					
			1st Fracture		2nd Fracture		3rd Fracture	
	kg/cm ²	psi	cm	in.	cm	in.	cm	in.
I	1.76	25	10.2	4	25.4	10	38.1	15
E	1.41	20	27.3	10 3/4	31.8	12 1/2		
V	1.41	20	27.9	11	31.8	12 1/2	39.4	15 1/2
III	1.27	18	29.2	11 1/2	36.2	14 1/2	56.6	22 1/4
11	1.12	16	25.4	10	62.2	24 1/2		
G	1.05	15	24.1	9 1/2	40.0	15 3/4		
10	0.84	12	39.4	15 1/2				
6	0.77	11	31.1	11 1/4	37.5	14 3/4		

Similar data to that on Table C is presented for the steel wire fibrous-reinforced concrete cylinders in Table D.

Table D

Steel Wire Fibrous-Reinforced Concrete

Fracture Locations

Specimen No.	Tank Pressure		Distance from Distal End							
			1st Fracture		2nd Fracture		3rd Fracture		4th Fracture	
	kg/cm ²	psi	cm	in.	cm	in.	cm	in.	cm	in.
PG 6-3	4.22	60	19.0	7 1/2	27.9	11	45.7	18		
PG 6-9	2.11	30	35.6	14						
PG 8-3	1.69	24	25.4	10	34.3	13 1/2	46.4	18 1/4		
PG 8-4	1.69	24	25.4	10	29.2	11 1/2	40.6	16	55.9	22
PG 7-4	1.55	22	27.9	11	33.2	13	38.1	15		
PG 8-1	1.48	21	28.6	11 1/4						
PG 6-4	1.41	20	26.8	10 1/2	27.9	11	45.7	18		
PG 8-7	1.34	19	25.4	10	41.9	16 1/2				
PG 7-1	1.27	18	30.5	12	35.6	14				
PG 7-11	1.20	17	38.1	15						
PG 6-11	1.12	16	35.6	14						
PG 7-9	1.05	15	27.9	11						
PG 7-6	0.98	14	33.0	13						

62. There appears to be no correlation of fracture location or number of spalls to tank pressure. This is attributed to the weakest link type of testing. Typical fractured specimens are shown in Plate 2. The failure with plain concrete, as pointed out previously, was by single or multiple spalling while the failure in the fibrous-reinforced concrete specimens was by development of hairline fractures. For the fibrous concretes, there appears to be no correlation of fracture location or number of fractured sections to tank pressure. This is attributed, as with the plain concrete, to the weakest link type of testing. Theoretical predictions of the length of the first fractured section may be made. However, since one needs to know the fracture strain, these predictions would be no better, and in fact worse, than the measurements.

Design Considerations

63. In contemporary analysis and design of structural elements exposed to stress wave loading, the idealization of a plane wave traveling through the body is frequently used (12). Usually fracture is taken to occur when the tensile capacity of the material is exceeded. Figure 5 shows that the critical normal fracture strain appears to approach a minimum value for large rise times. The implication to design and testing is that determinations of the fracture strength should be made under standardized testing procedures. Since the fracture strength does vary with changes in projectile configurations, the standardized procedures are necessary to insure that comparative measurements are obtained from test to test and among various testing agencies. The implication to research is that determination of the minimum dynamic tensile strength for various materials used in protective construction should be made. This would base material selection and spalling predictions on material strengths. The need for this research is also cited in Reference 11.

64. Recently, the dynamic tensile strength of unreinforced concrete has been studied with respect to model studies of piles (13). The author concluded that even when driving a pile against firm bottom, tensile cracks can occur. The research reported herein points out that the dynamic tensile strength is not a constant and hence would be dependent on the elastic properties of the concrete and the pile driving mechanism, the shape of the driving mechanism, and the impact velocity. More research in this area should lead to better understanding of the problem and also to better design techniques and materials.

Limitations

65. The most severe limitation imposed upon this data is the accuracy associated with the oscilloscope trace. Typical traces have already been presented on which each large grid represents one square centimeter. The vertical calibration was such that one centimeter equals $500 \mu\text{cm}/\text{cm}$ ($\mu\text{in.}/\text{in.}$) of strain and the horizontal calibration was such that one centimeter equals 100 microseconds in time. Each axis, vertical and horizontal, contained subdivisions to one-fifth of a centimeter. With interpolation, the values should be read to the nearest one-tenth of a centimeter. By the calibration, this would make the accuracy of the strain measurement equal to $\pm 25 \mu\text{cm}/\text{cm}$ ($\mu\text{in.}/\text{in.}$) and the accuracy of the time measurement equal to ± 5 microseconds. With an average seismic velocity of plain concrete equal to 3767 m/sec (12,360 ft/sec, Table 2) the reference of the position of the straining pulse with regard to the specimen length would be accurate to 3.8 cm (1.5 in.). Since the strain gradients associated with this type of test are high, the positioning of the pulse should not be against time. Therefore,

the positioning of the pulse was against strain magnitude and these magnitudes are limited in accuracy to $\pm 25 \mu\text{cm}/\text{cm}$ ($\mu\text{in.}/\text{in.}$).

66. A basic limitation to this type of testing is the number of actual data points gained versus the number of cylinders cast. This limitation may be examined using Tables 17 through 20. The actual number of data points obtained in these tests was approximately 75% of the total cylinders cast. This limitation can be improved with experience.

67. One limitation in the analysis should appear if tests are performed with very fast rise times. In the analysis presented, the amount of strain transmitted across the incipient fracture was read on the gaging location. This should be good for finite rise times. However, as the rise time becomes less, the pulse approaches a shock wave with an instantaneous pressure difference. If this is the testing pulse, and fracture occurs, the pulse should be reflected at the fracture location instead of transmitted. The actual rise time at which this occurs has not been examined.

68. The greatest limitation in the applicability of this work to design is the limited scope. The fracture strain data was produced only for one plain concrete type and one fibrous concrete type. It should be expected that, if one percentage of fibre increases the fracture strain of plain concrete (compare Figure 6 to Figure 5), then any other chosen percentage of fibre should increase the fracture strain of plain concrete and it cannot be assumed, a priori, that this increase is directly proportional to the amount of fibre used. Hence, the relationship of percentage of fibre to fracture strain should be evaluated to extend the results presented in this study. Other variables, such as maximum size coarse aggregate, should also have a direct effect on the fracture strains. From the theory of wave propagation across interfaces (References 2), it is known that an abrupt change in the specific acoustic impedance (product of mass density and seismic velocity) causes a portion of an incident wave to be reflected. Hence, a wave encountering a large piece of aggregate should certainly be portionally reflected. This would decrease the strain magnitudes with travel and should therefore have an effect on the apparent fracture strain. The overall implication is that the variables mentioned, as well as other variables that affect strength, should be evaluated in regard to separate effects on fracture strain. Investigations of the fracture strains of other types of concrete are necessary to extend the applicability of these results.

69. The estimate of t_f (time associated with macroscopic fracture of the cross section) was based only on the experimental data. The determination of whether the actual fracture of the cross section was by the propagation of one crack across the cross section or by the coalescence of many cracks forming a macroscopic fracture (microvoid coalescence) would aid in making predictions of t_f . This would allow comparison of the predicted time with the experimentally determined time.

PART VII: CONCLUSIONS

70. The following conclusions are based upon the test results given and the preceding discussion and are to be considered with reference to the limitations in the scope and test procedures.

a. The critical normal fracture strains of plain and steel wire fibrous-reinforced concrete test cylinders, of the type reported herein, are functionally dependent on the rise time of the straining pulse through the value of the critical normal fracture strain. (See Figures 5 and 6). The fracture strain of the plain concrete varies from three to six times the static strain limit. As well as can be defined by the data presented herein, the fracture strain of the steel wire fibrous-reinforced concrete varies from slightly under three to slightly over five times its static strain limit.

b. The conceptual model of the critical normal fracture strain $\xi_{CR} = \xi_c + [\xi_c / (RT - t_f) t_f]$ provides a reasonable fit to the fracture strain data obtained on the plain and fibrous-reinforced concrete. (See Figures 5 and 6 paragraphs 52 and 47).

c. The critical normal fracture strains, of the materials tested, appear to approach a minimal constant value to approximately three times their respective static strain limits for rise times to that fracture strain of greater than 80 microseconds. This is evidenced by Figures 5 and 6 which also show the scatter of data.

d. The critical normal fracture strain of plain concrete can be slightly increased, over the range of rise times cited, by the incorporation of the randomly placed steel wire fibrous-reinforcement of the type tested. (See Figures 5 and 6). However, only one fibrous concrete has been evaluated and this conclusion should be considered with regard to the limitation in scope discussed in paragraph 67.

e. The induced strains, necessary to actually cause spallation of the steel wire fibrous-reinforced concrete cylinders, were in excess of the highest induced strains employed here (See Figure 75). The highest value of critical fracture strain recorded for steel wire fibrous-reinforced concrete was 790 $\mu\text{cm}/\text{cm}$ ($\mu\text{in.}/\text{in.}$) (See Tables 19 and 20).

f. The fibres, as evidenced by their resistance to separation of the concrete matrix, provide a post-fracture resistance to tensile loads (See paragraph 59).

PART VIII: RECOMMENDATIONS

71. Based upon the data and discussion presented herein, and upon the background of laboratory research in fibrous concrete, the following recommendations are made:

a. That the critical normal fracture strain of plain and steel wire fibrous-reinforced concrete test specimens be examined over rise times to that fracture strain less than 20 microseconds and greater than 120 microseconds (See paragraph 57). This should be pursued with regard to the inferences discussed in paragraph 26 and supported by Figures 5 and 6.

b. That a digital computer program be developed to refine the construction of the fracture graphs. The compressional wave shape may be read from the strain time traces taken from the gage location closest to the impact end. This wave shape should be used to predict the shape of the net tensional pulse at reflection presented as a fracture graph. Some work along these lines has been done by others (14).

c. That the fracture surfaces be investigated by electron fractography. To determine the failure cause as microvoid coalescence would allow estimates to be made of the time associated with macroscopic fracture (See paragraph 69).

d. That the influence of such variables as the percentage of fibre, the maximum size coarse aggregate, and the water-cement ratio on the critical normal fracture strain be investigated (See paragraph 68).

e. That the cross-sectional size effect and the volumetric size effect inferred by the conceptual model be investigated. The cross-sectional size effect is associated with the time to complete macroscopic fracture. The volumetric size is associated with the higher probability of finding a crack sufficiently large to initiate fracture in a large volume (See paragraph 60).

f. That the minimum value of the critical normal fracture strain be developed for various materials to aid in material selection for protective construction (See paragraph 68).

g. That a state-of-the-art survey be conducted to ascertain the influence of transient loadings on the design and construction of various elements in structural systems.

BLANK PAGE

REFERENCES

1. G. R. Williamson, "A Method for Determining the Critical Normal Fracture Stress for Rock and Concrete Specimens," Miscellaneous Paper No. 5-3, U. S. Army Engineer Division, Ohio River, Corps of Engineers, Ohio River Division Laboratories, Cincinnati, Ohio 45227, August 1964.
2. J. S. Rinehart, "On Fractures Caused by Explosions and Impacts," Quarterly of the Colorado School of Mines, Volume 55, Number 4, Colorado School of Mines, Golden, Colorado, October 1960.
3. "Instrumentation Development and Evaluation - Ohio River Division Laboratories," Miscellaneous Paper No. 5-4, U. S. Army Engineer Division, Ohio River, Corps of Engineers, Ohio River Division Laboratories, Cincinnati, Ohio 45227, November 1964.
4. D. L. Birkimer, "Fibrous Concrete Under Dynamic Tension," University of Cincinnati, Cincinnati, Ohio 1965.
5. G. R. Williamson, "Fibrous Reinforcements for Portland Cement Concrete," Technical Report No. 2-40, U. S. Army Engineer Division, Ohio River, Corps of Engineers, Ohio River Division Laboratories, Cincinnati, Ohio 45227, May 1965.
6. G. R. Williamson, "The Use of Fibrous-Reinforced Concrete in Structures Exposed to Explosive Hazards," Miscellaneous Paper No. 5-5, U. S. Army Engineer Division, Ohio River, Corps of Engineers, Ohio River Division Laboratories, Cincinnati, Ohio 45227, August 1965.
7. G. R. Williamson, "Response of Fibrous-Reinforced Concrete to Explosive Loading," Technical Report No. 2-48, U. S. Army Engineer Division, Ohio River, Corps of Engineers, Ohio River Division Laboratories, Cincinnati, Ohio 45227, January 1966.
8. F. M. Mellinger and D. L. Birkimer, "Measurements of Stress and Strain on Cylindrical Test Specimens of Rock and Concrete Under Impact Loading," Technical Report No. 4-46, U. S. Army Engineer Division, Ohio River, Corps of Engineers, Ohio River Division Laboratories, Cincinnati, Ohio 45227, April 1966.
9. D. L. Birkimer and J. R. Hossley, "Comparison of Static and Dynamic Behavior of Plain and Fibrous-Reinforced Concrete Cylinders," Technical Report No. 4-69, U. S. Army Engineer Division, Ohio River, Corps of Engineers, Ohio River Division Laboratories, Cincinnati, Ohio 45227, December 1968.

10. D. L. Birkimer, "Critical Normal Fracture Strain of Portland Cement Concrete," University of Cincinnati, Cincinnati, Ohio; in publication at this time.
11. S. K. Takahashi and J. R. Allgood, "Static Versus Dynamic Testing of Deep Slabs," Technical Note N-9051, (DASA RS 53318) Naval Civil Engineering Laboratory, Port Hueneme, California, August 1967; Confidential.
12. Ammann & Whitney, Consulting Engineers, "Industrial Engineering Study to Establish Safety Design Criteria for Use in Engineering of Explosive Facilities and Operations - Wall Response," A Report Submitted to Process Engineering Branch, A. P. M. E. D., Picatinny Arsenal, Dover, New Jersey, April 1963.
13. Sven Sahlin and Lars Hellman, "Dynamic Tensile Strength of Model Unreinforced Concrete," Author's Summary, Bulletin No. 63, Kungliga Tekniska Hogskolan Institutionen for Byggnadsstatik, Stockholm, Sweden; Printed in Technical Reviews, Journal of the American Concrete Institute, No. 12, Proceedings, V. 64, December 1967.
14. C. G. Lyons, "Energy Reflection in a Cylindrical Steel Rod Subjected to Longitudinal Impact," Master of Science Thesis, Civil Engineering Department, Texas A&M University, May 1966.

Table 1
Fine Aggregate Gradation

Sieve Size	Sieve Openings		% Passing
	mm	in.	
8	2.38	0.094	98
16	1.19	0.047	61
30	0.59	0.023	46
50	0.297	0.012	26
100	0.149	0.006	7
200	0.074	0.003	0

U. S. Standard Sieve Series
 (ASTM E 11-61)

Table 2

Average Physical Properties of Concrete Test Specimens

	Plain Concrete		Steel Wire Fibrous-Reinforced Concrete	
*Static Direct Pull Ultimate Tensile Strength	34.4 kg/cm ²	490 psi	40.3 kg/cm ²	573 psi
*Static Direct Pull Ultimate Tensile Strain	100 μ cm/cm	100 μ in./in.	150 μ cm/cm	150 μ in./in.
*Static Initial Young's Modulus of Elasticity in Tension	3.24x10 ⁵ kg/cm ²	4.61x10 ⁶ psi	2.64x10 ⁵ kg/cm ²	3.75x10 ⁶ psi
**Static Ultimate Unconfined Compressive Strength	450 kg/cm ²	6830 psi	421 kg/cm ²	5990 psi
Specific Gravity	2.28	2.28	2.29	2.29
Mass Density	2278 kg/cm ³	4.42 slugs/ft ³	2294 kg/cm ³	4.45 slugs/ft ³
Fundamental Frequency: Specimens (89 cm, 35 in.)	2120 cps	2120 cps	2140 cps	2140 cps
Seismic Velocity	3710 m/sec	12360 ft/sec	3780 m/sec	12390 ft/sec
Dynamic Young's Modulus of Elasticity	3.44x10 ⁵ kg/cm ²	4.90x10 ⁶ psi	3.34x10 ⁵ kg/cm ²	4.75x10 ⁶ psi
*Average of 30 Tests	NOTE: All properties determined at 9 Day Age			
**Average of Six Tests				

Table 3

Plain Concrete

Specific Gravity and Mass Density

Specimen A through K

Specimen	Weight in Air gm	Weight in Water gm	Specific Gravity	Mass Density kg/m ³	Mass Density slug/ft ³
B	57.6	32.5	2.29	2289	4.44
C	42.5	23.9	2.28	2279	4.42
D	52.8	30.0	2.31	2309	4.48
E	58.8	33.0	2.27	2268	4.40
F	46.8	26.2	2.27	2268	4.40
G	56.6	31.6	2.26	2258	4.38
H	12.6	6.7	2.13	2129	4.13
I	43.2	24.0	2.24	2237	4.34
J	52.6	29.3	2.26	2258	4.38
K	46.4	26.0	2.27	2268	4.40
K	44.1	25.5	2.38	2376	4.61
Arithmetic Average			2.27	2267	4.40

Table 4

Plain Concrete
Specific Gravity and Mass Density
Specimen 1 through 11

Specimen	Weight in Air gm	Weight in Water gm	Specific Gravity	Mass Density	
				kg/m ³	slug/ft ³
1	80.3	45.5	2.31	2309	4.48
2	69.0	38.8	2.28	2279	4.42
3	73.6	41.3	2.28	2279	4.42
4	66.4	37.6	2.31	2309	4.48
5	54.2	30.5	2.29	2289	4.44
6	50.5	28.2	2.26	2258	4.38
7	69.7	39.1	2.28	2279	4.42
8	56.9	31.8	2.27	2268	4.40
9	108.8	62.3	2.34	2335	4.53
10	67.9	38.2	2.29	2289	4.44
11	77.6	43.3	2.26	2258	4.38
Arithmetic Average				2286	4.44

Table 5

Plain Concrete
Specific Gravity and Mass Density
Specimen I through XII

Specimen	Weight in Air gm	Weight in Water gm	Specific Gravity	Mass Density	
				kg/m ³	slug/ft ³
I	46.7	25.4	2.30	2299	4.46
II	58.7	33.0	2.28	2330	4.52
III	62.4	34.8	2.26	2258	4.38
IV	57.6	32.3	2.28	2279	4.42
V	47.5	26.7	2.28	2279	4.42
VI	53.3	29.7	2.26	2258	4.38
VII	47.5	26.9	2.31	2309	4.48
VIII	35.4	18.7	2.12	2119	4.11
IX	48.8	27.5	2.29	2289	4.44
X	52.9	28.6	2.18	2175	4.22
XI	56.3	31.2	2.24	2237	4.34
XII	62.1	35.1	2.30	2299	4.46
Arithmetic Average			2.26	2261	4.38

Table 6

Plain Concrete
Specific Gravity and Mass Density
Specimen PG 4-1 through PG 4-12

Specimen	Weight in Air gm	Weight in Water gm	Specific Gravity	Mass Density	
				kg/m ³	slug/ft ³
PG 4-1	79.5	44.9	2.30	2299	4.46
PG 4-2	50-8	28.7	2.30	2299	4.46
PG 4-3	72.2	40.9	2.31	2309	4.48
PG 4-4	69.2	39.3	2.31	2309	4.48
PG 4-5	43.7	25.1	2.35	2336	4.55
PG 4-6	42.9	24.8	2.37	2366	4.59
PG 4-7	235.7	131.4	2.26	2259	4.38
PG 4-8	67.8	38.2	2.29	2289	4.44
PG 4-9	49.5	28.3	2.33	2330	4.52
PG 4-10	29.8	17.1	2.35	2336	4.55
PG 4-11	60.8	33.9	2.26	2259	4.38
PG 4-12	54.1	30.8	2.32	2320	4.50
Arithmetic Average			2.31	2309	4.48

Table 7

Steel Wire Fibrous-Reinforced Concrete

Specific Gravity and Mass Density

Specimen PG 6-1 through PG 6-11

Specimen	Weight in Air gm	Weight in Water gm	Specific Gravity	Mass Density	
				kg/m ³	slug/ft ³
PG 6-1	116.4	66.3	2.32	2335	4.53
PG 6-2	110.1	62.0	2.29	2304	4.47
PG 6-3	125.1	70.2	2.28	2294	4.45
PG 6-4	169.9	92.1	2.18	2191	4.25
PG 6-5	125.8	71.5	2.32	2335	4.53
PG 6-6	128.3	72.0	2.28	2294	4.45
PG 6-7	140.0	78.5	2.28	2294	4.45
PG 6-8	109.5	62.0	2.31	2325	4.51
PG 6-9	149.0	84.0	2.29	2304	4.47
PG 6-10	126.6	72.5	2.34	2356	4.57
PG 6-11	81.5	46.0	2.30	2309	4.48
Arithmetic Average			2.29	2304	4.47

Table 8

Steel Wire Fibrous-Reinforced Concrete
Specific Gravity and Mass Density
Specimen PG 7-1 through PG 7-12

Specimen	Weight in Air gm	Weight in Water gm	Specific Gravity	Mass Density kg/m ³	Mass Density slug/ft ³
PG 7-1	102.0	58.3	2.37	2387	4.63
PG 7-2	137.6	80.6	2.40	2413	4.68
PG 7-3	95.7	55.1	2.36	2376	4.61
PG 7-4	85.1	48.0	2.29	2304	4.47
PG 7-5	116.8	67.3	2.36	2376	4.61
PG 7-6	64.0	37.2	2.39	2407	4.67
PG 7-7	97.65	55.3	2.30	2309	4.48
PG 7-8	86.4	48.9	2.30	2309	4.48
PG 7-9	95.7	54.3	2.31	2330	4.52
PG 7-10	97.2	56.2	2.36	2376	4.61
PG 7-11	99.3	57.2	2.36	2376	4.61
PG 7-12	117.0	66.4	2.31	2330	4.52
Arithmetic Average			2.34	2356	4.57

Table 9

Steel Wire Fibrous-Reinforced Concrete

Specific Gravity and Mass Density

Specimen PG 8-1 through PG 8-12

Specimen	Weight in Air gm	Weight in Water gm	Specific Gravity	Mass Density	
				kg/m ³	slug/ft ³
PG 8-1	110.2	61.0	2.24	2237	4.34
PG 8-2	87.7	48.3	2.23	2227	4.32
PG 8-3	89.0	49.0	2.23	2227	4.32
PG 8-4	81.2	44.5	2.21	2206	4.28
PG 8-5	100.9	55.2	2.21	2206	4.28
PG 8-6	98.0	52.5	2.15	2150	4.17
PG 8-7	77.6	42.5	2.21	2206	4.28
PG 8-8	103.2	57.9	2.28	2279	4.42
PG 8-9	128.9	71.8	2.26	2258	4.38
PG 8-10	94.7	52.7	2.25	2248	4.36
PG 8-11	103.6	58.2	2.28	2279	4.42
PG 8-12	81.9	45.0	2.22	2217	4.30
Arithmetic Average			2.23	2227	4.32

Table 10

Plain Concrete
Seismic Velocity and Dynamic Young's Modulus of Elasticity
Specimen A through K

Specimen	Fundamental Frequency	Seismic Velocity		Dynamic Young's Modulus of Elasticity	
		m/sec	ft/sec	kg/cm ² x 10 ⁵	psi x 10 ⁶
A	2190	3885	12,746	3.63	5.17
B	2175	3858	12,658	3.56	5.07
C	2180	3867	12,688	3.63	5.17
D	2180	3867	12,688	3.57	5.08
E	2175	3858	12,658	3.55	5.05
F	2170	3849	12,629	3.52	5.01
G	2200	3909	12,826	3.42	4.87
H	2175	3858	12,658	3.50	4.98
I	2170	3849	12,629	3.52	5.01
J	2180	3867	12,688	3.57	5.08
K	2190	3885	12,746	3.78	5.37
Arithmetic Average		3868	12,692	3.57	5.08

Table 11

Plain Concrete
Seismic Velocity and Dynamic Young's Modulus of Elasticity
Specimen 1 through 11

Specimen	Fundamental Frequency	Seismic Velocity		Dynamic Young's Modulus of Elasticity	
	cps	m/sec	ft/sec	kg/cm ² x 10 ⁵	psi x 10 ⁶
1	2190	3885	12,746	3.66	5.21
2	2190	3885	12,746	3.61	5.14
3	2195	3894	12,775	3.63	5.17
4	2190	3885	12,746	3.66	5.21
5	2170	3849	12,629	3.56	5.07
6	2160	3832	12,571	3.49	4.96
7	2180	3867	12,688	3.59	5.10
8	2180	3867	12,688	3.56	5.07
9	2185	3876	12,717	3.70	5.26
10	2190	3885	12,746	3.63	5.17
11	2195	3894	12,775	3.60	5.12
Arithmetic Average		3874	12,711	3.61	5.13

Table 12

Plain Concrete
Seismic Velocity and Dynamic Young's Modulus of Elasticity
Specimen I through XII

Specimen	Fundamental Frequency	Seismic Velocity		Dynamic Young's Modulus of Elasticity	
		m/sec	ft/sec	kg/cm ² x 10 ⁵	psi x 10 ⁶
I	2200	3901	12,800	3.68	5.23
II	2175	3859	12,660	3.52	5.01
III	2180	3868	12,690	3.55	5.05
IV	2190	3886	12,750	3.62	5.15
V	2170	3850	12,630	3.55	5.05
VI	2170	3850	12,630	3.52	5.01
VII	2170	3850	12,630	3.59	5.10
VIII	2180	3868	12,690	3.32	4.72
IX	2175	3859	12,660	3.54	5.03
X	2180	3868	12,690	3.43	4.88
XI	2190	3886	12,750	3.56	5.06
XII	2170	3850	12,630	3.59	5.10
Arithmetic Average		3866	12,684	3.54	5.03

Table 13

Plain Concrete
Seismic Velocity and Dynamic Young's Modulus of Elasticity
Specimen PG 4-1 through PG 4-12

Specimen	Fundamental Frequency	Seismic Velocity		Dynamic Young's Modulus of Elasticity	
		m/sec	ft/sec	kg/cm ² x 10 ⁵	psi x 10 ⁶
PG 4-1	2140	3795	12,450	3.38	4.81
PG 4-2	2160	3834	12,580	3.45	4.91
PG 4-3	2160	3834	12,580	3.47	4.93
PG 4-4	2125	3764	12,350	3.34	4.75
PG 4-5	2125	3764	12,350	3.40	4.84
PG 4-6	2160	3834	12,580	3.56	5.06
PG 4-7	2140	3795	12,450	3.33	4.73
PG 4-8	2140	3795	12,450	3.36	4.78
PG 4-9	2140	3795	12,450	3.43	4.88
PG 4-10	2125	3764	12,350	3.40	4.84
PG 4-11	2140	3795	12,450	3.33	4.73
PG 4-12	2125	3764	12,350	3.35	4.77
Arithmetic Average		3794	12,450	3.40	4.84

Table 14

Steel Wire Fibrous-Reinforced Concrete
Seismic Velocity and Dynamic Young's Modulus of Elasticity
Specimen PG 6-1 through PG 6-11

Specimen	Fundamental Frequency	Seismic Velocity		Dynamic Young's Modulus of Elasticity	
		m/sec	ft/sec	kg/cm ² x 10 ⁵	psi x 10 ⁶
PG 6-1	2060	3667	12,030	3.20	4.55
PG 6-2	2060	3667	12,030	3.16	4.49
PG 6-3	2060	3667	12,030	3.14	4.47
PG 6-4	2060	3667	12,030	3.00	4.27
PG 6-5	2090	3667	12,030	3.20	4.55
PG 6-6	2090	3722	12,210	3.24	4.61
PG 6-7	2080	3703	12,150	3.21	4.56
PG 6-8	2060	3667	12,030	3.18	4.53
PG 6-9	2070	3685	12,090	3.19	4.54
PG 6-10	2080	3703	12,150	3.29	4.68
PG 6-11	2070	3685	12,090	3.20	4.55
Arithmetic Average		3682	12,080	3.18	4.53

Table 15

Steel Wire Fibrous-Reinforced Concrete
Seismic Velocity and Dynamic Young's Modulus of Elasticity
Specimen PG 7-1 through PG 7-12

Specimen	Fundamental Frequency	Seismic Velocity		Dynamic Young's Modulus of Elasticity	
		m/sec	ft/sec	kg/cm ² x 10 ⁵	psi x 10 ⁶
PG 7-1	2175	3865	12,680	3.63	5.17
PG 7-2	2150	3816	12,520	3.58	5.09
PG 7-3	2190	3895	12,780	3.68	5.23
PG 7-4	2160	3840	12,600	3.47	4.93
PG 7-5	2190	3895	12,780	3.68	5.23
PG 7-6	2160	3840	12,600	3.62	5.15
PG 7-7	2165	3850	12,630	3.49	4.96
PG 7-8	2165	3850	12,630	3.49	4.96
PG 7-9	2180	3874	12,710	3.56	5.07
PG 7-10	2160	3840	12,600	3.57	5.08
PG 7-11	2170	3856	12,650	3.60	5.12
PG 7-12	2180	3874	12,710	3.56	5.07
Arithmetic Average		3859	12,660	3.58	5.09

Table 16

Steel Wire Fibrous-Reinforced Concrete
Seismic Velocity and Dynamic Young's Modulus of Elasticity
Specimen PG 8-1 through PG 8-12

Specimen	Fundamental Frequency	Seismic Velocity		Dynamic Young's Modulus of Elasticity	
		m/sec	ft/sec	kg/cm ² x 10 ⁵	psi x 10 ⁶
PG 8-1	2100	3734	12,250	3.18	4.52
PG 8-2	2150	3822	12,540	3.32	4.72
PG 8-3	2120	3770	12,370	3.23	4.59
PG 8-4	2120	3770	12,370	3.20	4.55
PG 8-5	2130	3786	12,420	3.22	4.58
PG 8-6	2110	3752	12,310	3.09	4.39
PG 8-7	2150	3816	12,520	3.28	4.66
PG 8-8	2130	3786	12,370	3.33	4.73
PG 8-9	2120	3770	12,370	3.27	4.65
PG 8-10	2140	3804	12,480	3.32	4.72
PG 8-11	2140	3804	12,480	3.36	4.78
PG 8-12	2120	3770	12,370	3.21	4.57
Arithmetic Average		3783	12,410	3.25	4.62

Table 17

Plain Concrete
Summary of Critical Normal Fracture Strain Data

Specimen No.	ϵ_{CR}	Rise Time to ϵ_{CR}	Remarks
	μ in./in.	μ sec	
A	425	162	--
B	--	--	Not Tested
C	--	--	Not Tested
D	--	--	Electronic Misfire
E	510	28	--
F	--	--	Not Tested
G	500	34	--
H	280	113	--
I	520	30	--
J	300	90	--
K	--	--	Uninterpretable
1	415	110	--
2	--	--	Uninterpretable
3	--	--	Electronic Misfire
4	340	75	--
5	380	114	--
6	400	49	--
7	--	--	Electronic Misfire
8	350	62	--
9	300	120	--
10	440	60	--
11	630	40	--

Table 18

Plain Concrete
Summary of Critical Normal Fracture Strain Data

Specimen No.	ϵ_{CR}	Rise Time to ϵ_{CR}	Remarks
	μ in./in.	μ sec	
I	510	122	--
II	--	--	Electronic Misfire
III	600	26	--
IV	360	120	--
V	600	37	--
VI	200	160	*No Fracture
VII	500	130	--
VIII	--	--	Electronic Misfire
IX	510	112	--
X	450	140	--
XI	190	150	*No Fracture
XII	--	--	Not Tested
PG 4-1	510	57	--
PG 4-2	490	50	--
PG 4-3	520	60	--
PG 4-4	460	55	--
PG 4-5	550	60	--
PG 4-6	430	140	--
PG 4-7	--	--	Electronic Misfire
PG 4-8	300	210	*No Fracture
PG 4-9	430	125	--
PG 4-10	450	64	--
PG 4-11	--	--	Electronic Misfire
PG 4-12	--	--	Not Tested

* VALUES GIVEN ARE FOR PEAK STRAIN AND CORRESPONDING RISE TIME.

Table 19

Steel Wire Fibrous-Reinforced Concrete
Summary of Critical Normal Fracture Strain Data

Specimen No.	ϵ_{CR}	Rise Time to ϵ_{CR}	Remarks
	$\mu\text{in./in.}$	$\mu\text{ sec}$	
PG 6-1	470	102	--
PG 6-2	530	70	--
PG 6-3	700	20	--
PG 6-4	600	46	--
PG 6-5	400	100	*No Fracture
PG 6-6	--	--	Electronic Misfire
PG 6-7	450	79	--
PG 6-8	--	--	Electronic Misfire
PG 6-9	500	40	--
PG 6-10	--	--	Electronic Misfire
PG 6-11	650	60	--
PG 7-1	640	26	Second Fracture
PG 7-2	540	86	--
PG 7-3	400	75	--
PG 7-4	790	42	Second Fracture
PG 7-5	--	--	Inconclusive
PG 7-6	430	56	--
PG 7-7	490	55	--
PG 7-8	--	--	Electronic Misfire
PG 7-9	490	42	--
PG 7-10	470	60	*No Fracture
PG 7-11	620	60	--
PG 7-12	--	--	Not Tested

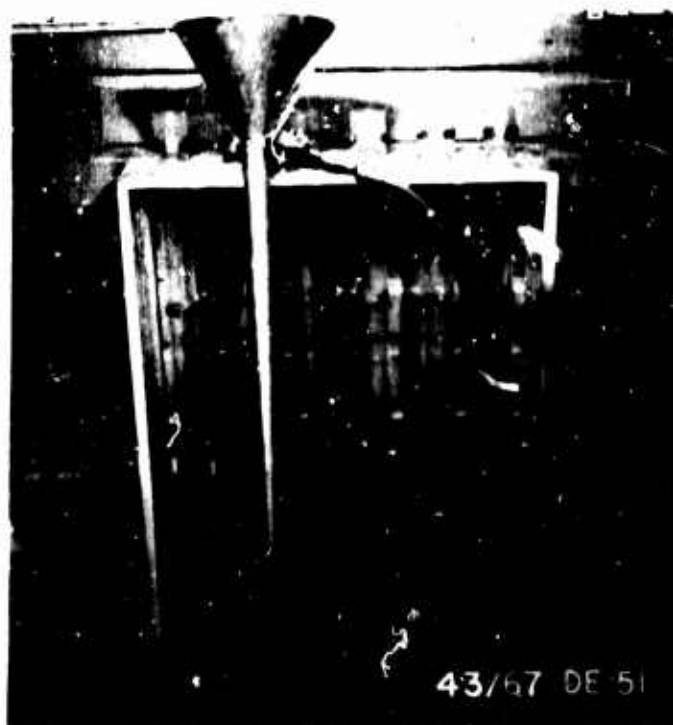
* VALUES GIVEN ARE FOR PEAK STRAIN AND CORRESPONDING RISE TIME.

Table 20

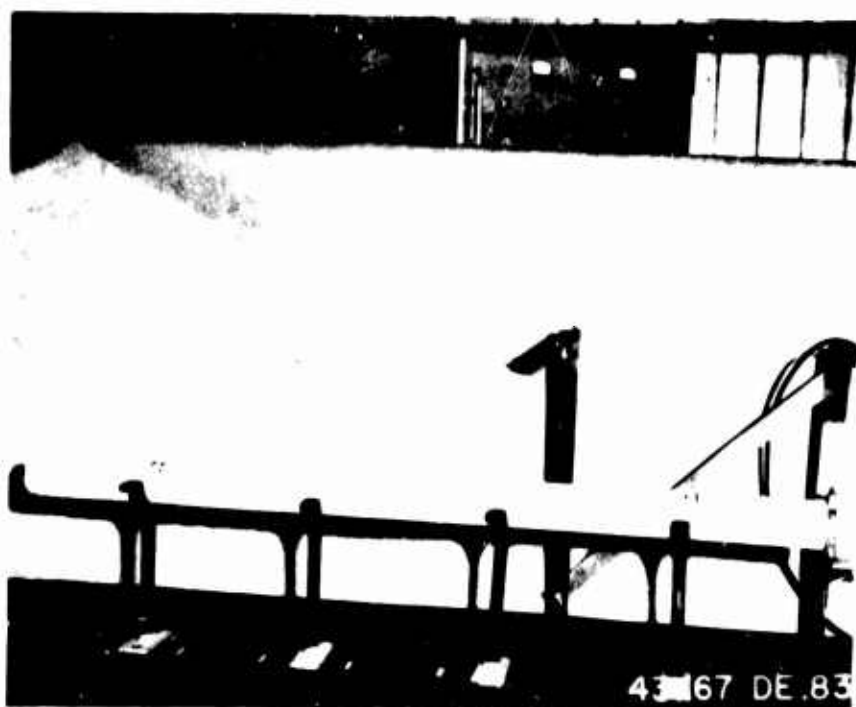
Steel Wire Fibrous-Reinforced Concrete
Summary of Critical Normal Fracture Strain Data

Specimen No.	ϵ_{CR}	Rise Time to ϵ_{CR}	Remarks
	$\mu\text{in./in.}$	μsec	
PG 8-1	590	56	--
PG 8-2	520	70	*No Fracture
PG 8-3	700	47	--
PG 8-4	650	49	--
PG 8-5	500	49	--
PG 8-6	333	100	*No Fracture
PG 8-7	790	50	--
PG 8-8	233	60	*No Fracture
PG 8-9	500	91	--
PG 8-10	525	74	Second Fracture
PG 8-11	--	--	Inconclusive
PG 8-12	530	55	--

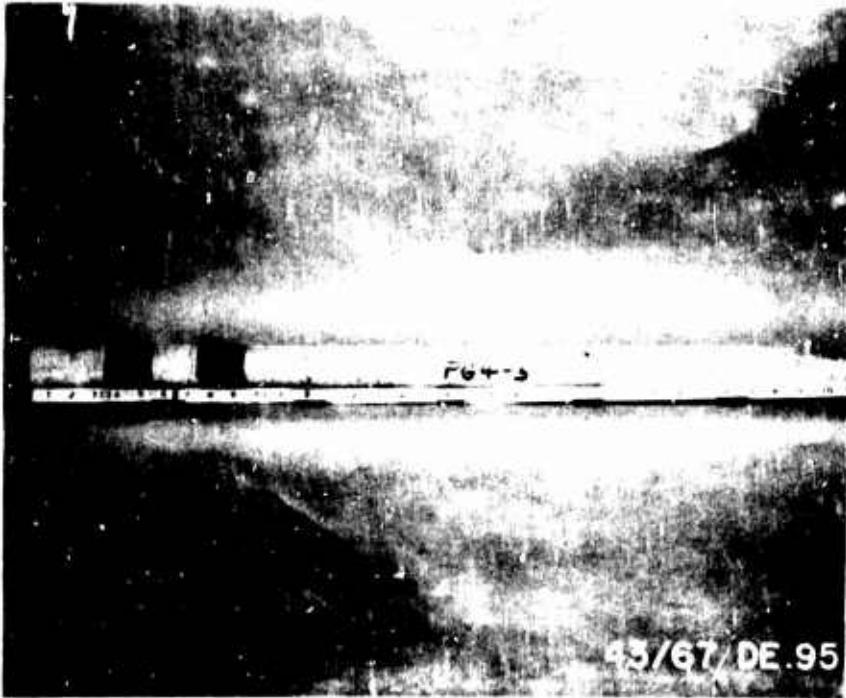
* VALUES GIVEN ARE FOR PEAK STRAIN AND CORRESPONDING RISE TIME.



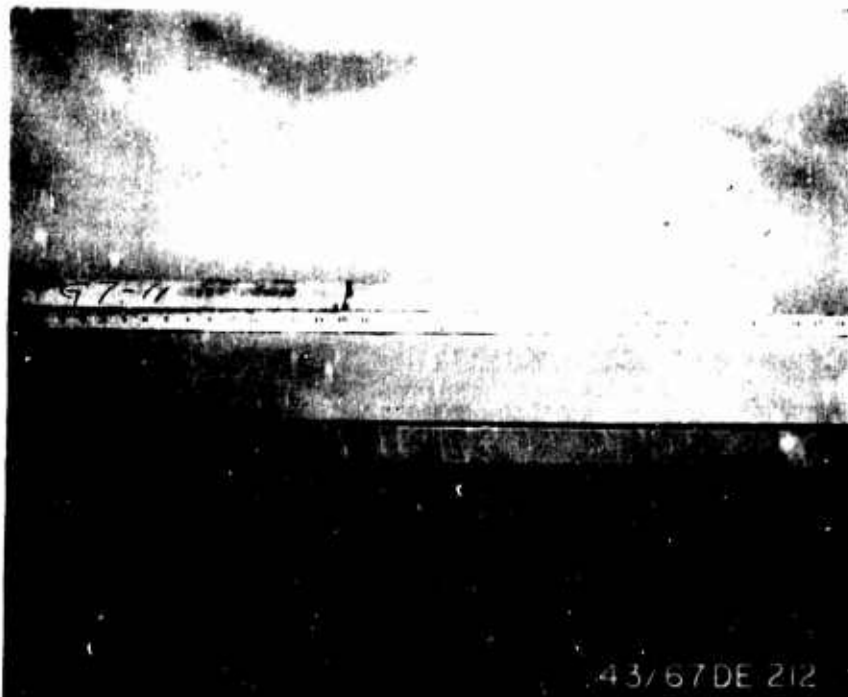
a. Specimen Casting Apparatus



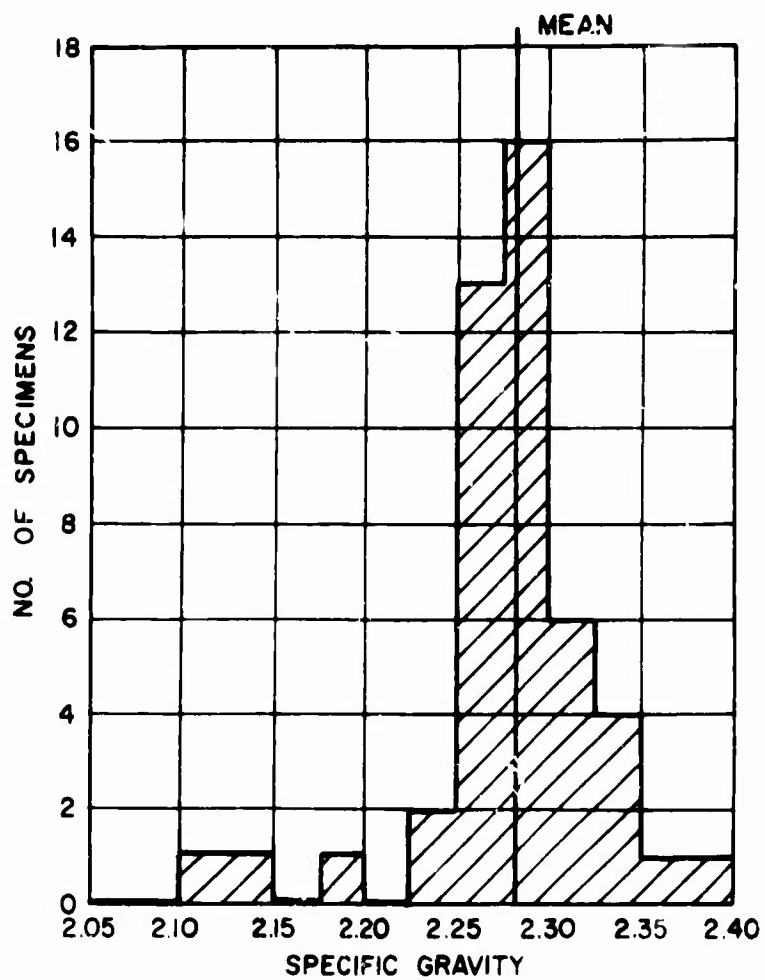
b. Specimen Support System



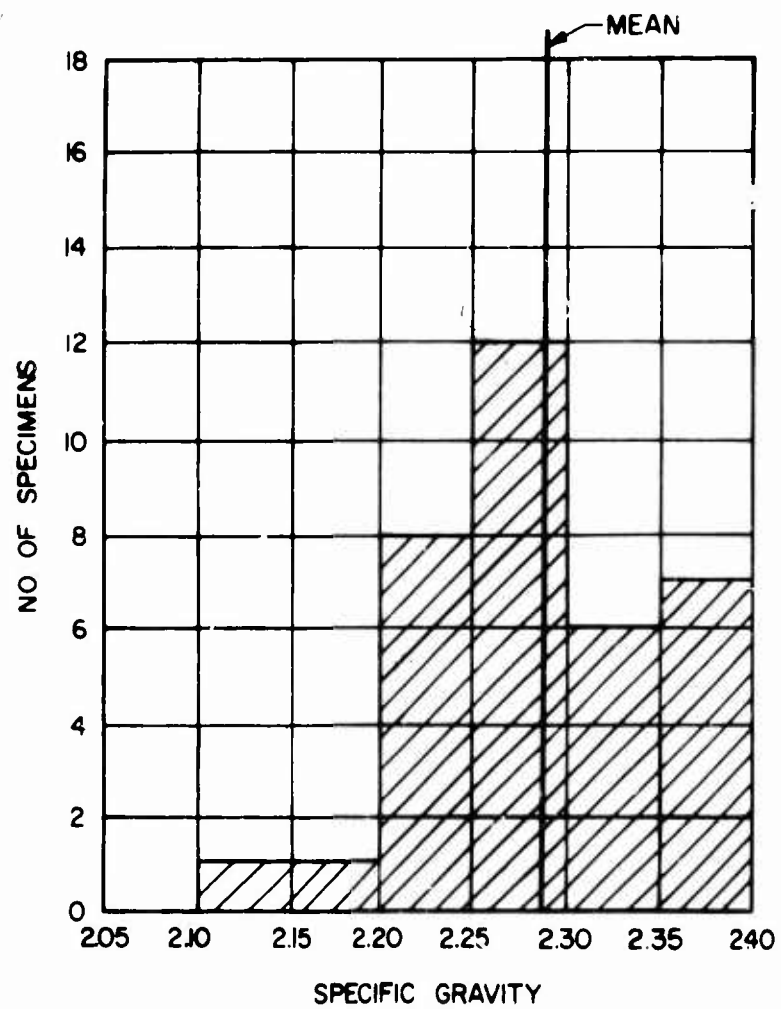
- a. Typical Plain Concrete Fracture Specimen . Note Double Spalls and Fracturing at Impact End.



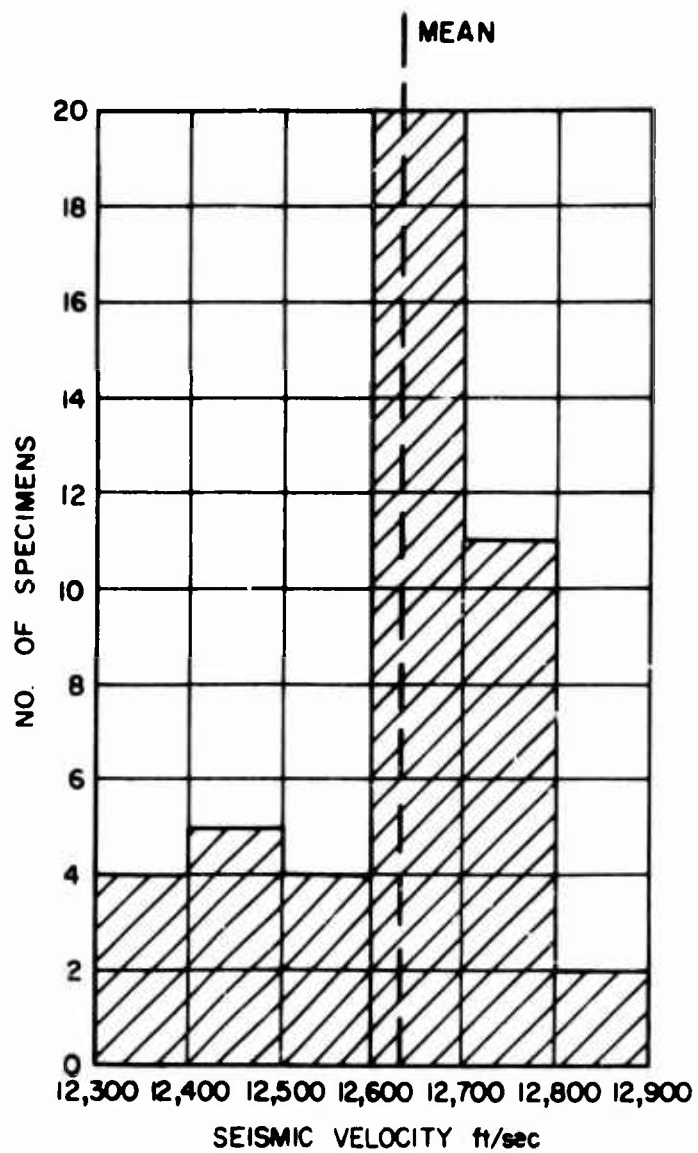
- b. Typical Fibrous Concrete Fractured Specimen. Hairline Fracture Marked With Black Ink.



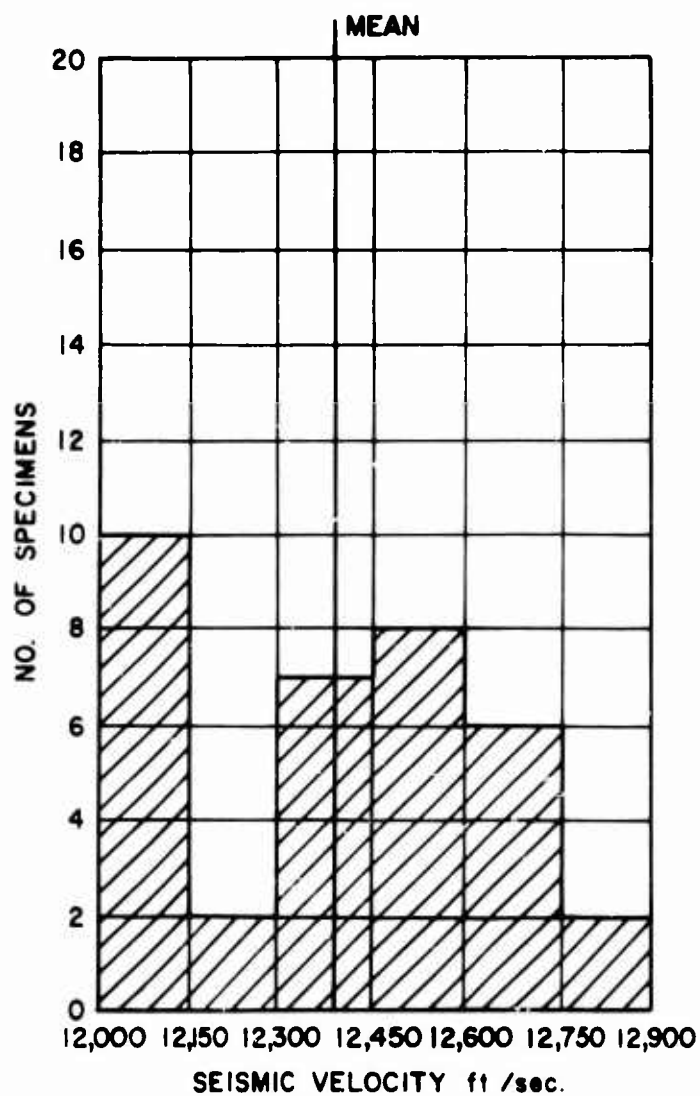
HISTOGRAM FOR DISTRIBUTION OF
SPECIFIC GRAVITY
PLAIN CONCRETE



HISTOGRAM FOR DISTRIBUTION OF
SPECIFIC GRAVITY
STEEL WIRE FIBROUS-REINFORCED CONCRETE

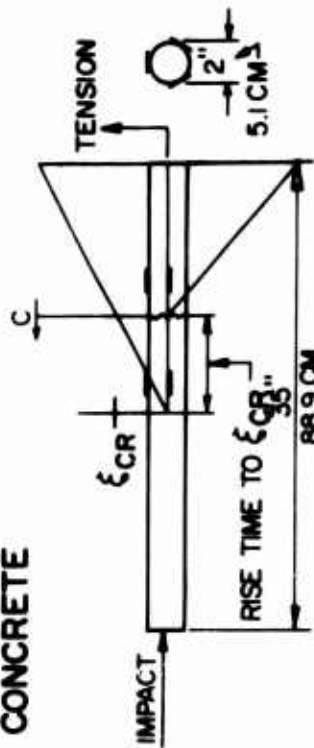


HISTOGRAM FOR DISTRIBUTION OF
SEISMIC VELOCITY
PLAIN CONCRETE

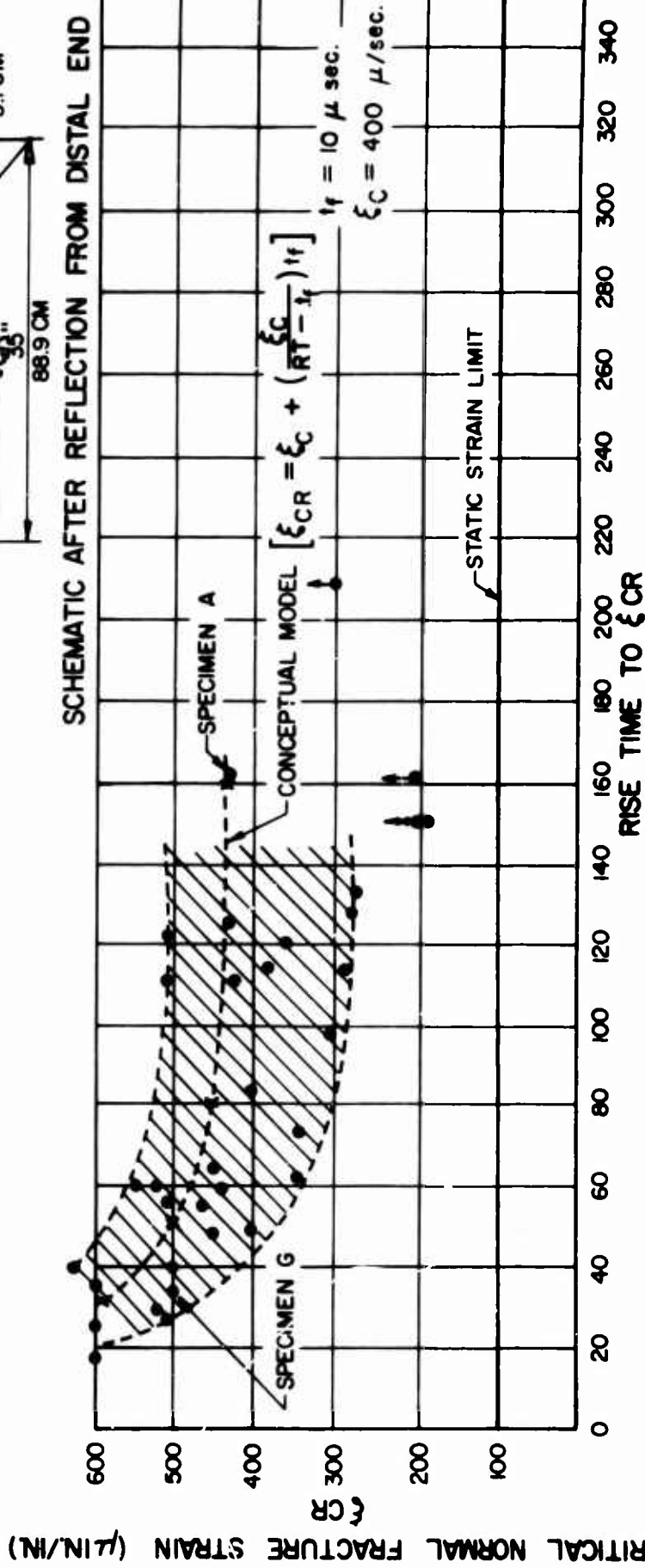


HISTOGRAM FOR DISTRIBUTION OF
SEISMIC VELOCITY
STEEL WIRE FIBROUS-REINFORCED CONCRETE

CRITICAL NORMAL FRACTURE STRAIN VS
RISE TIME OF STRAINING PULSE TO
FRACTURE STRAIN - PLAIN CONCRETE



SCHEMATIC AFTER REFLECTION FROM DISTAL END



RISE TIME OF STRAINING PULSE TO FRACTURE STRAIN (μSEC)

CRITICAL NORMAL FRACTURE STRAIN VS.
RISE TIME OF STRAINING PULSE TO FRACTURE STRAIN
STEEL WIRE FIBROUS - REINFORCED CONCRETE

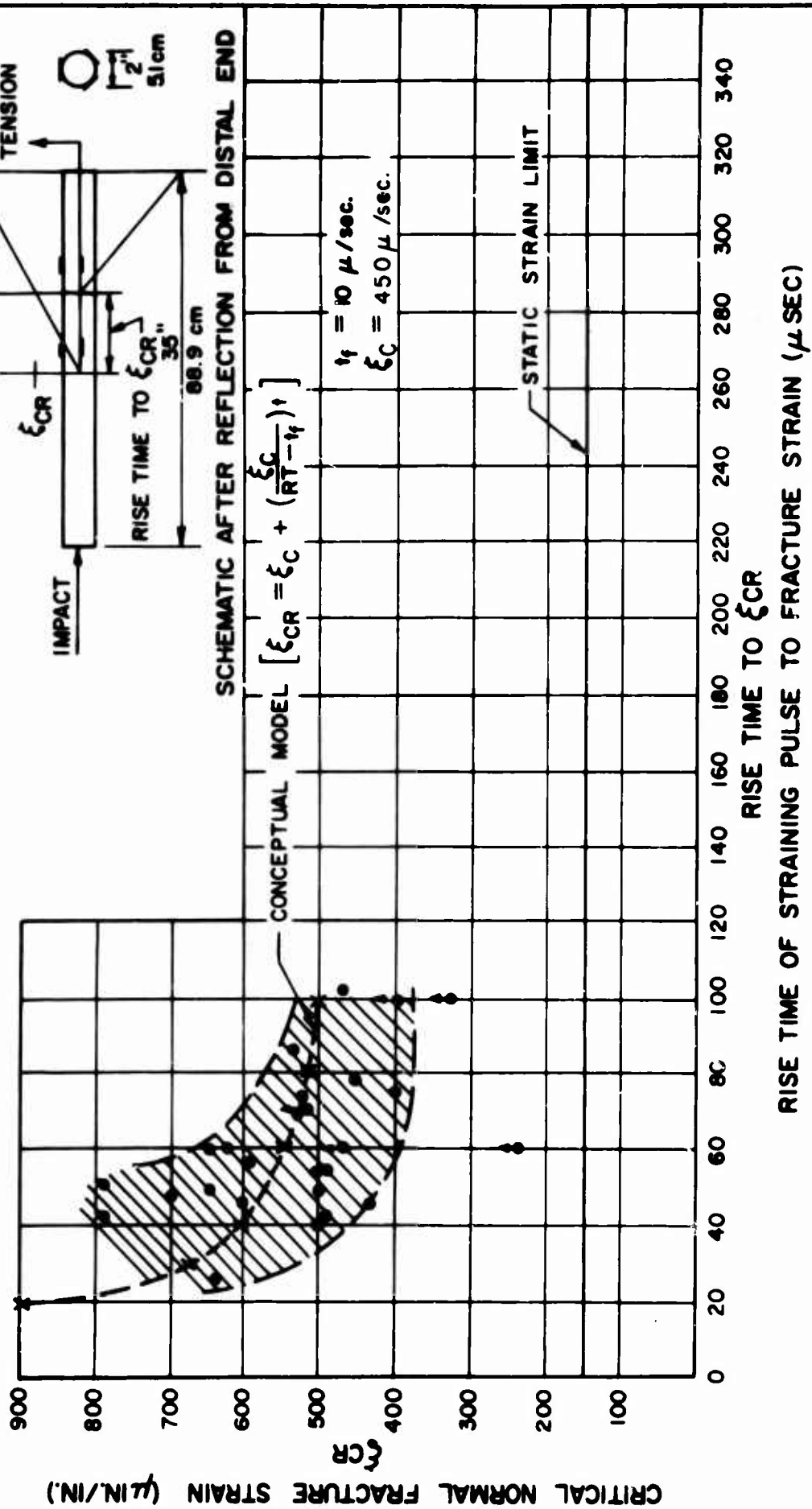


FIGURE 6

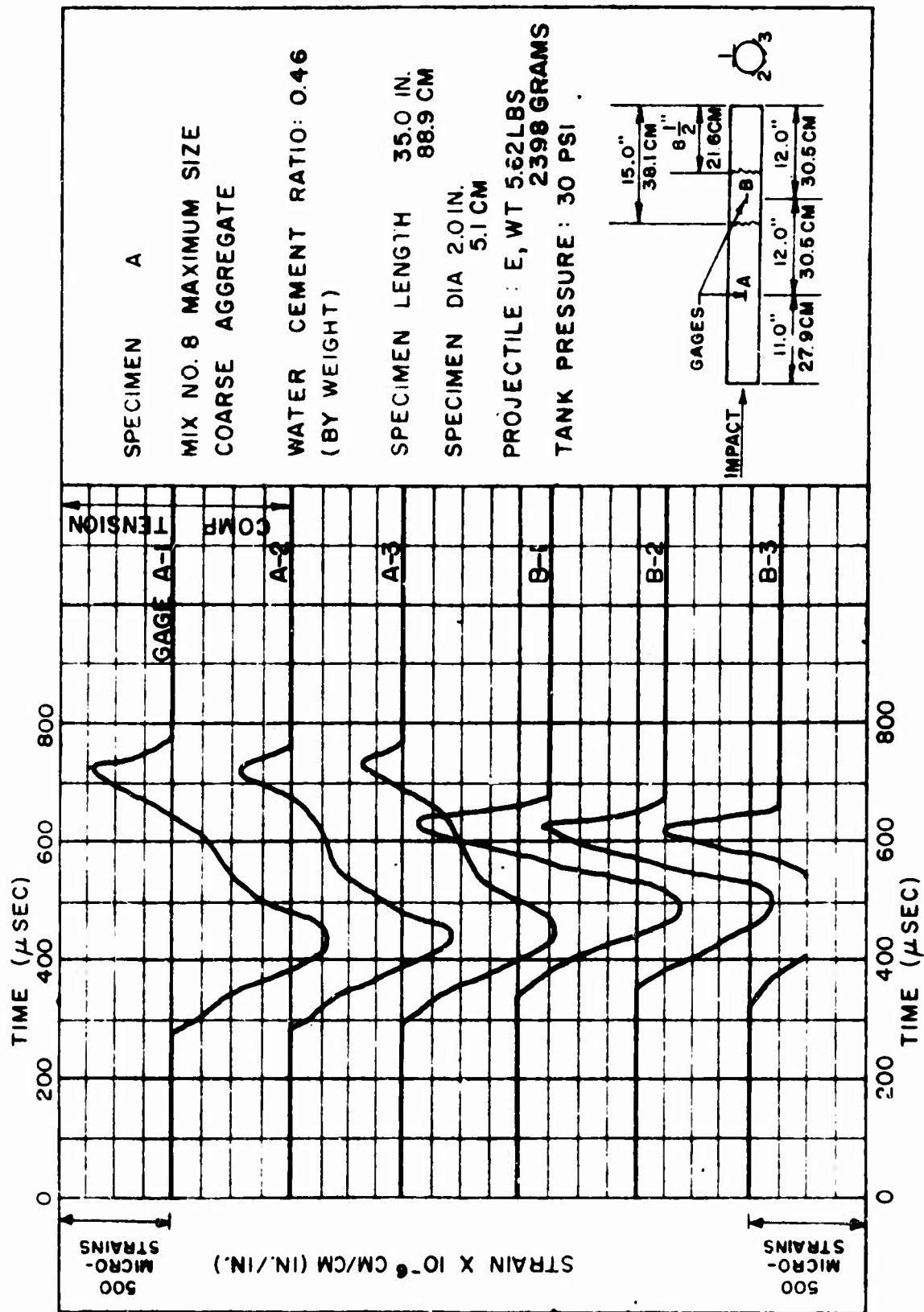
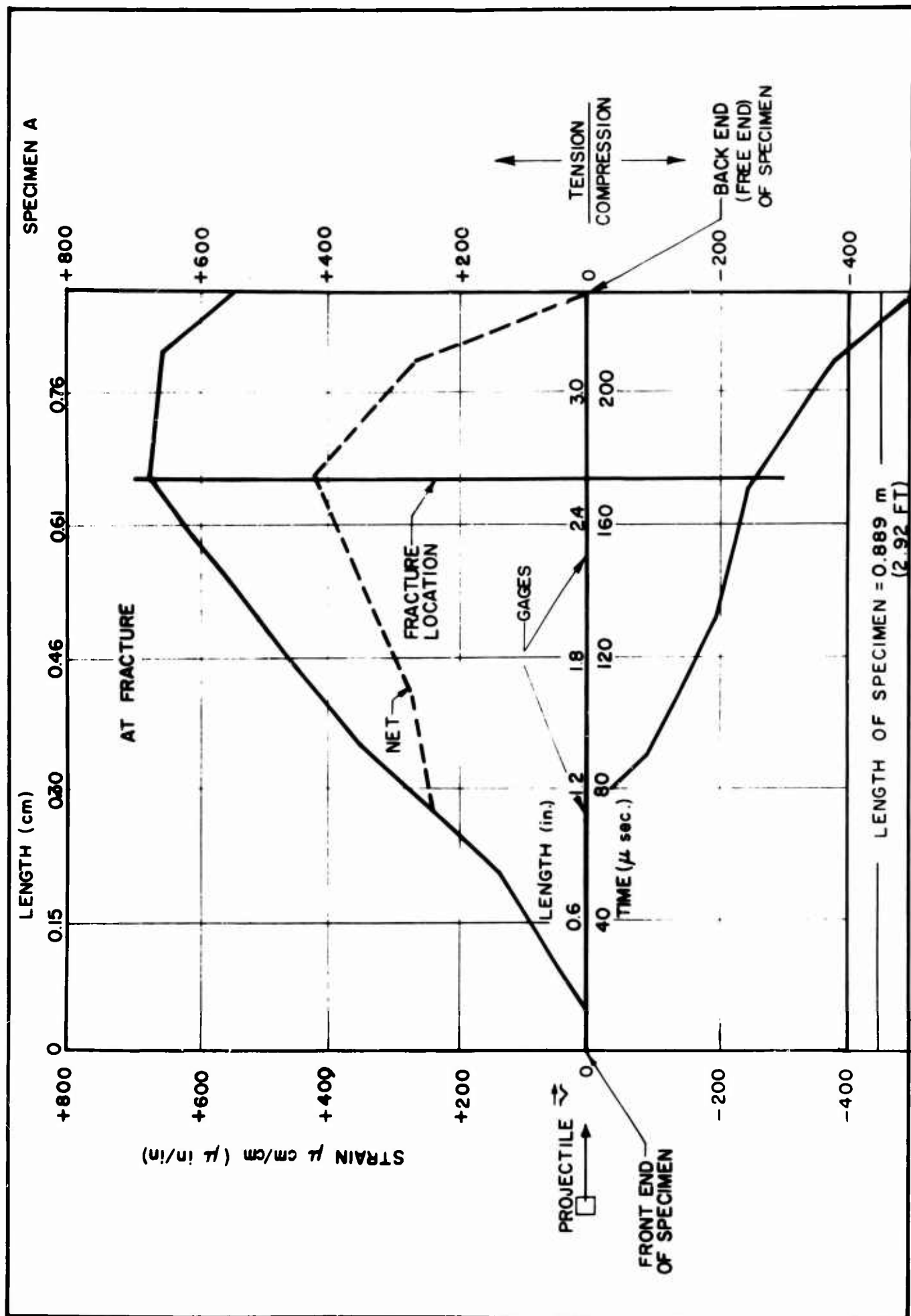
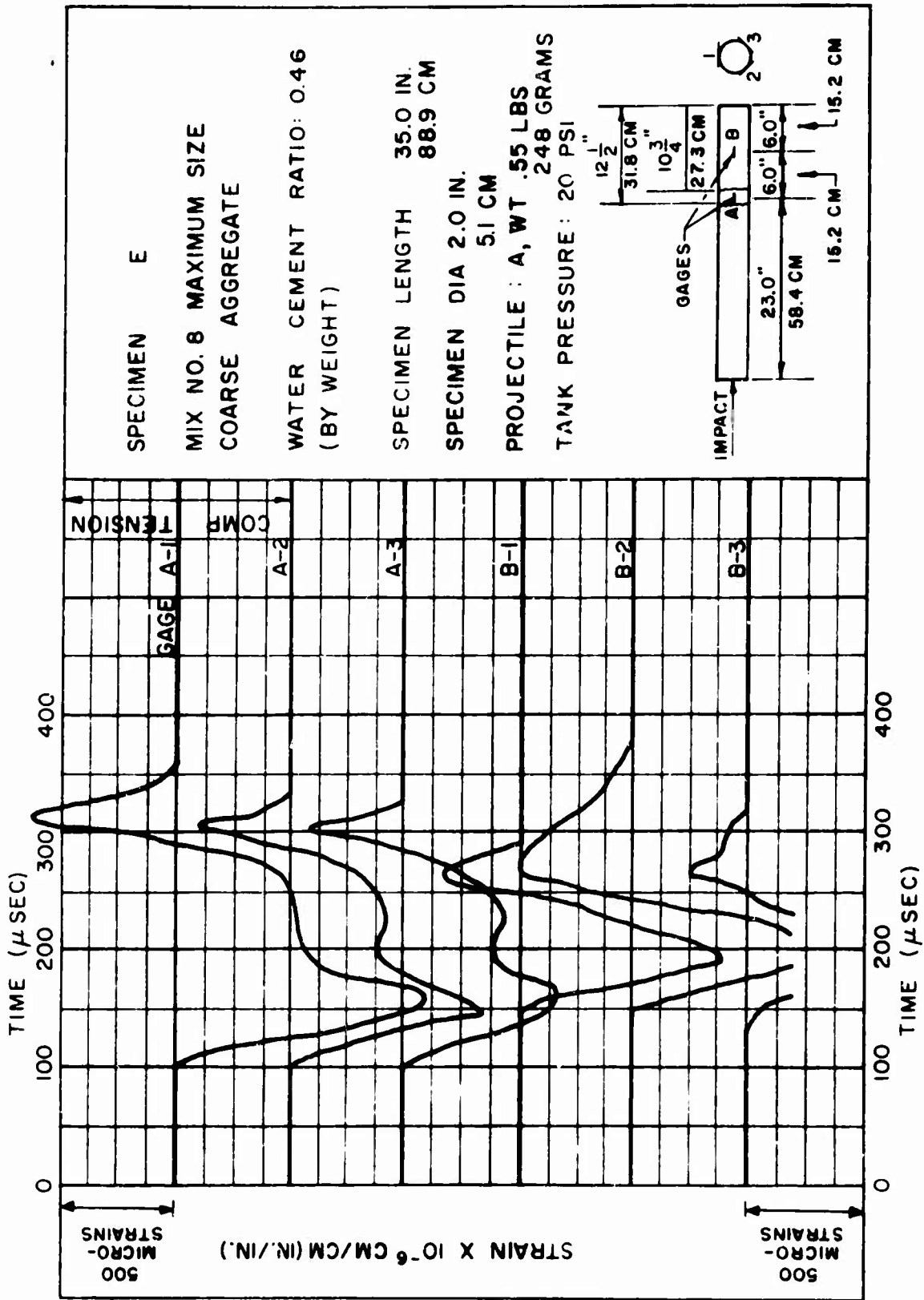


FIGURE 7





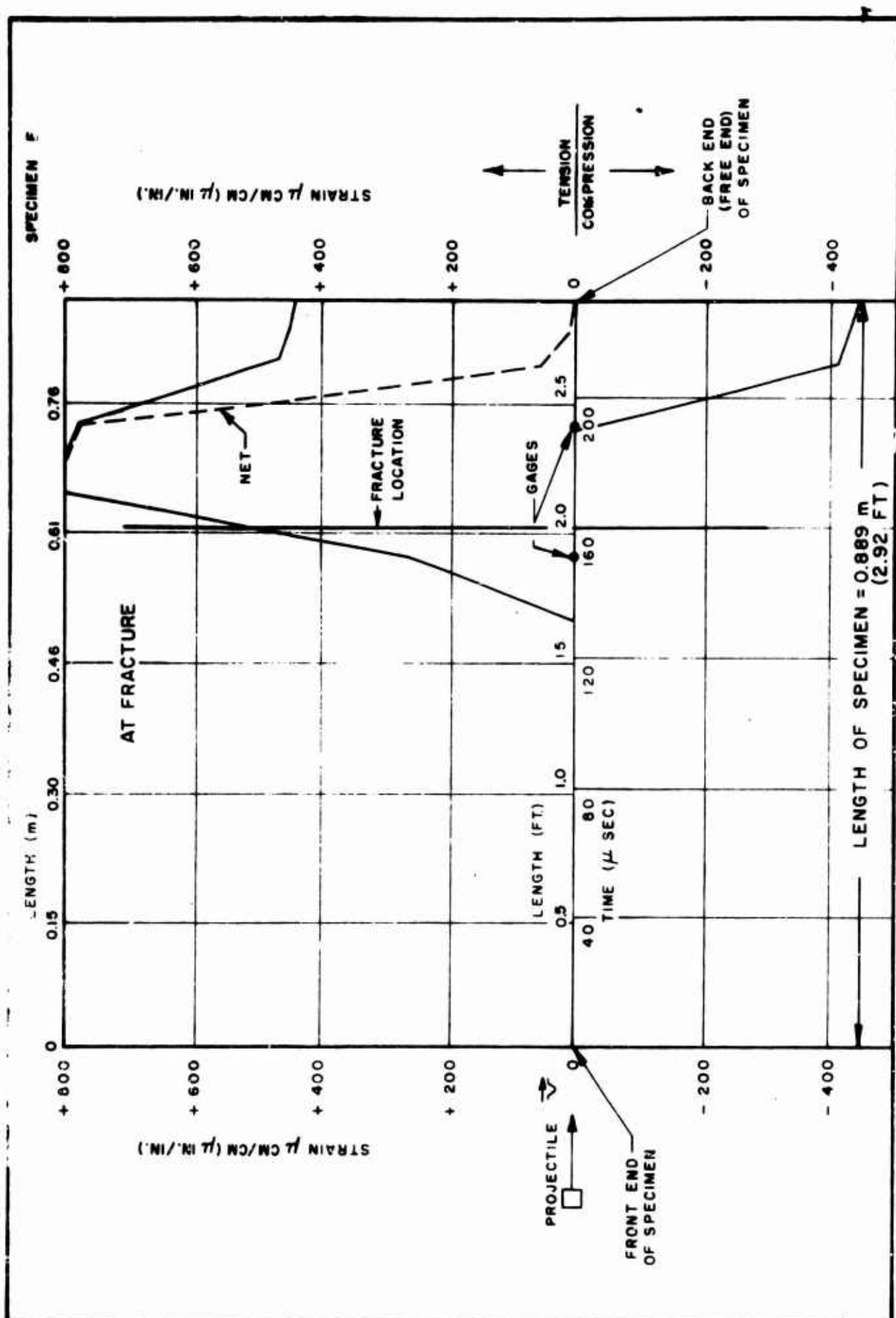


FIGURE 10

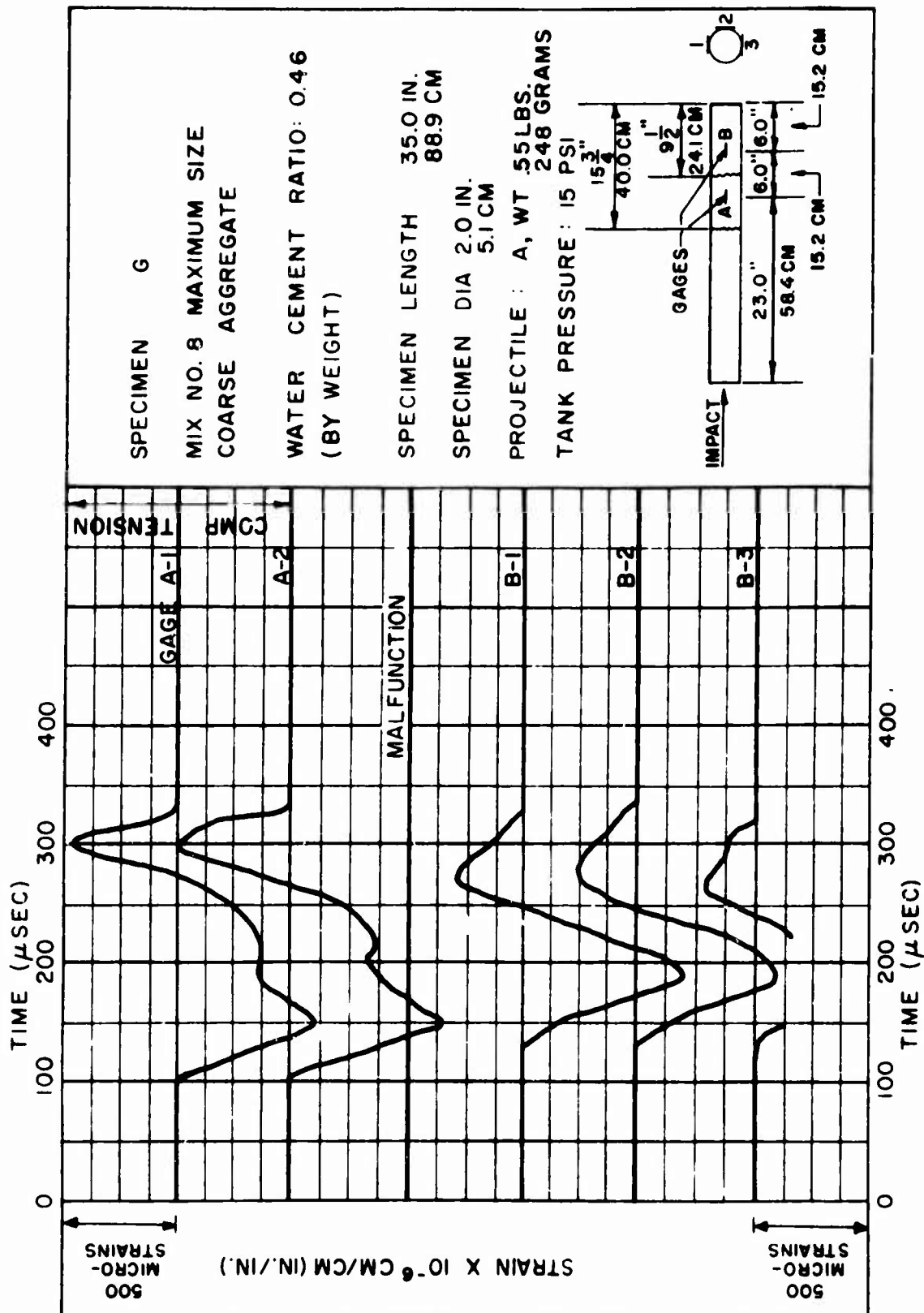


FIGURE II

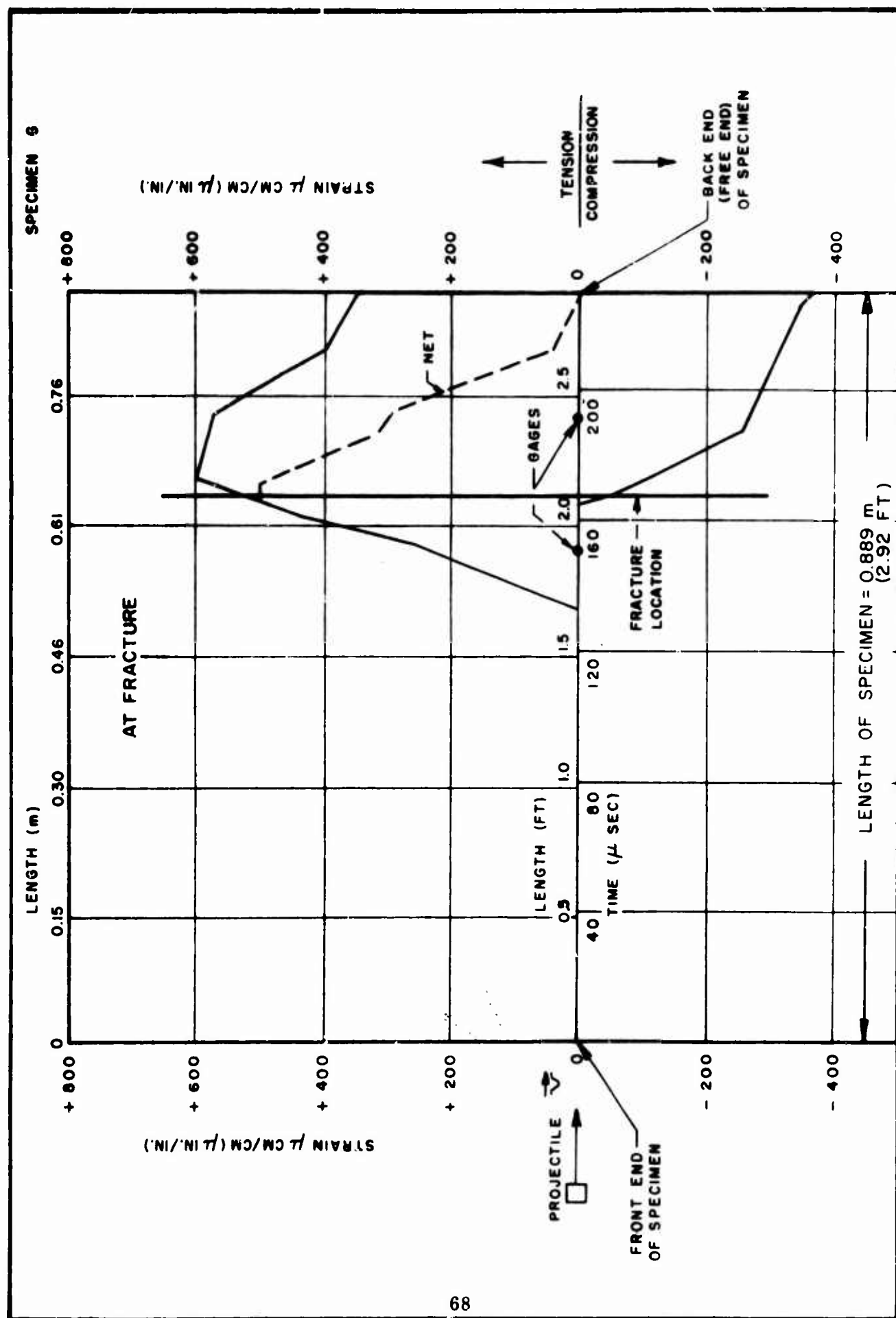


FIGURE 12

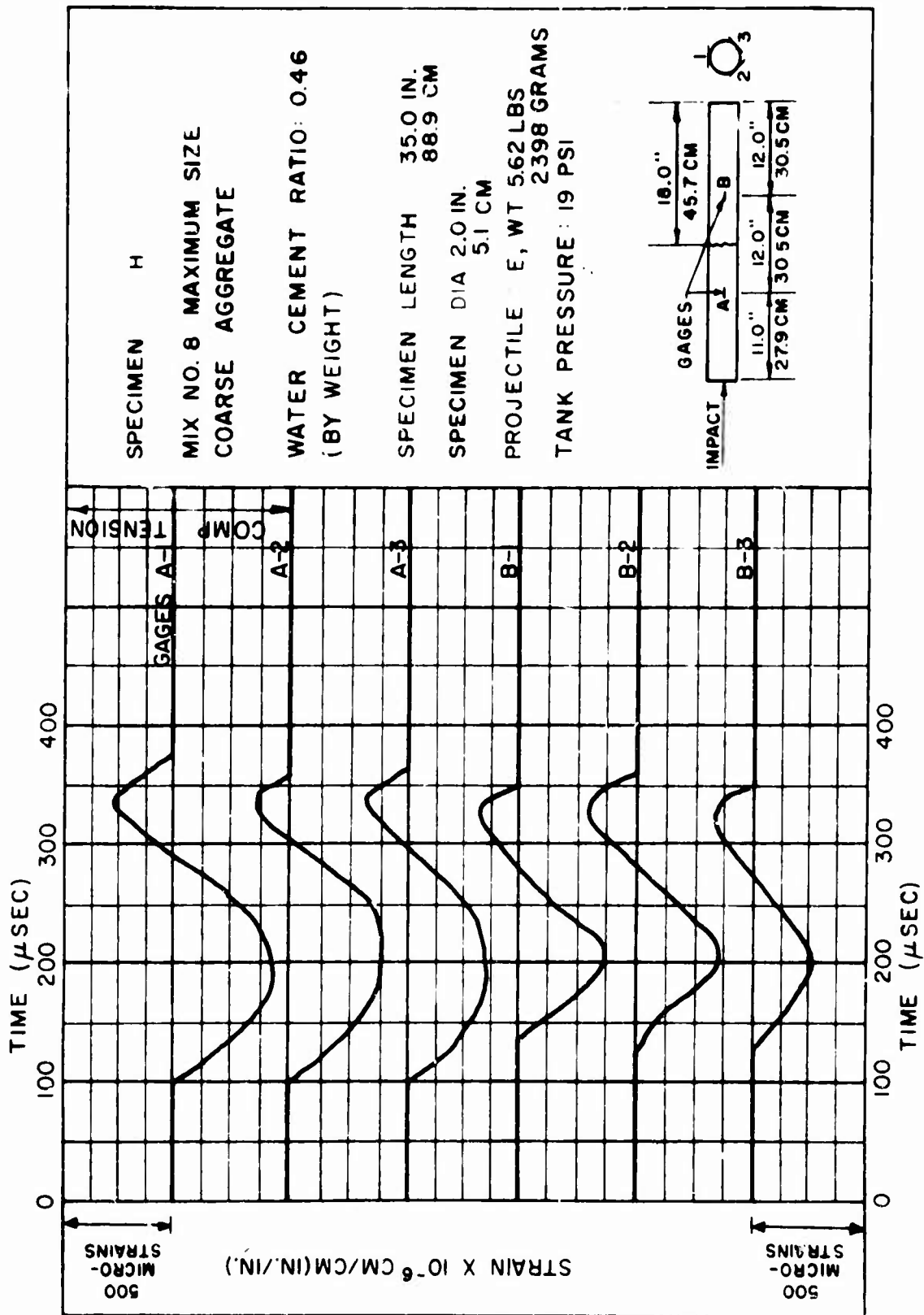
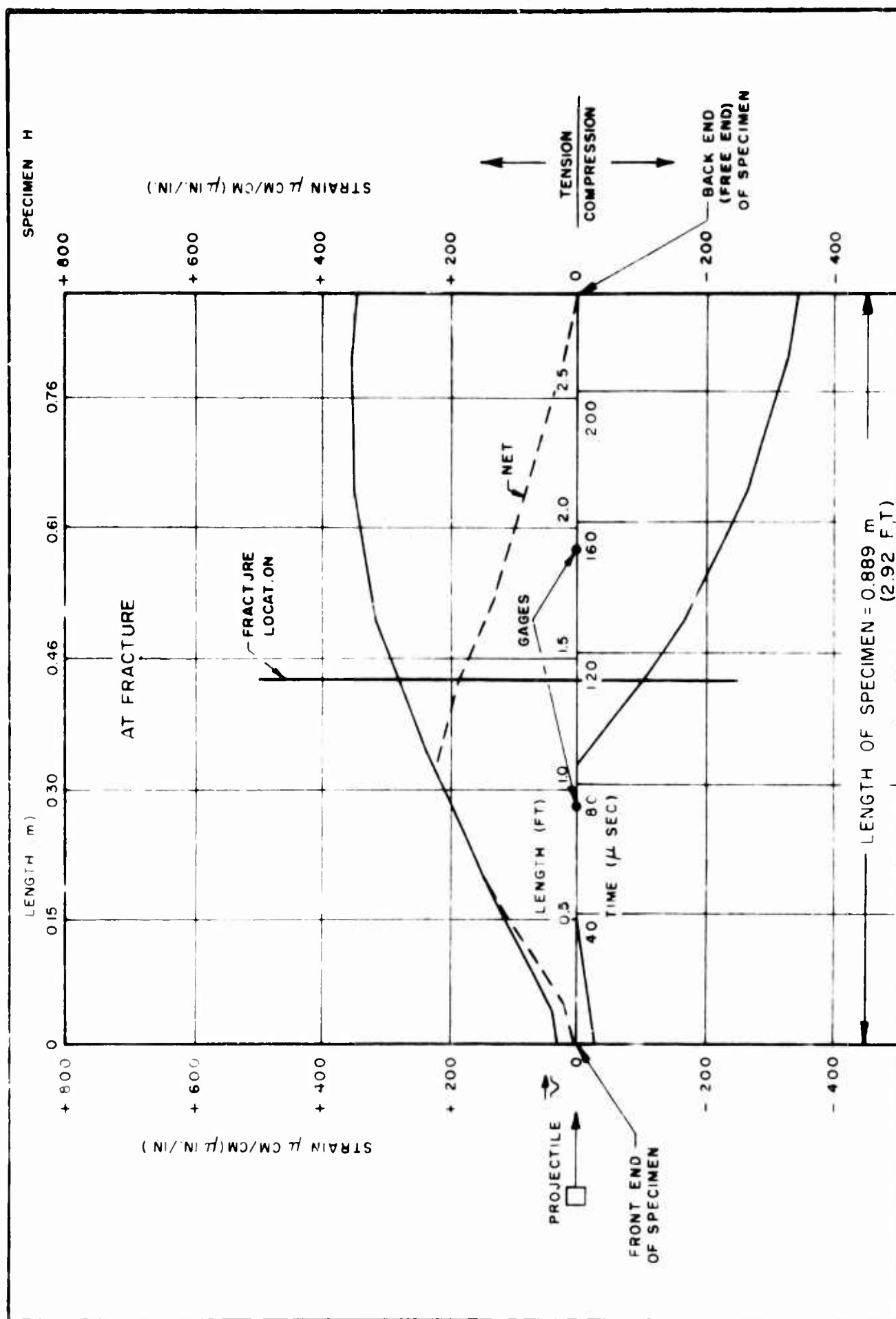


FIGURE 13



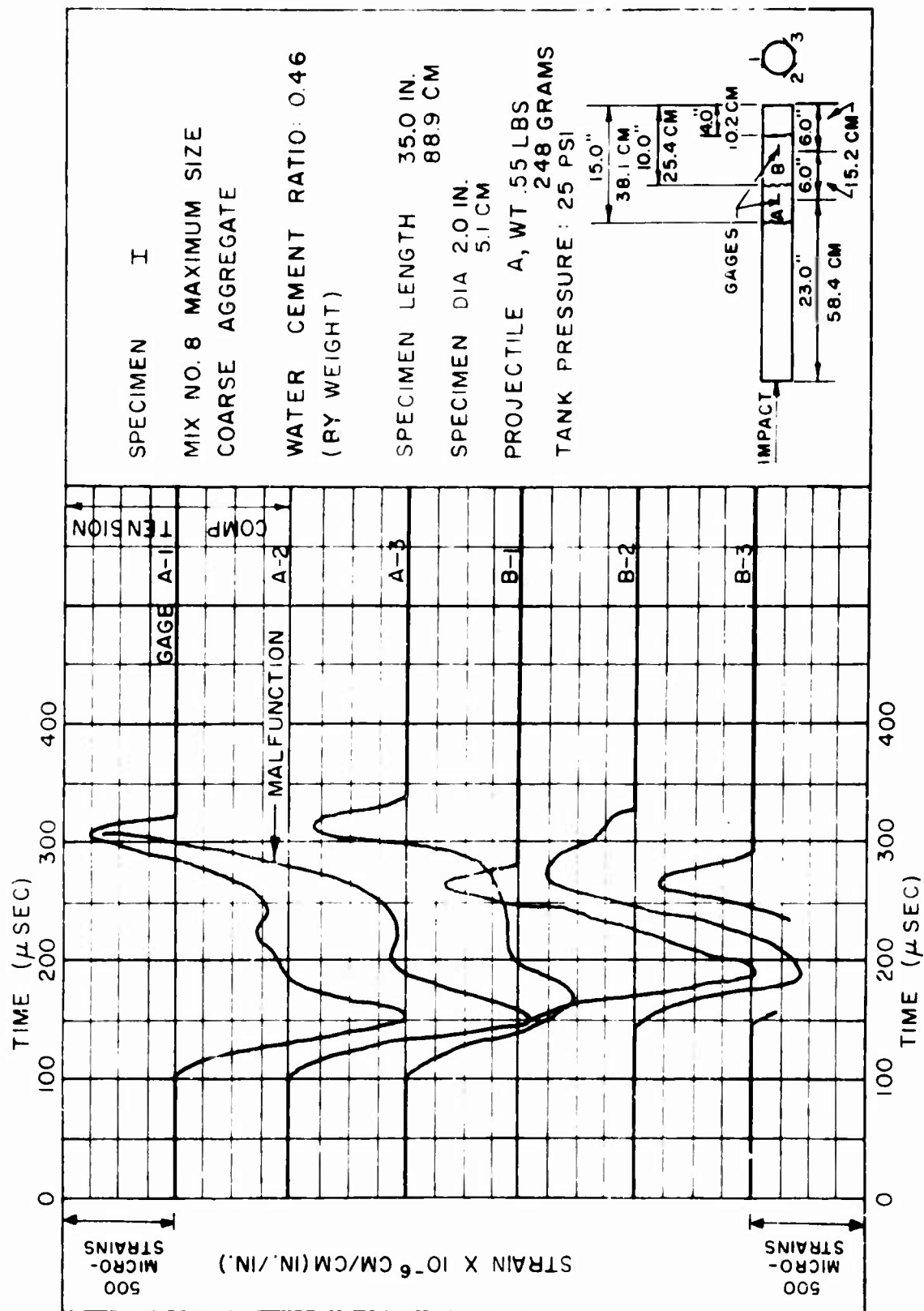
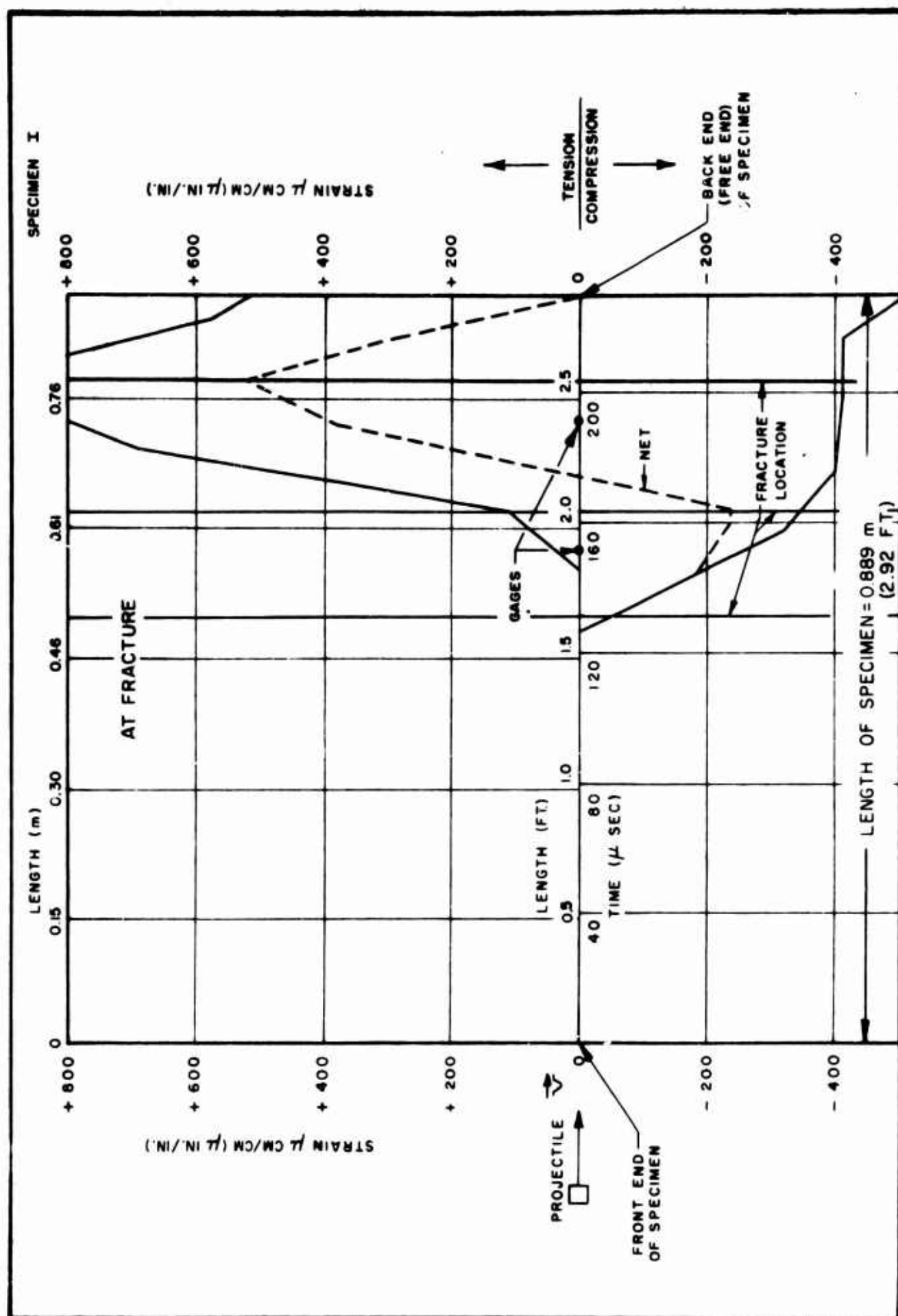


FIGURE 15



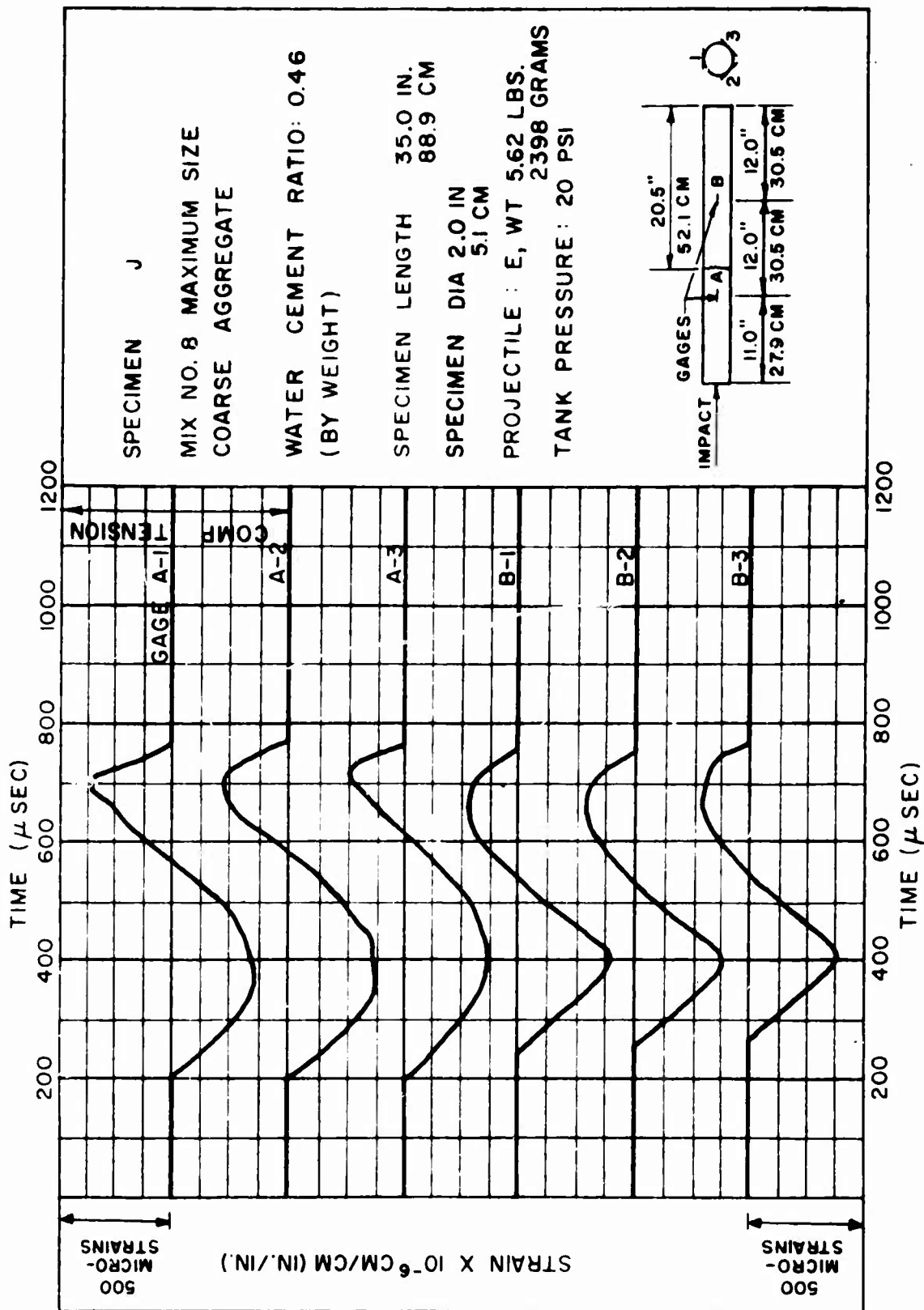
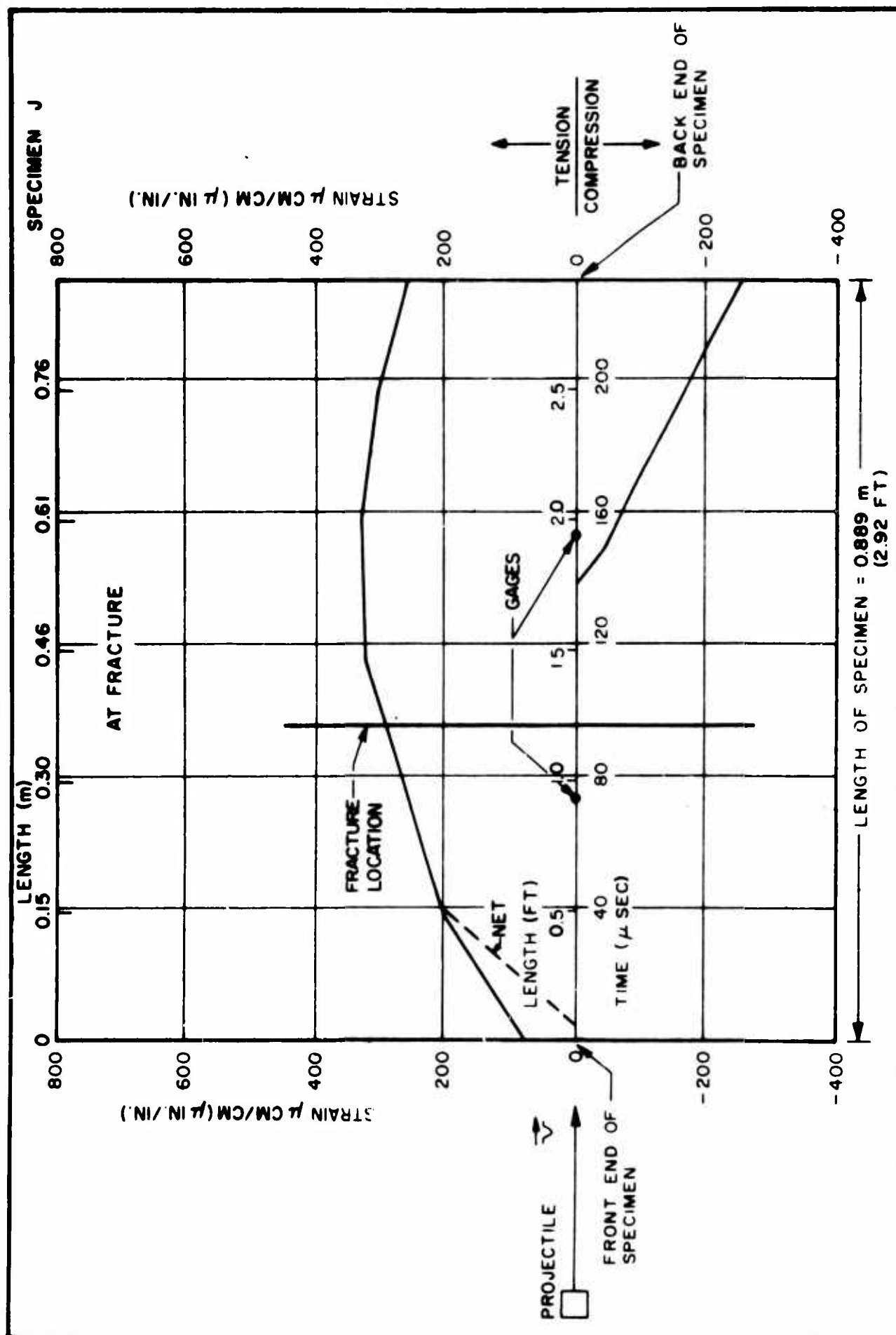


FIGURE 17



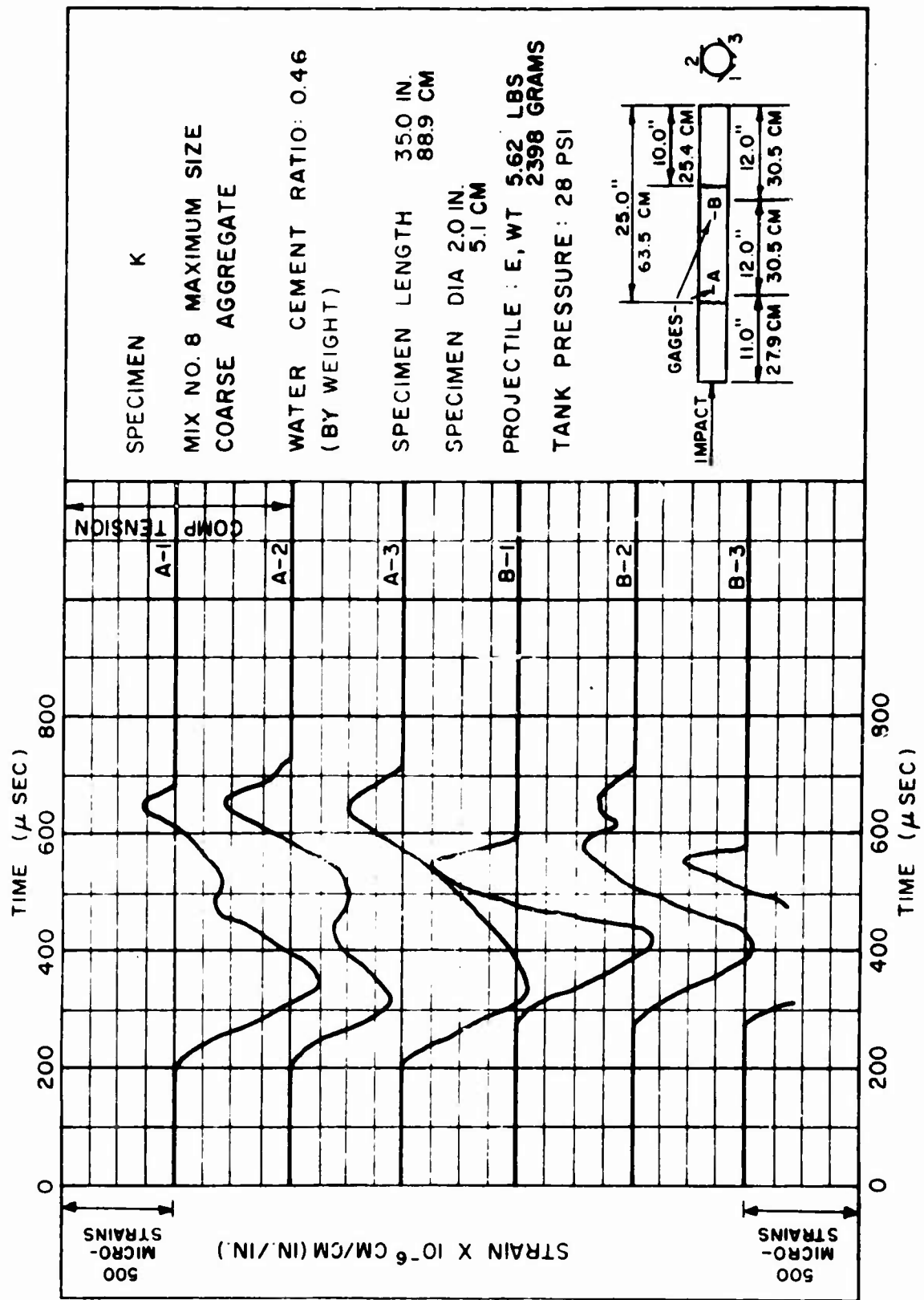
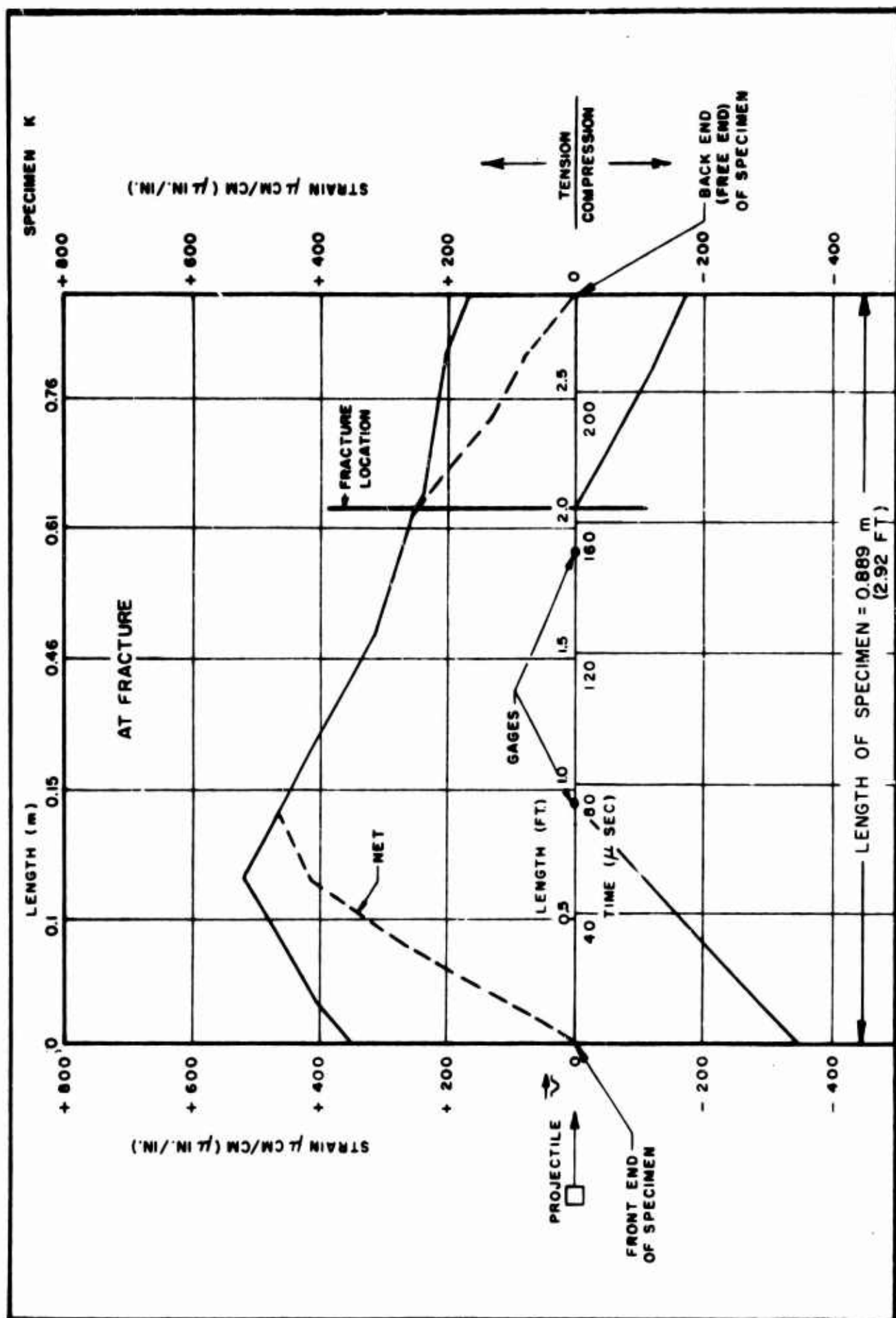
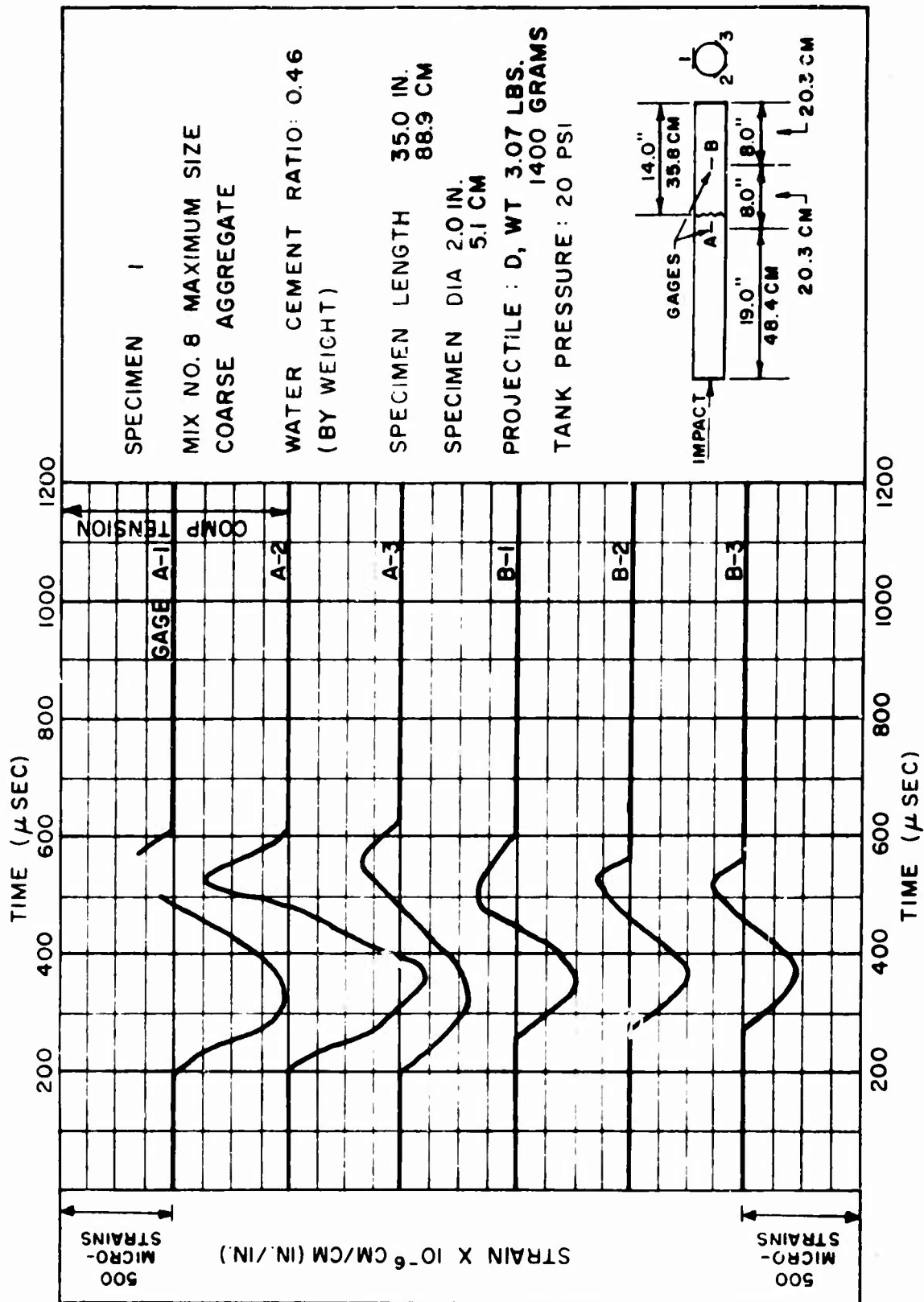
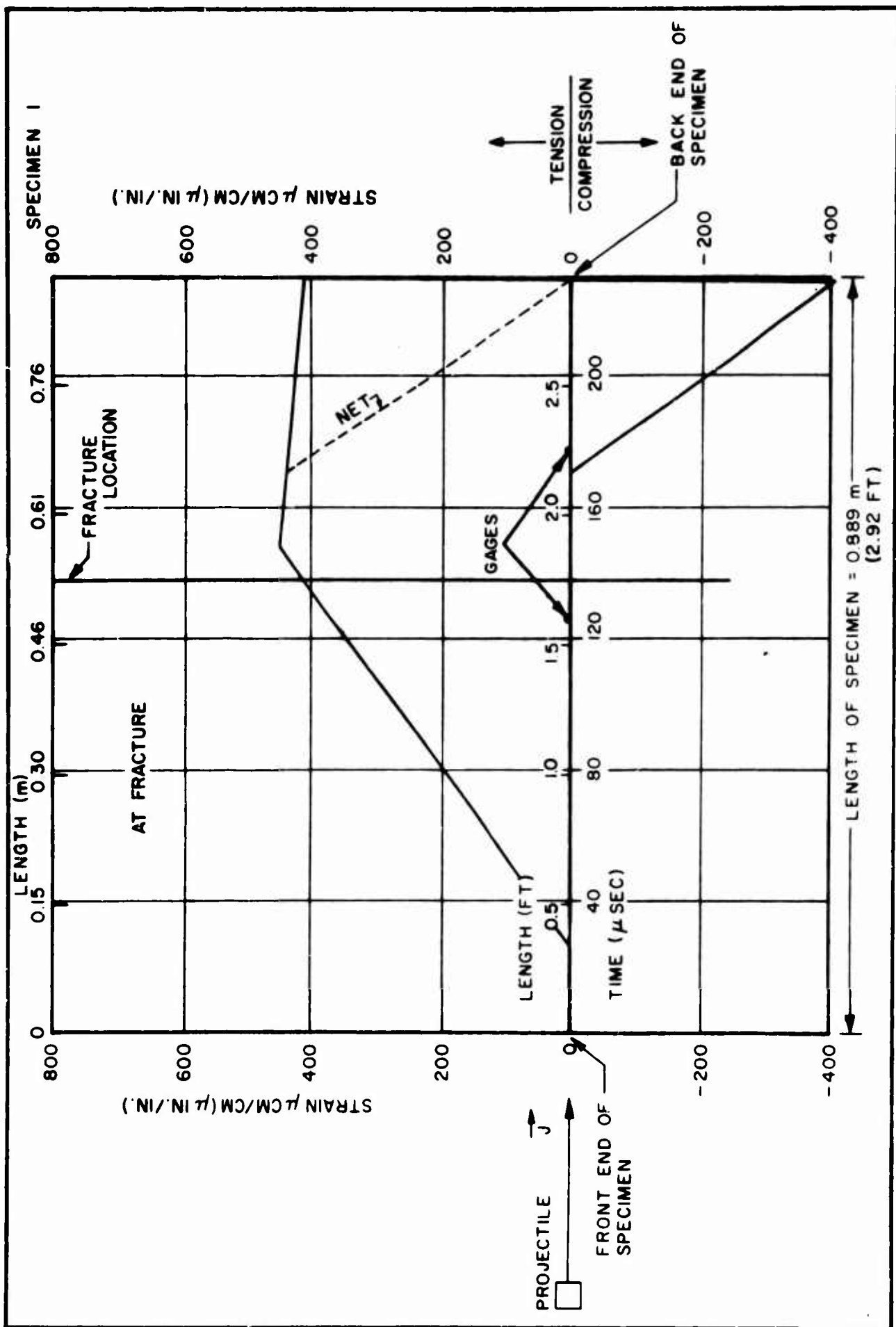
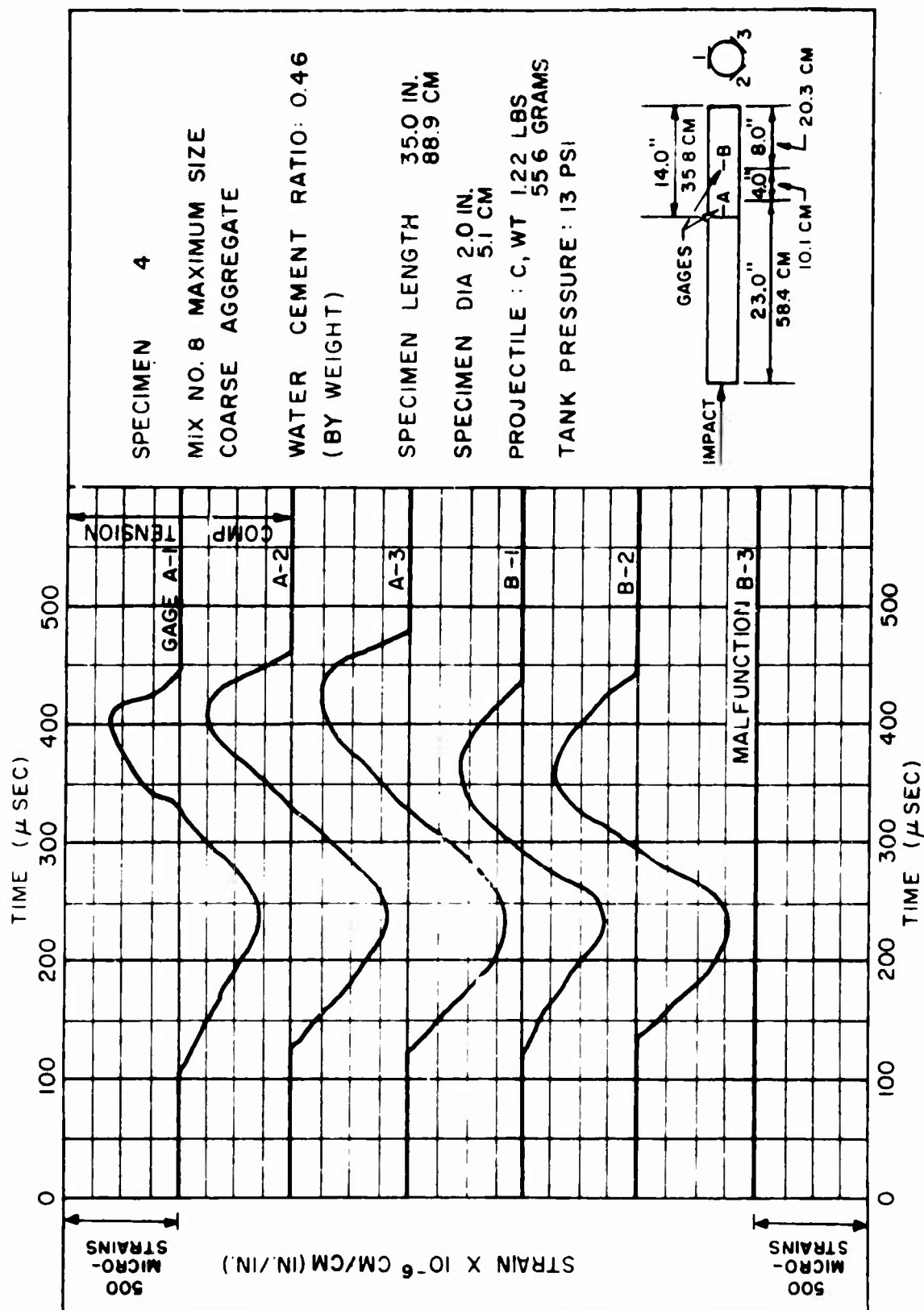


FIGURE 19









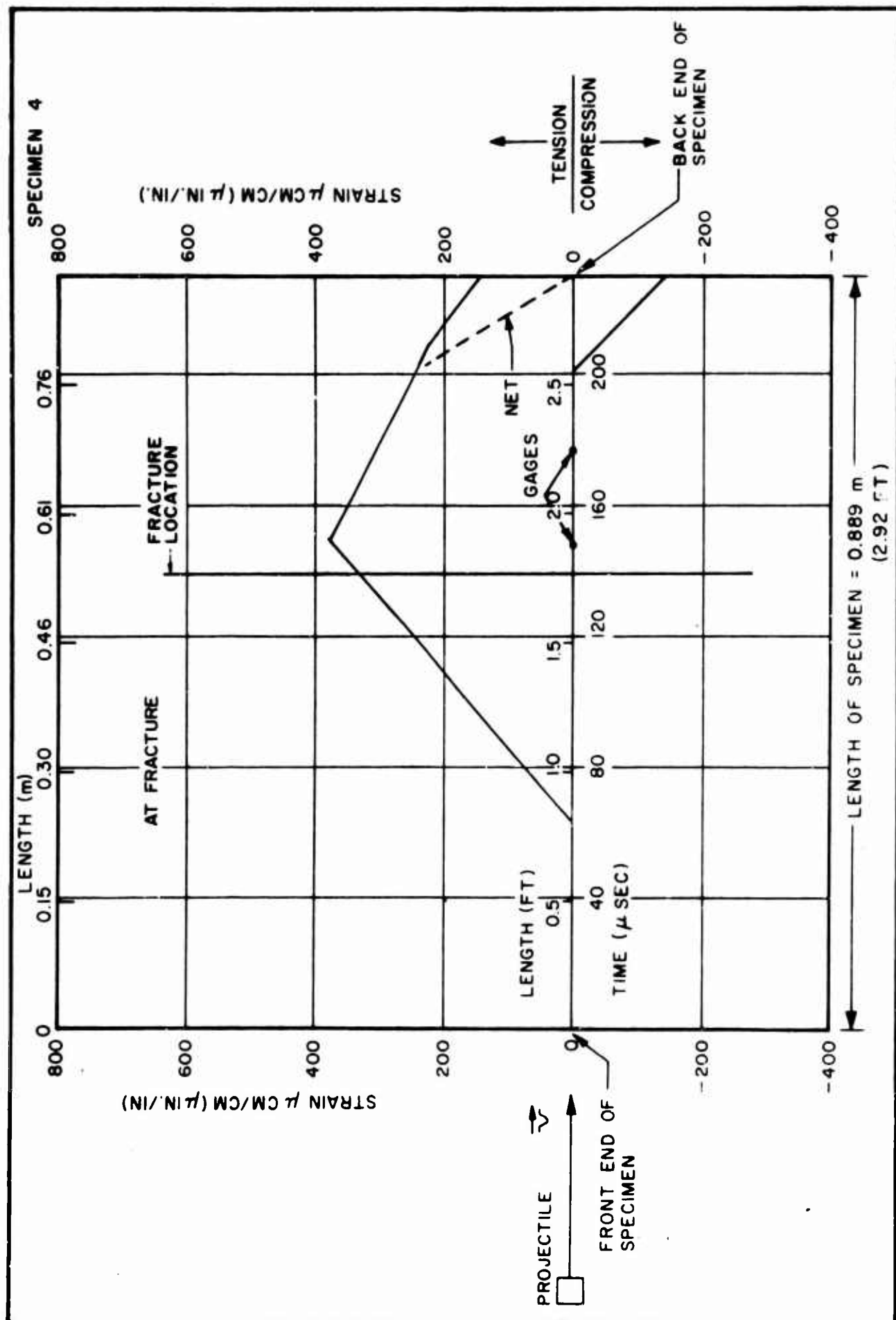
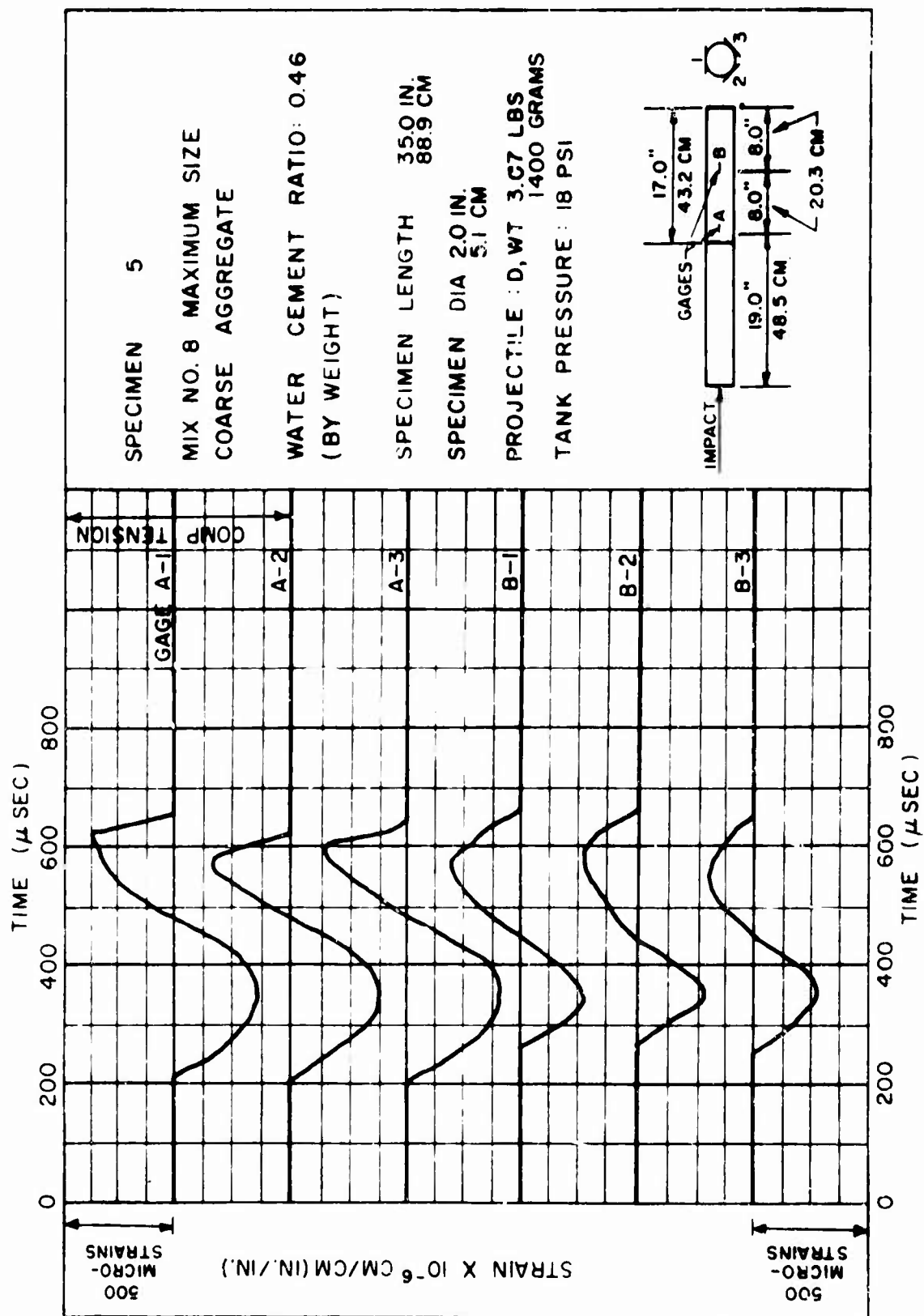
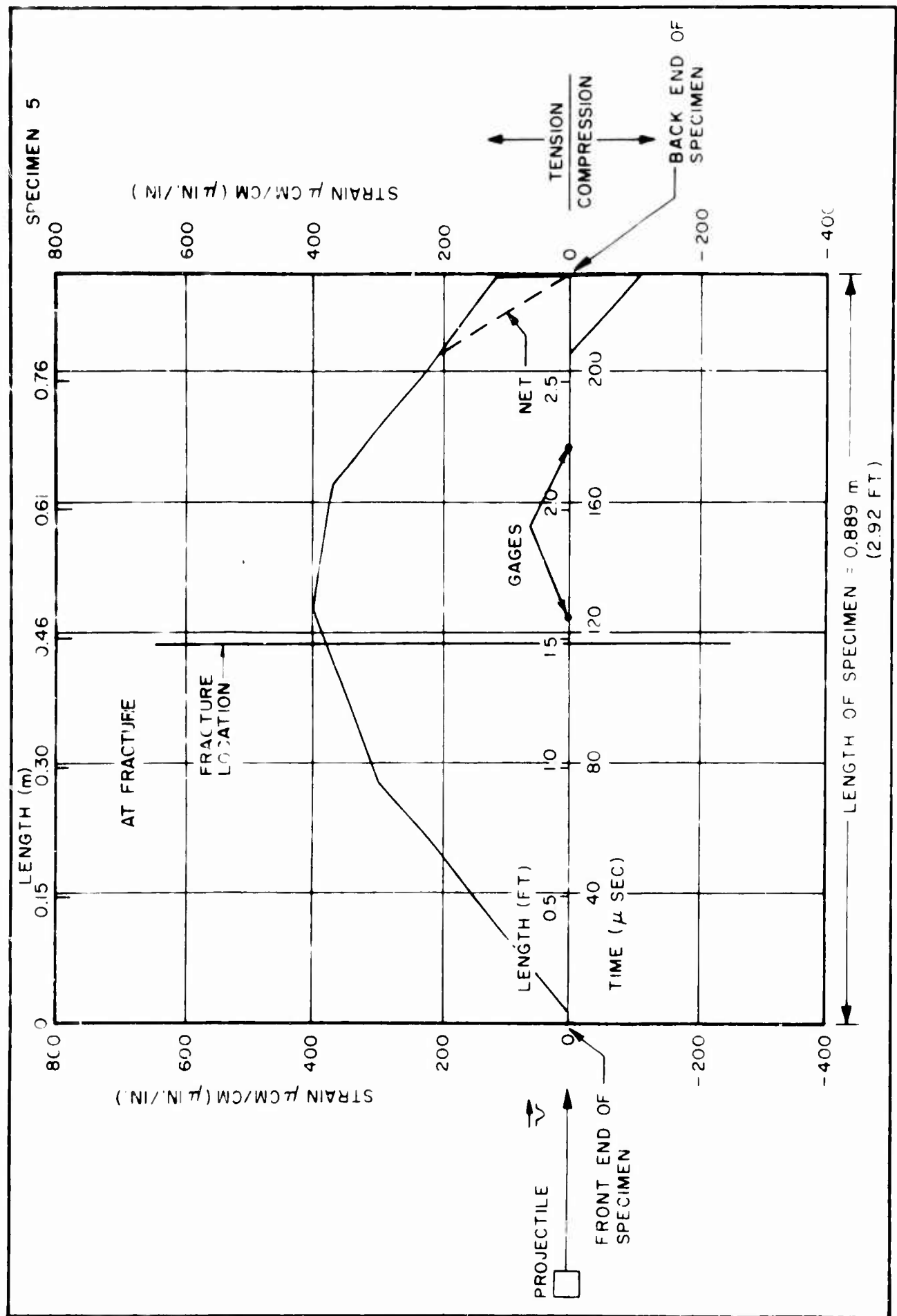
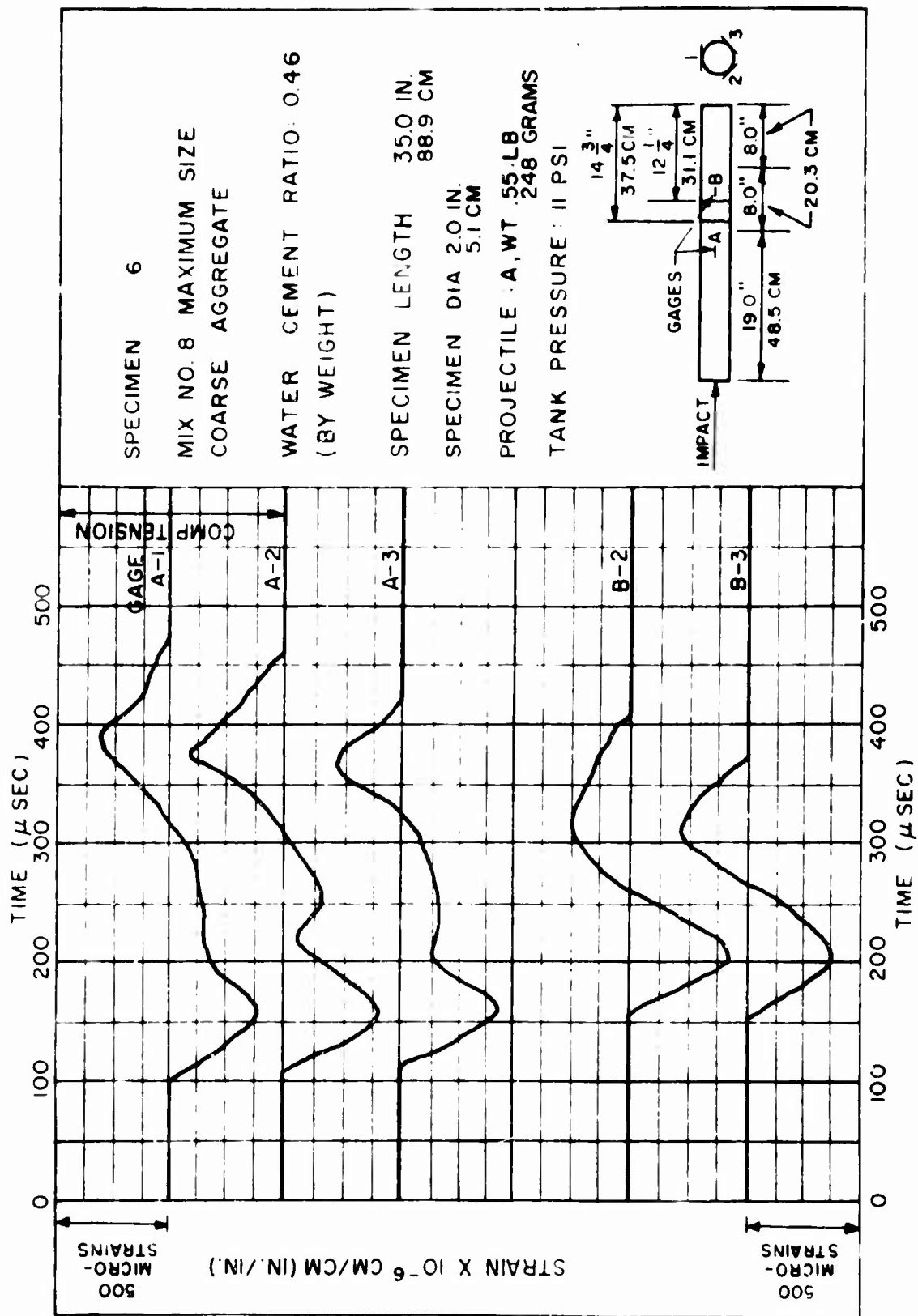


FIGURE 24







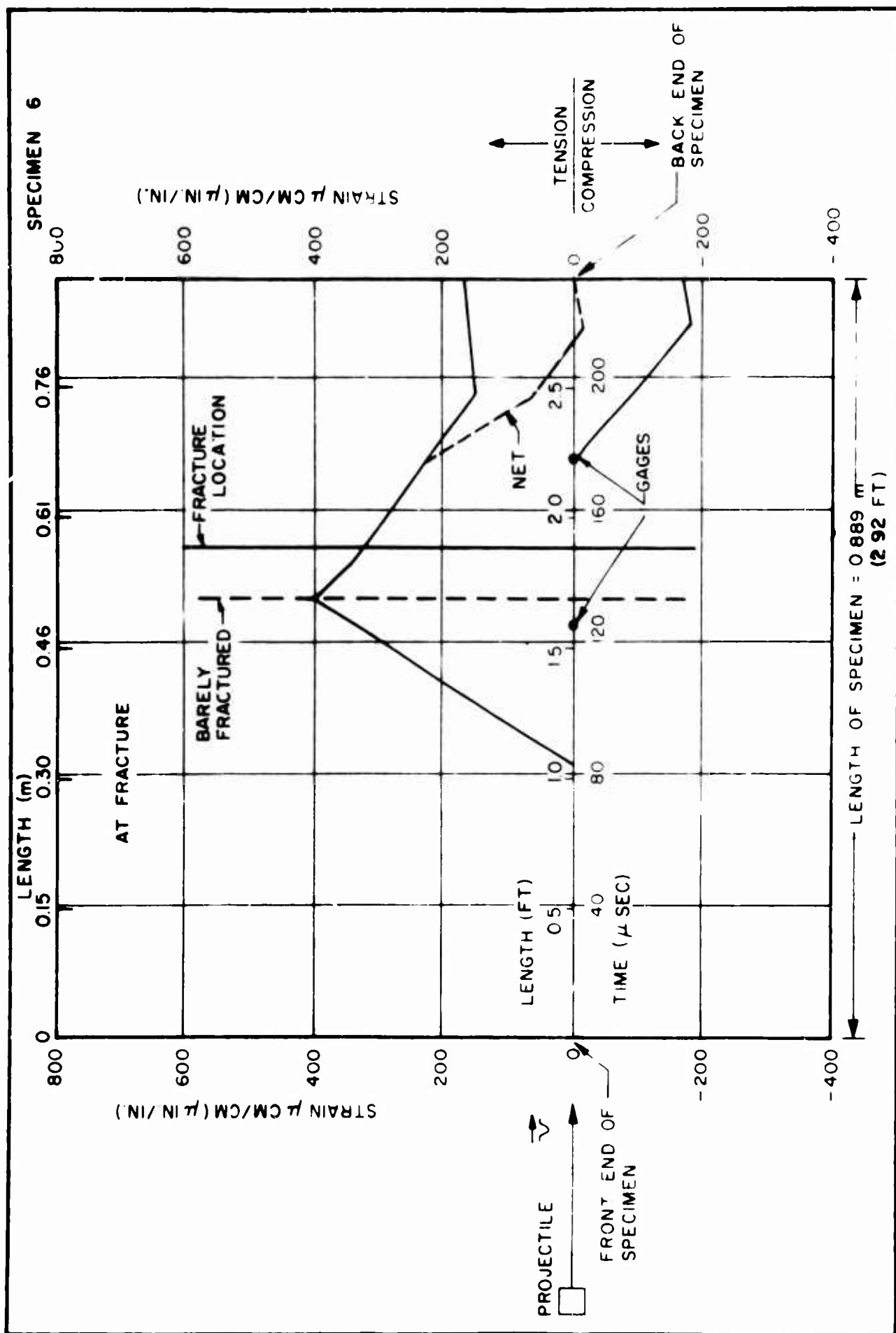
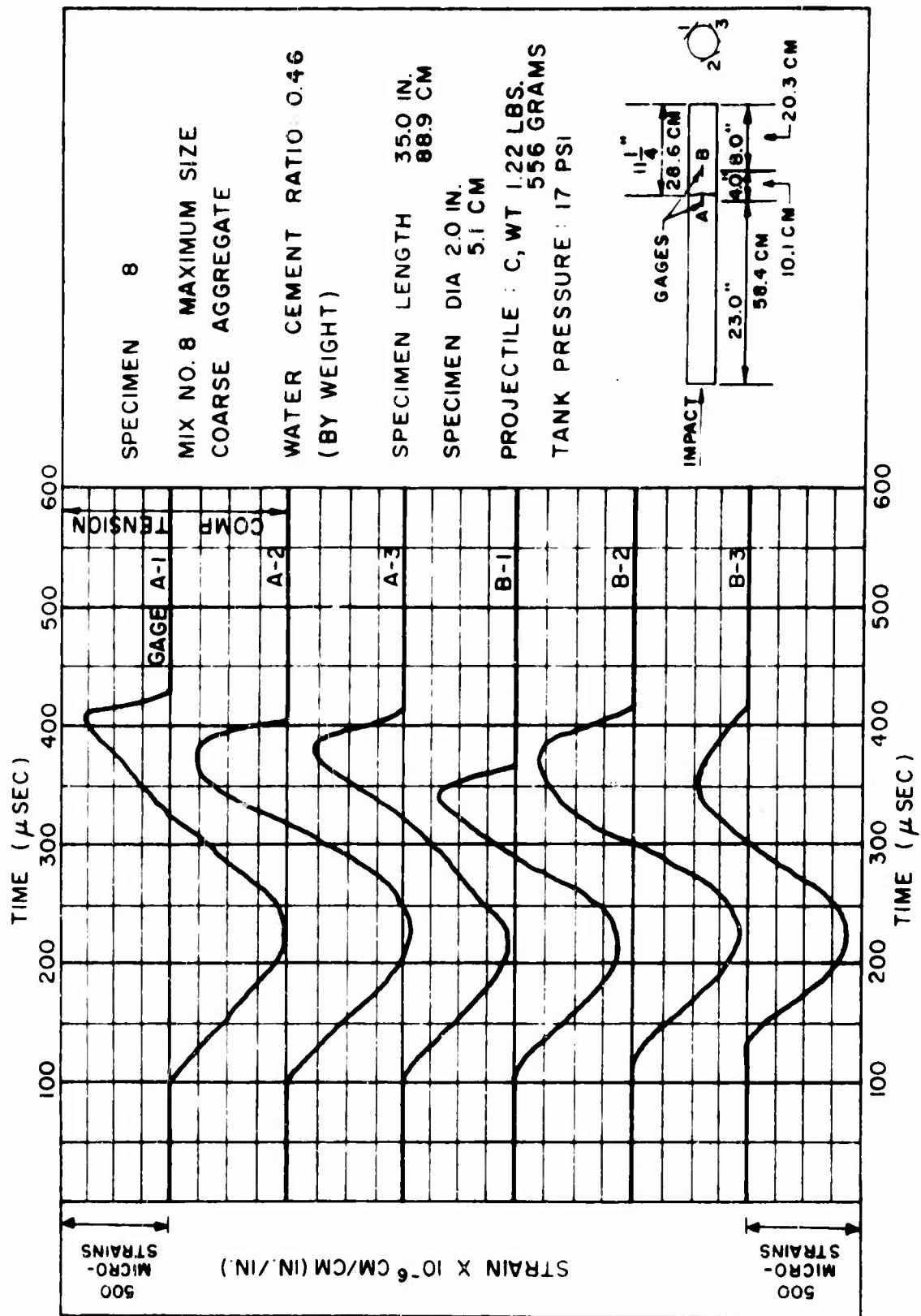


FIGURE 28



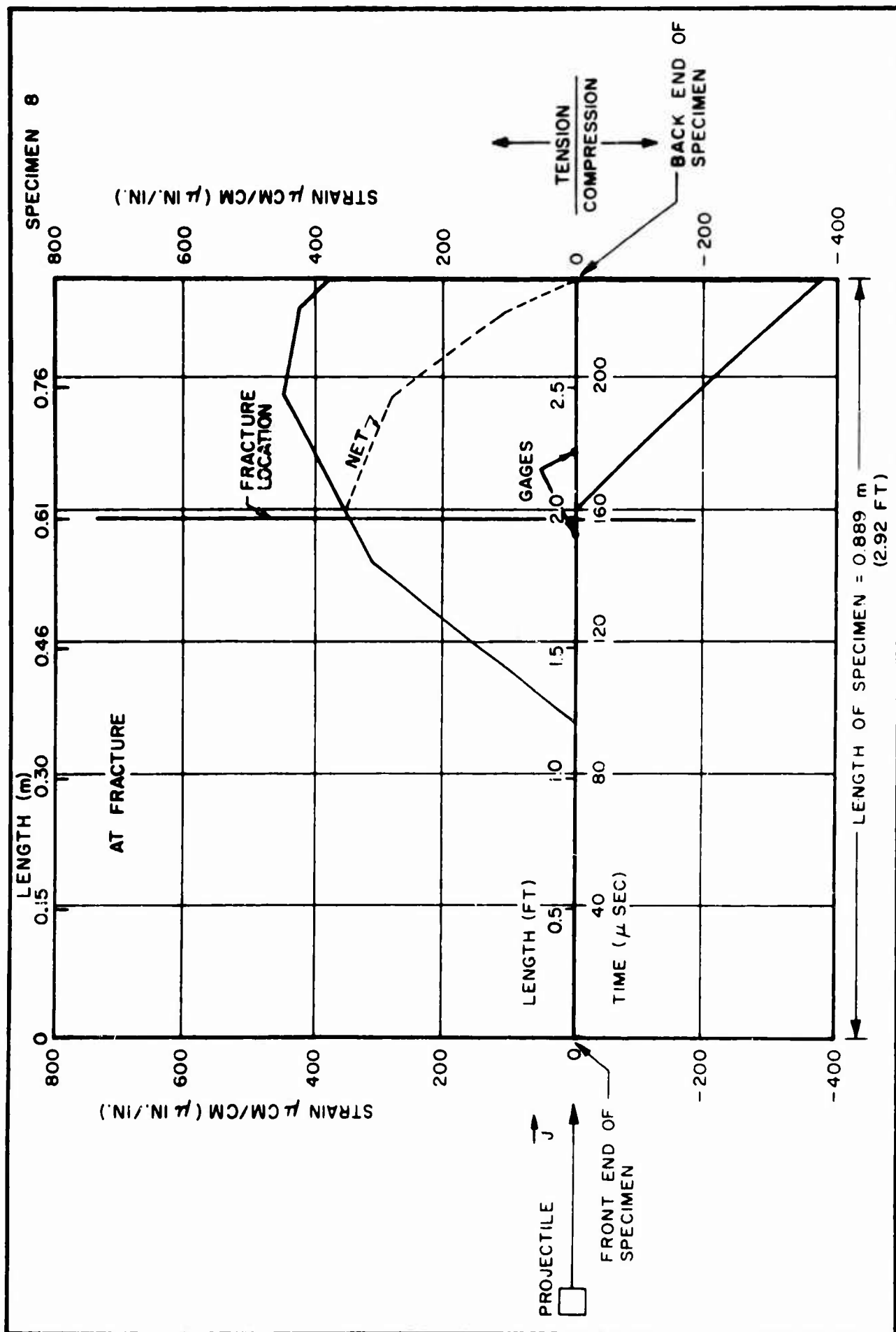
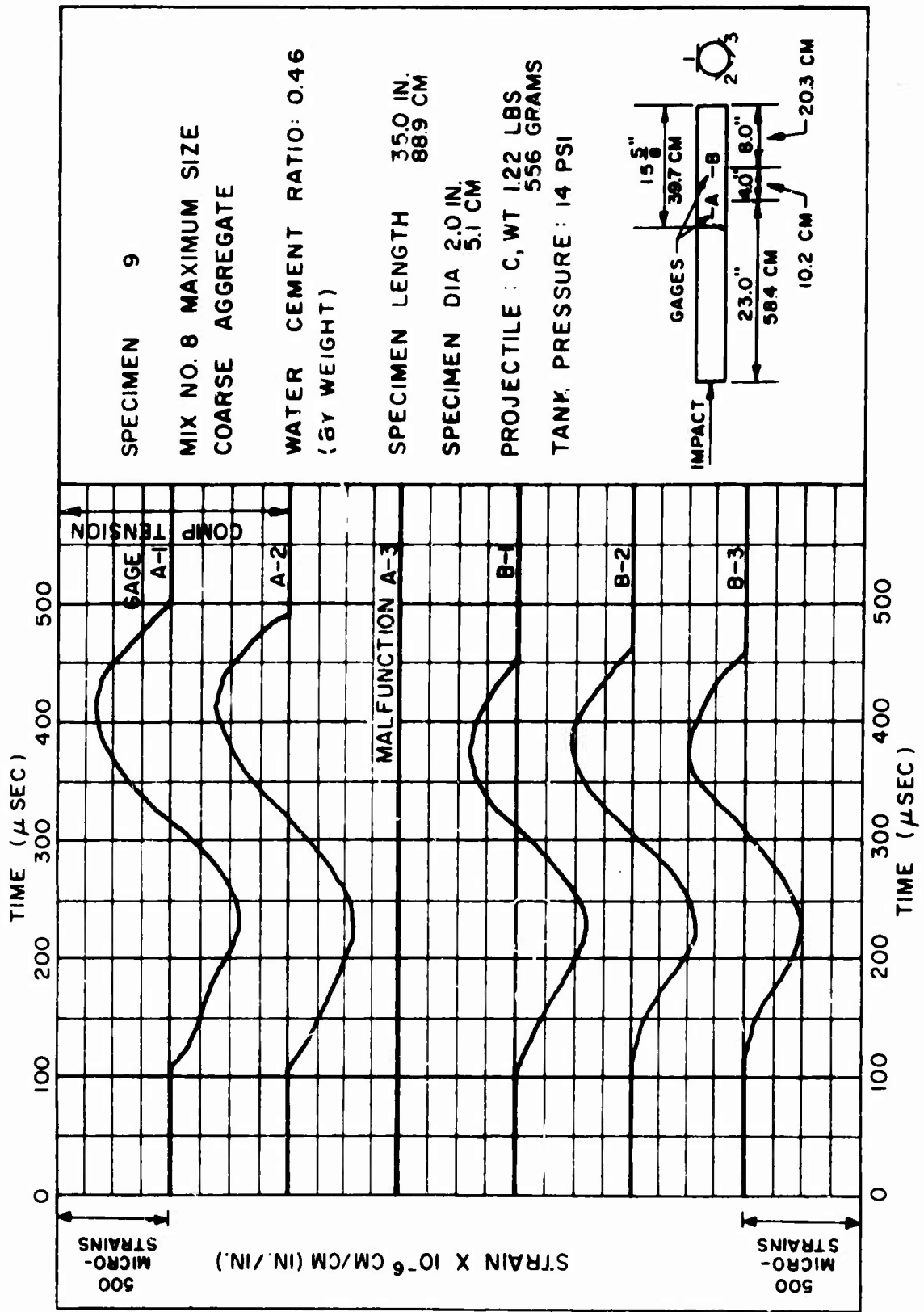


FIGURE 30



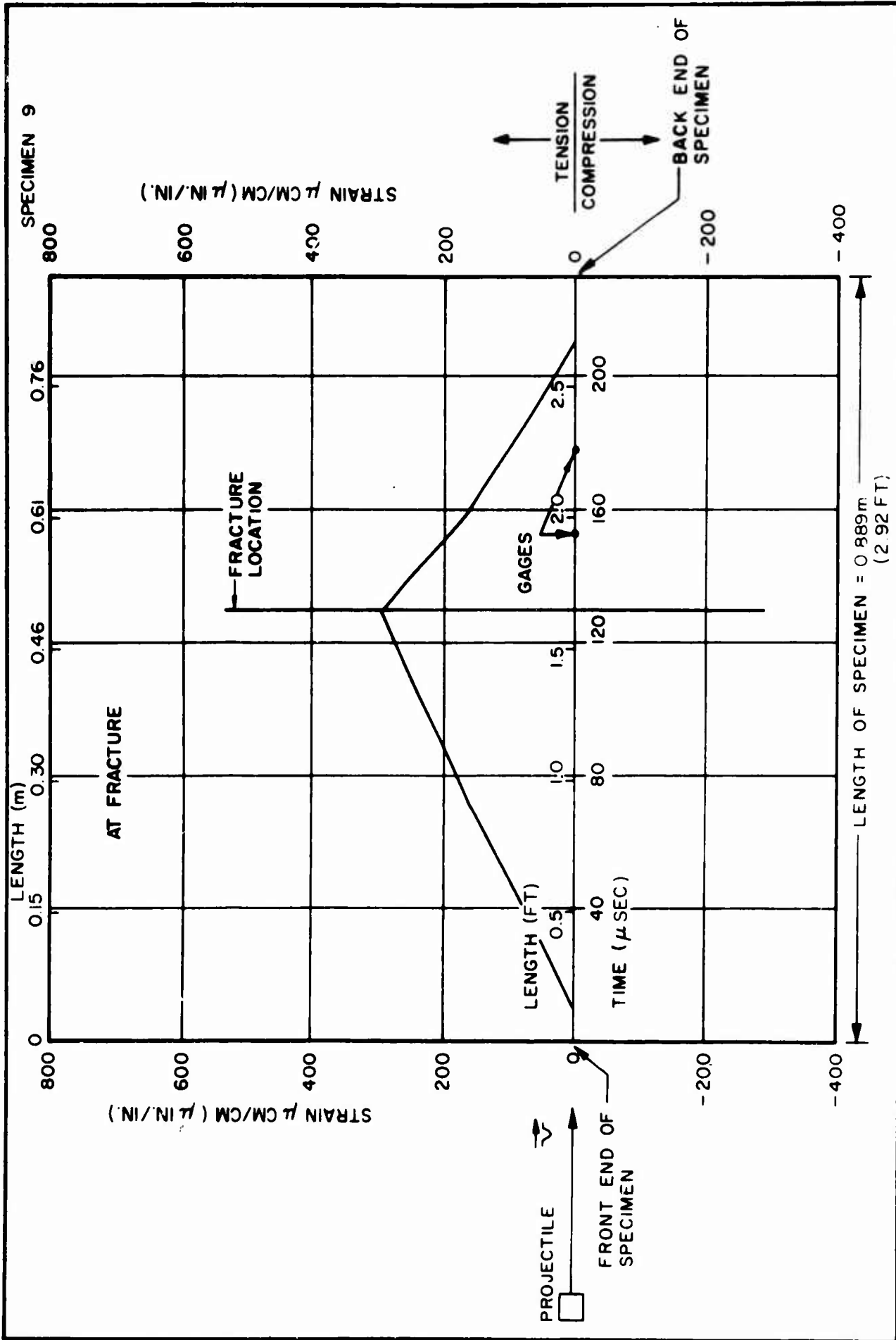


FIGURE 32

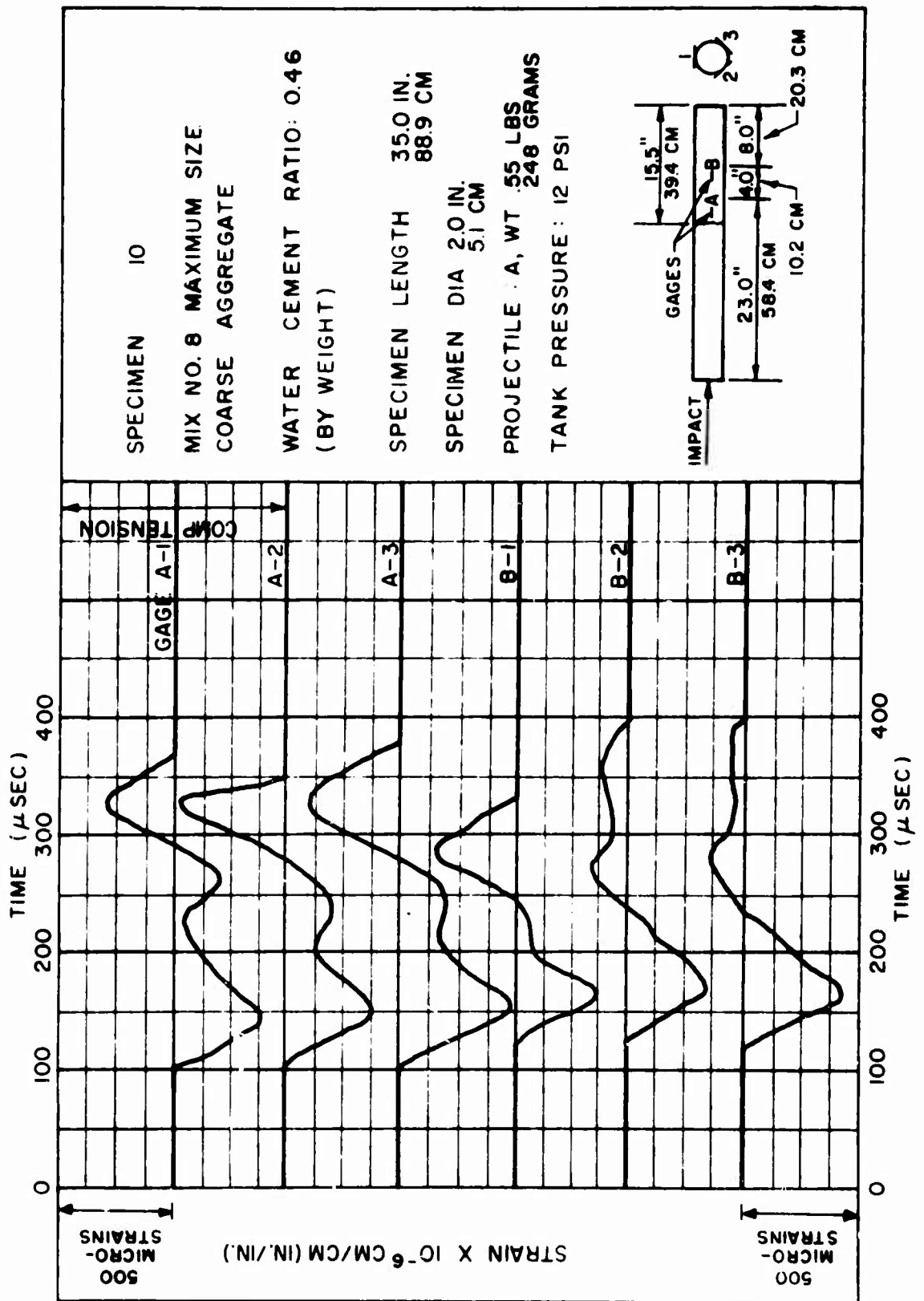
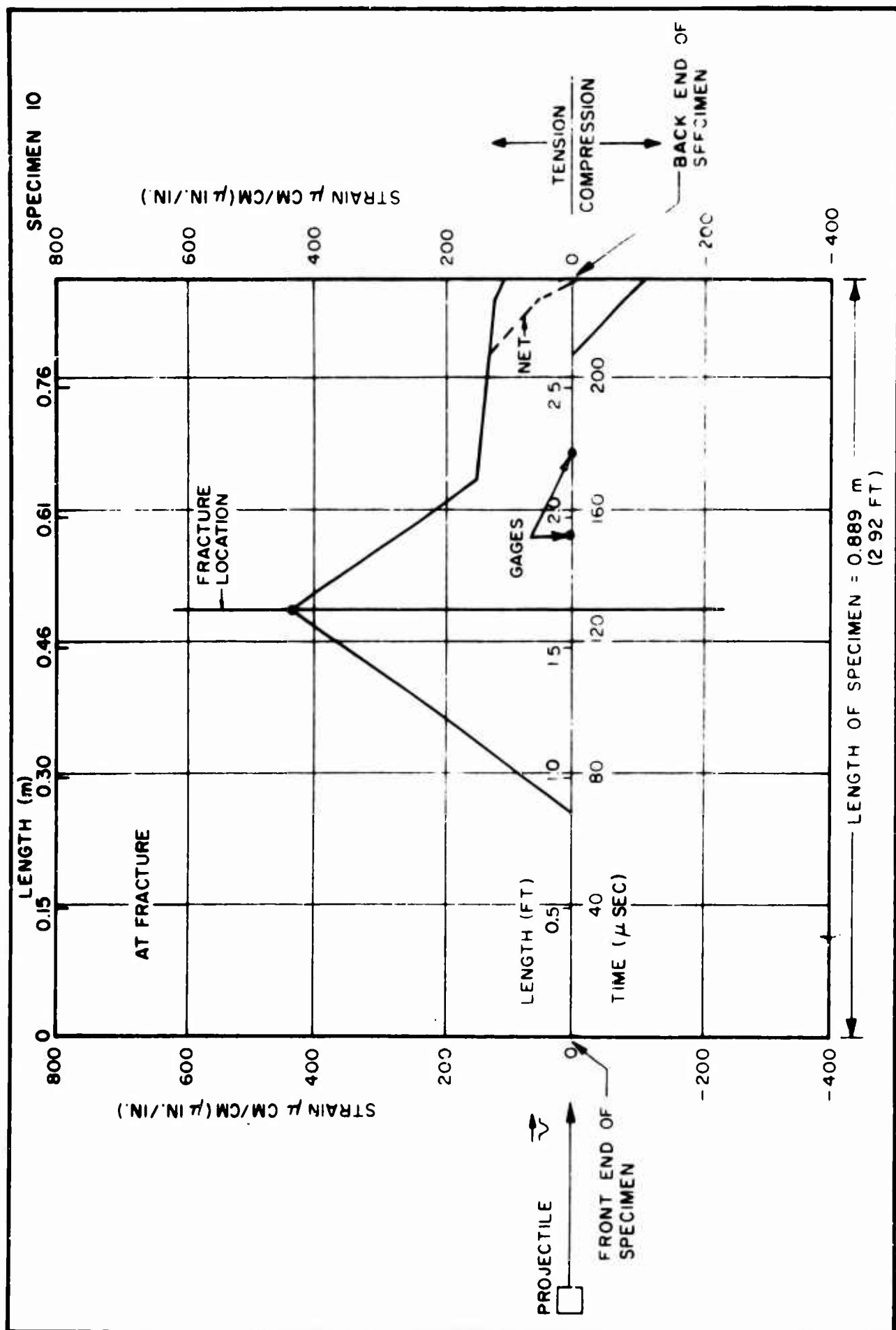


FIGURE 33



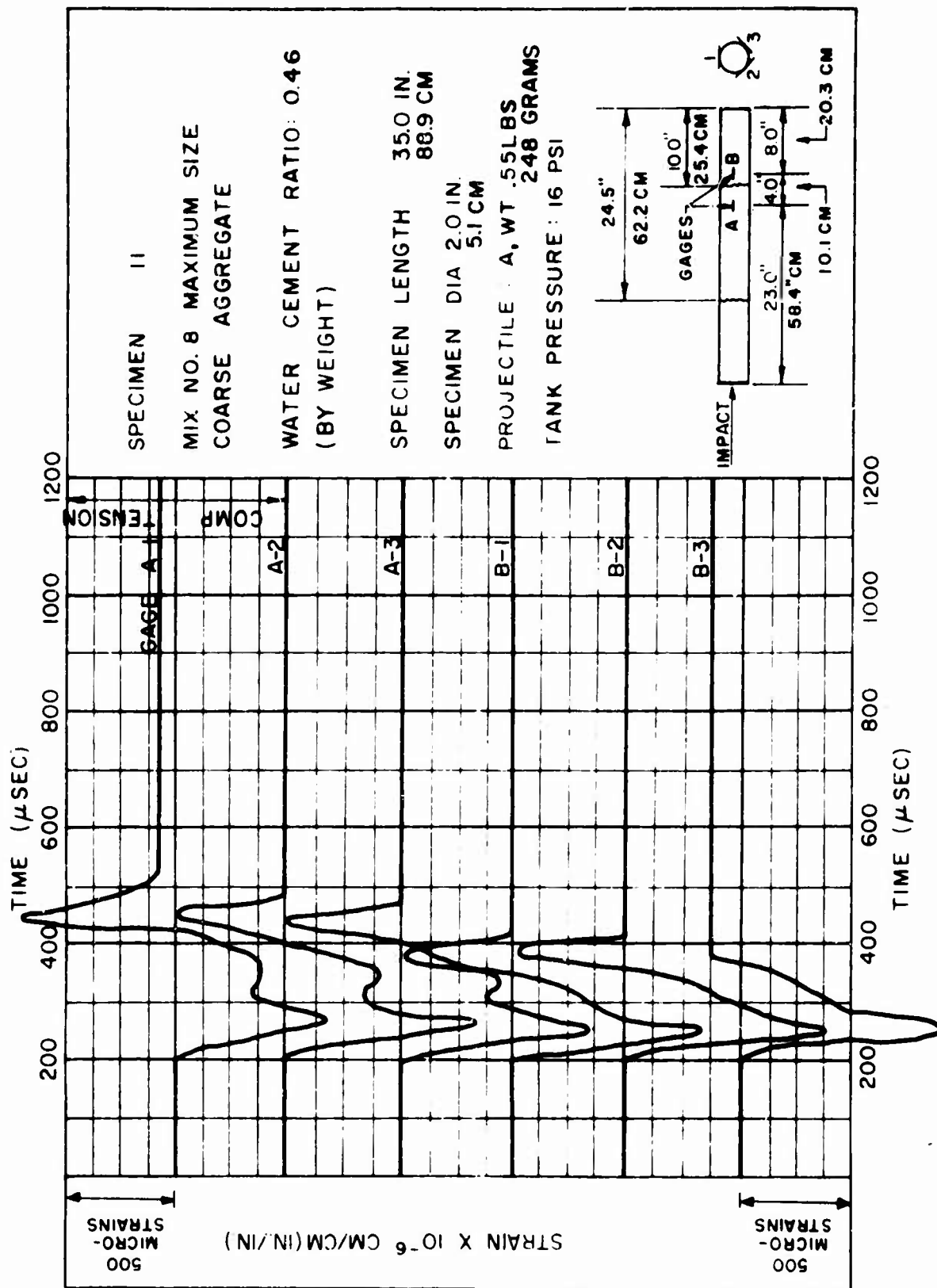
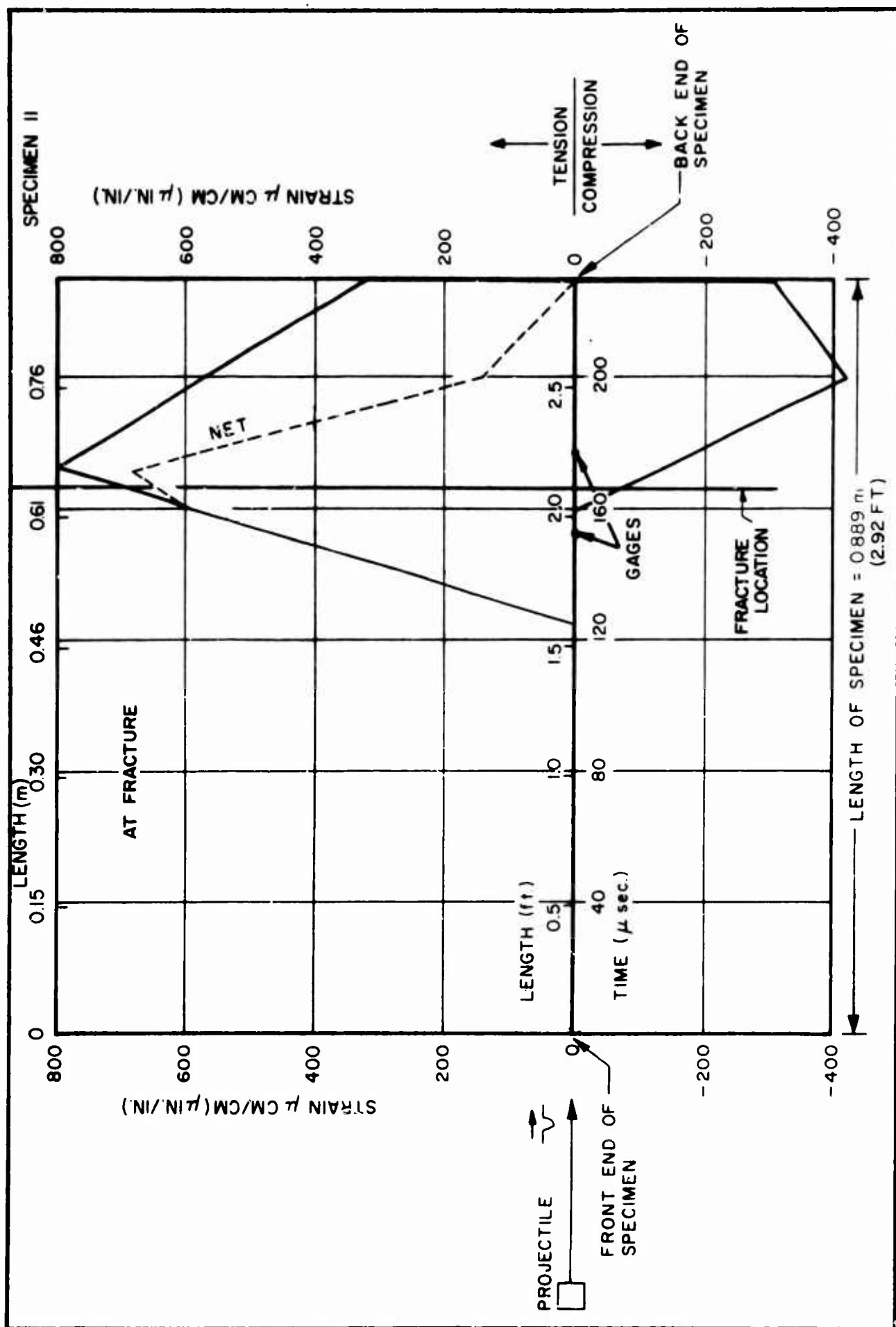
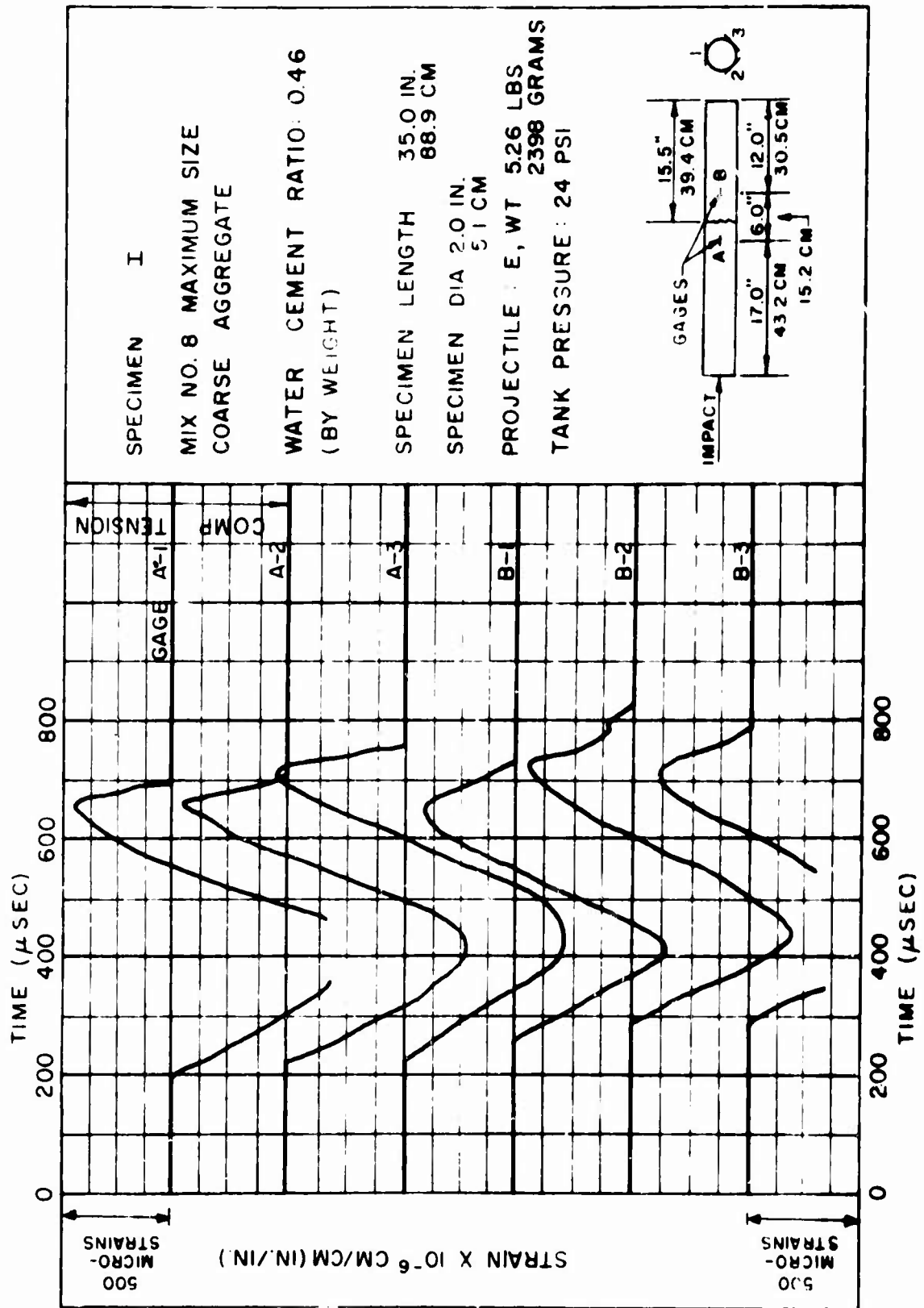


FIGURE 35





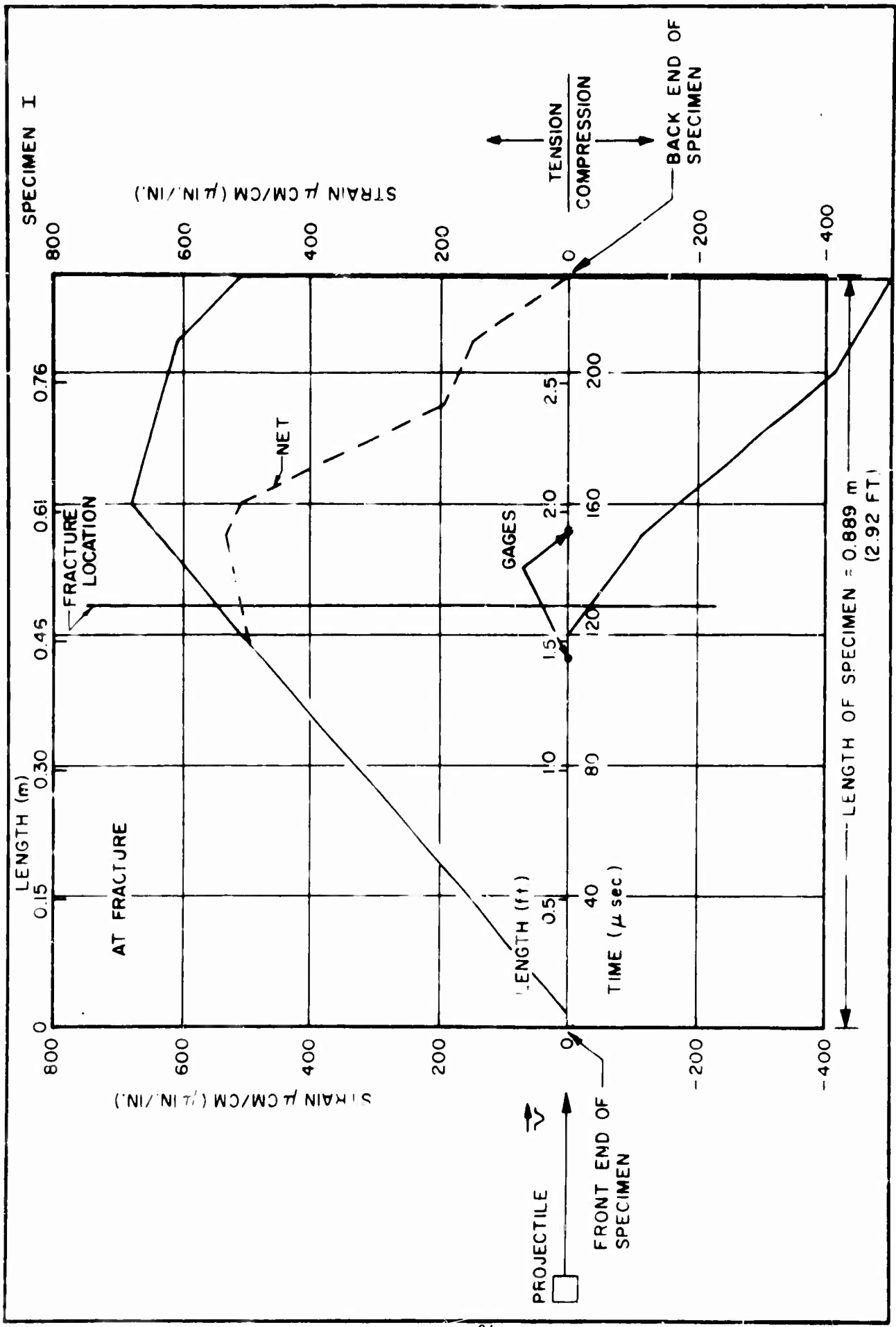


FIGURE 38

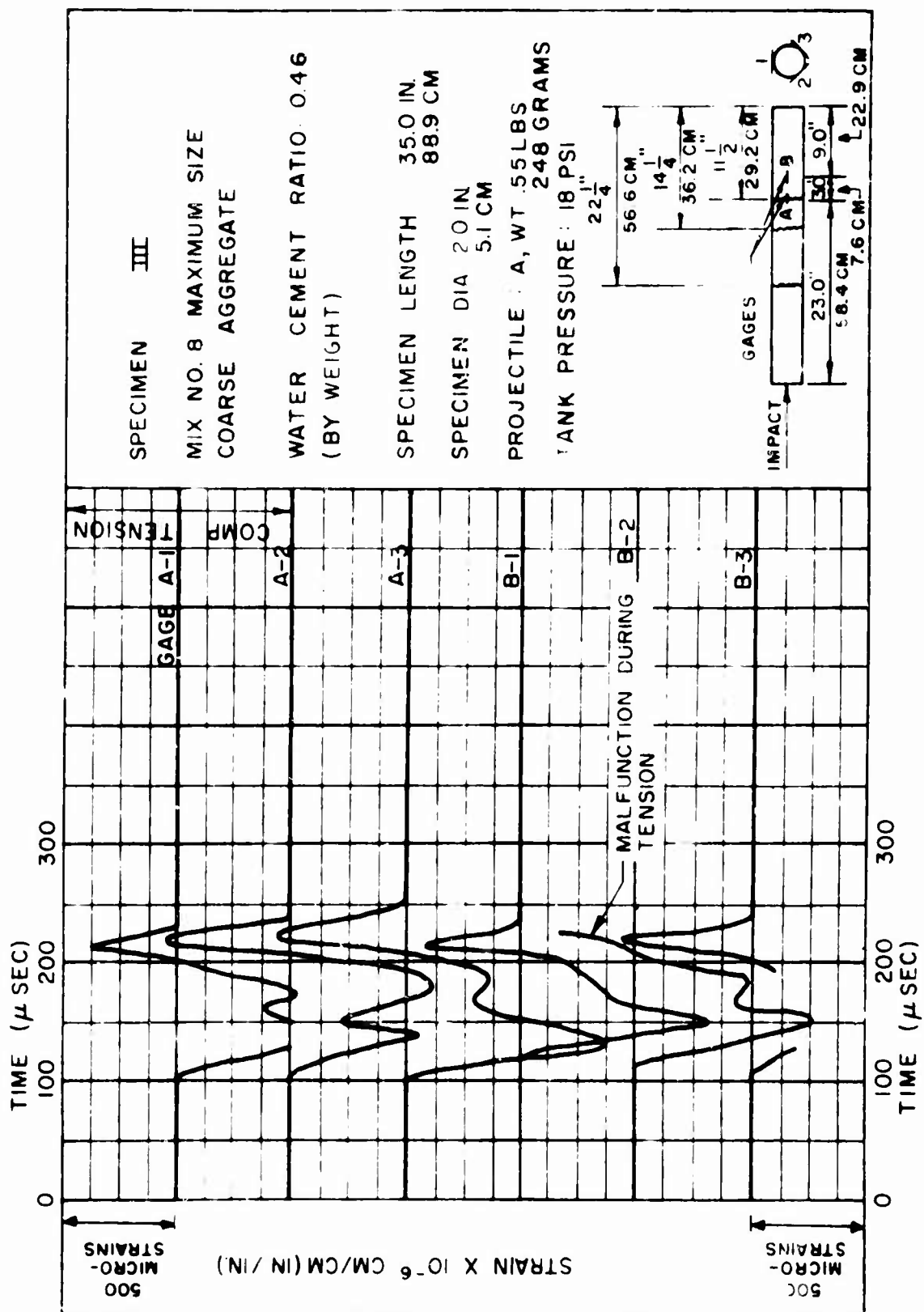


FIGURE 39

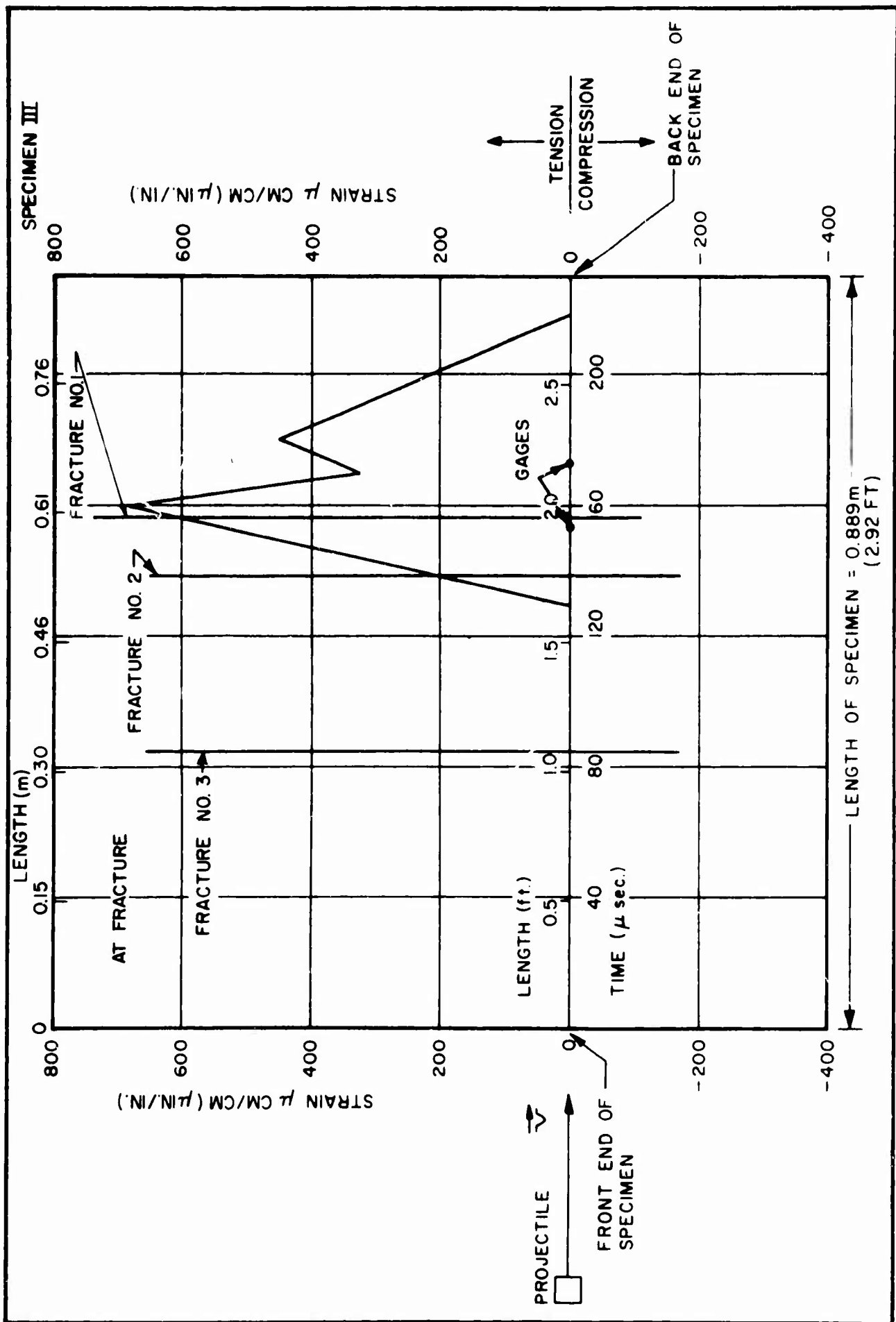


FIGURE 40

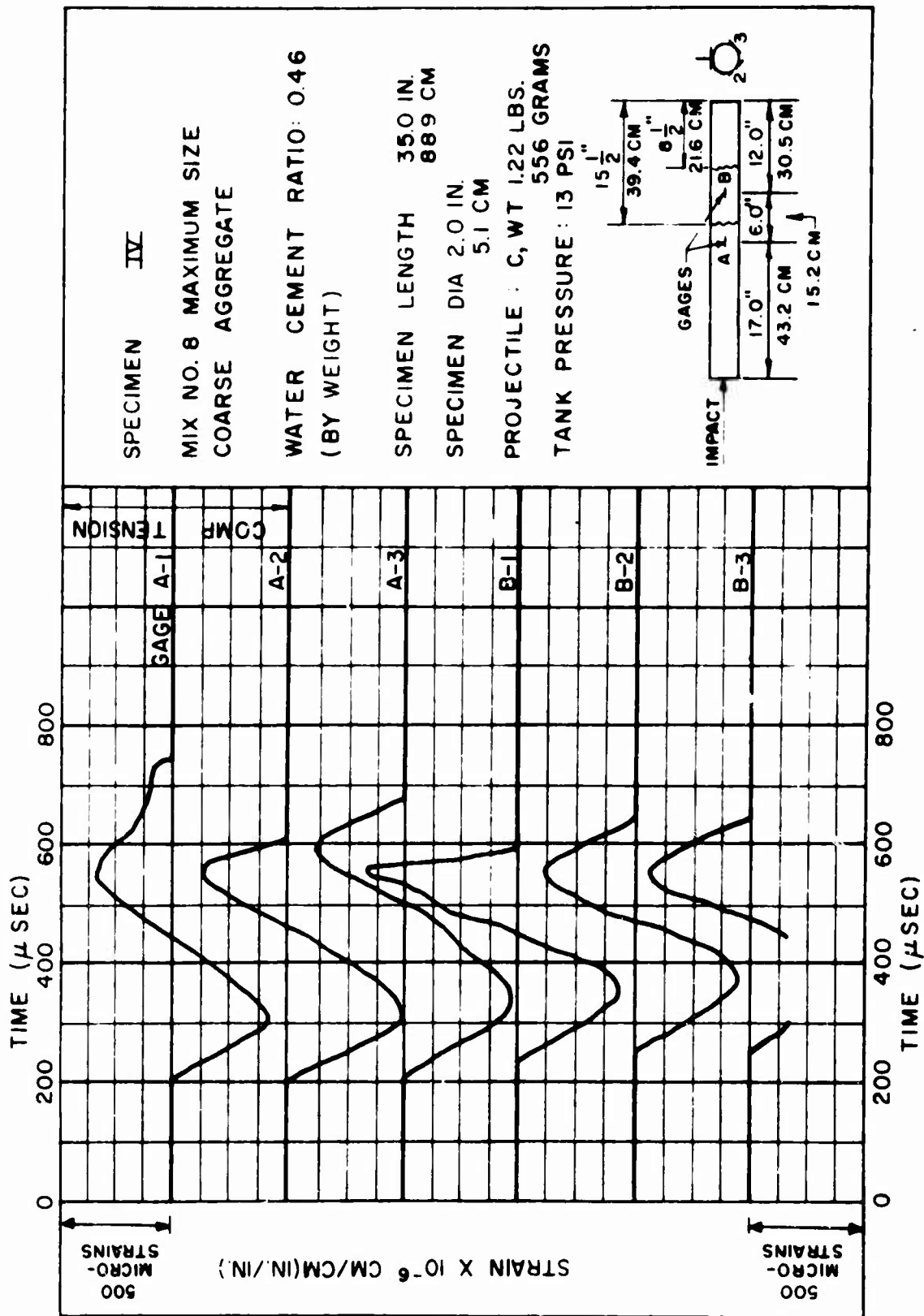


FIGURE 41

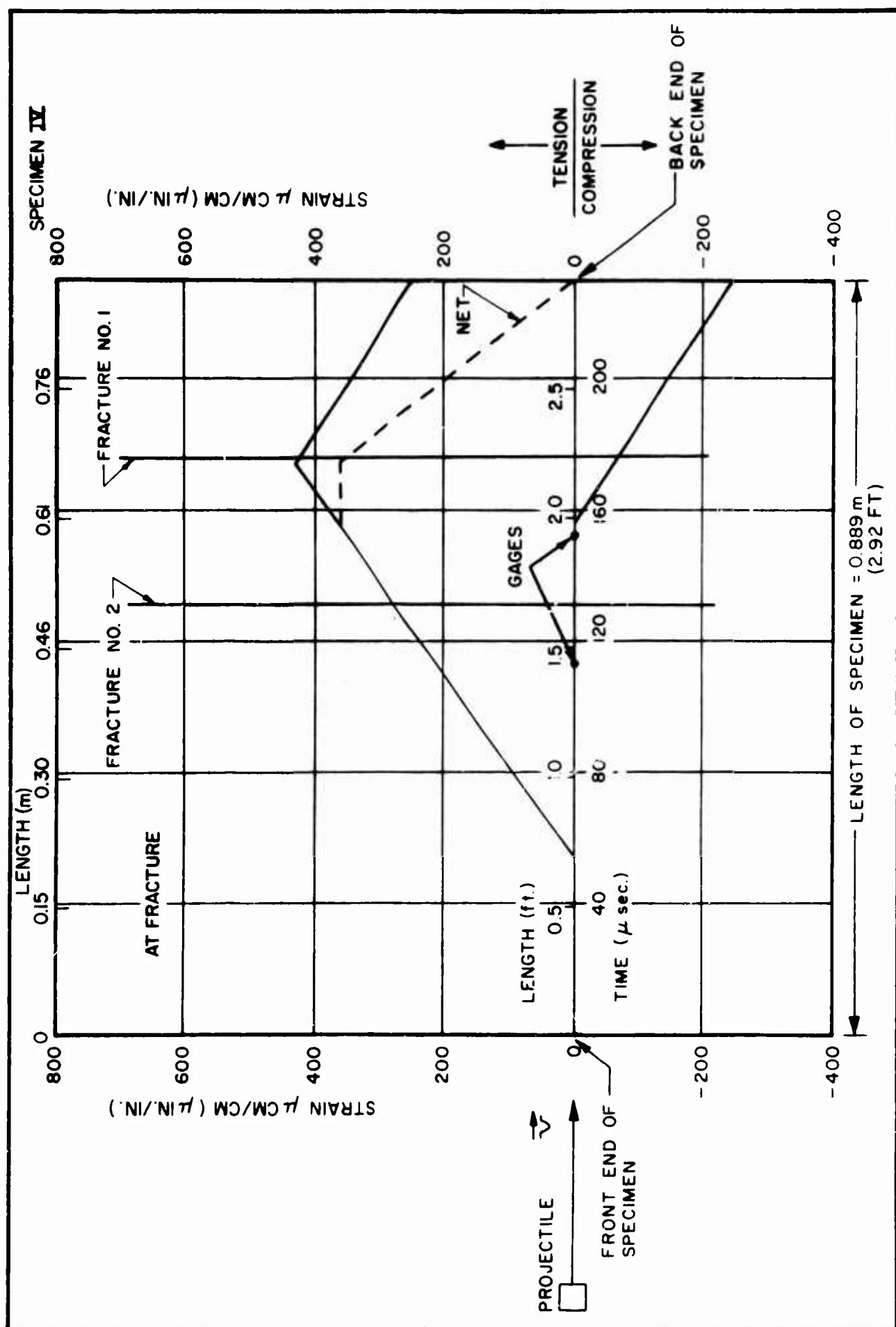


FIGURE 42

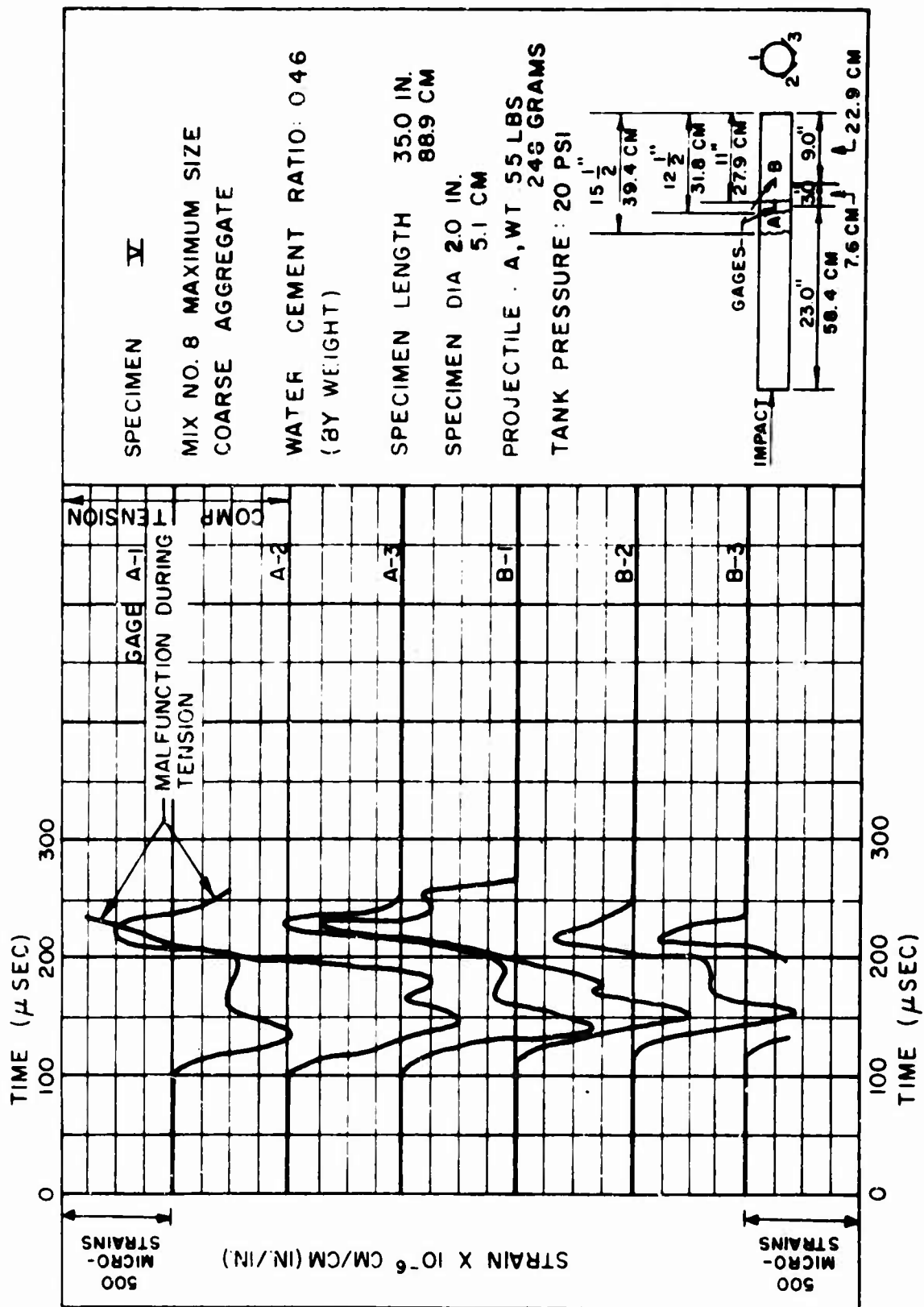
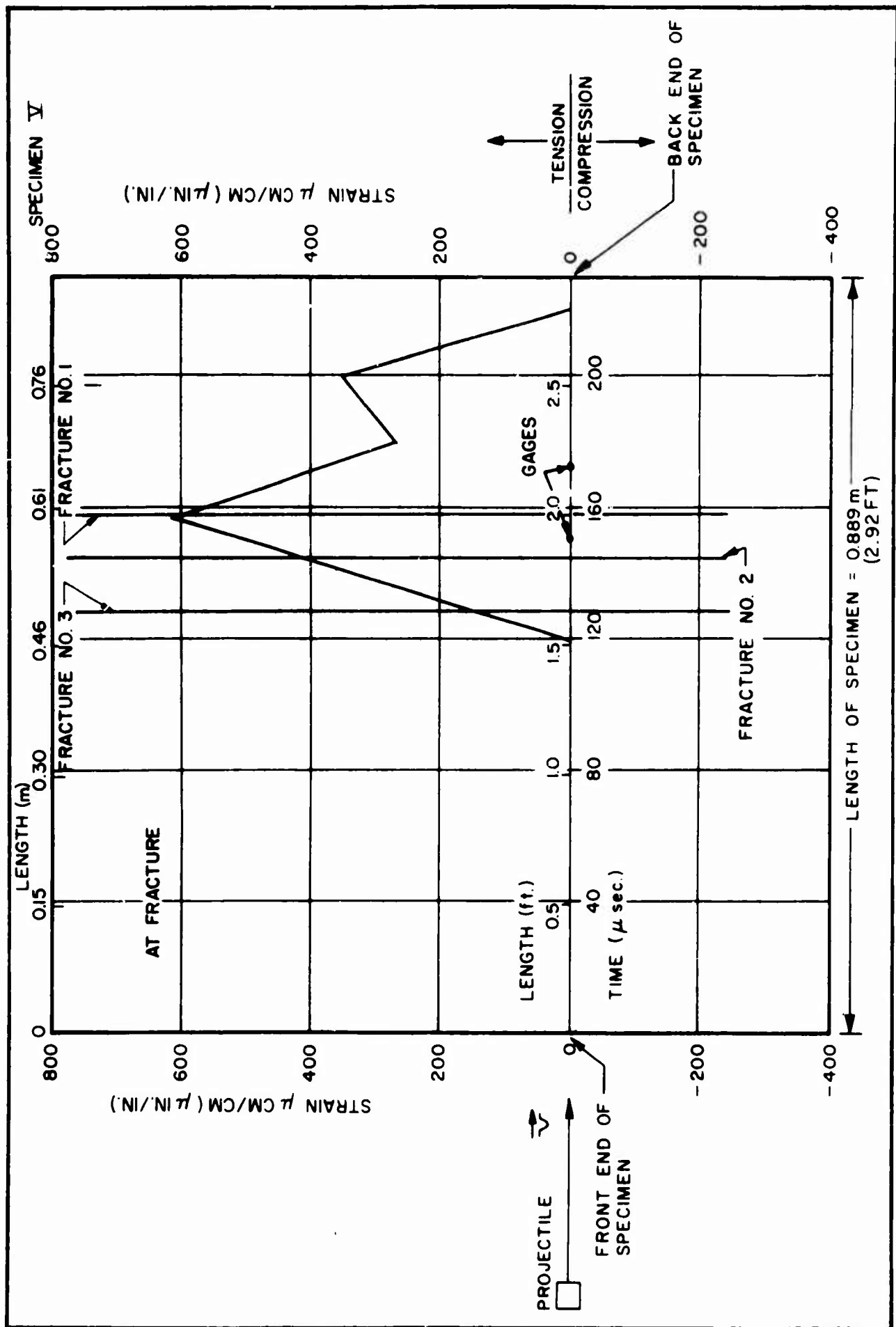
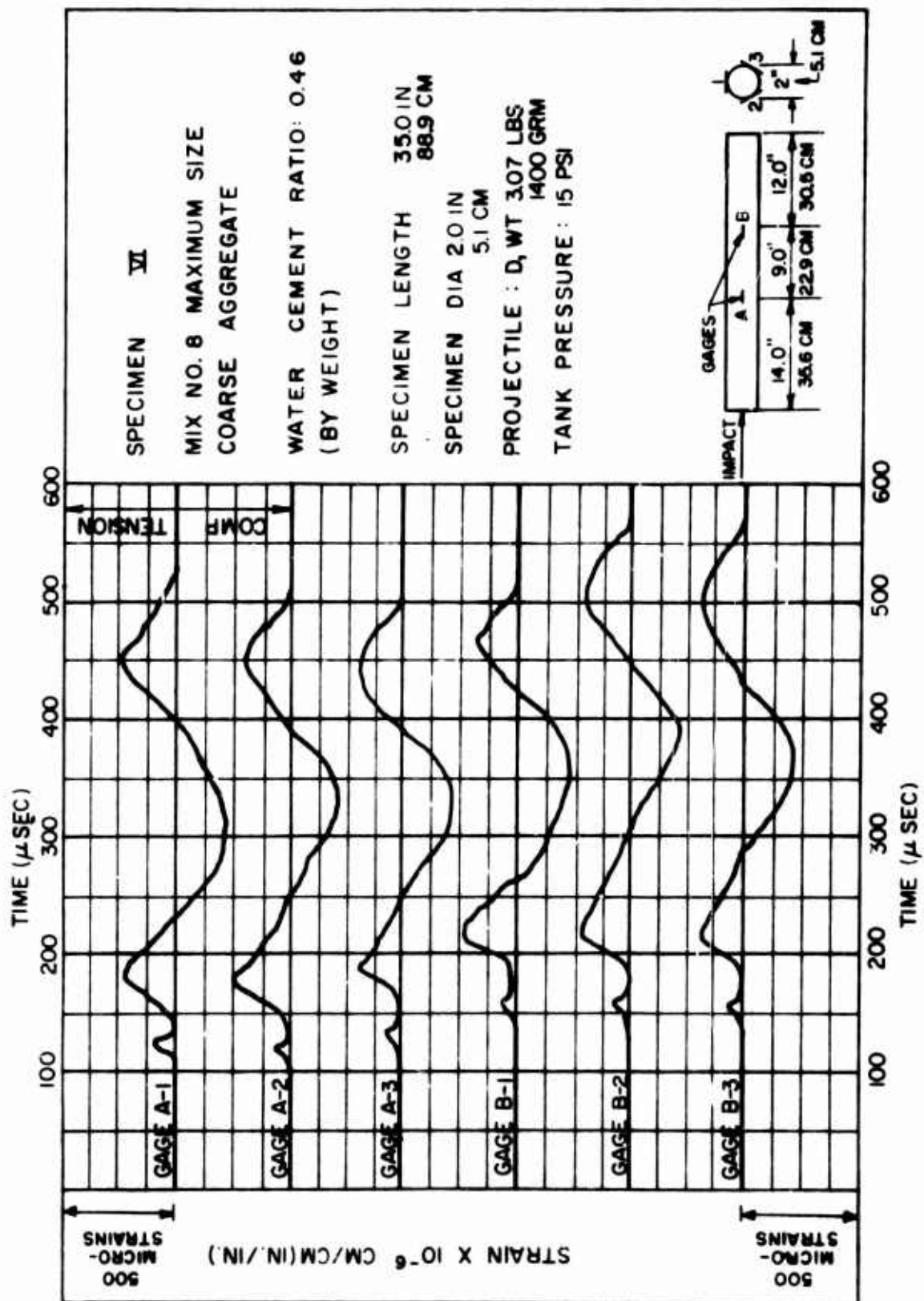


FIGURE 43





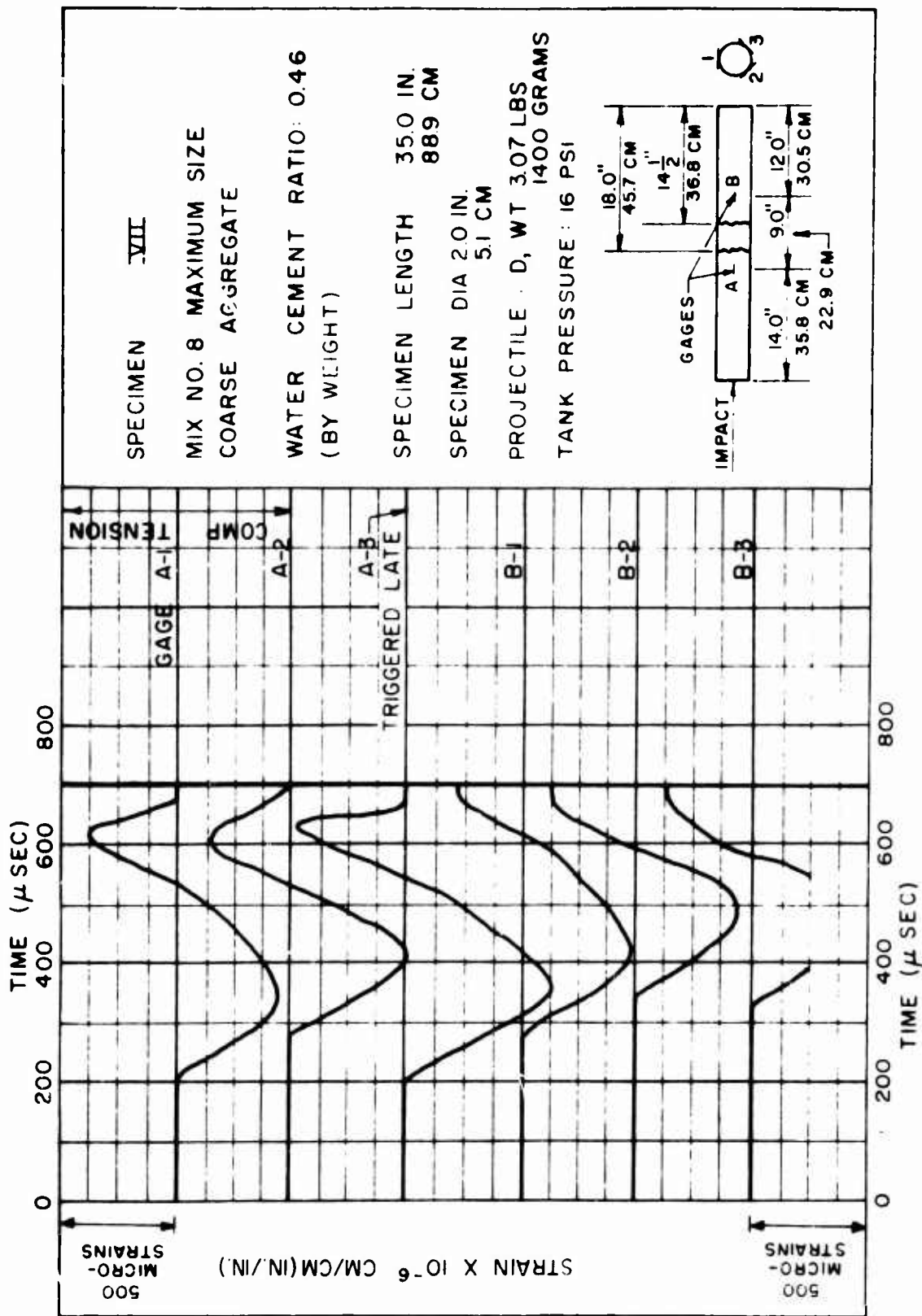
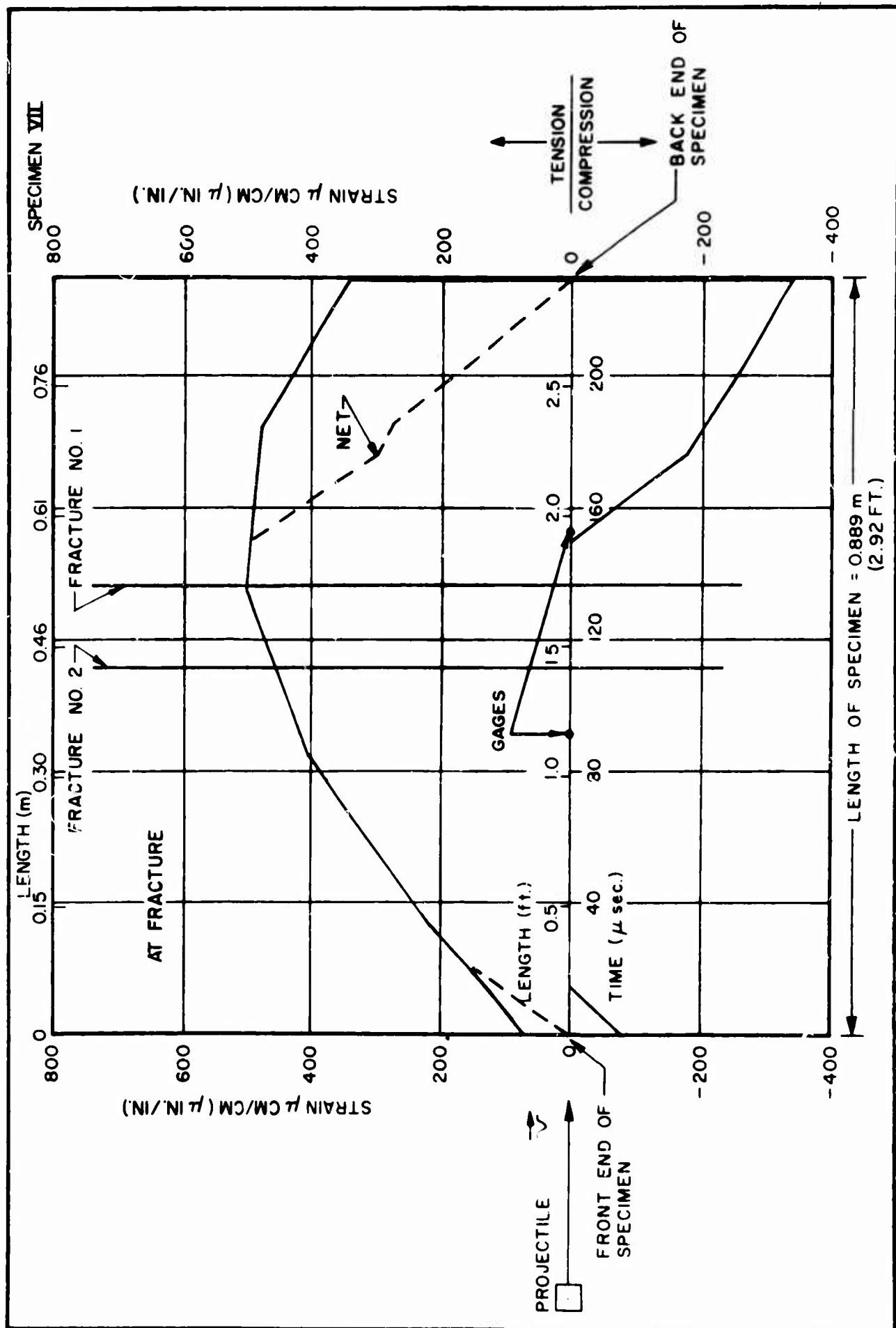


FIGURE 46



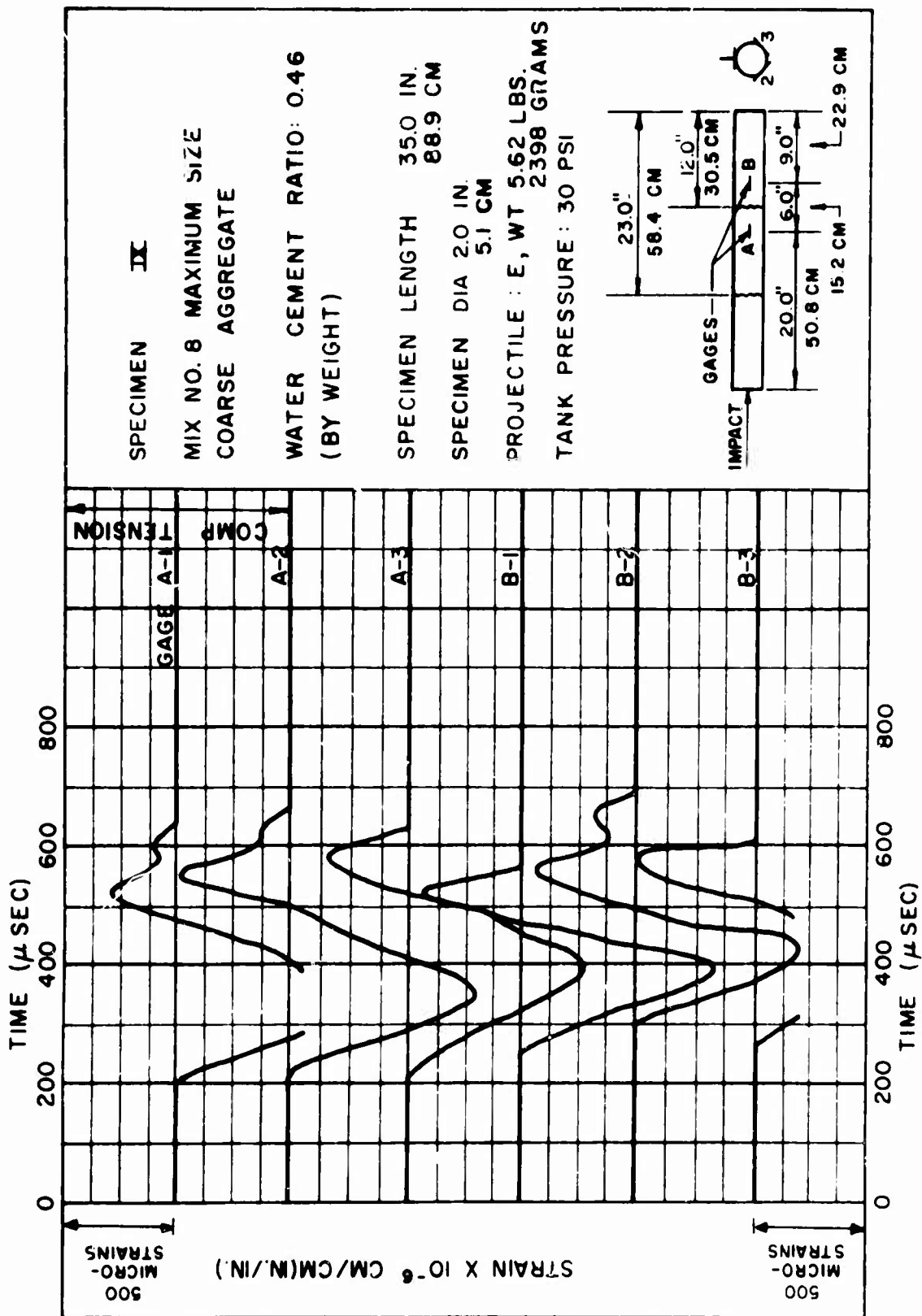
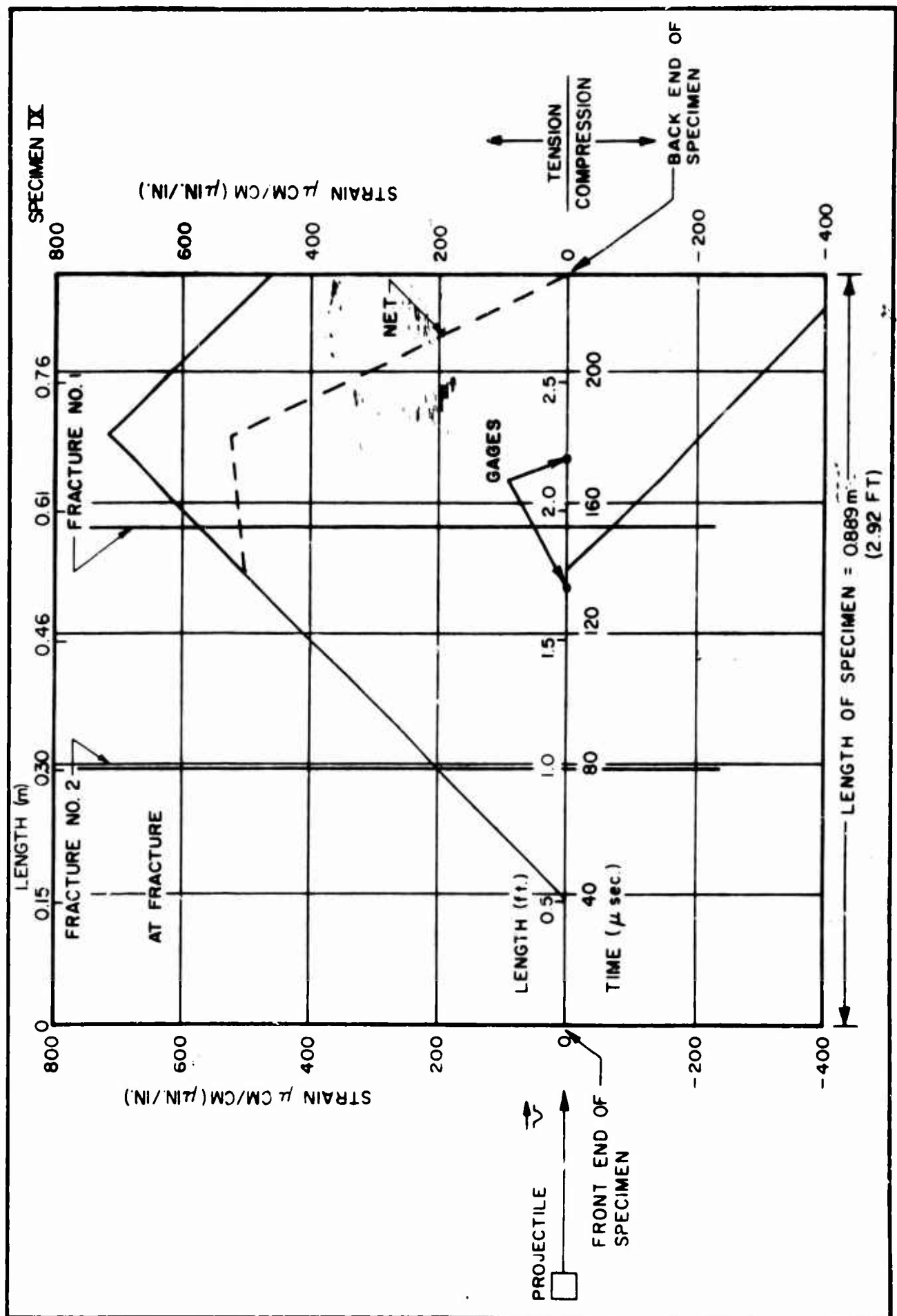


FIGURE 48



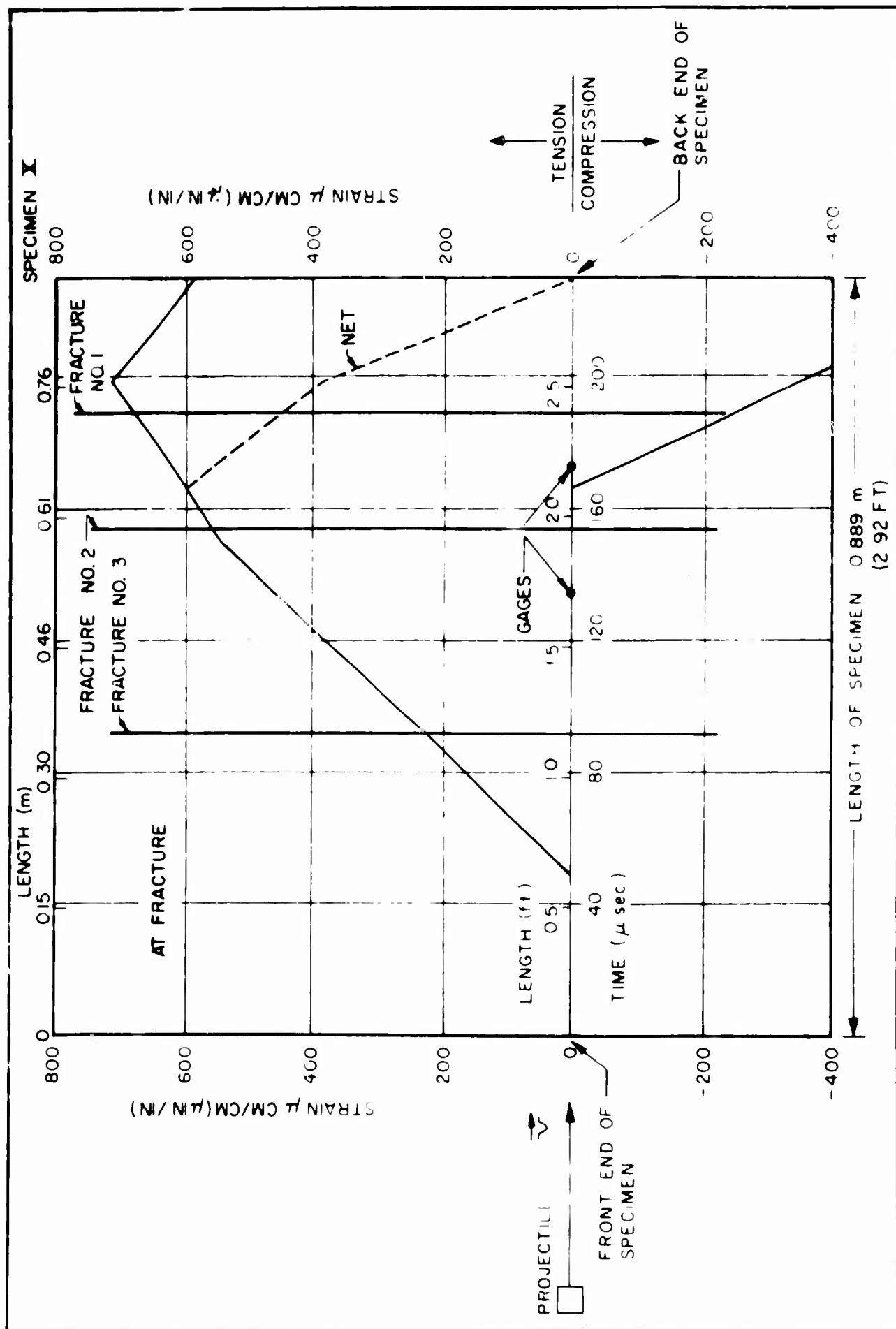


FIGURE 51

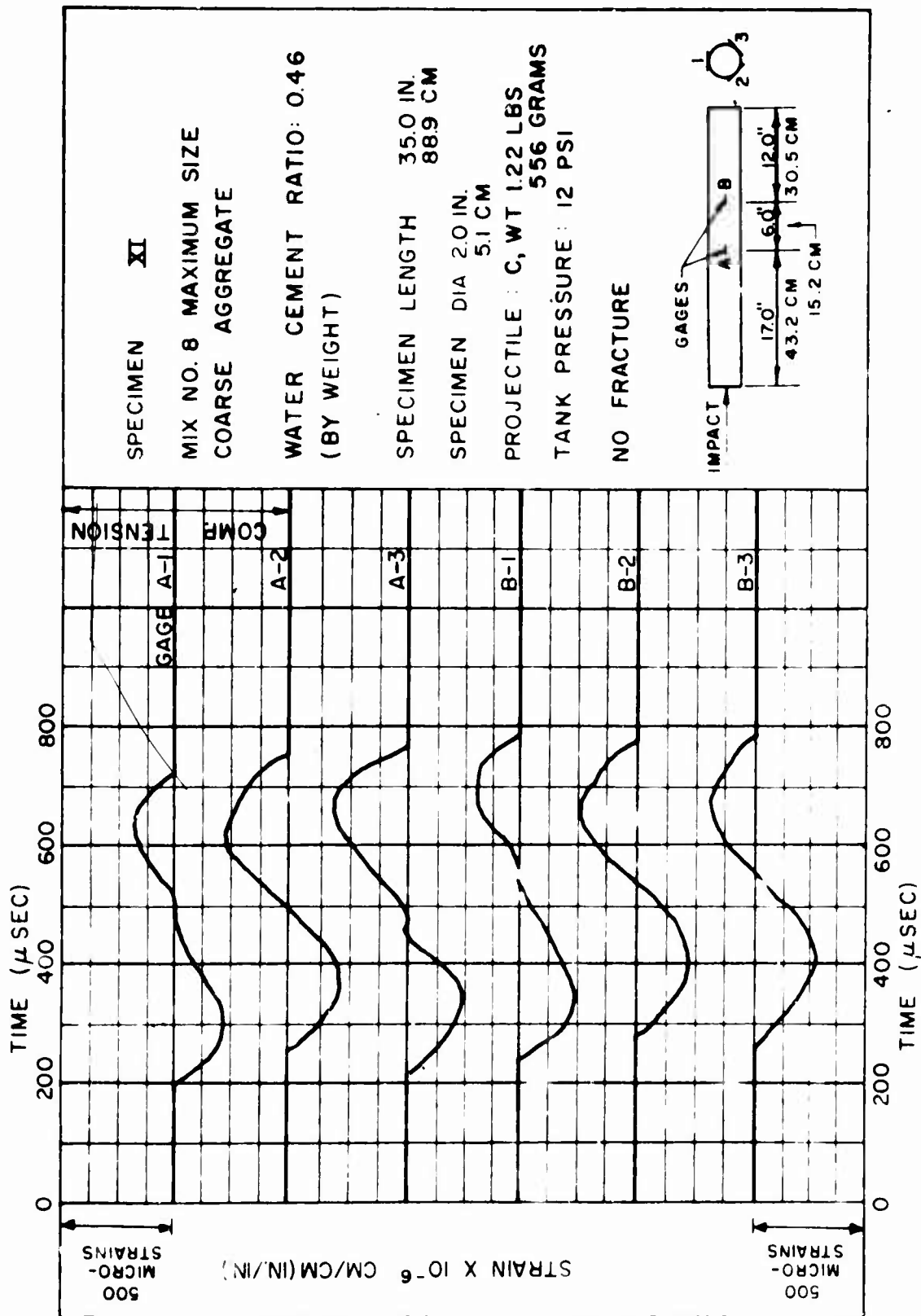
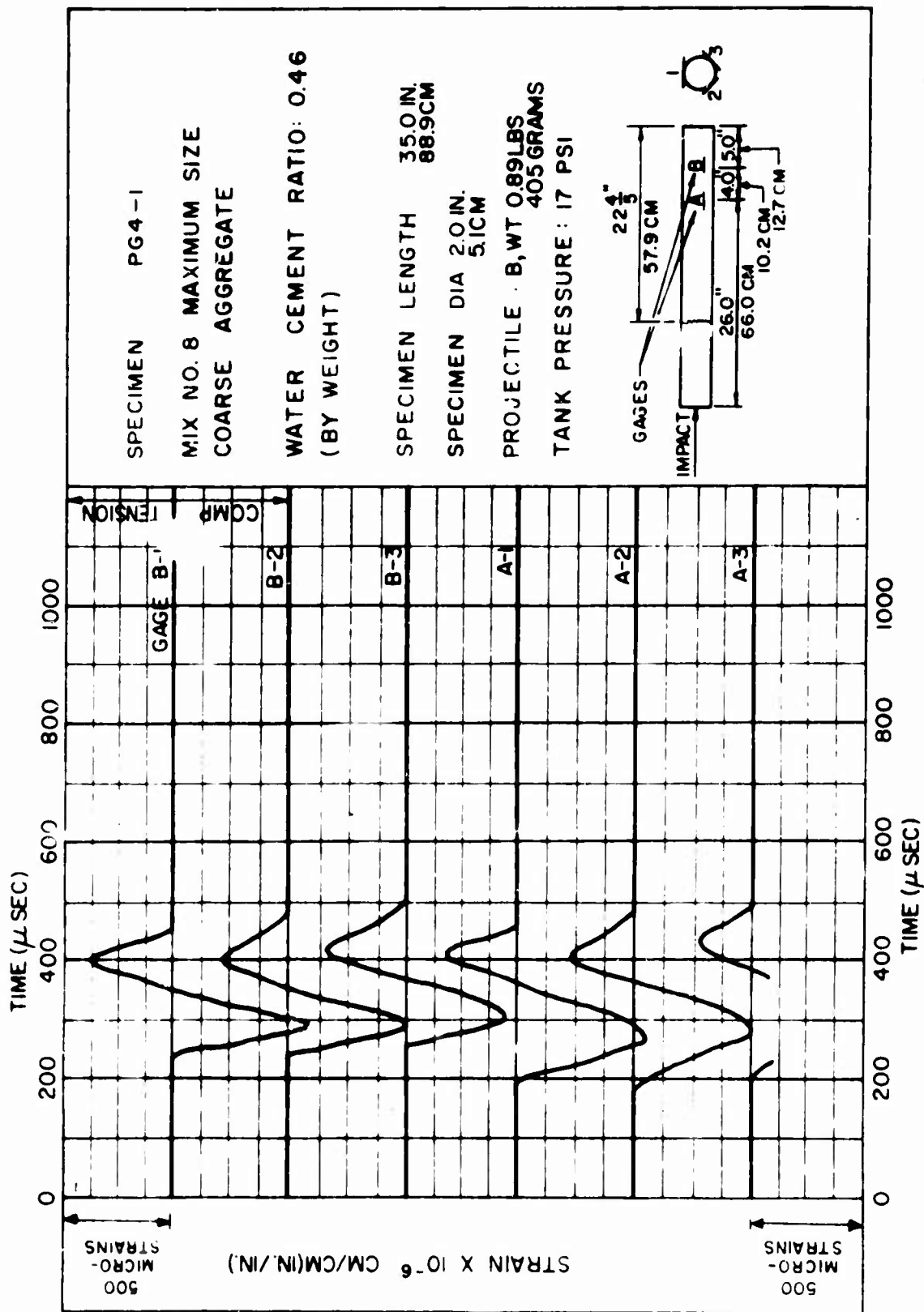
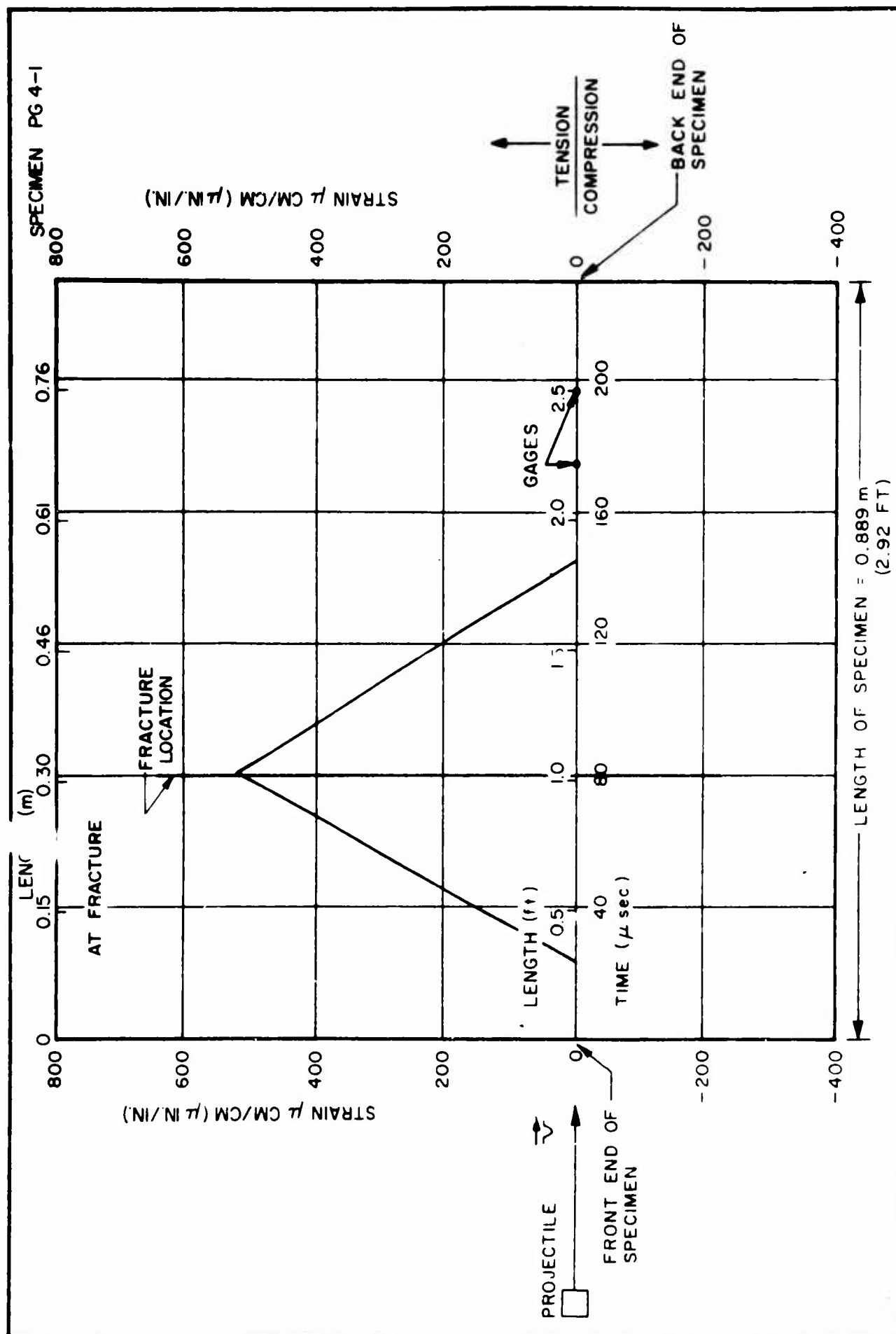


FIGURE 52





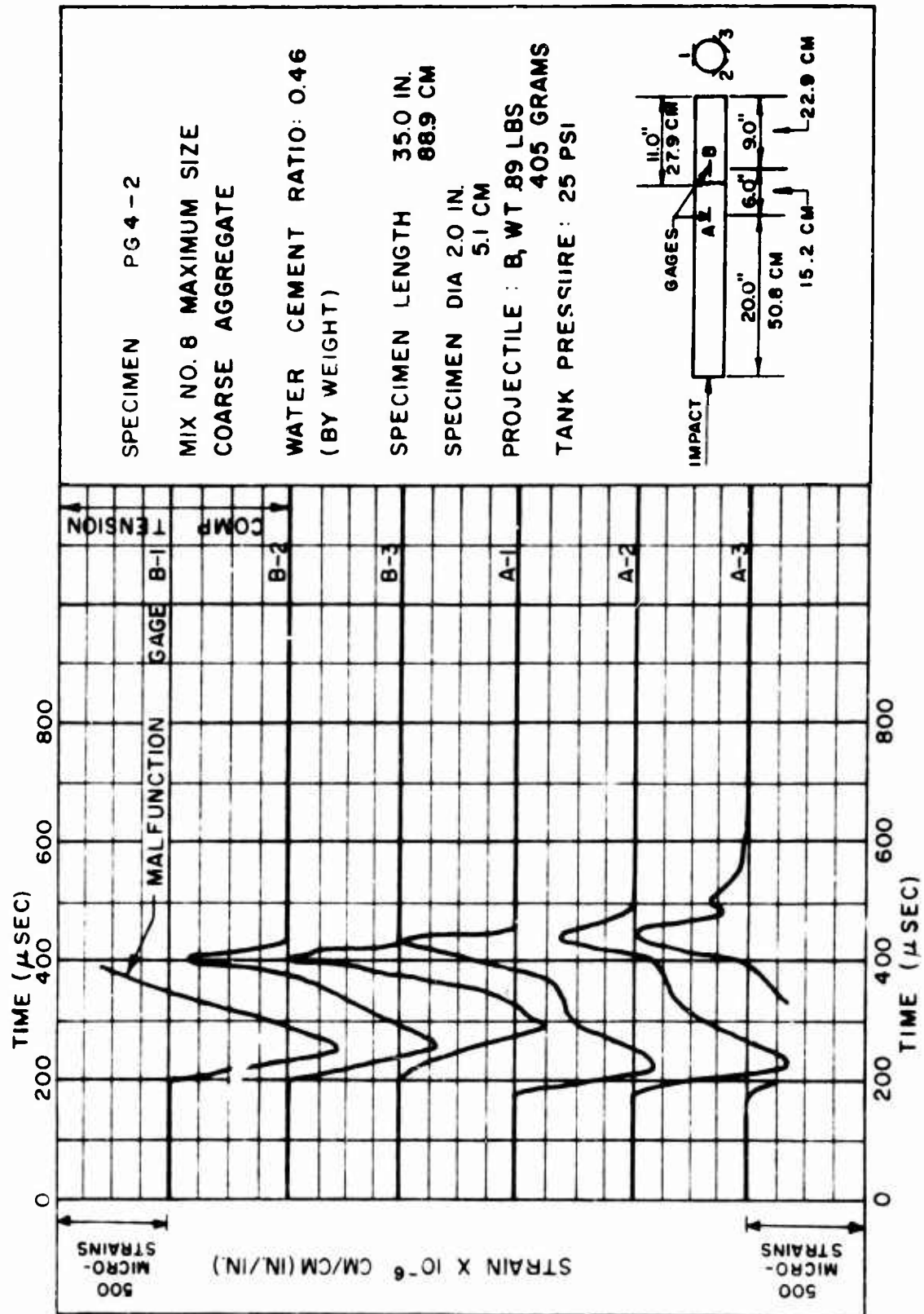
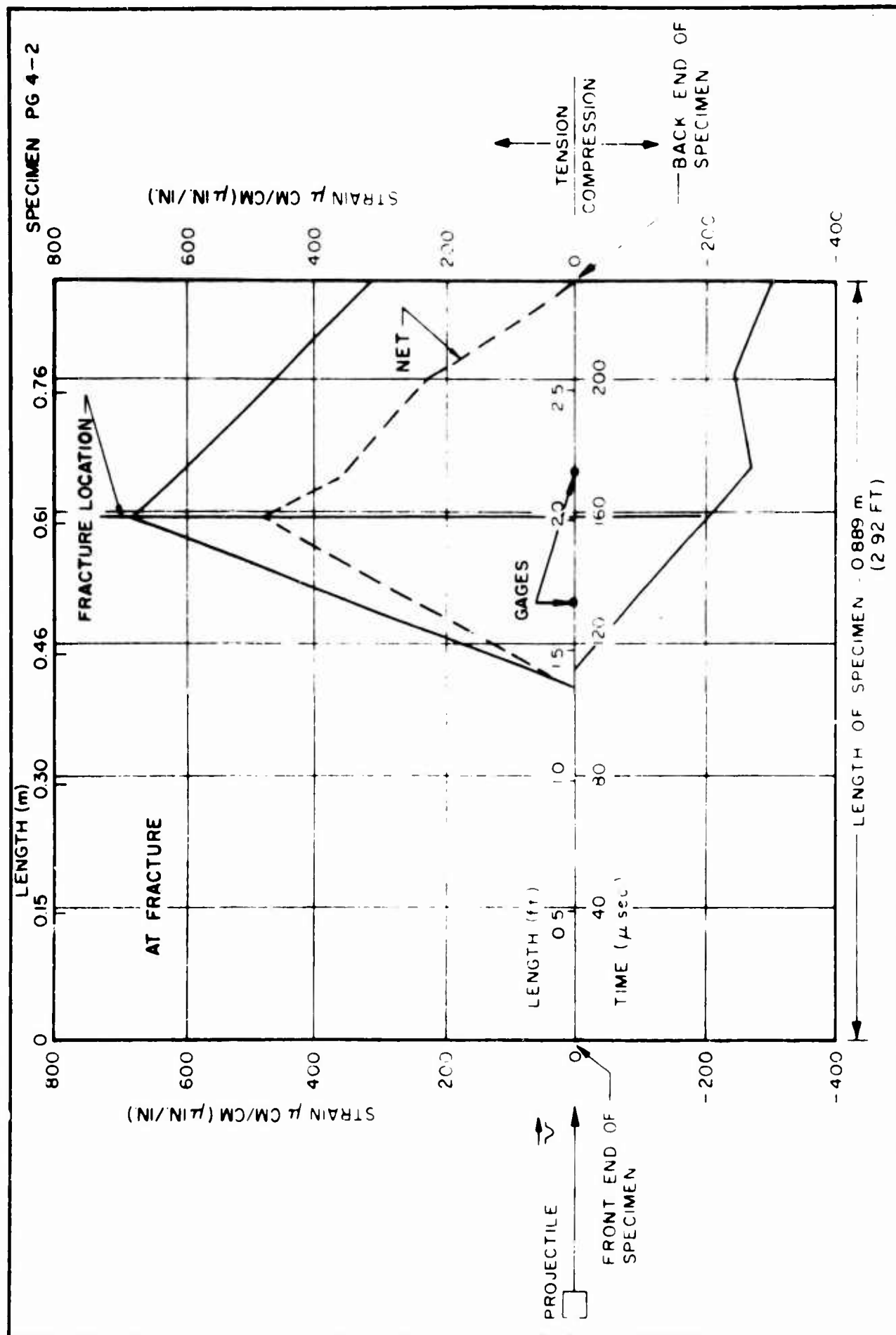
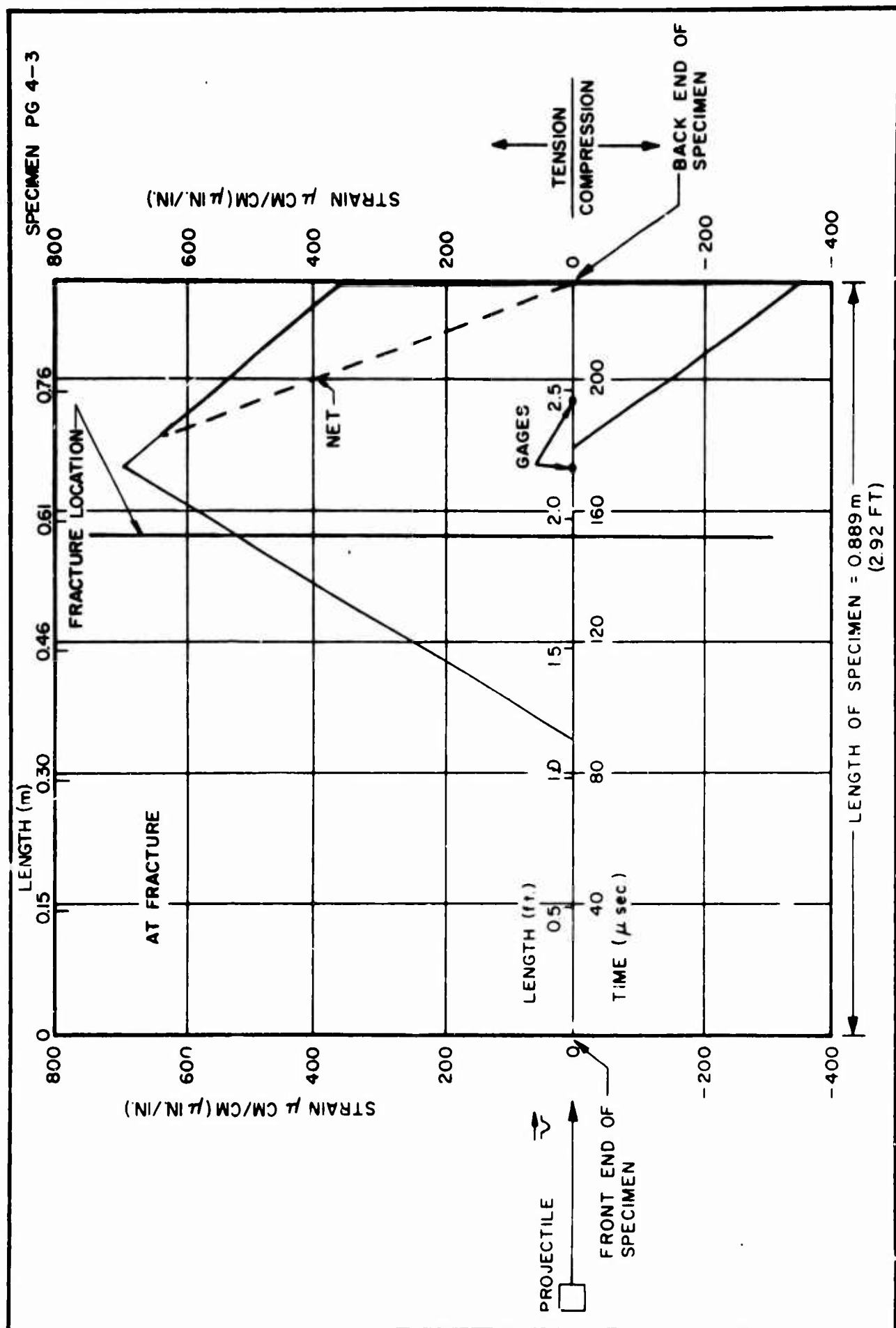


FIGURE 55





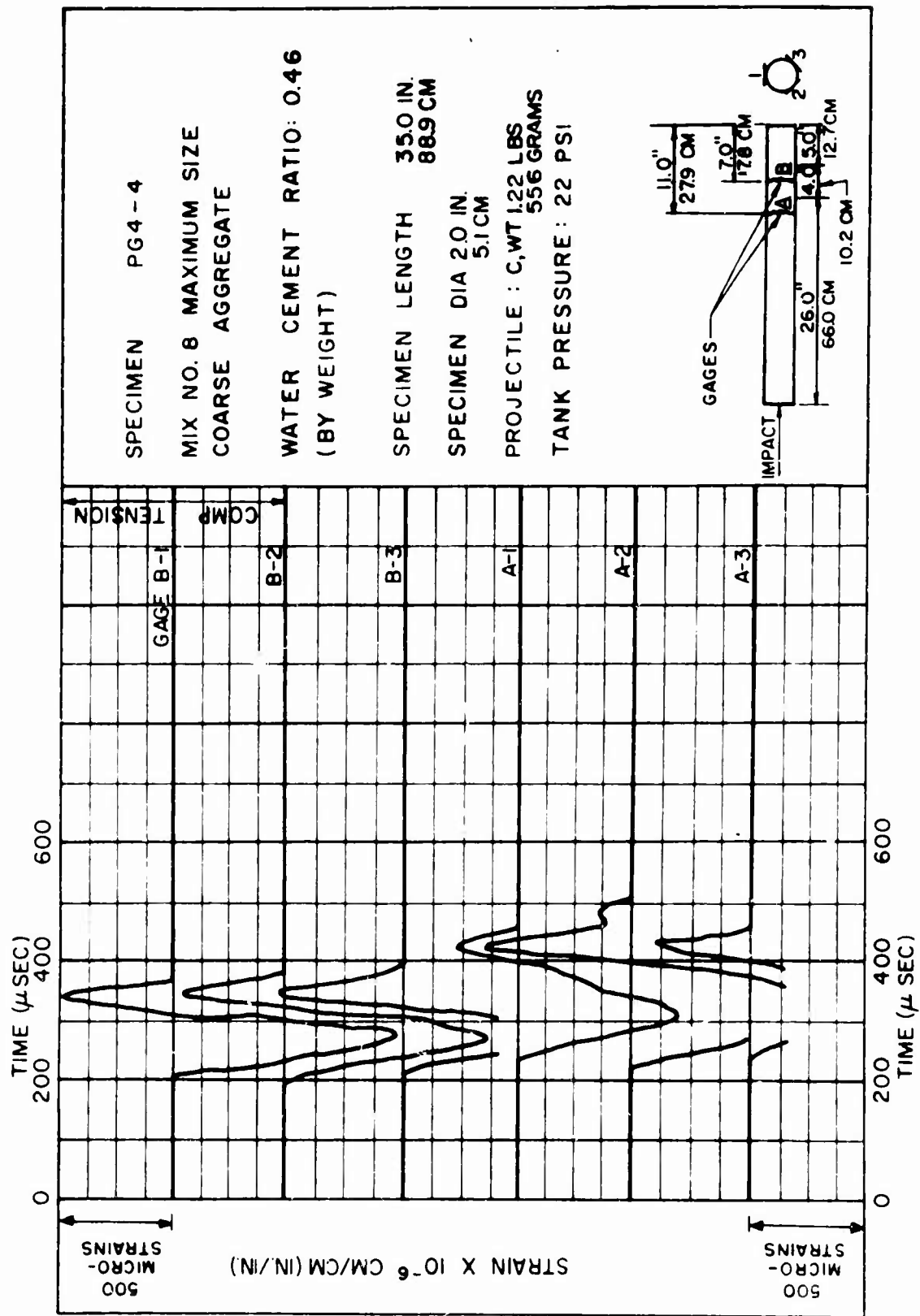
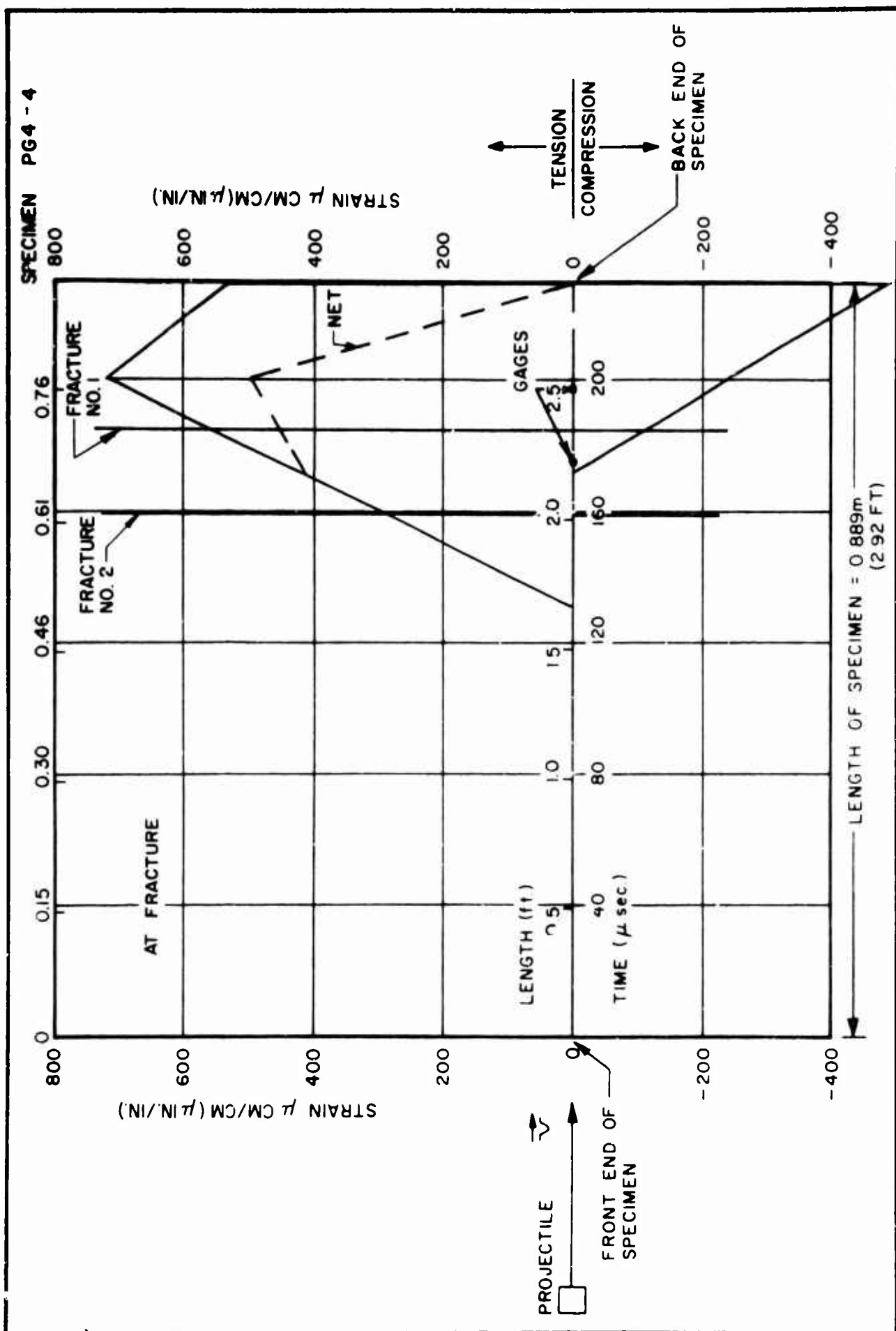
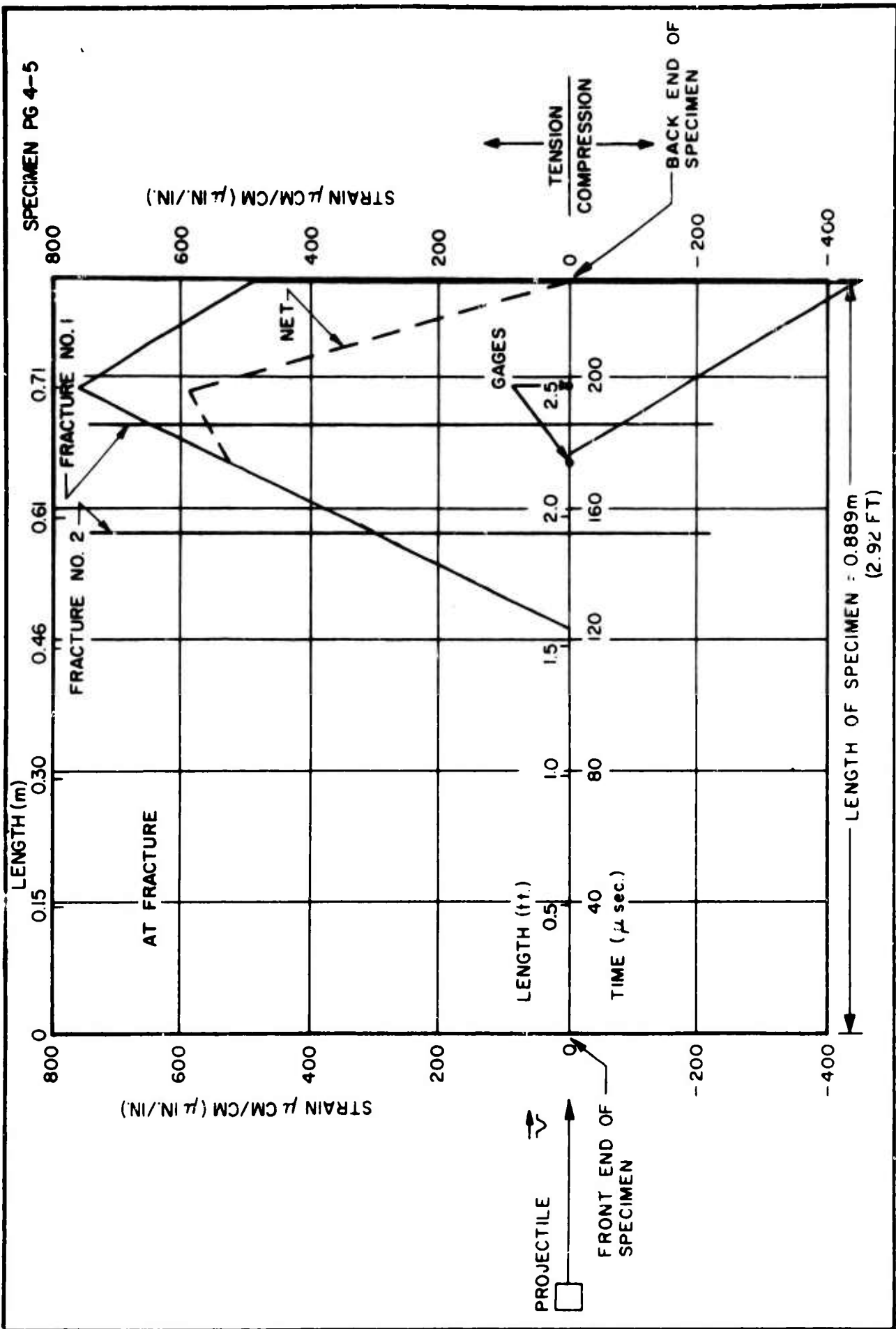
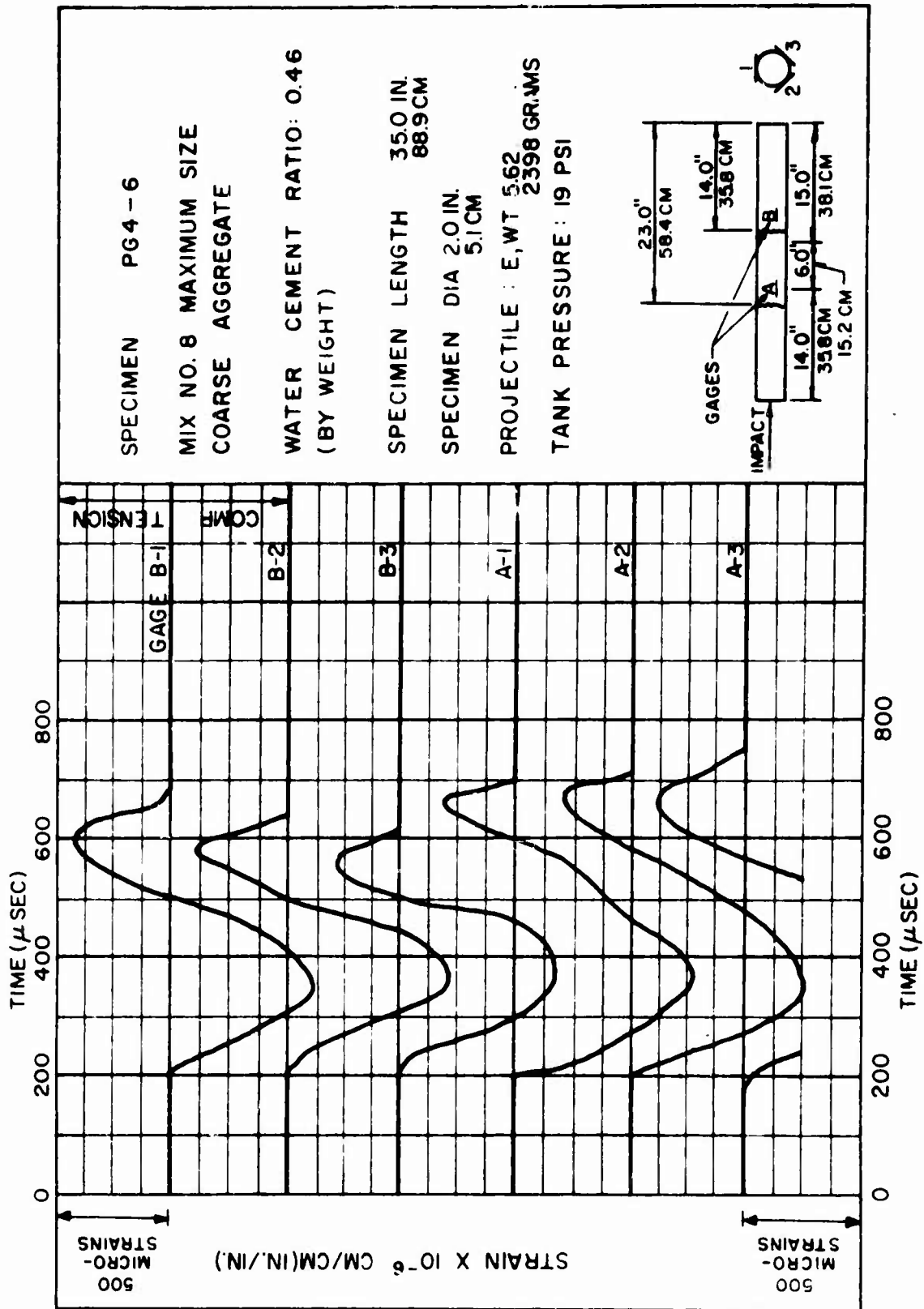
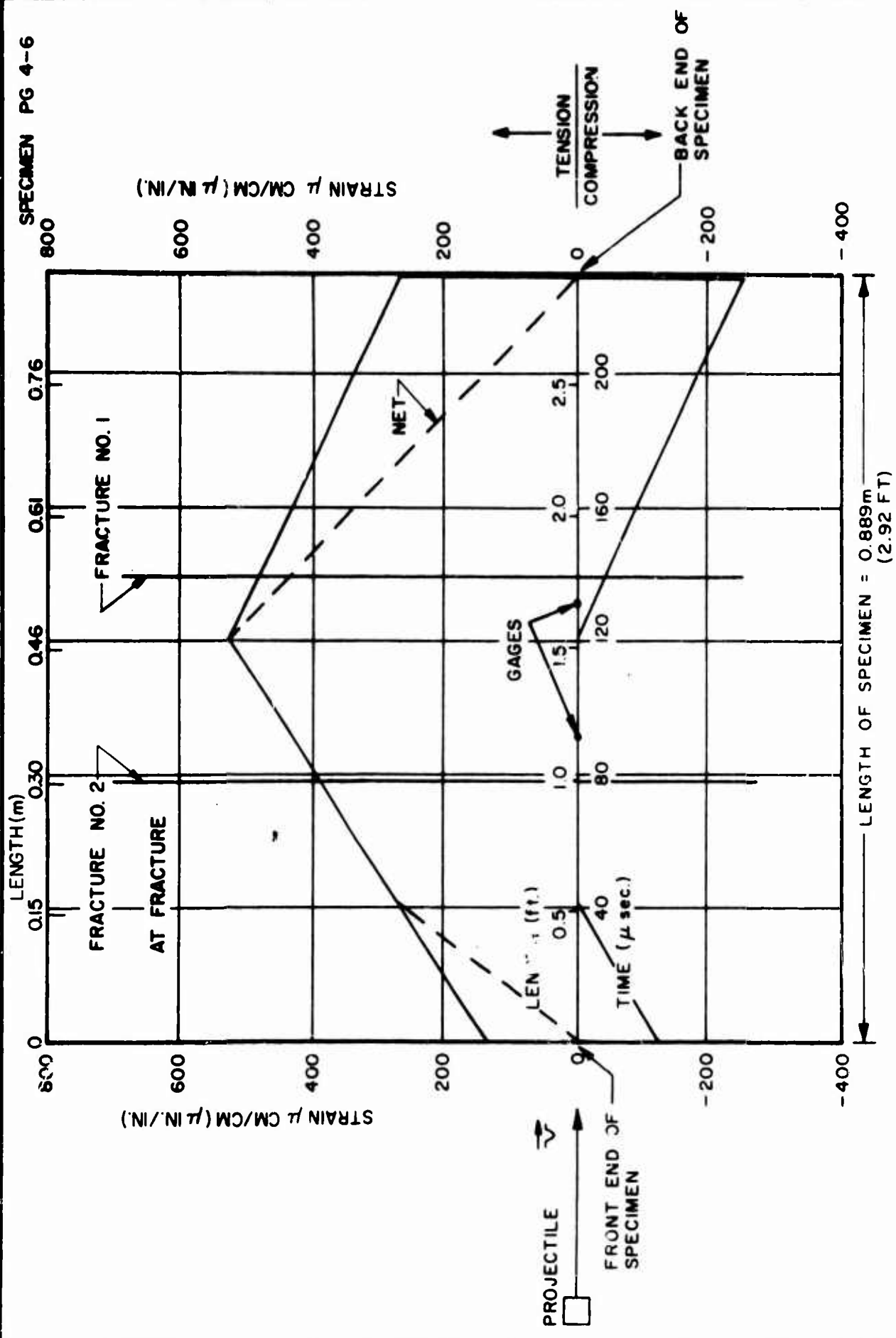


FIGURE 59









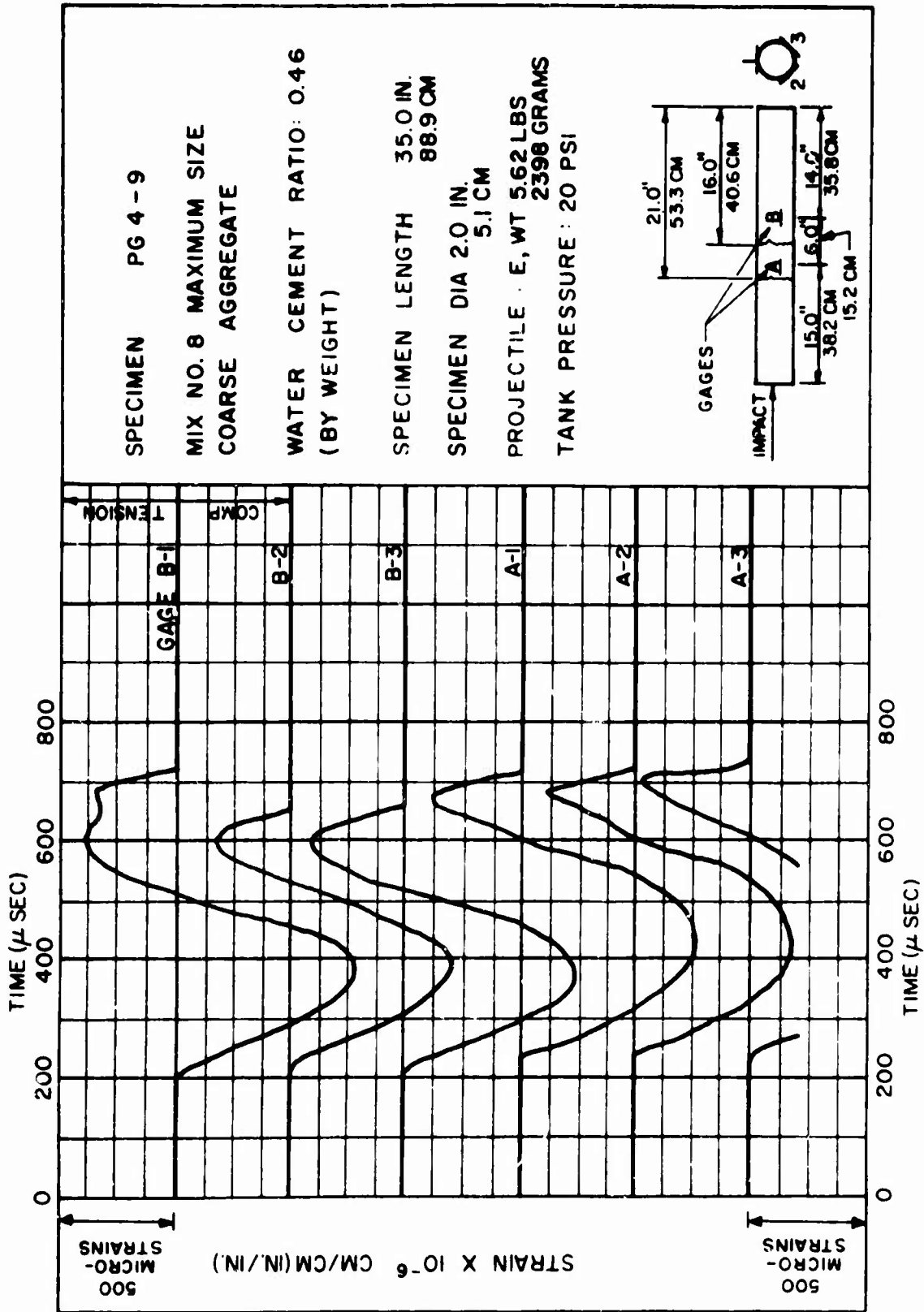
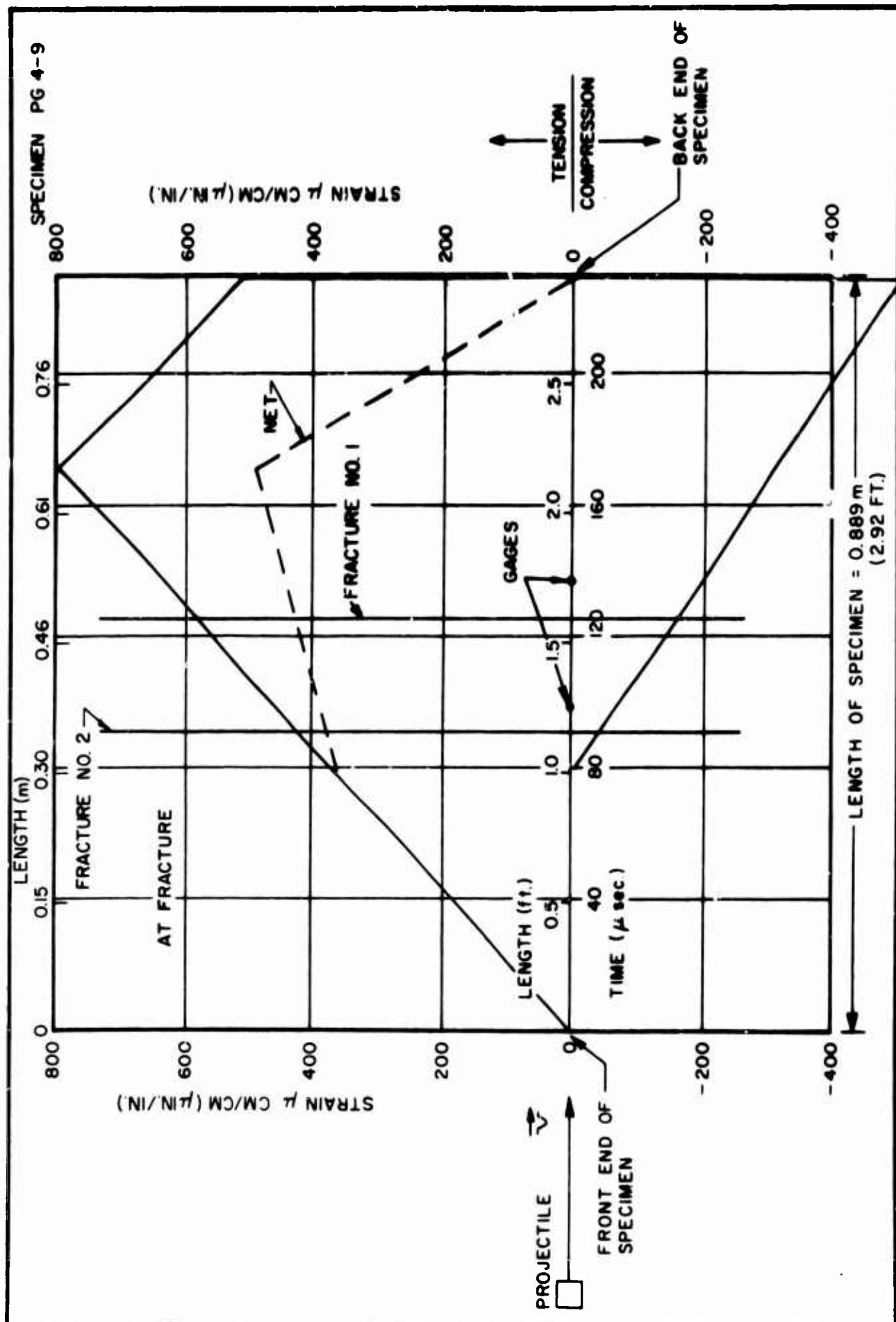


FIGURE 66



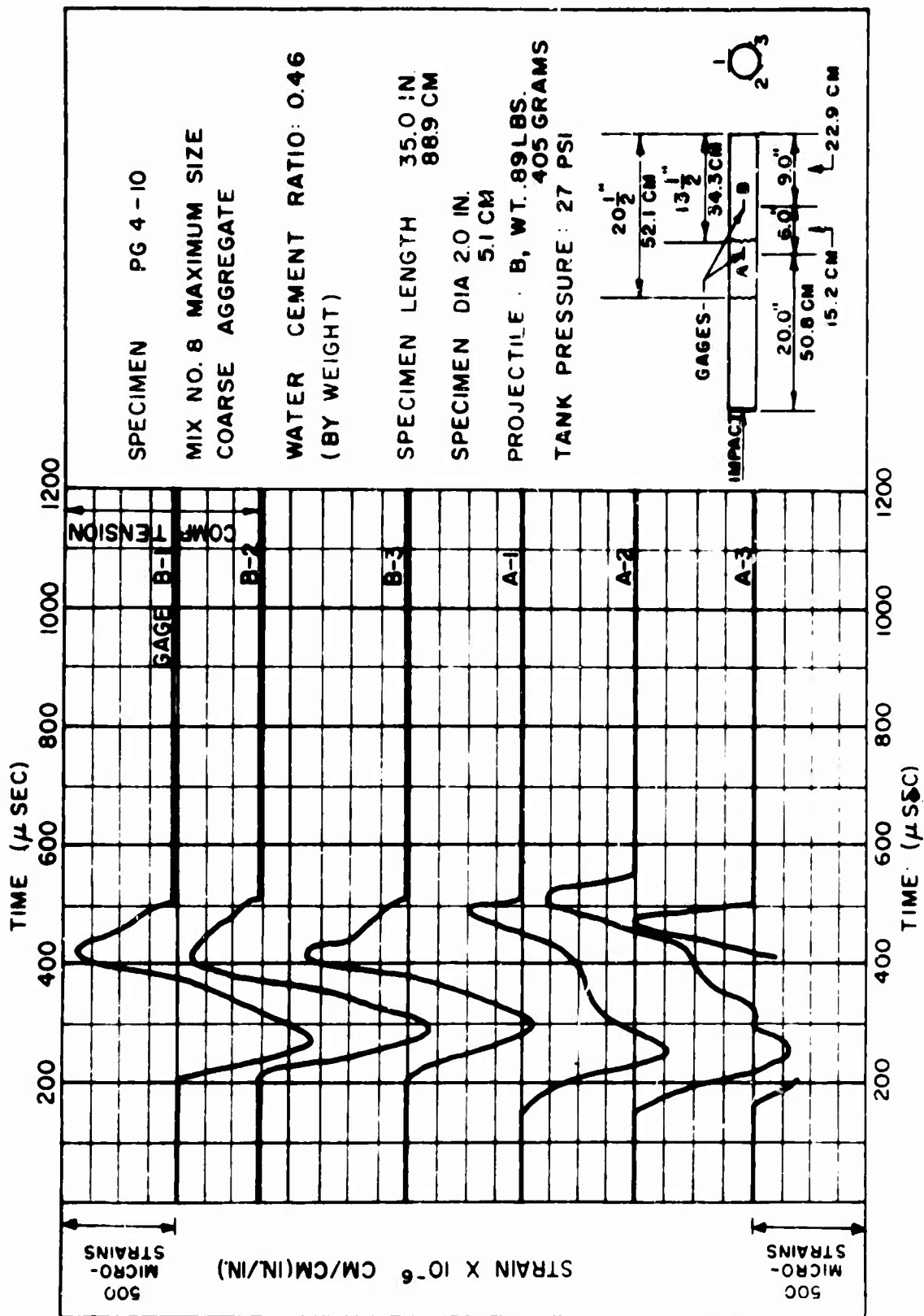
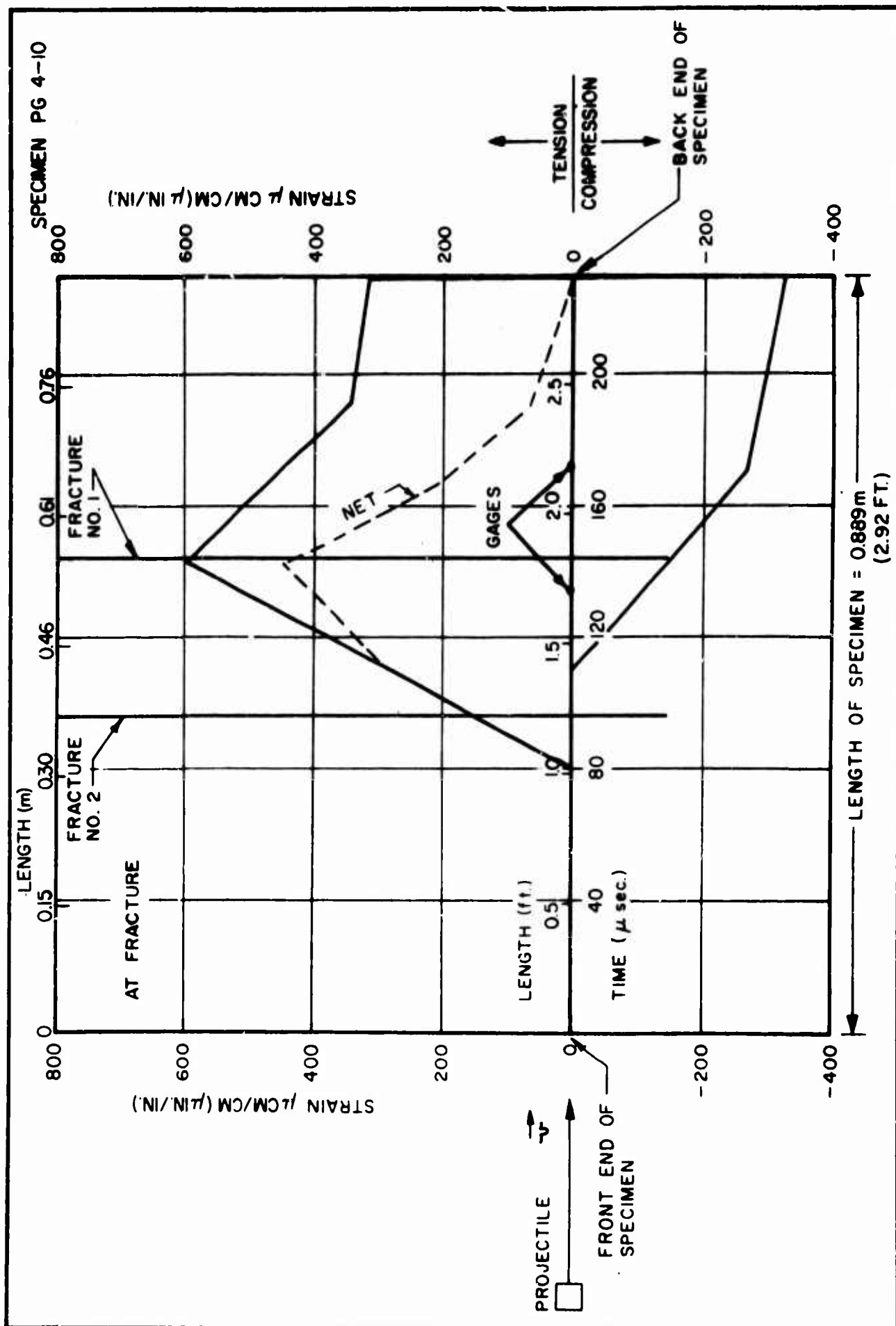
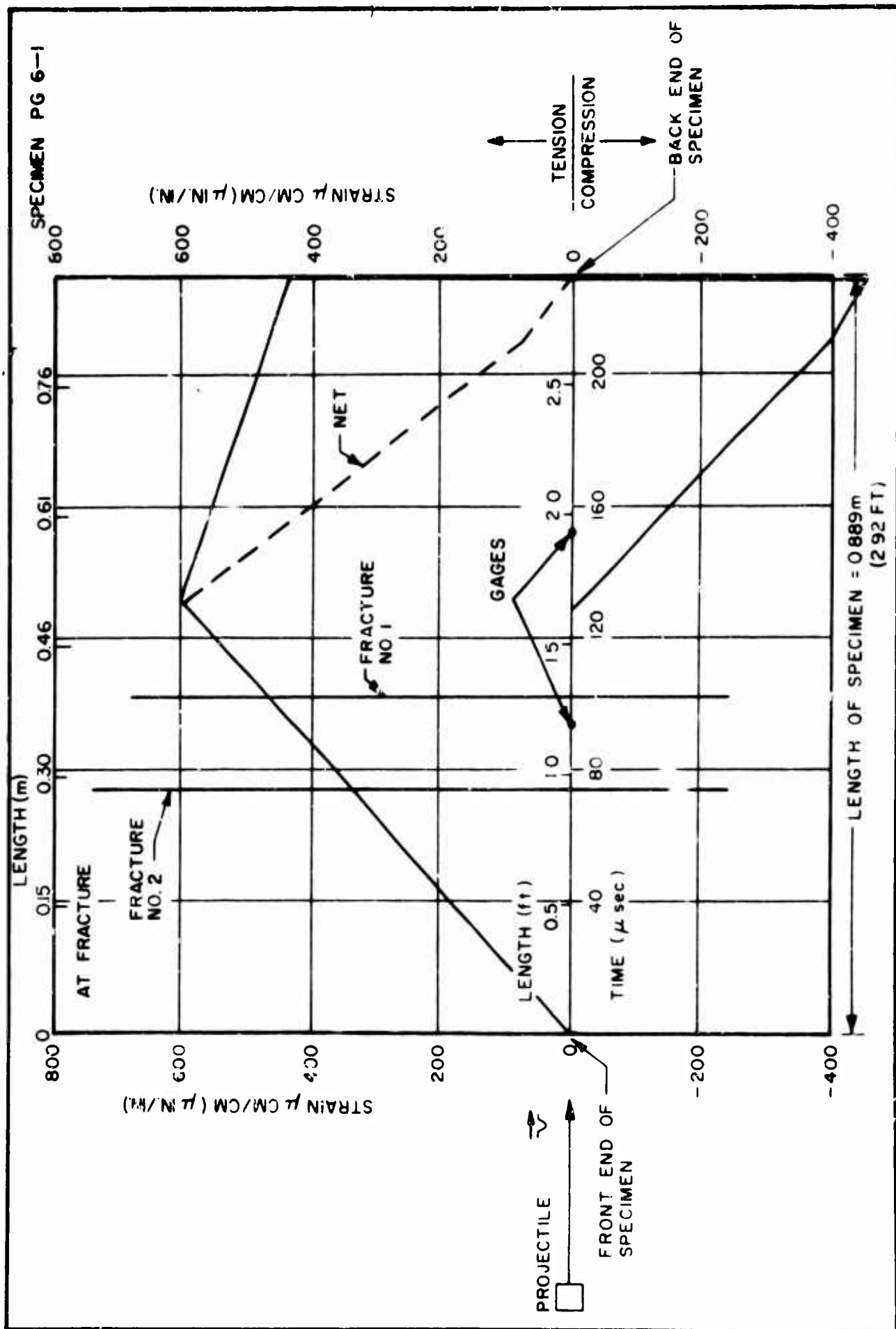


FIGURE 68





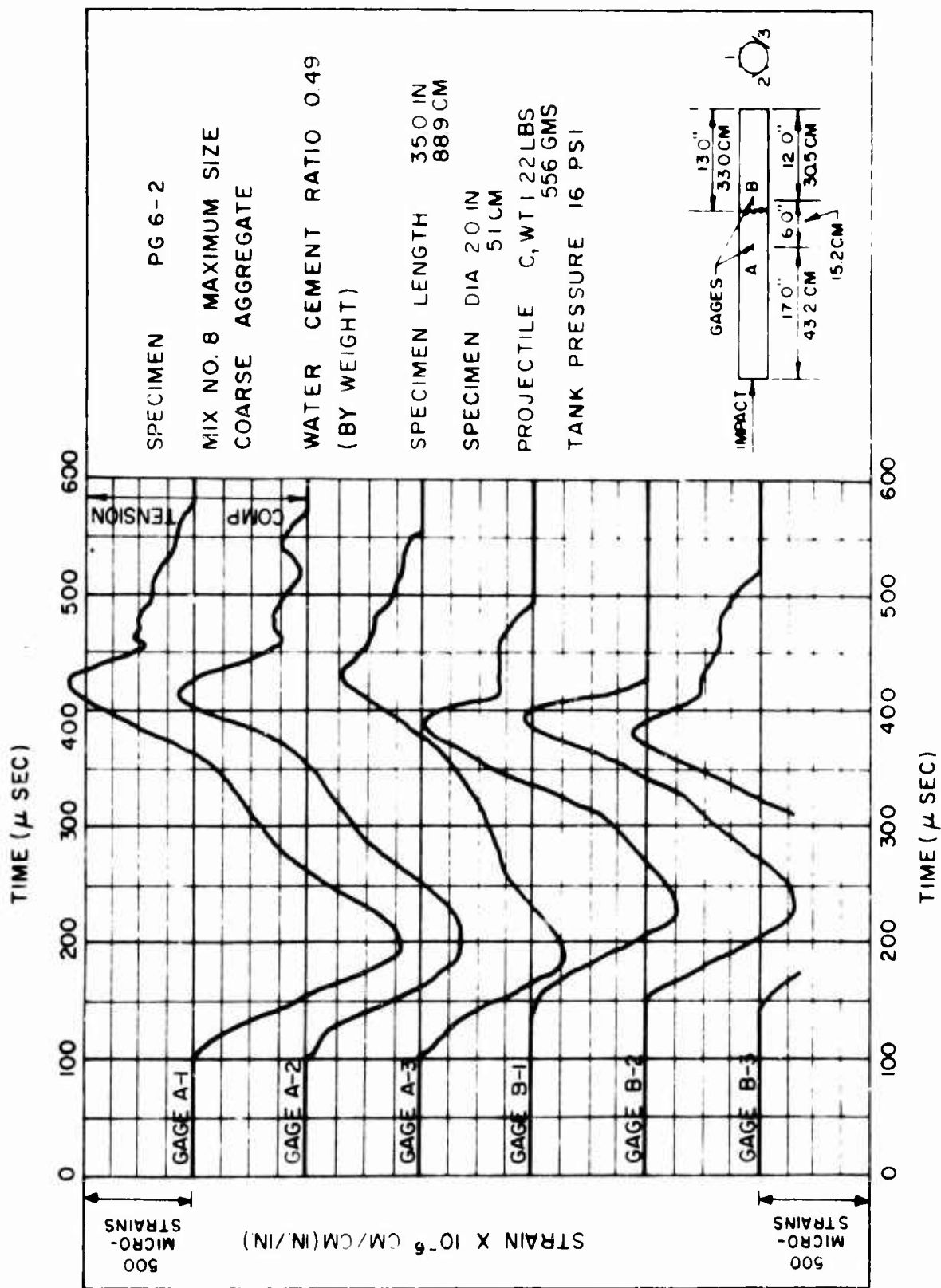
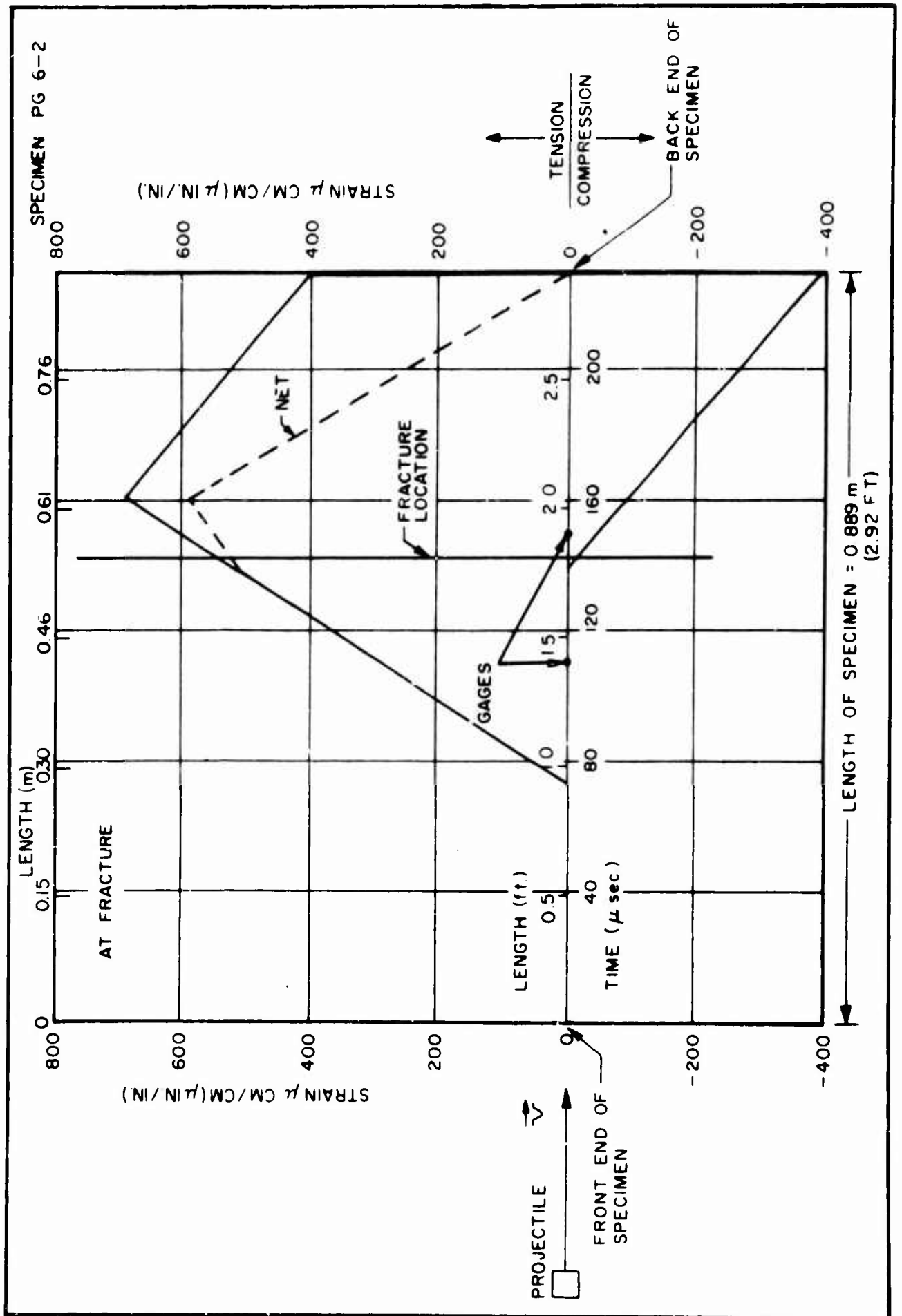


FIGURE 72



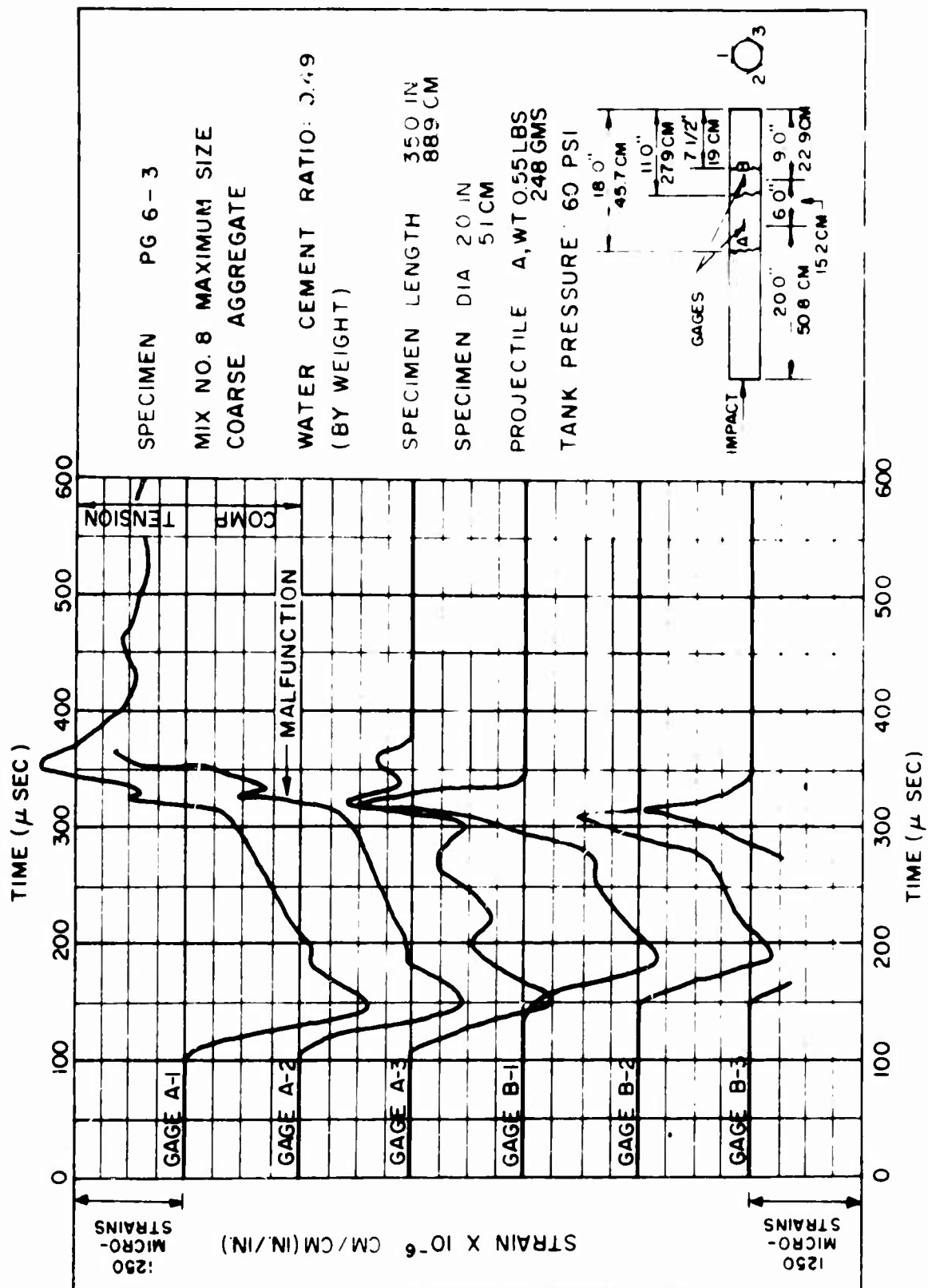
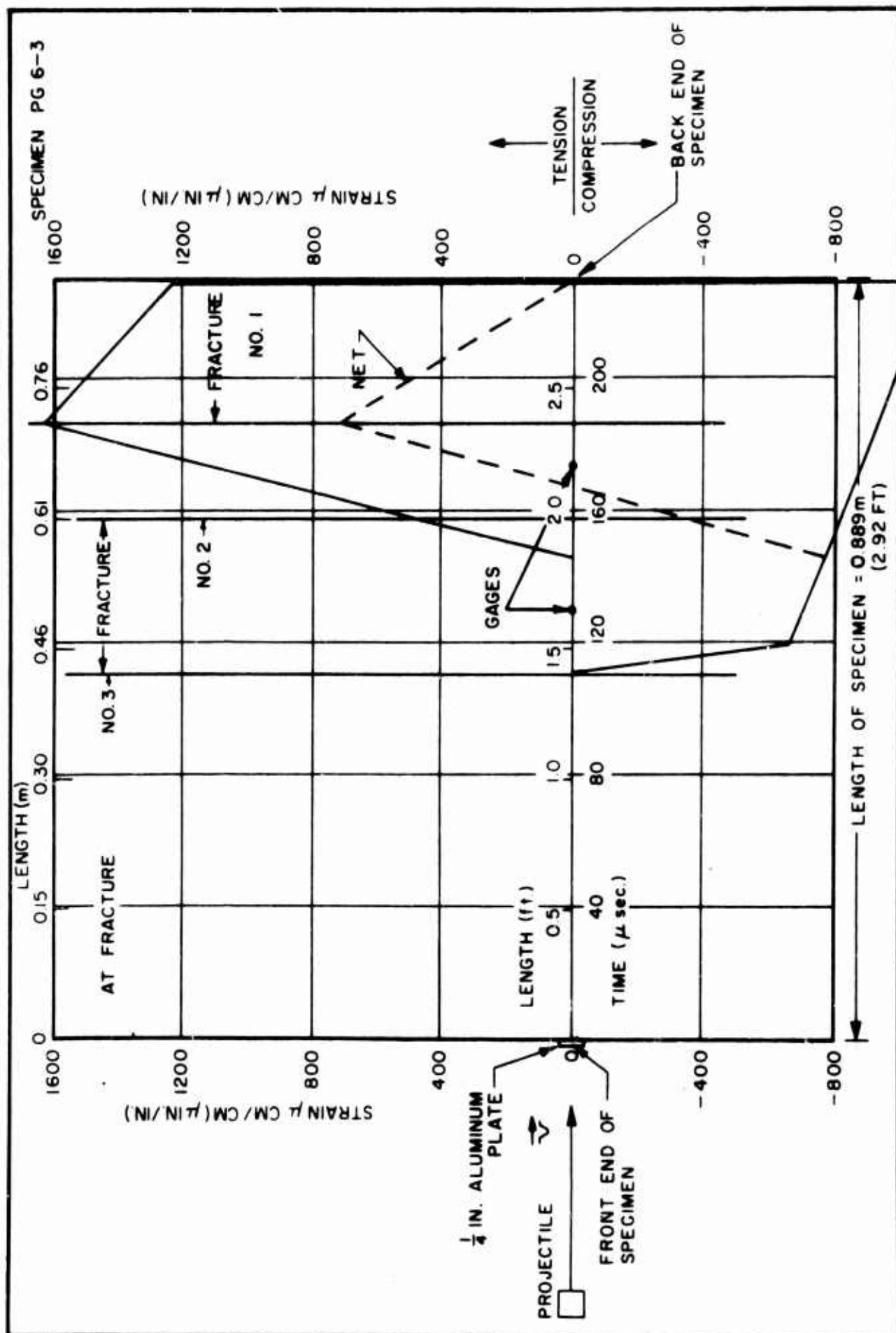


FIGURE 74



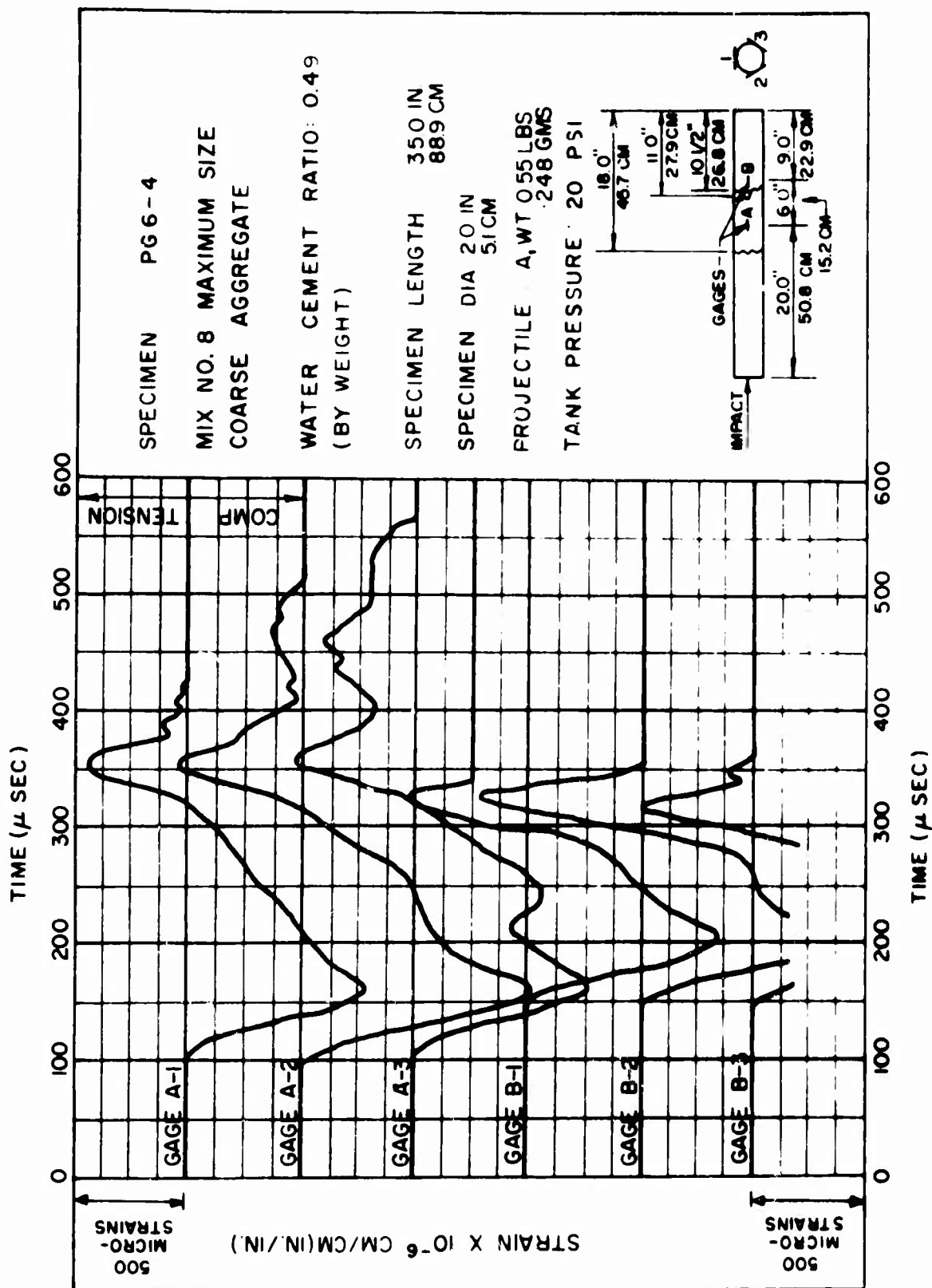
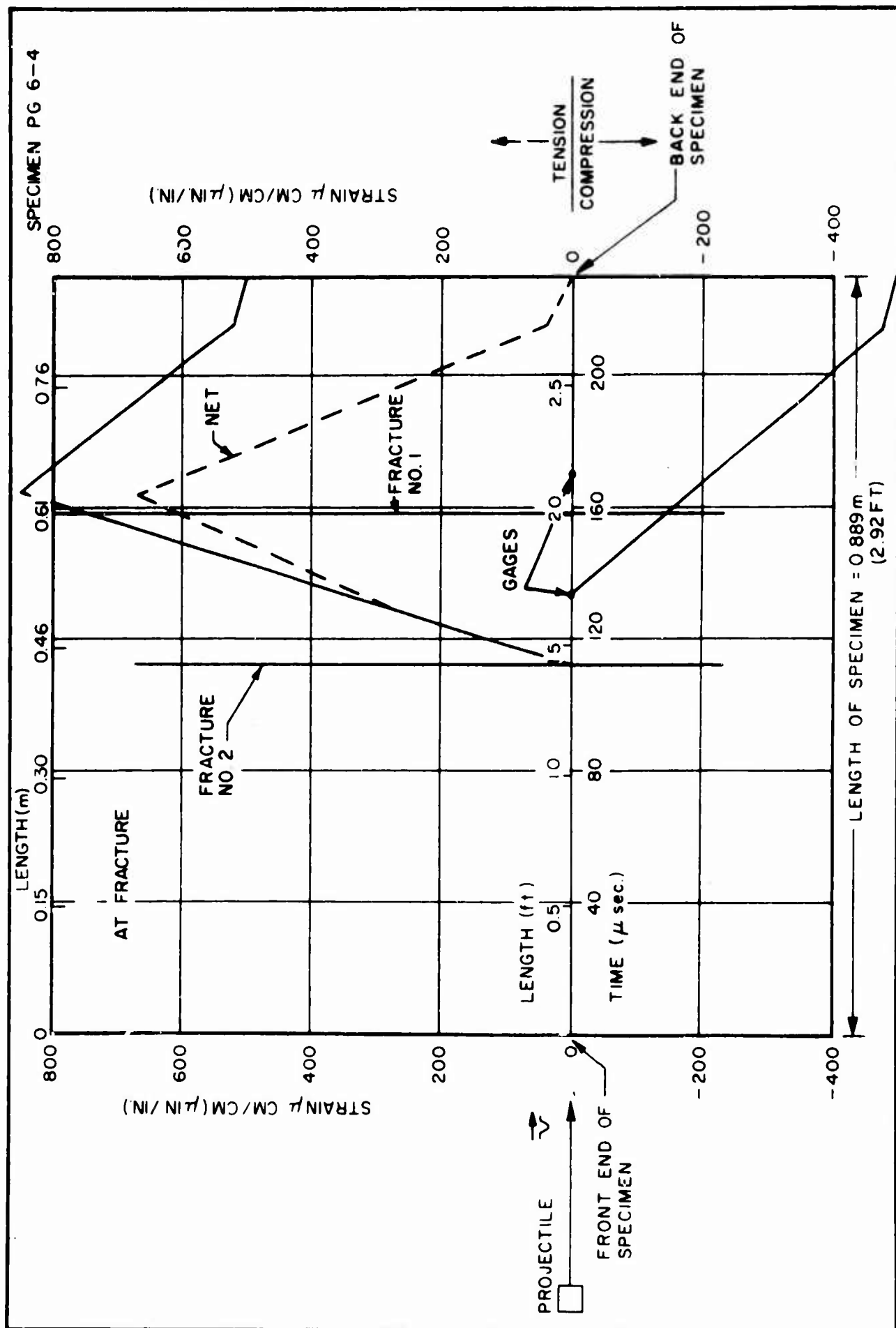


FIGURE 76



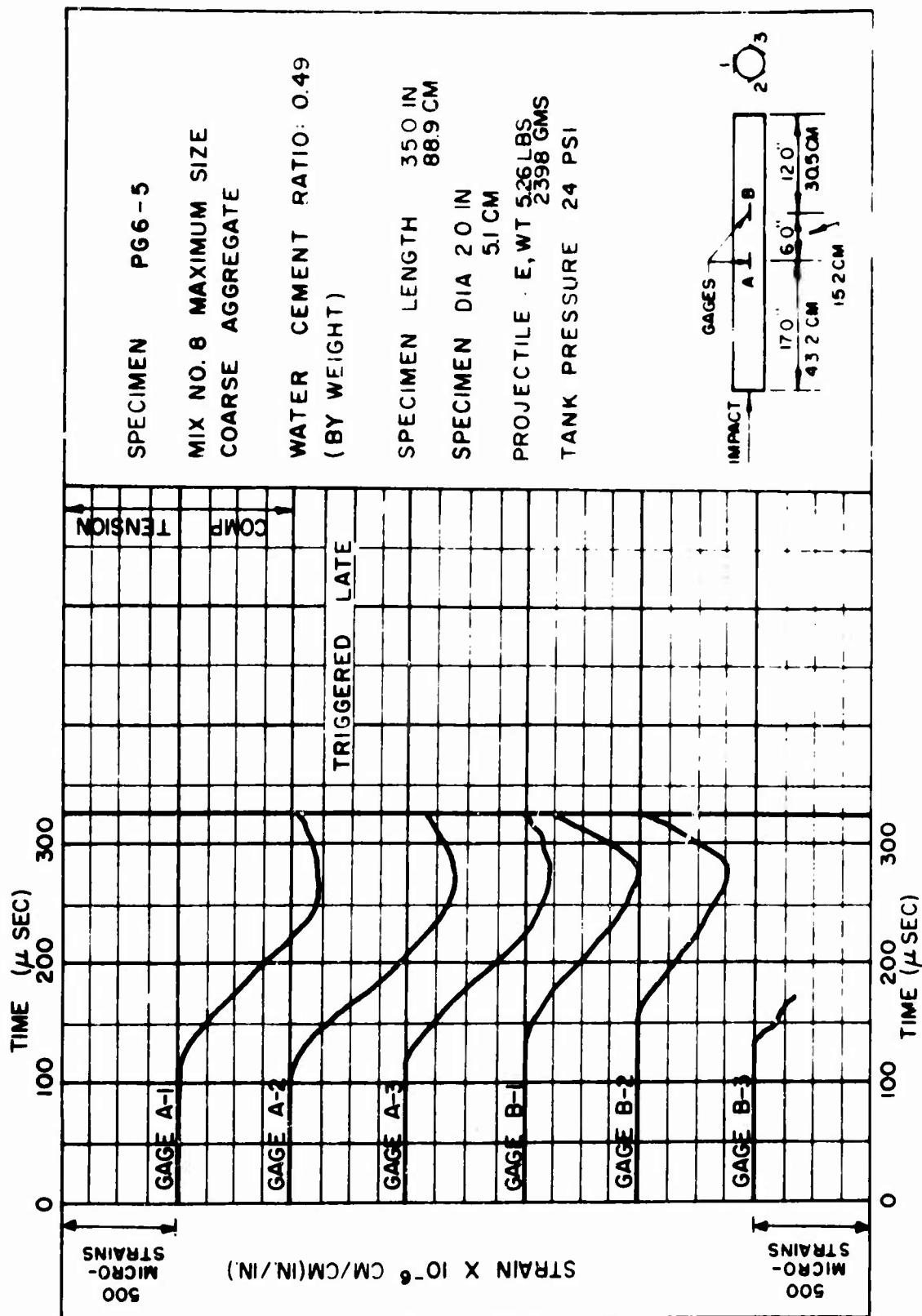
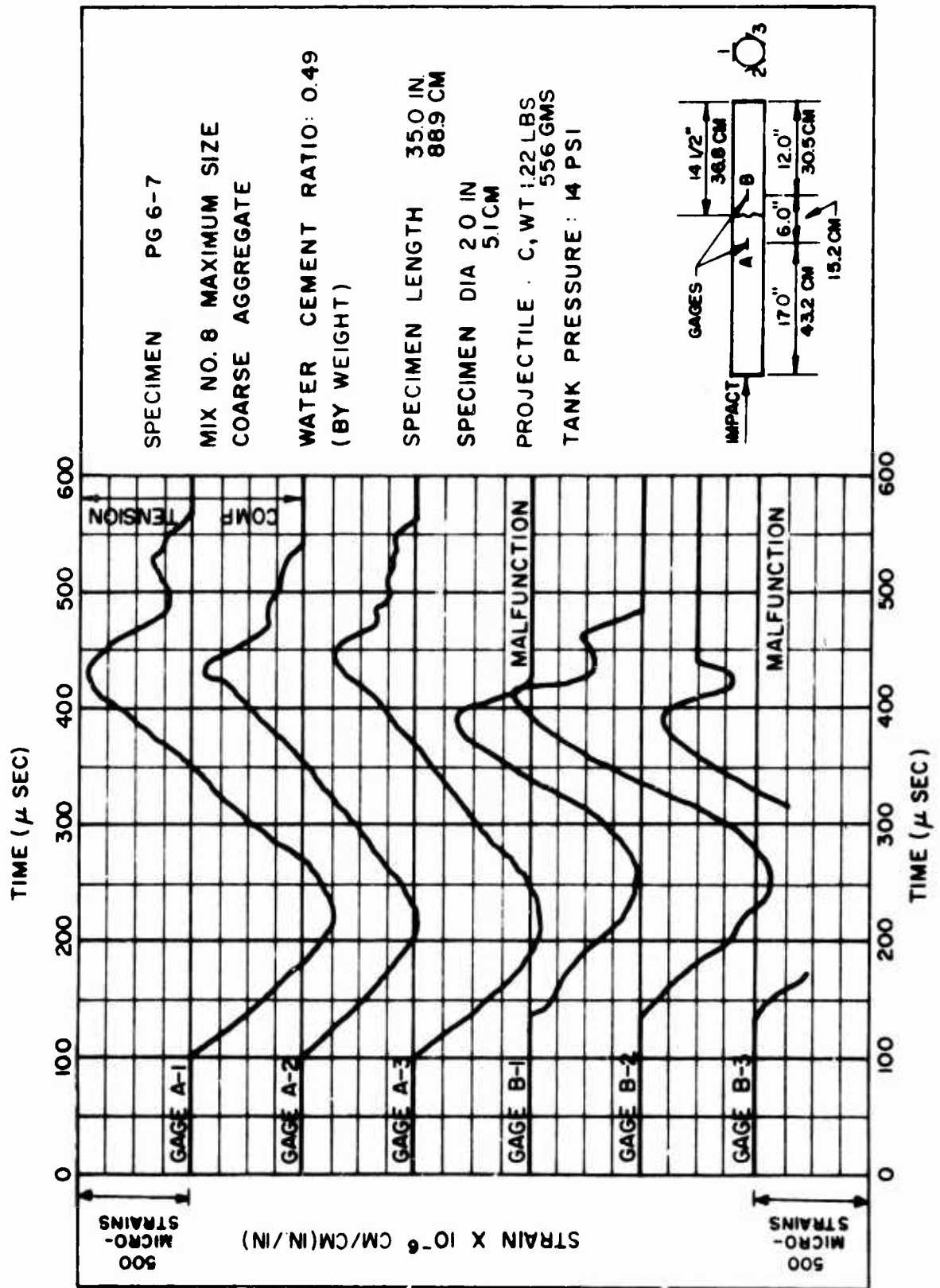
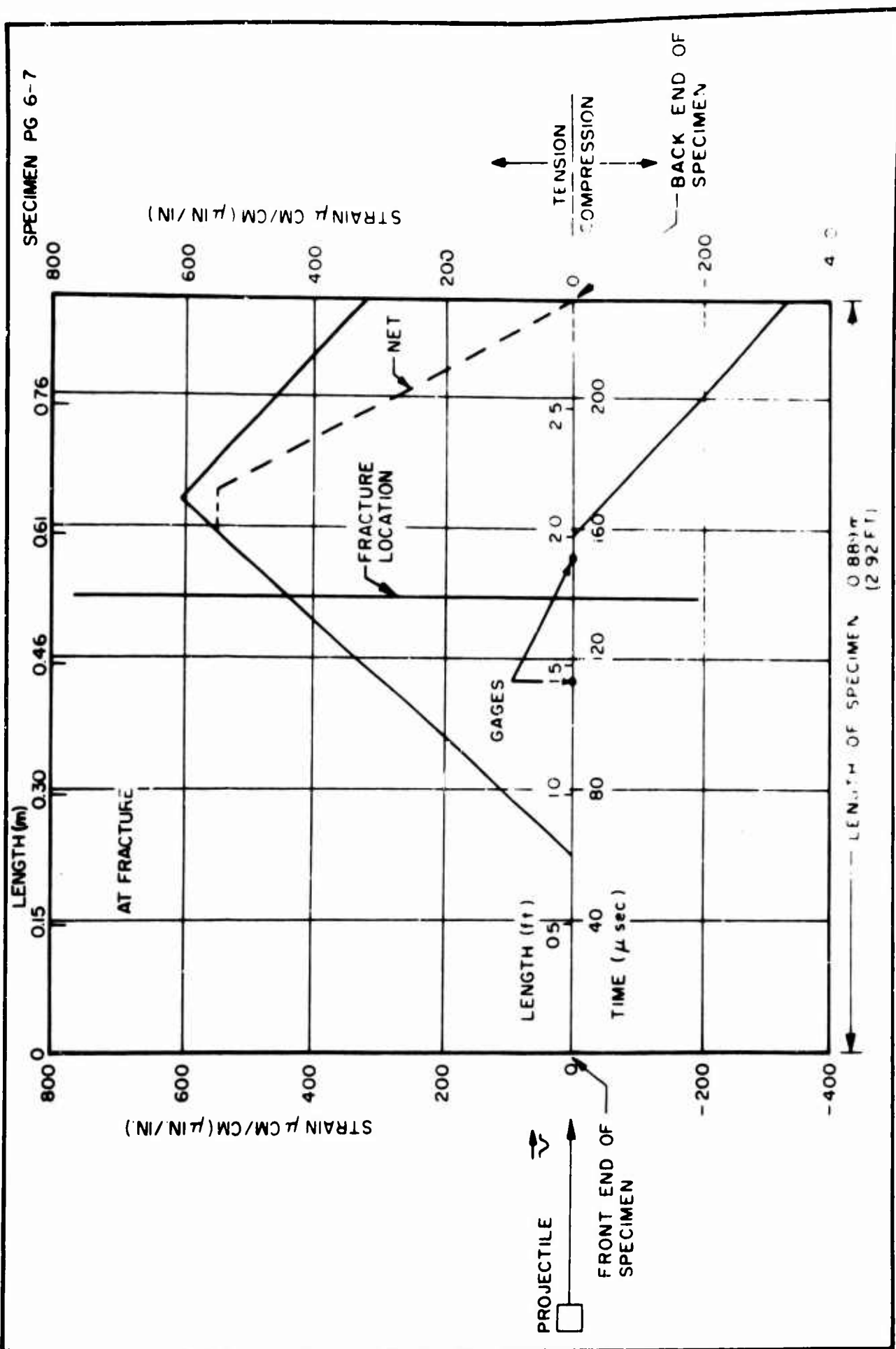
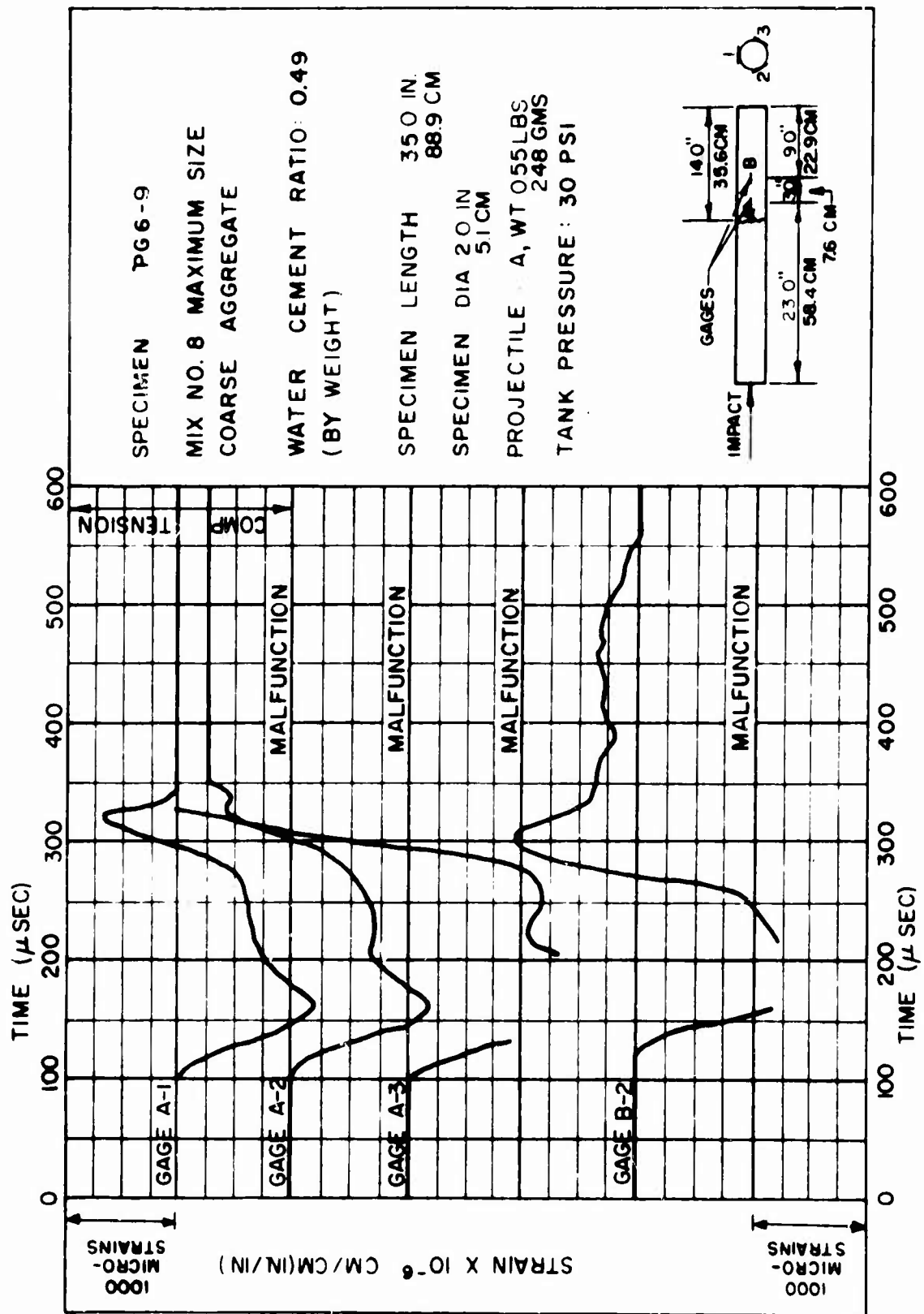
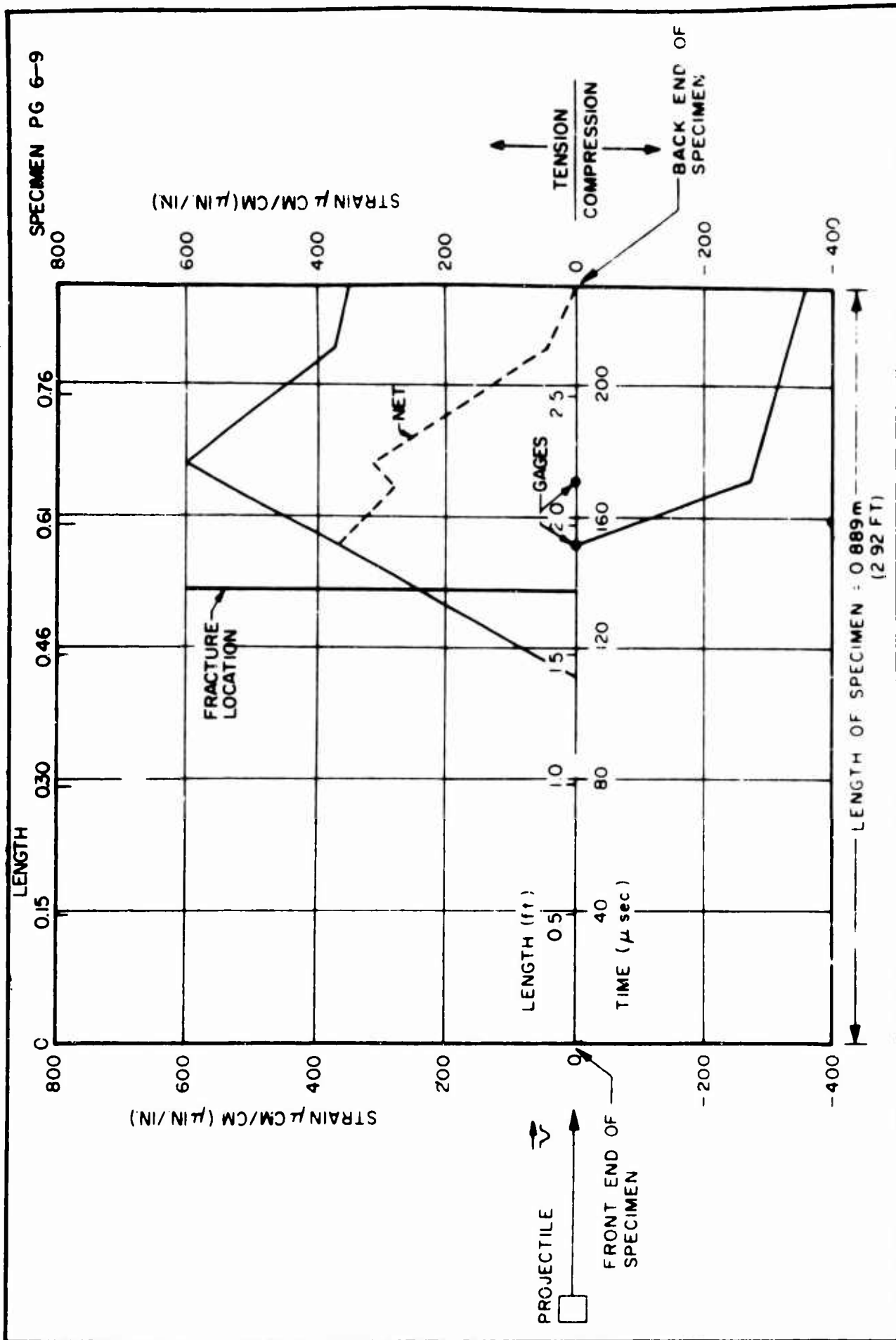


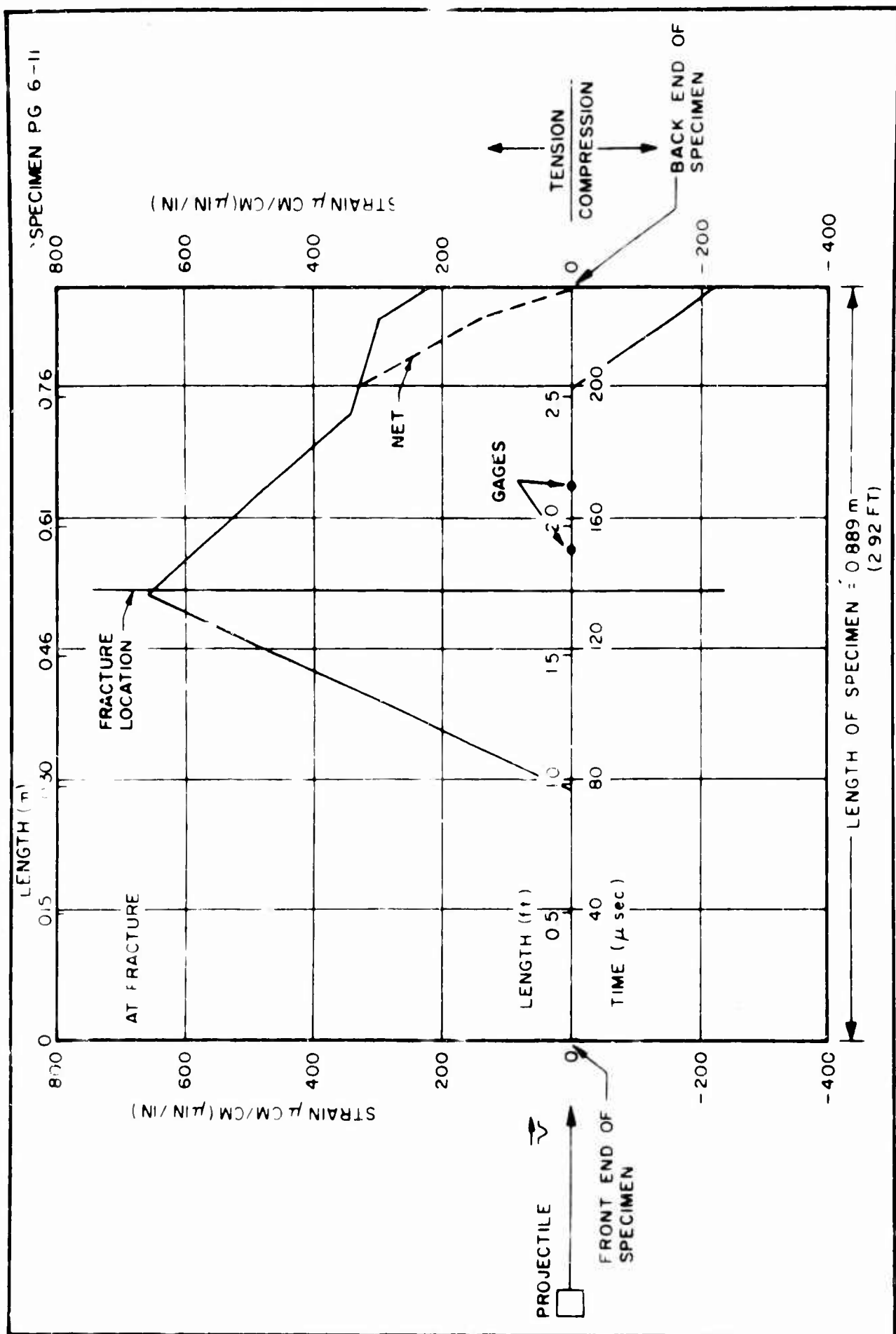
FIGURE 78











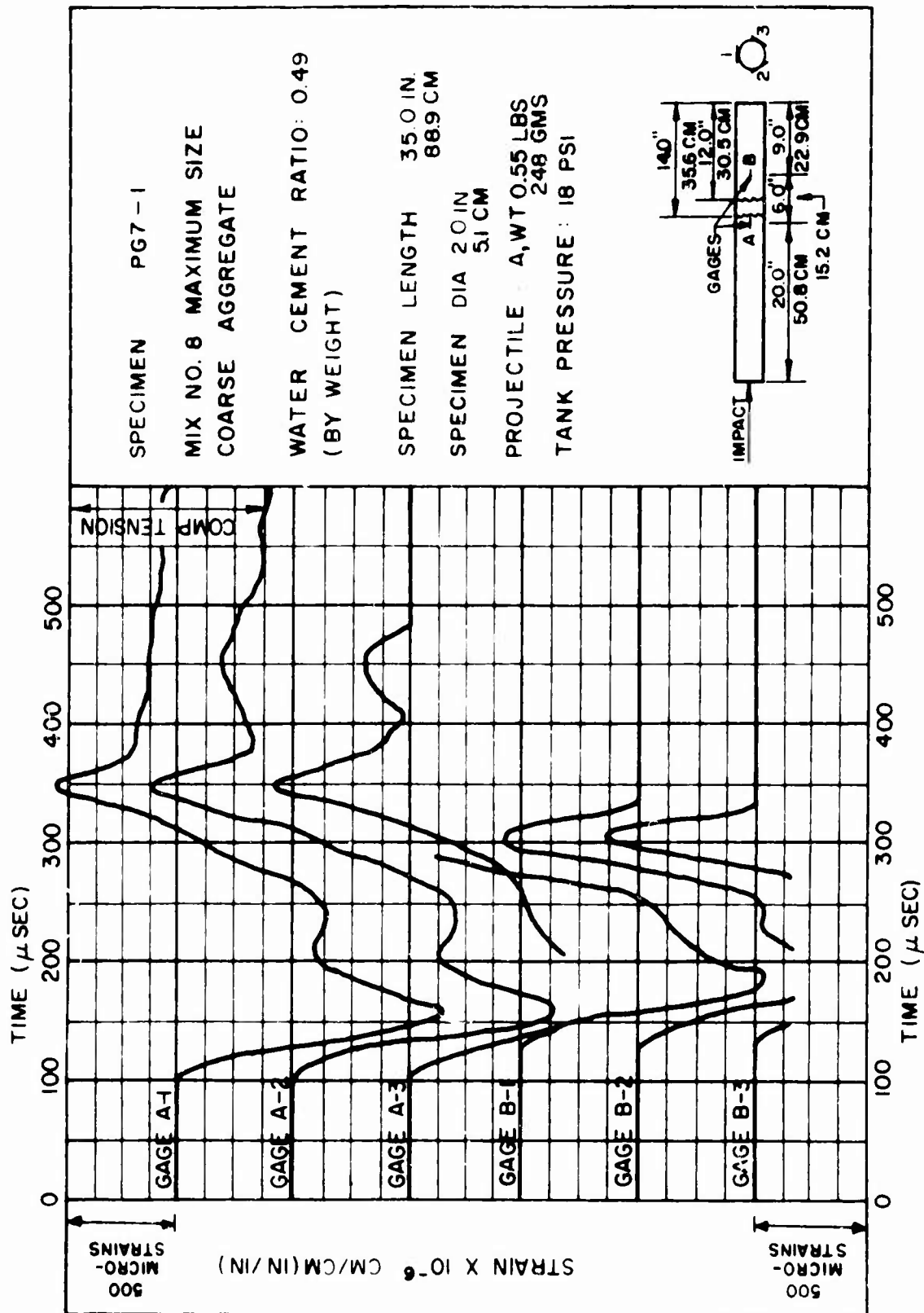
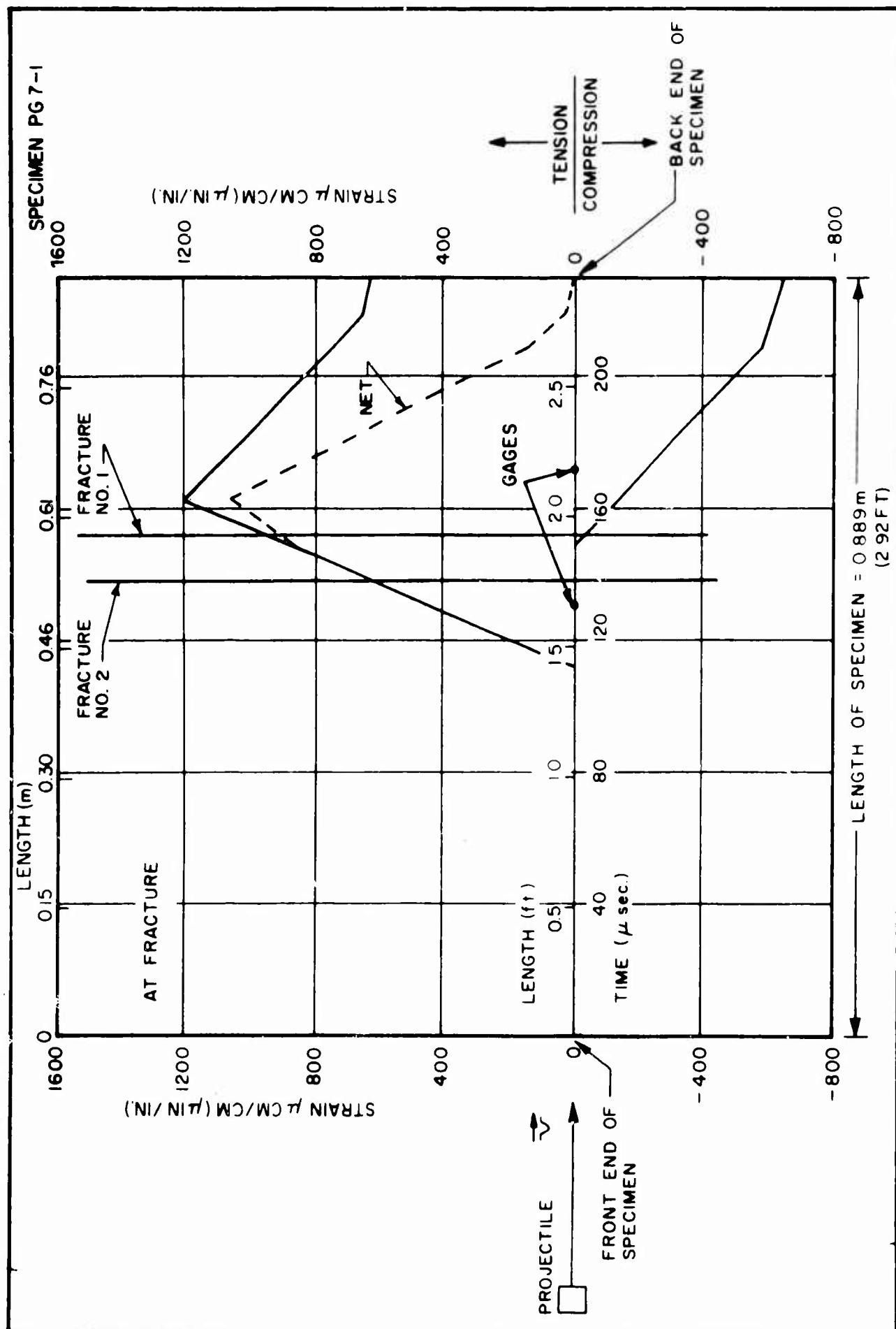


FIGURE 85



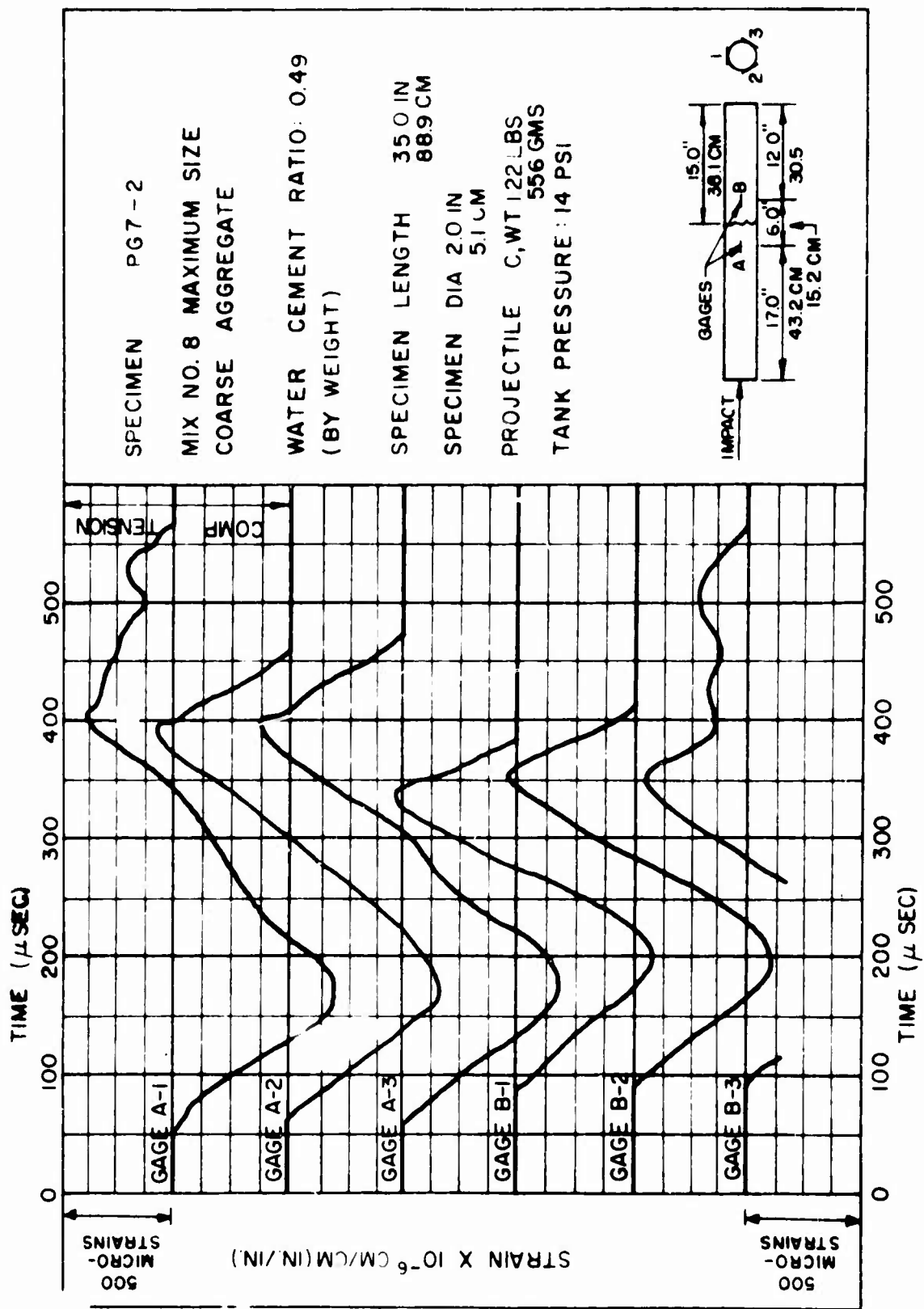
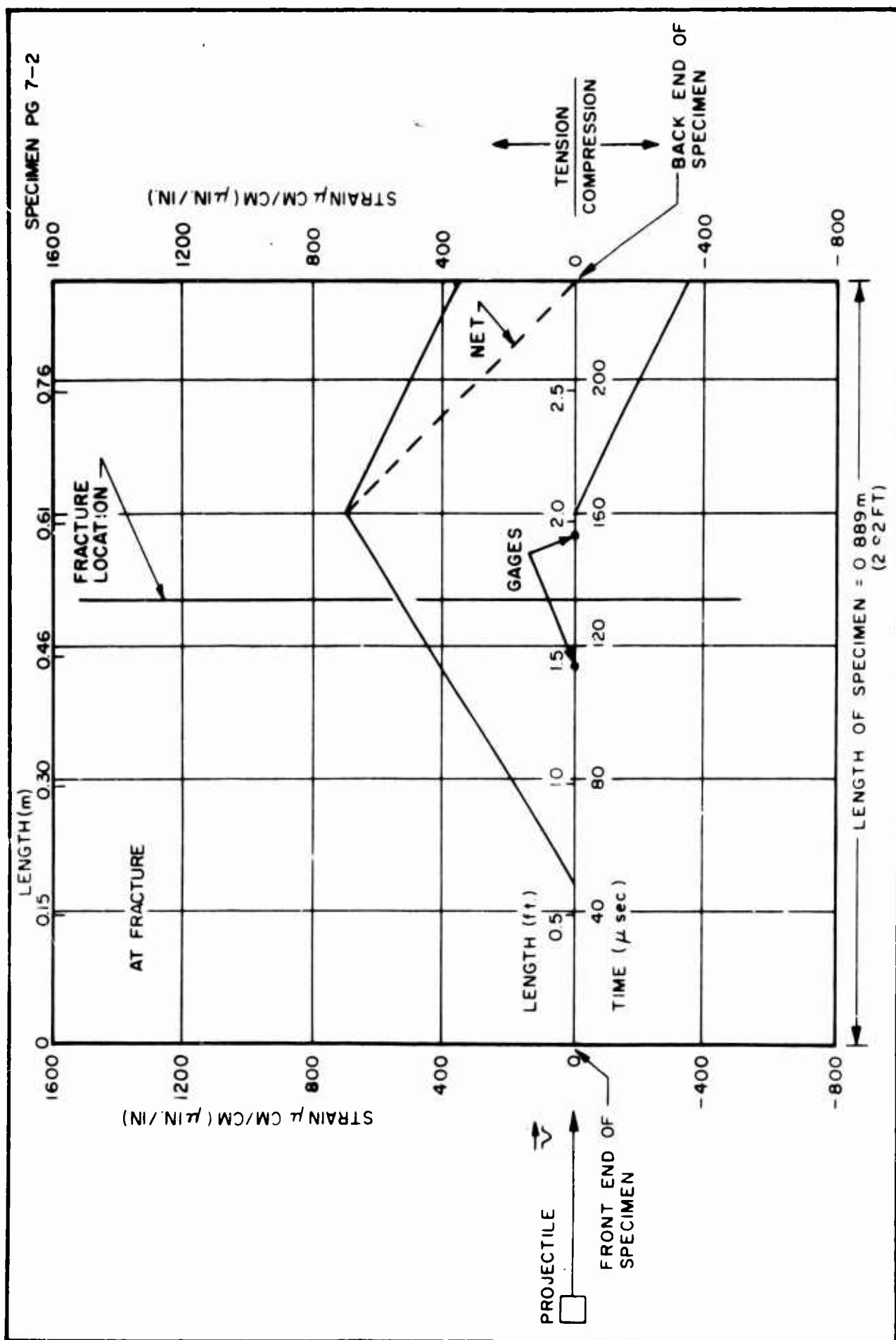
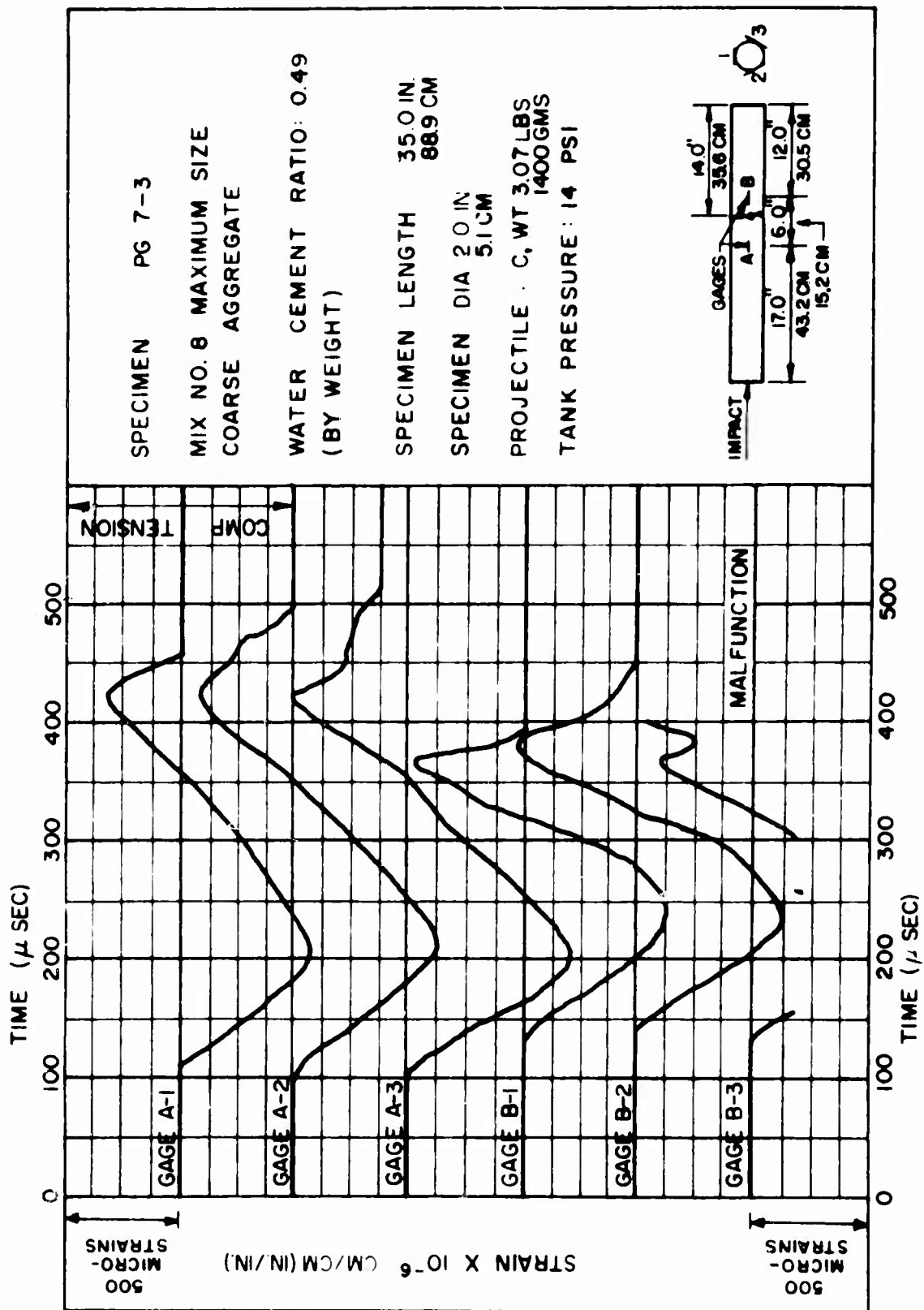
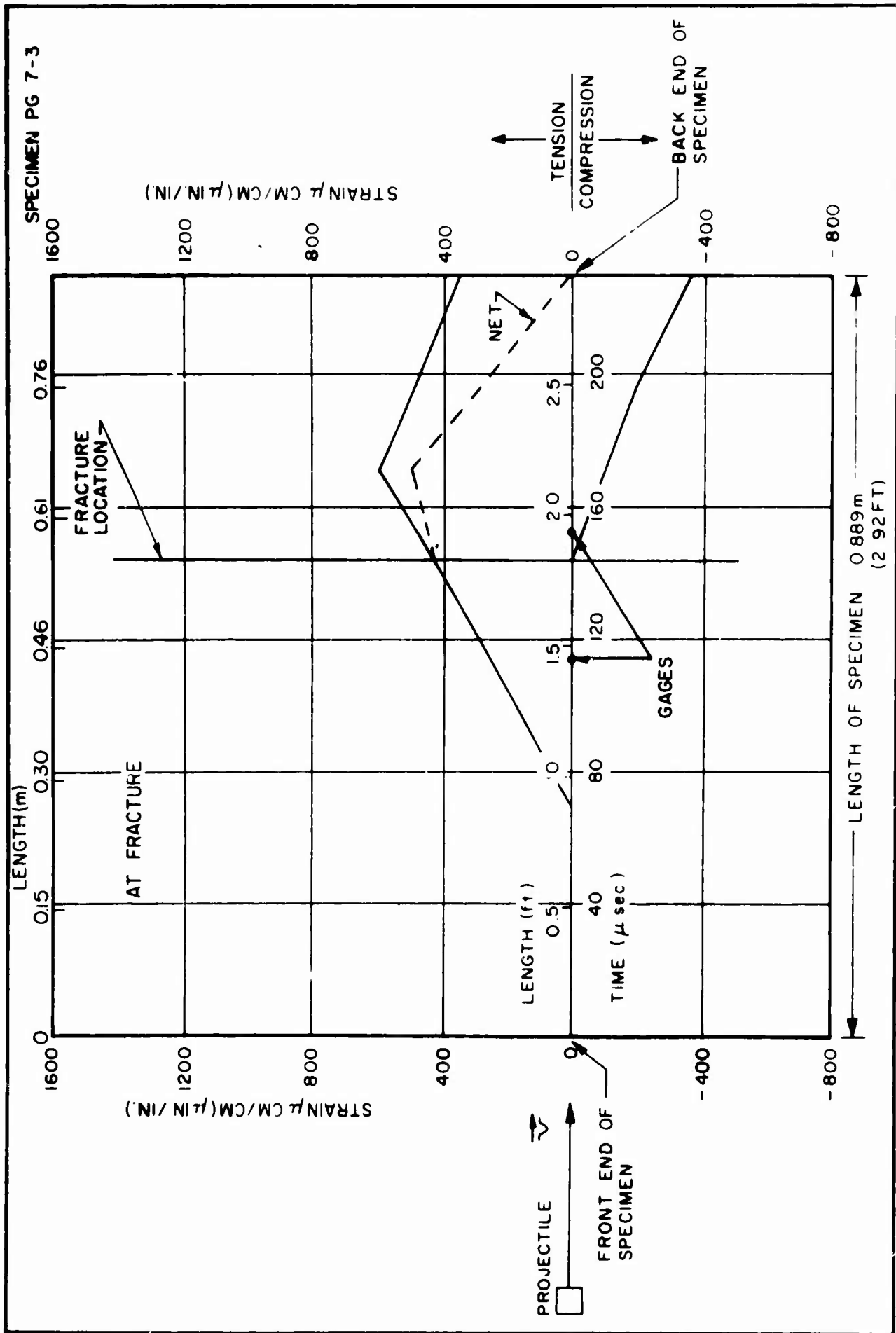
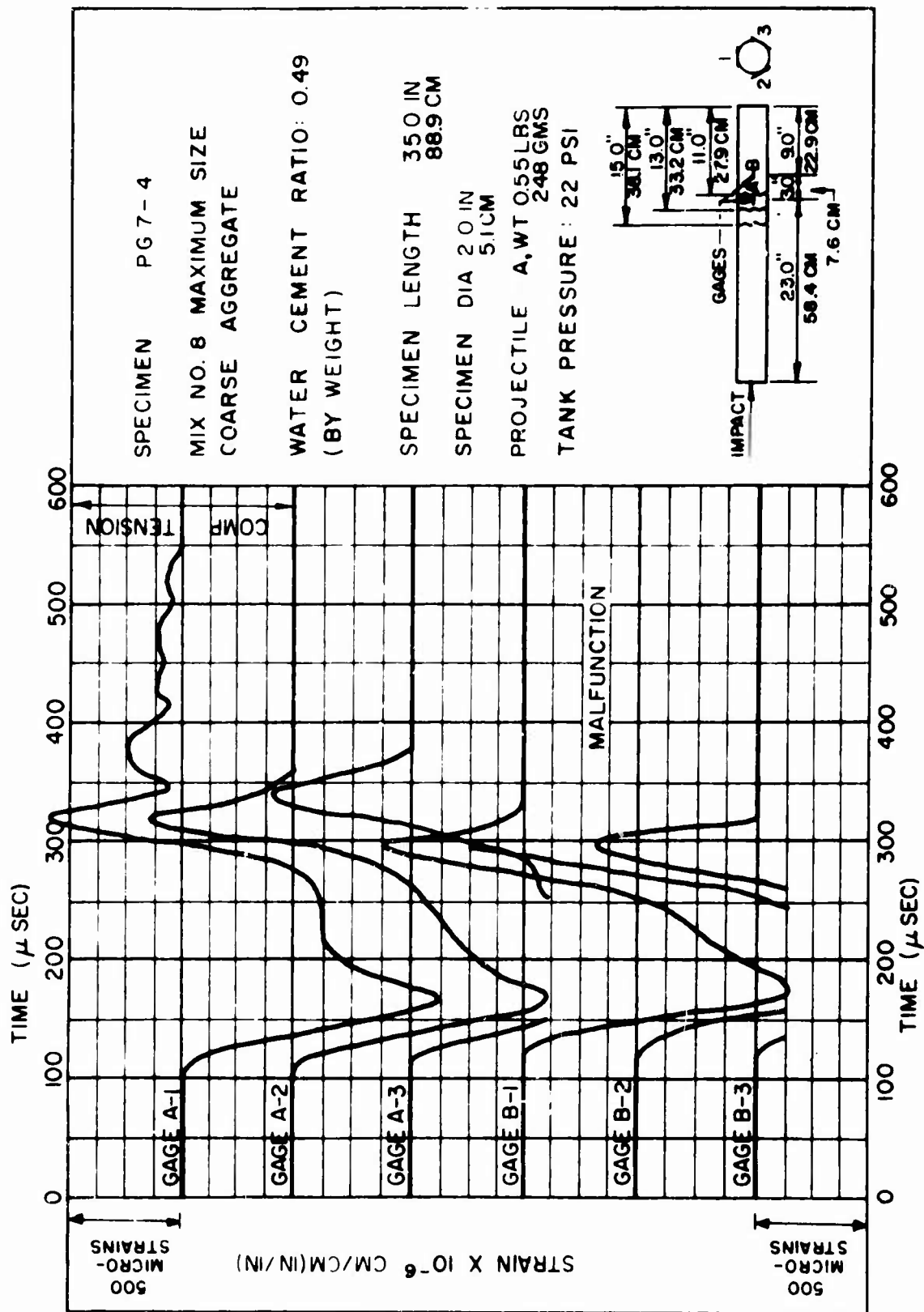


FIGURE 87









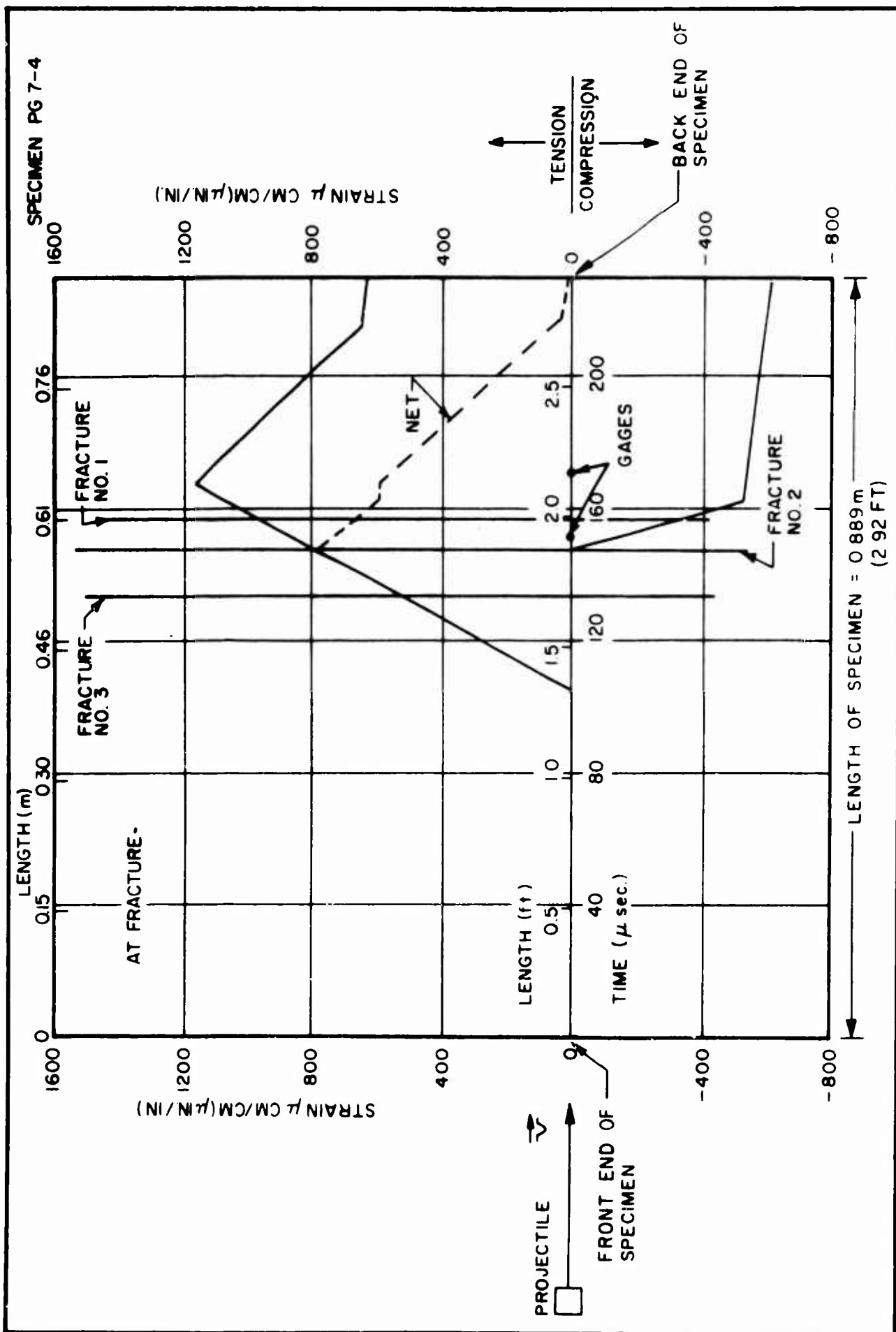
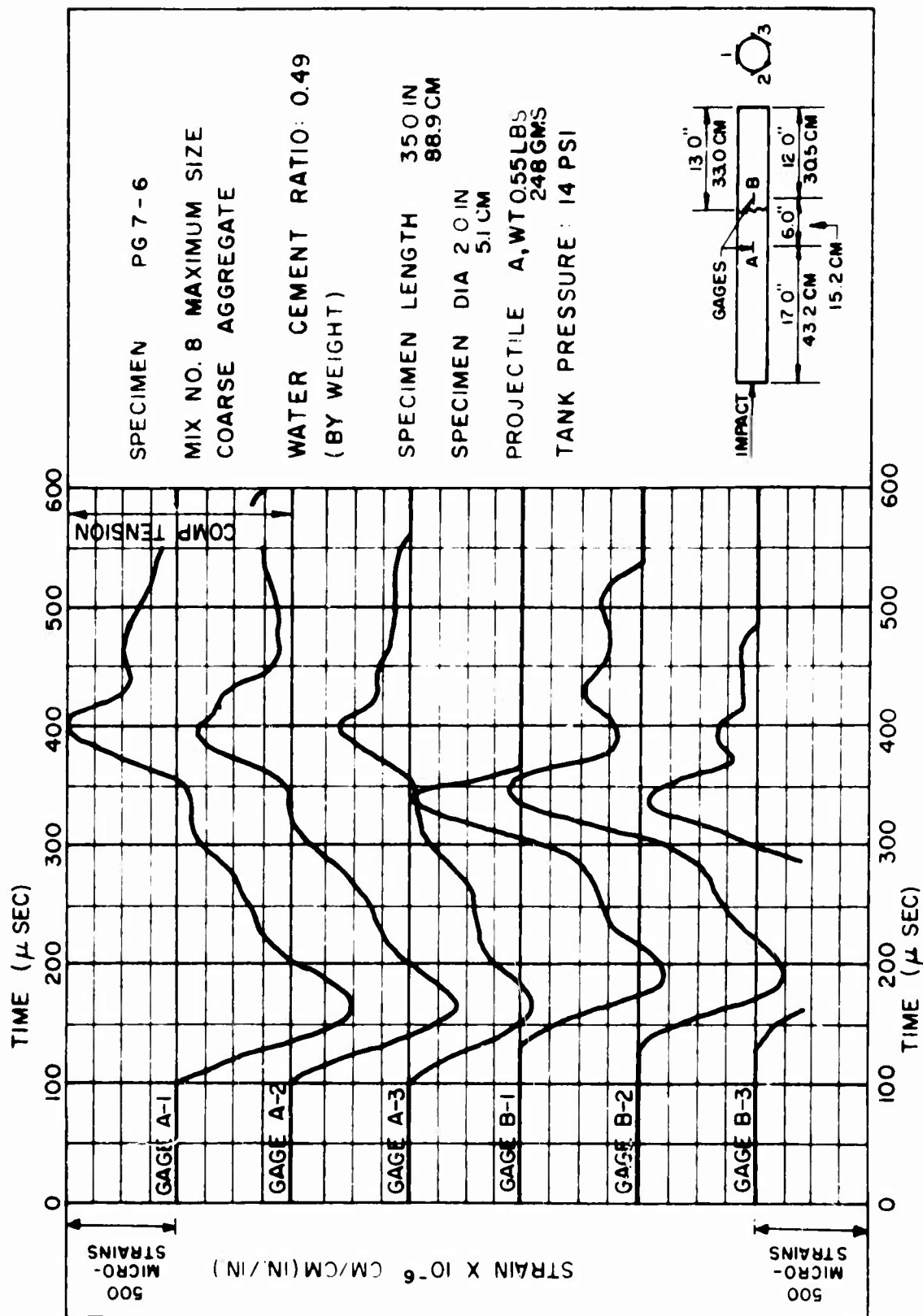
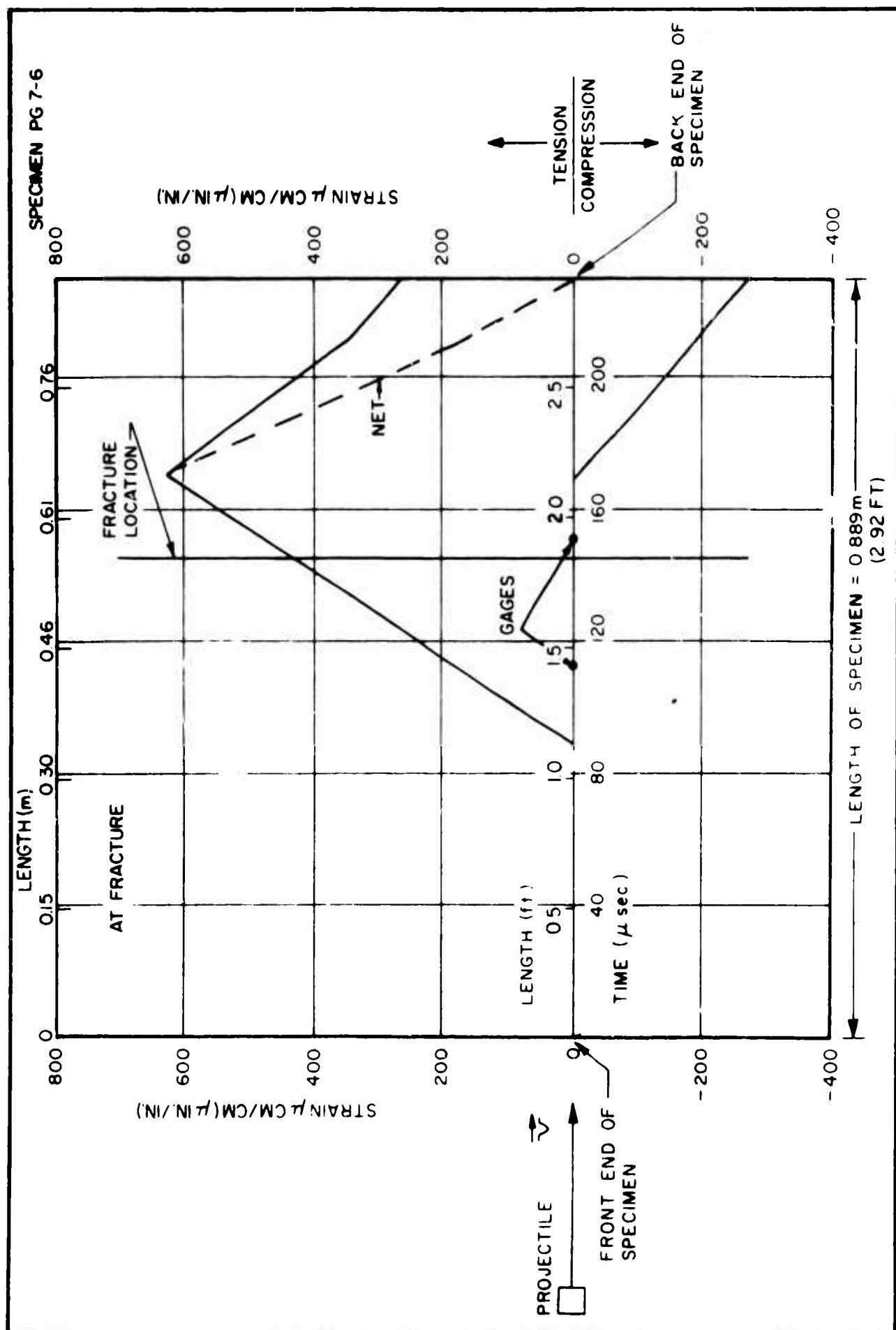
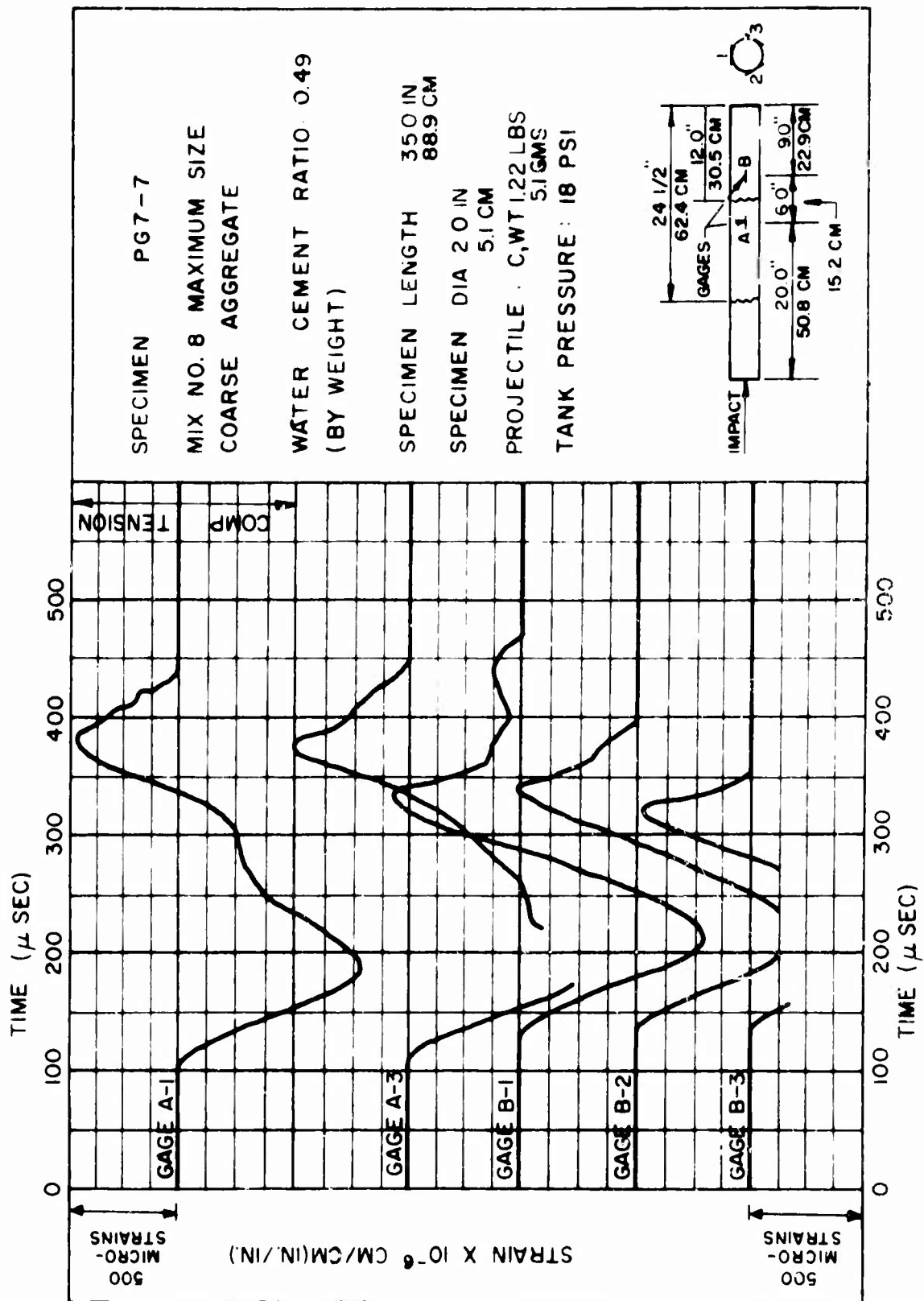
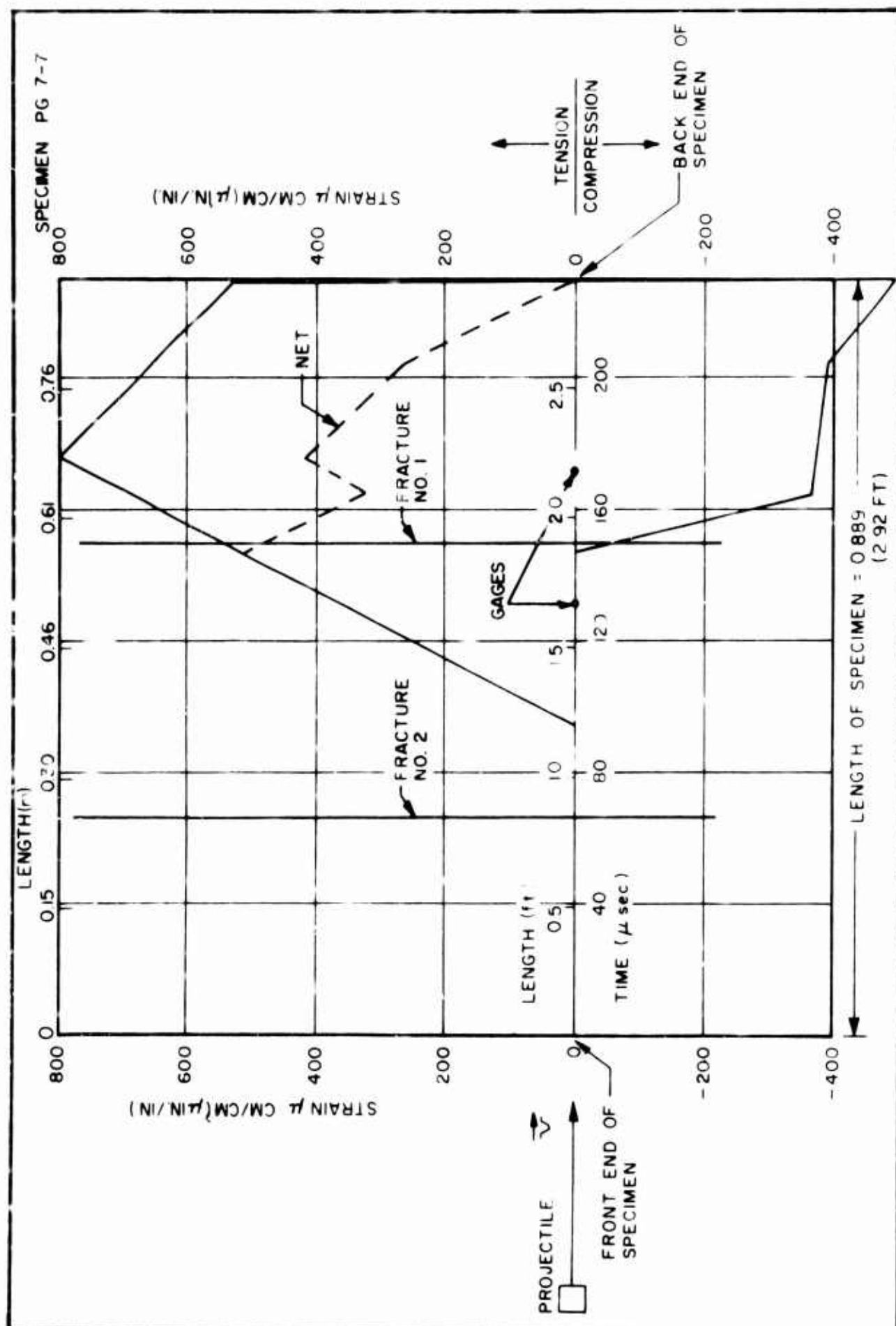


FIGURE 92









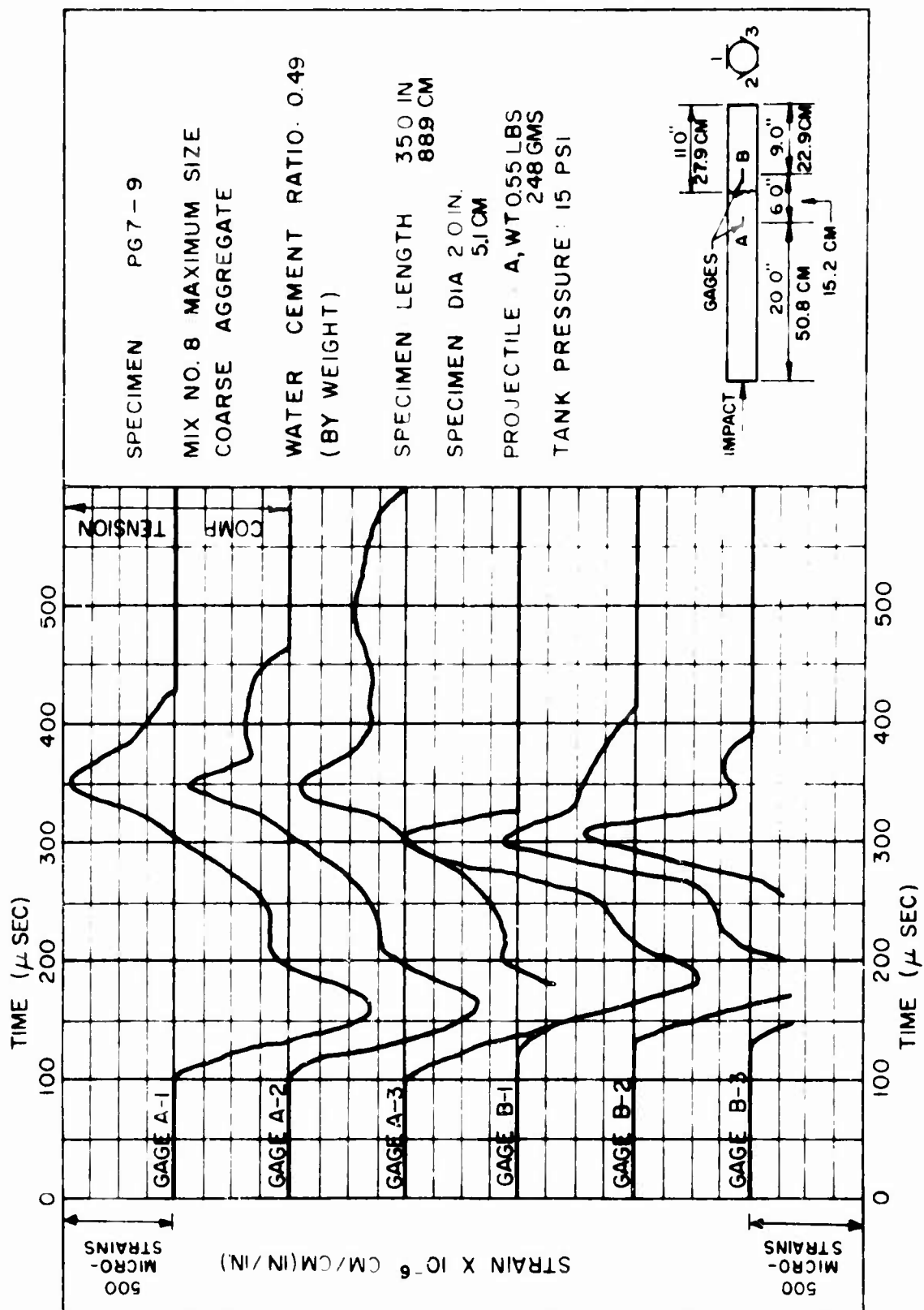
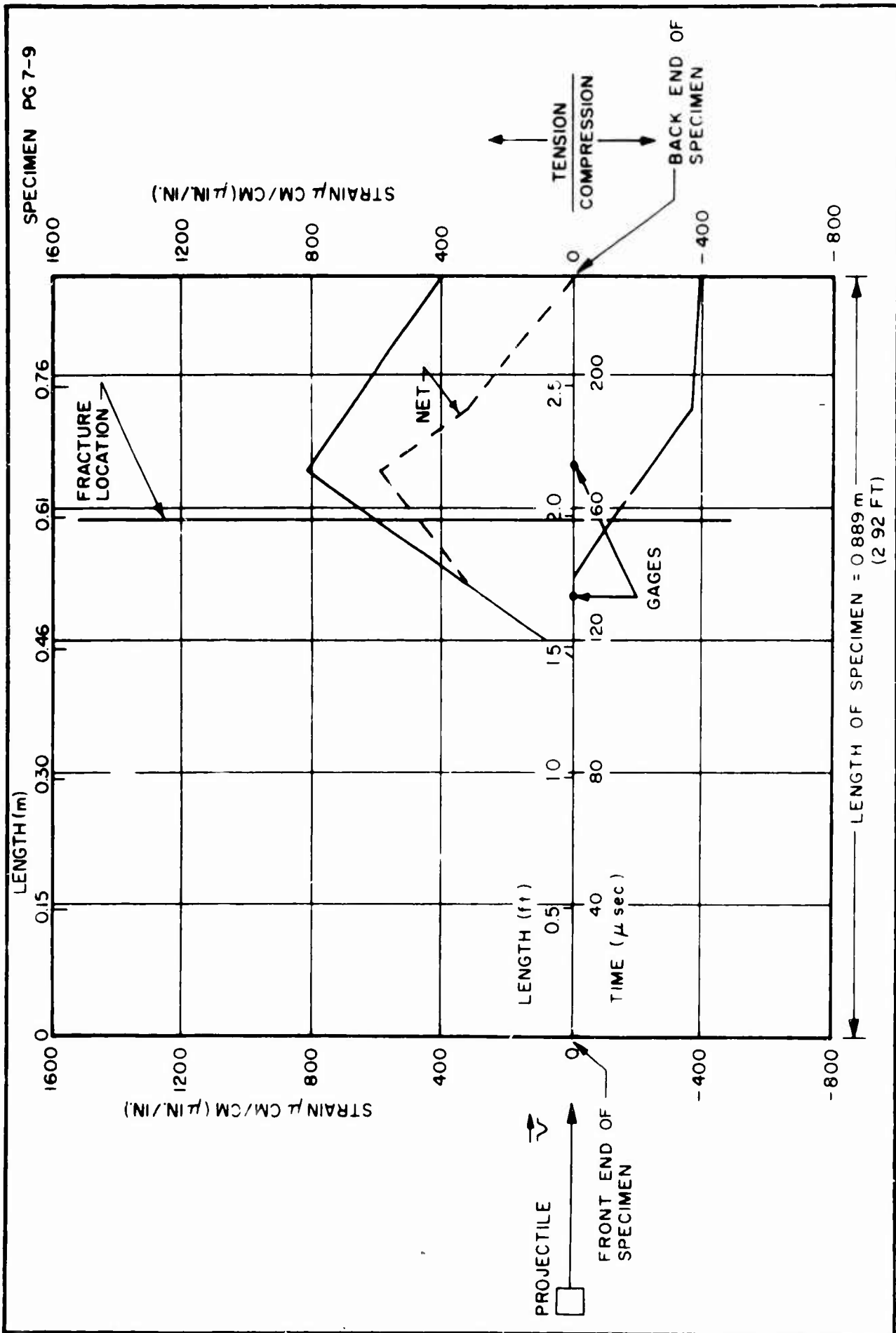
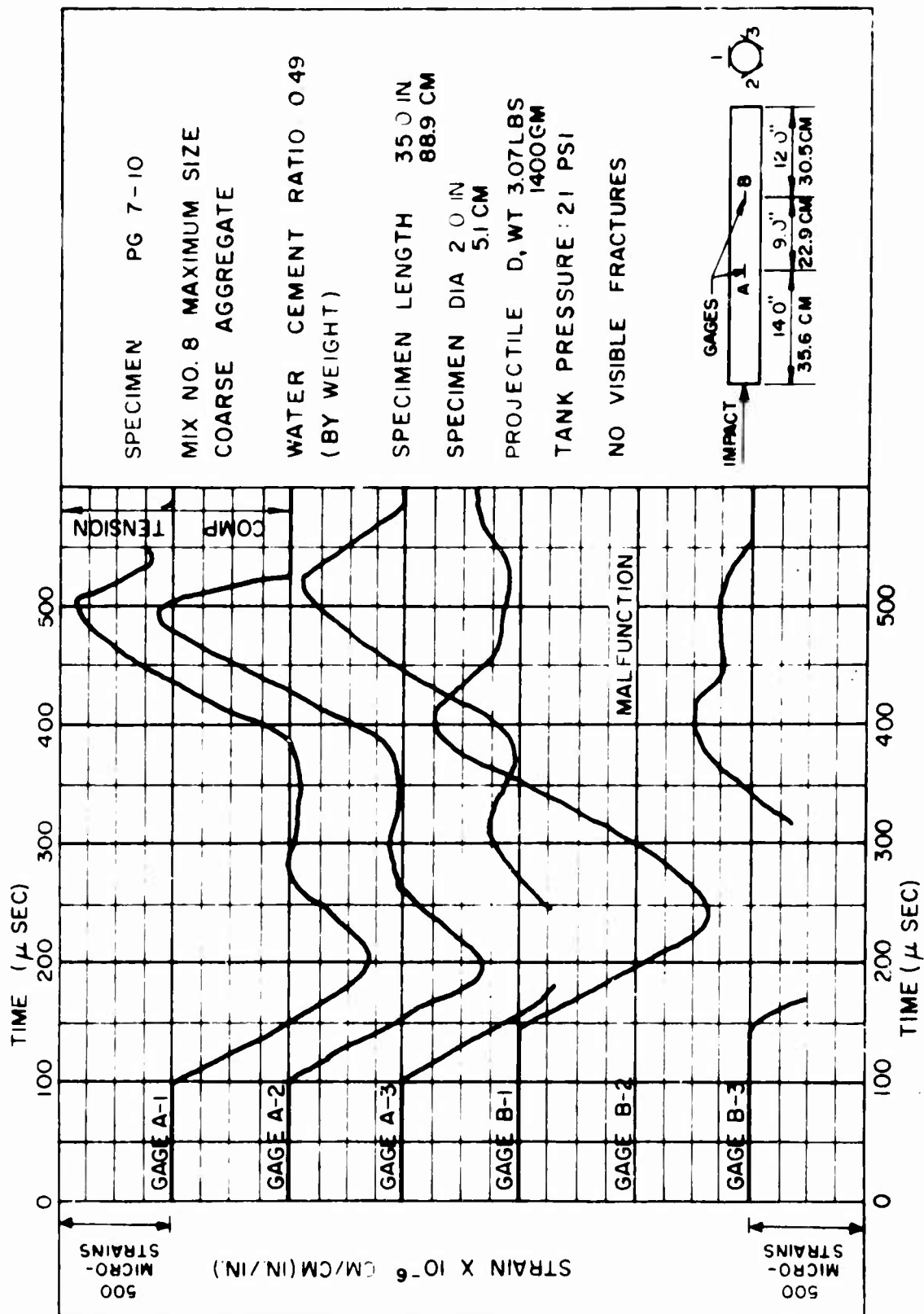
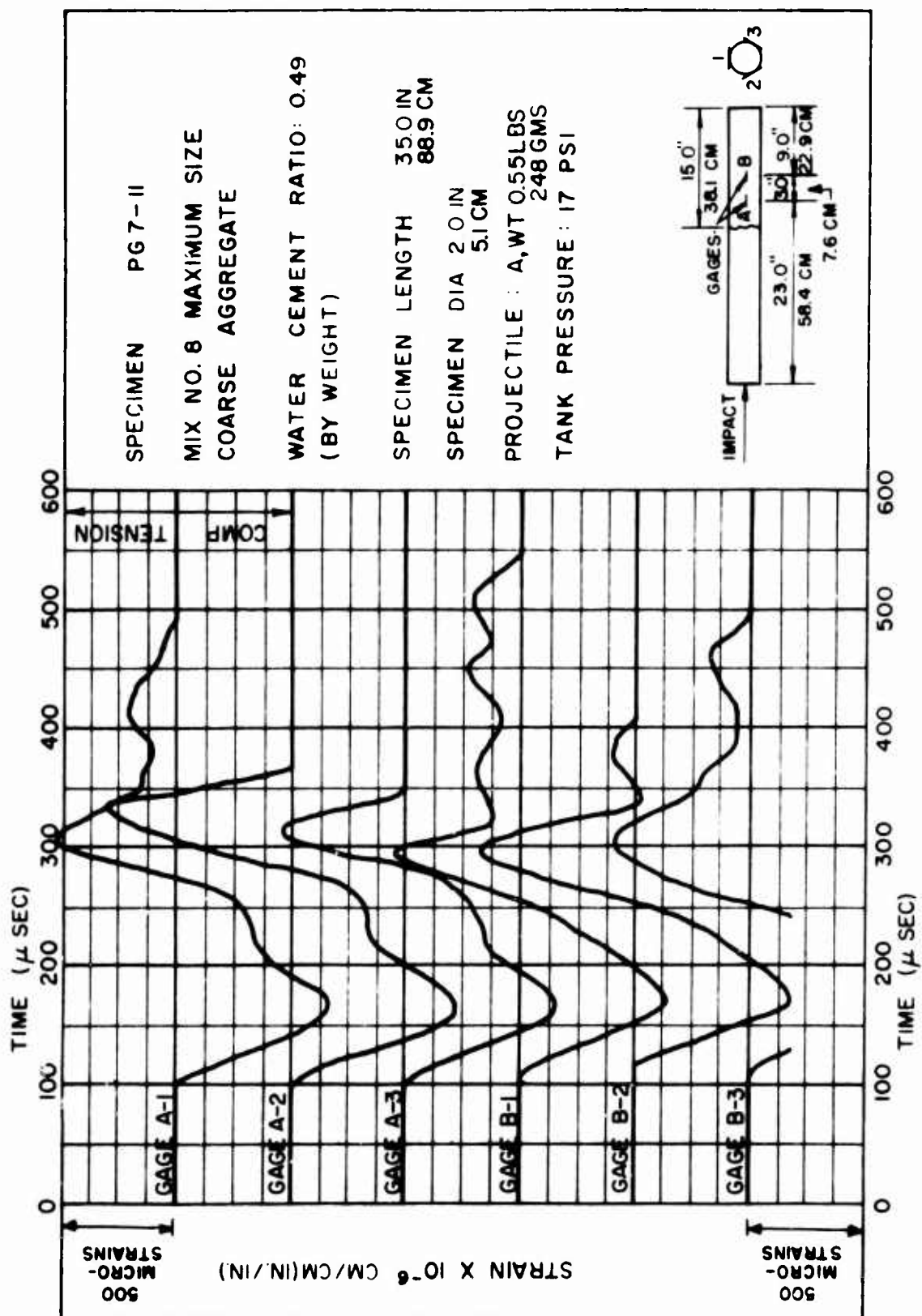
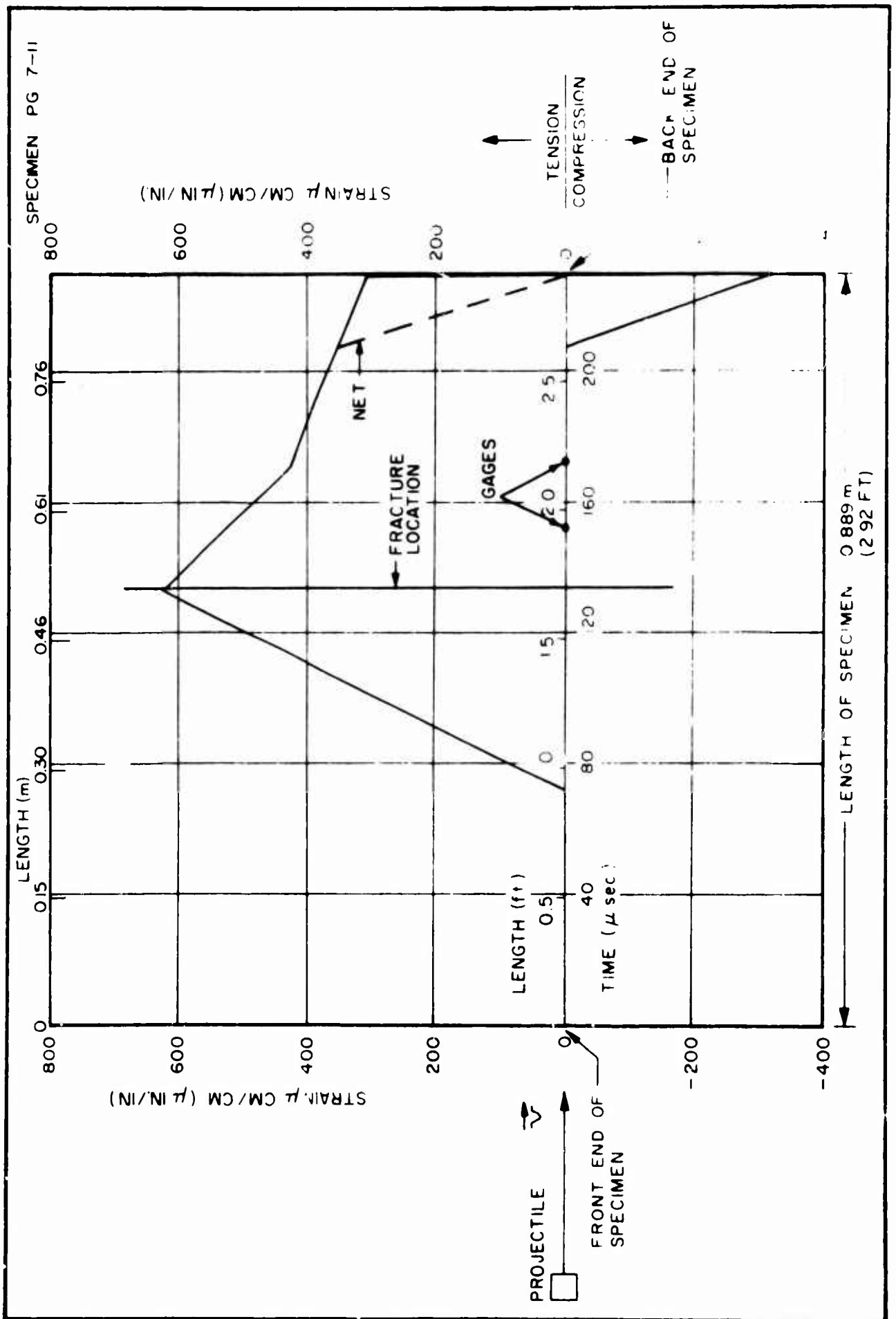


FIGURE 97









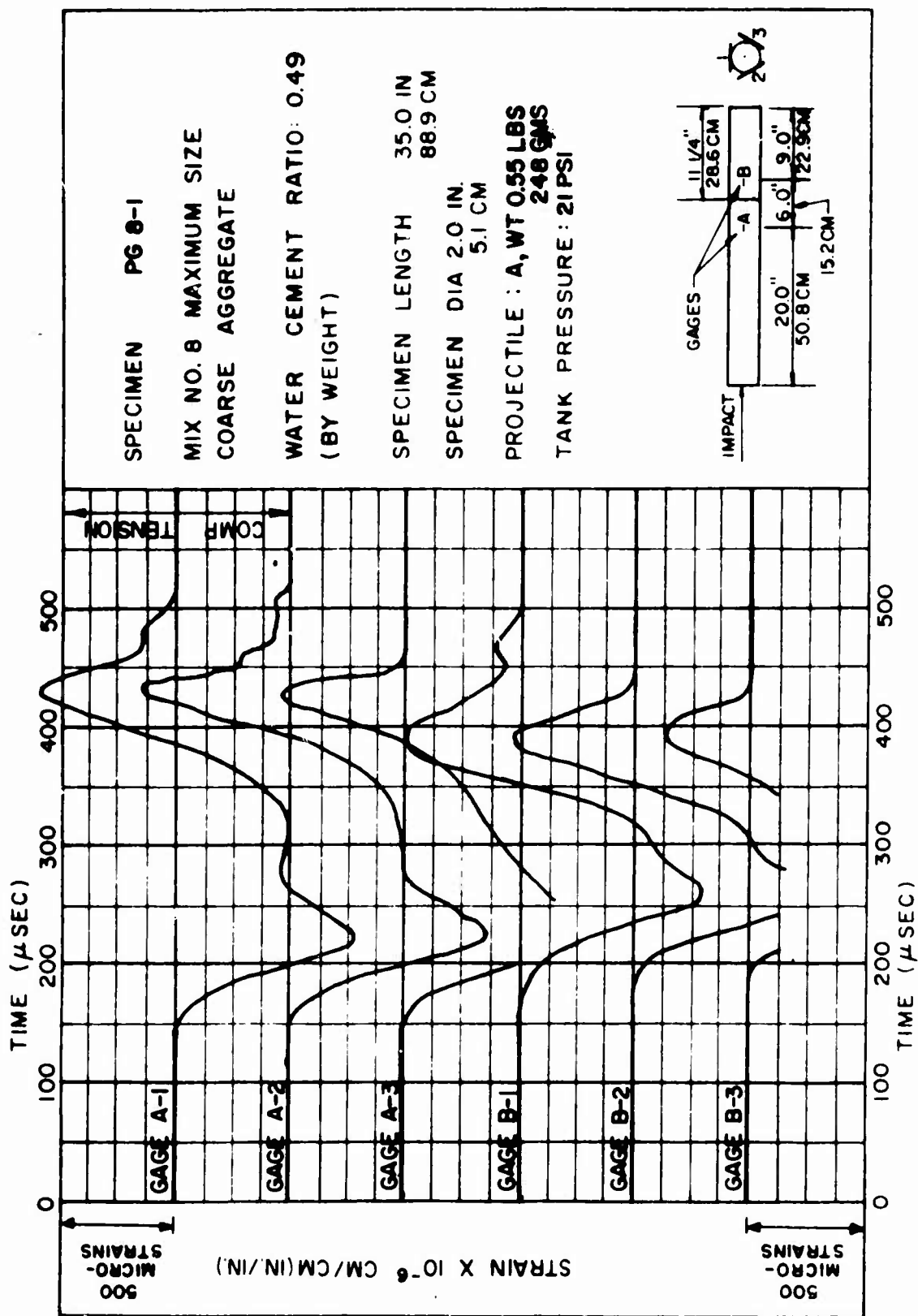
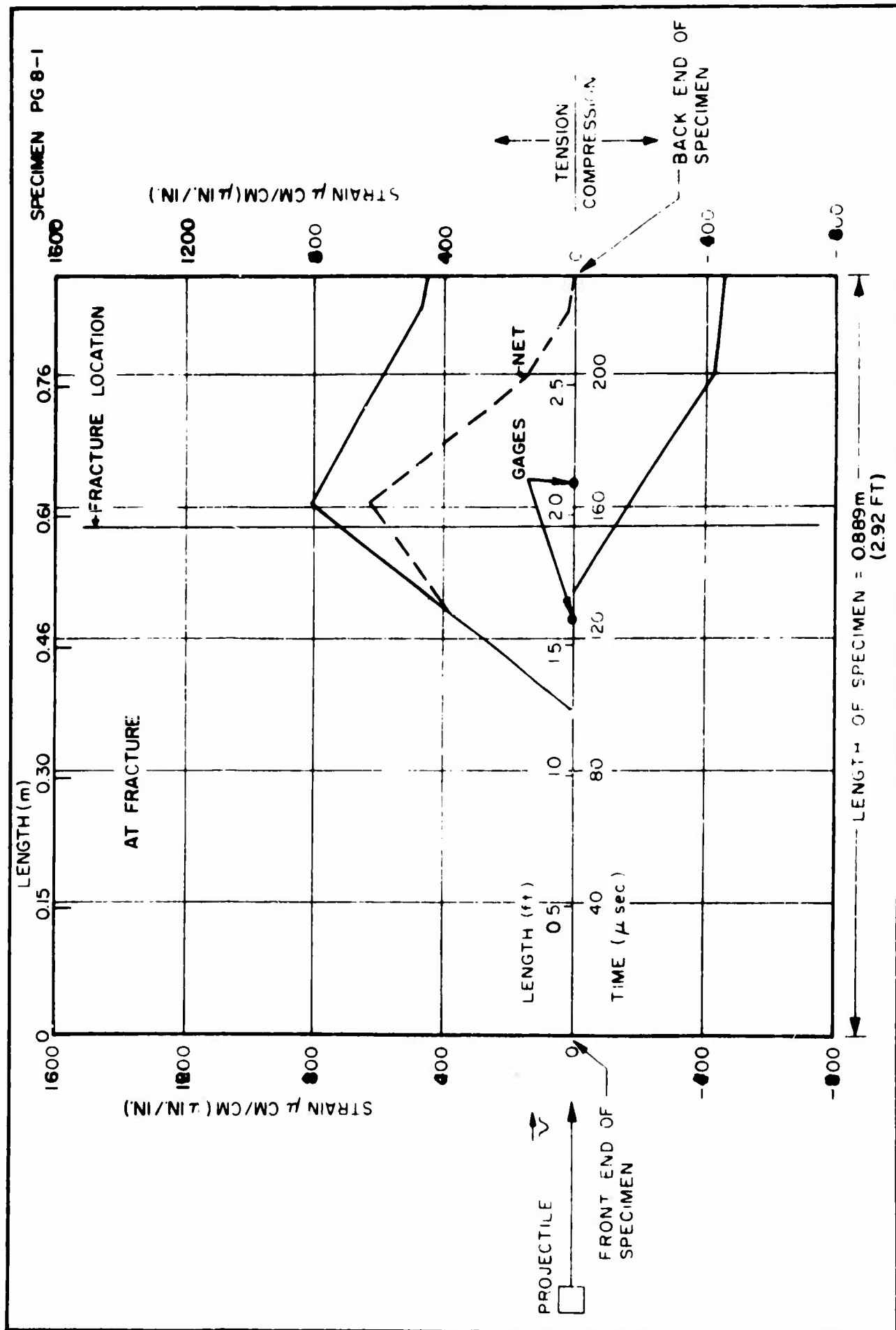


FIGURE 102



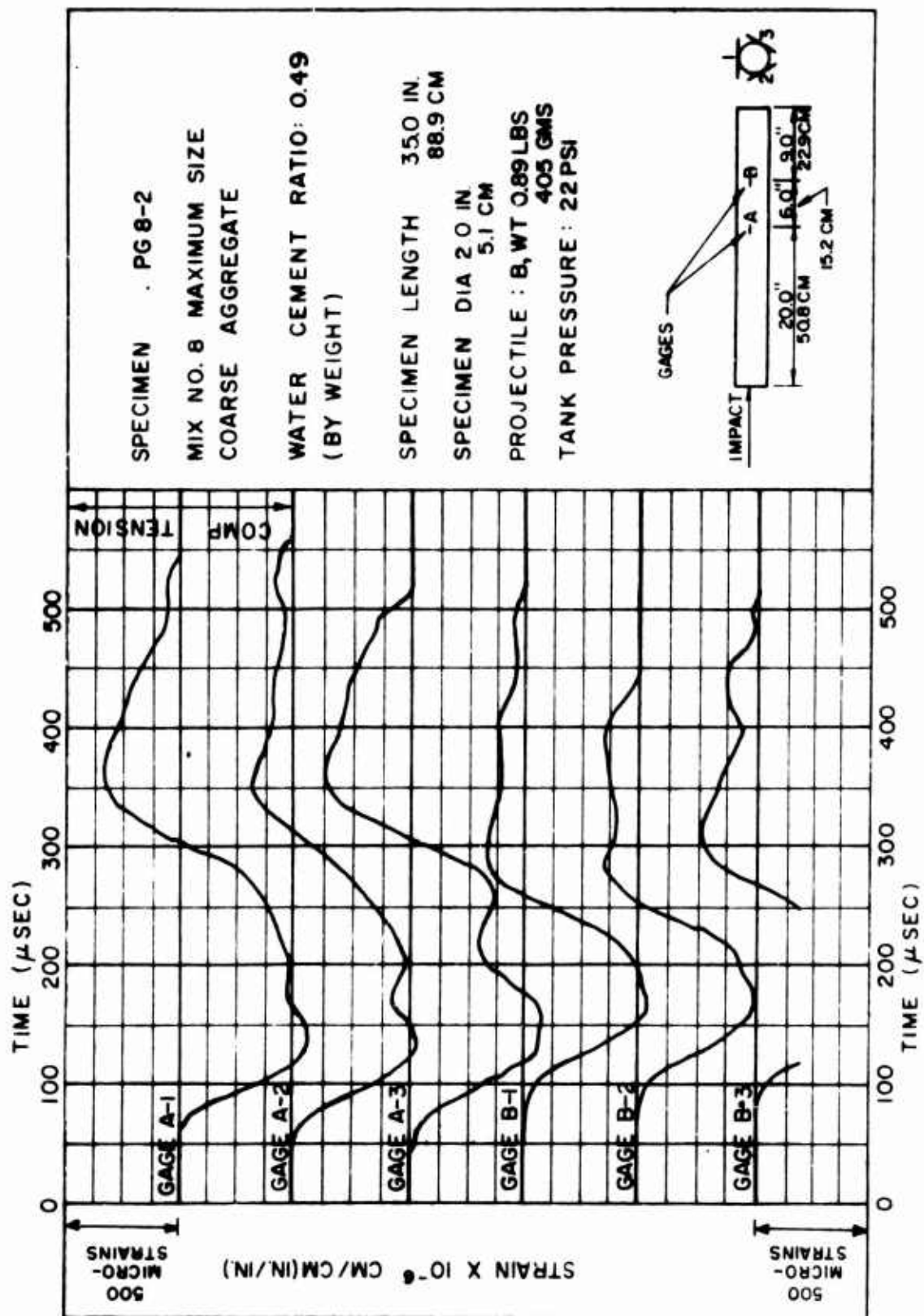
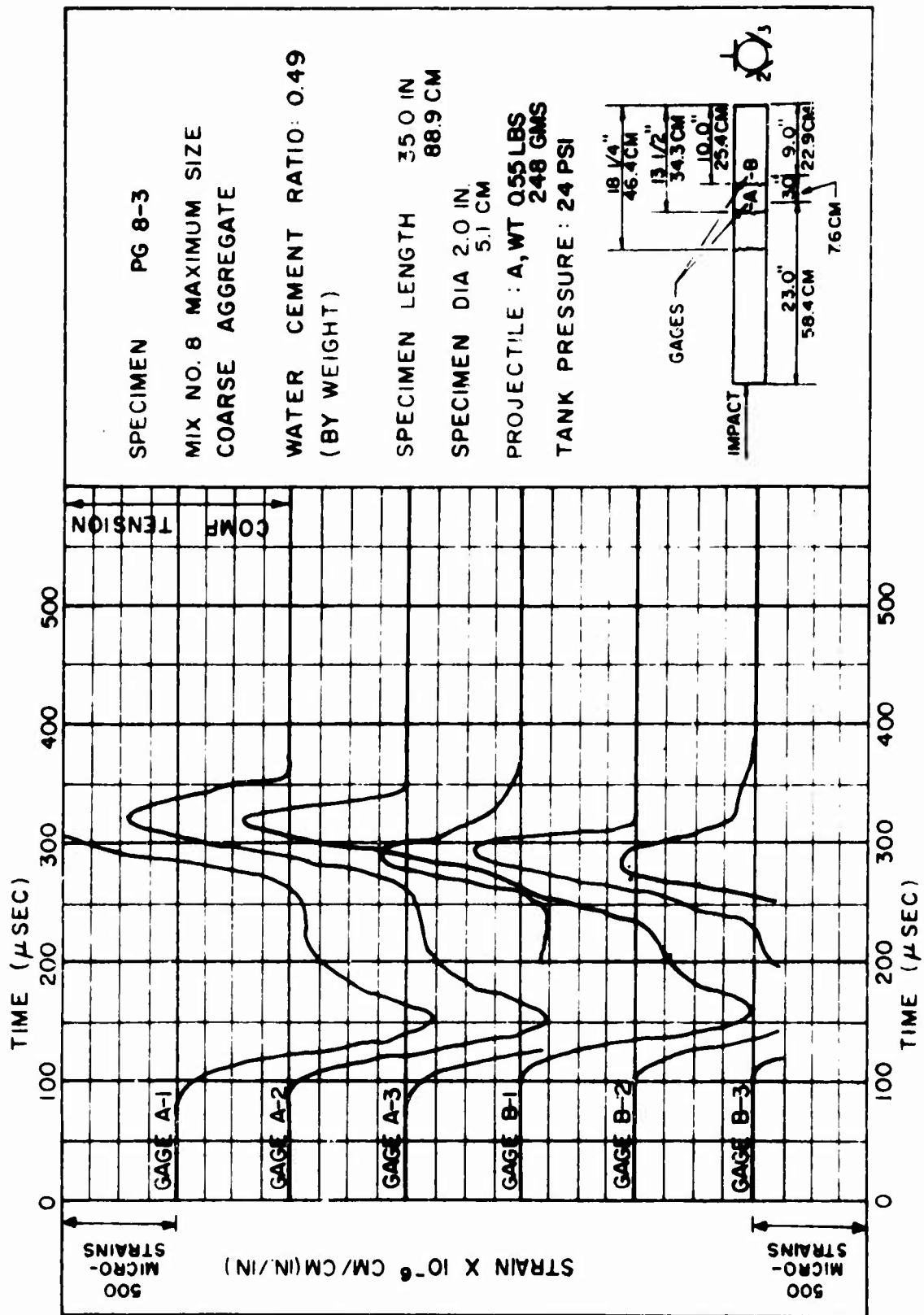
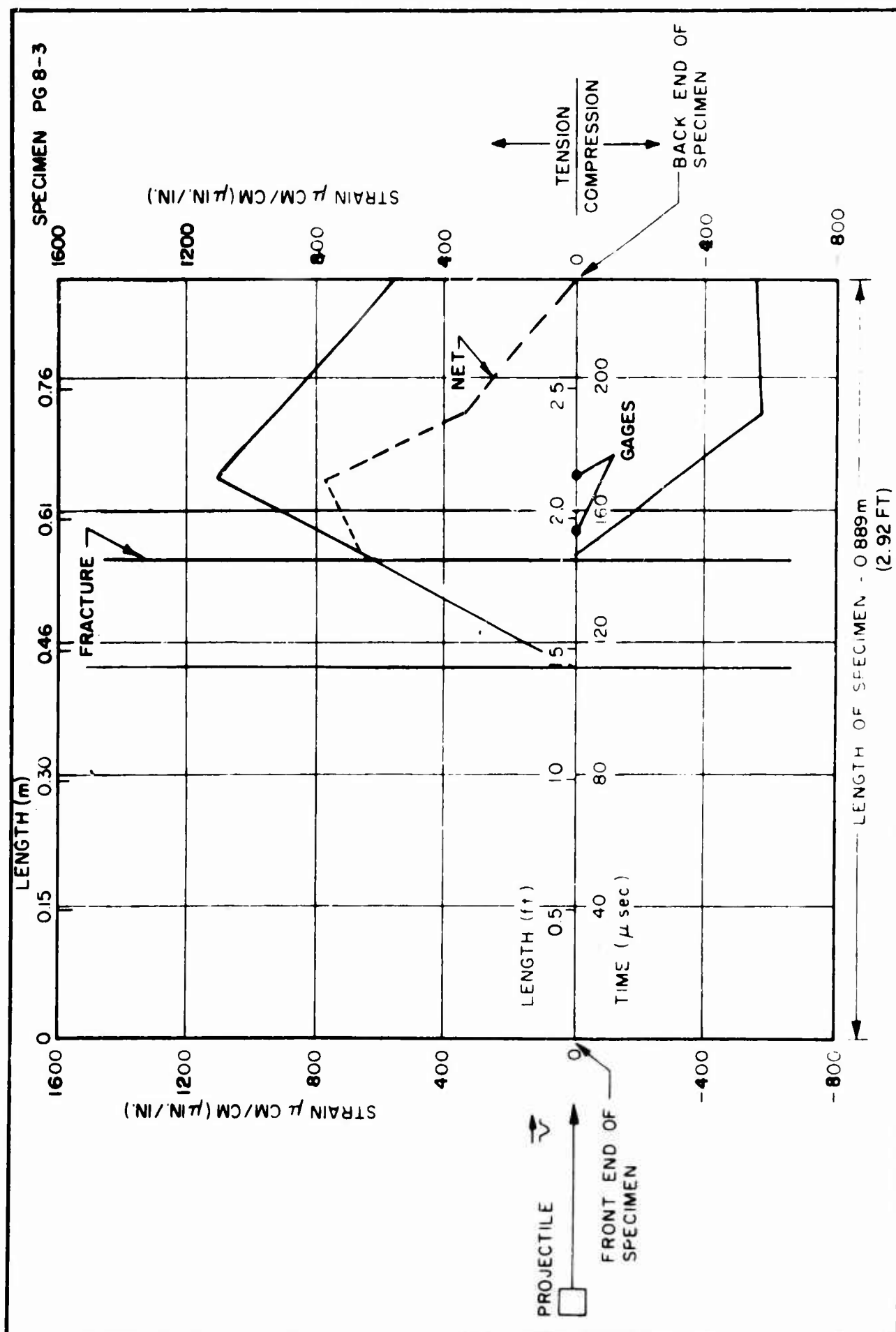
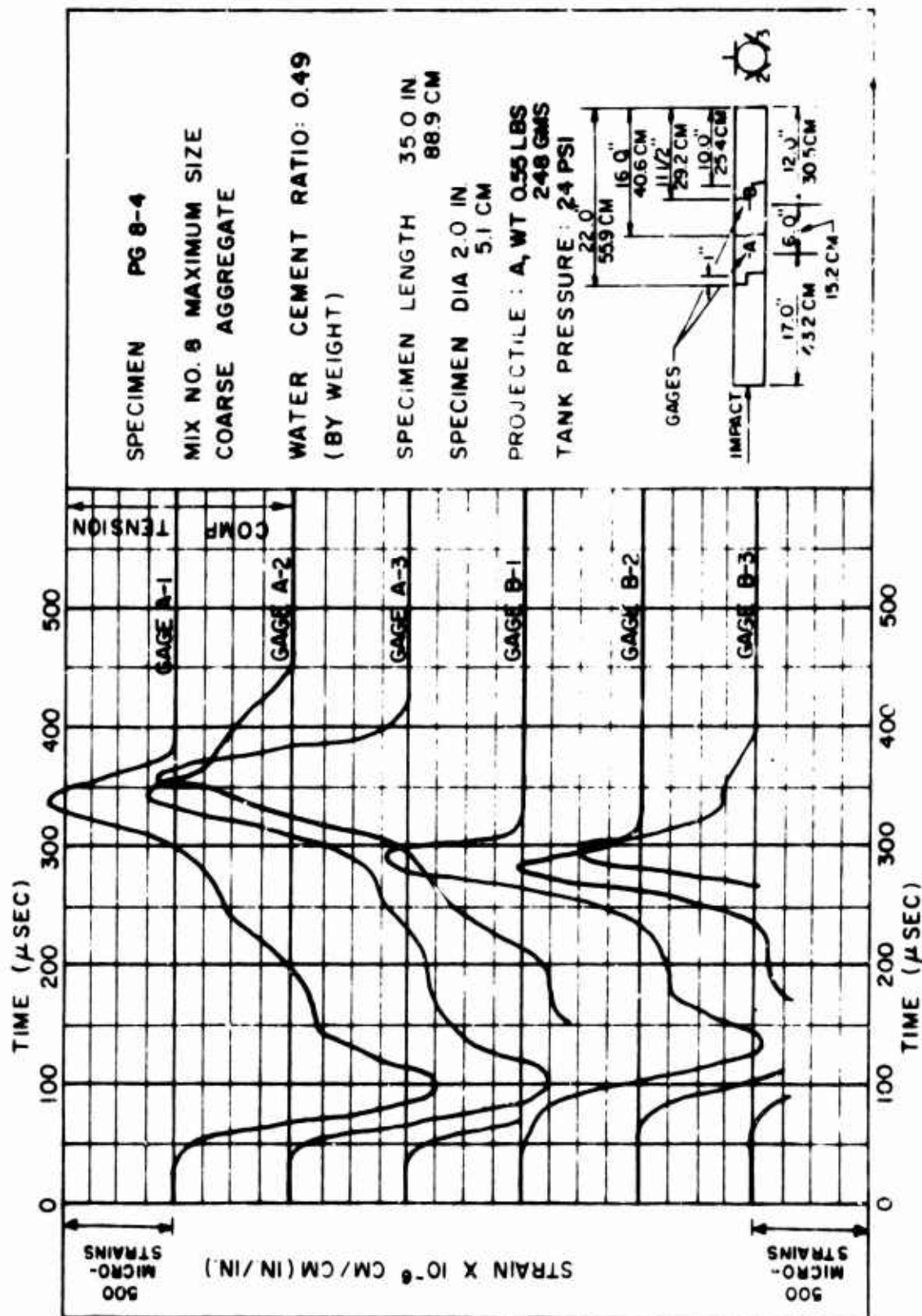
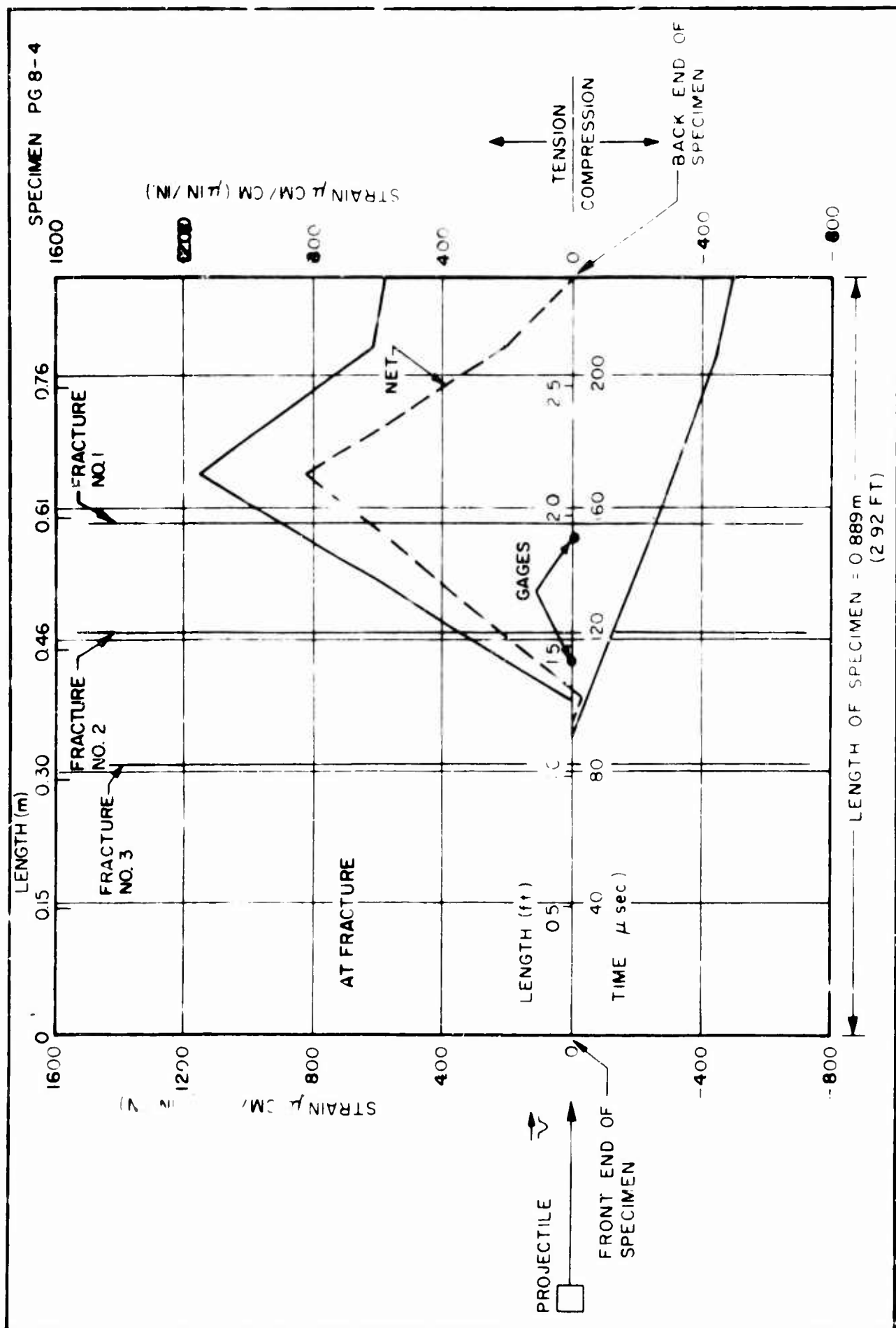


FIGURE 104









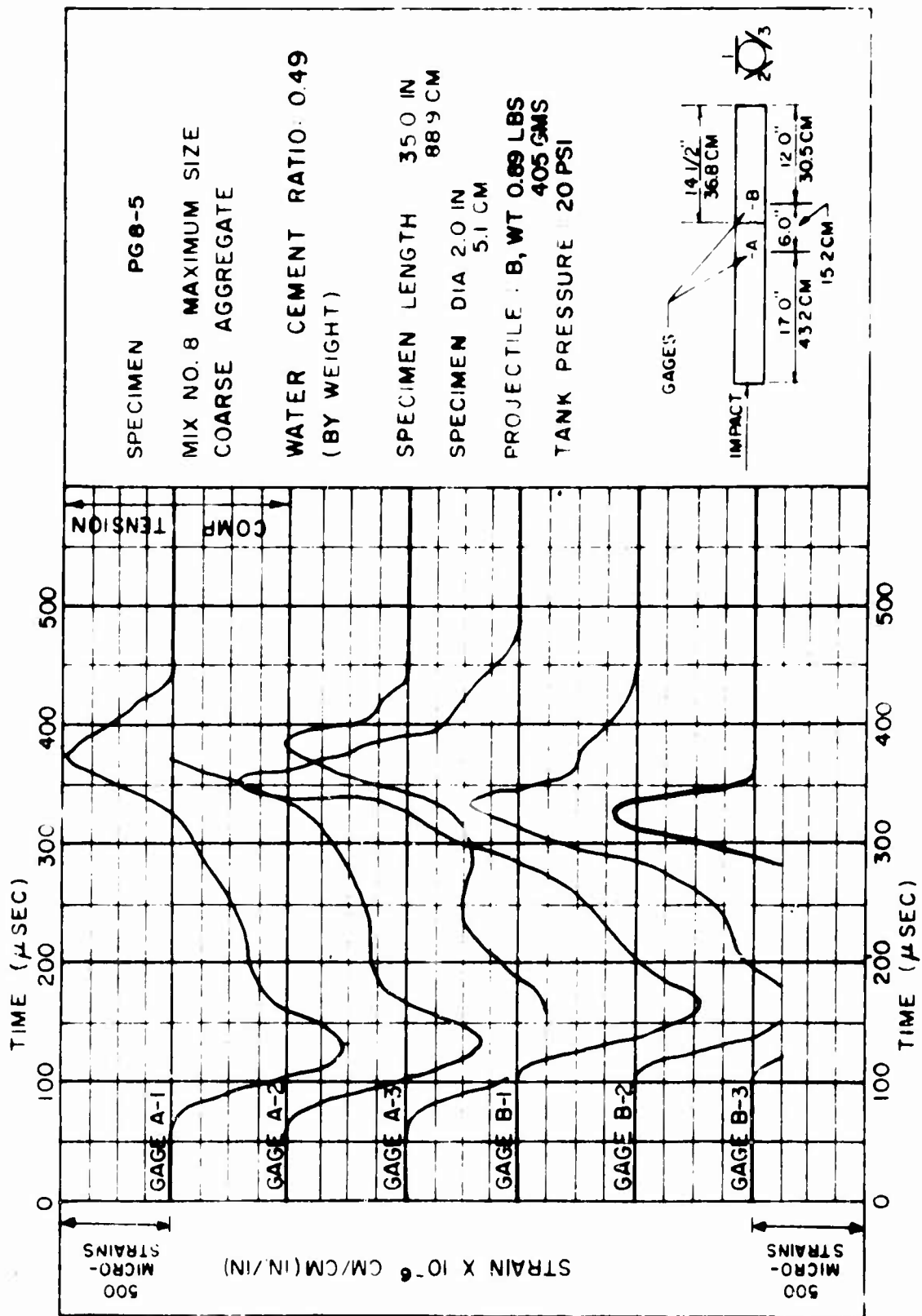
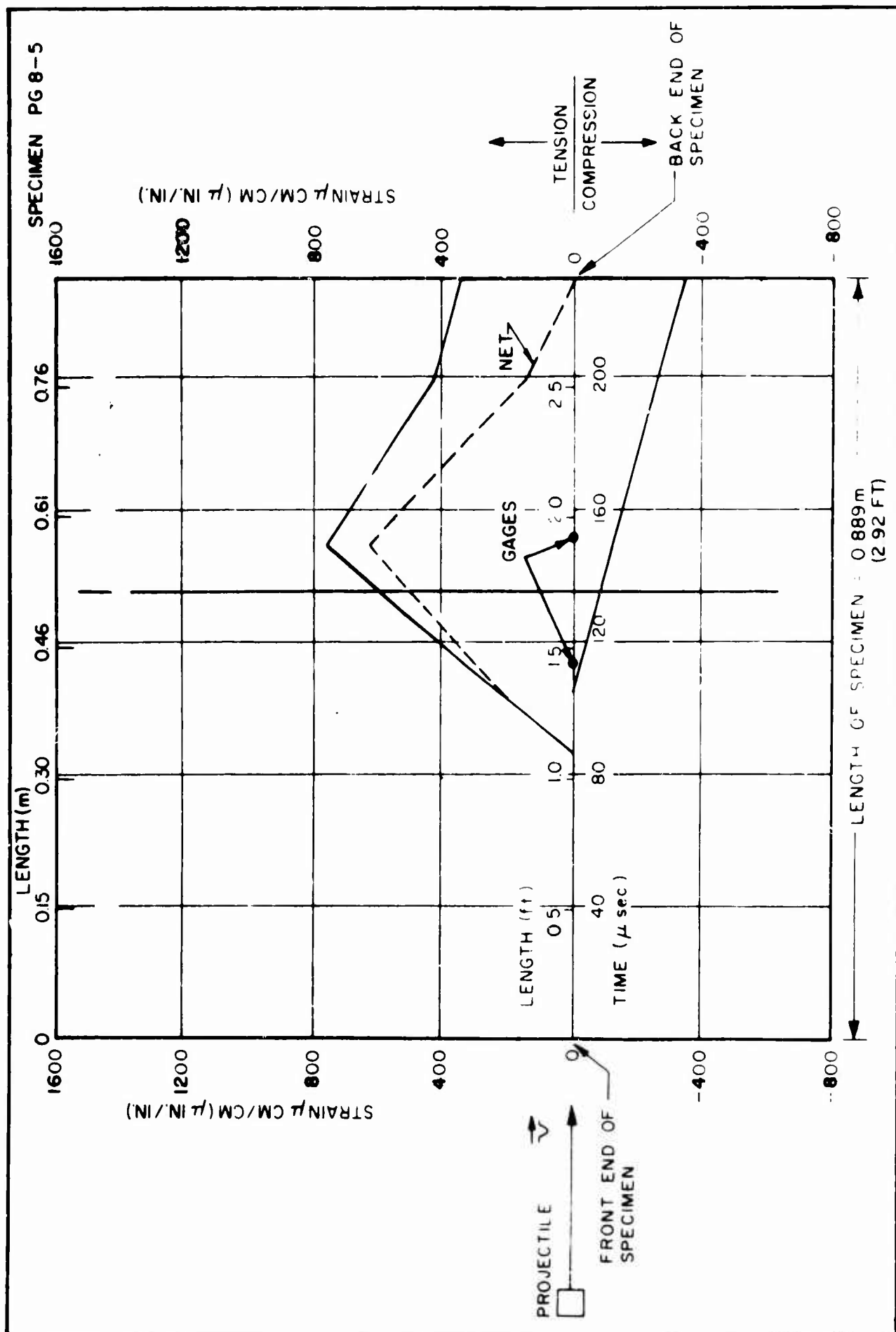
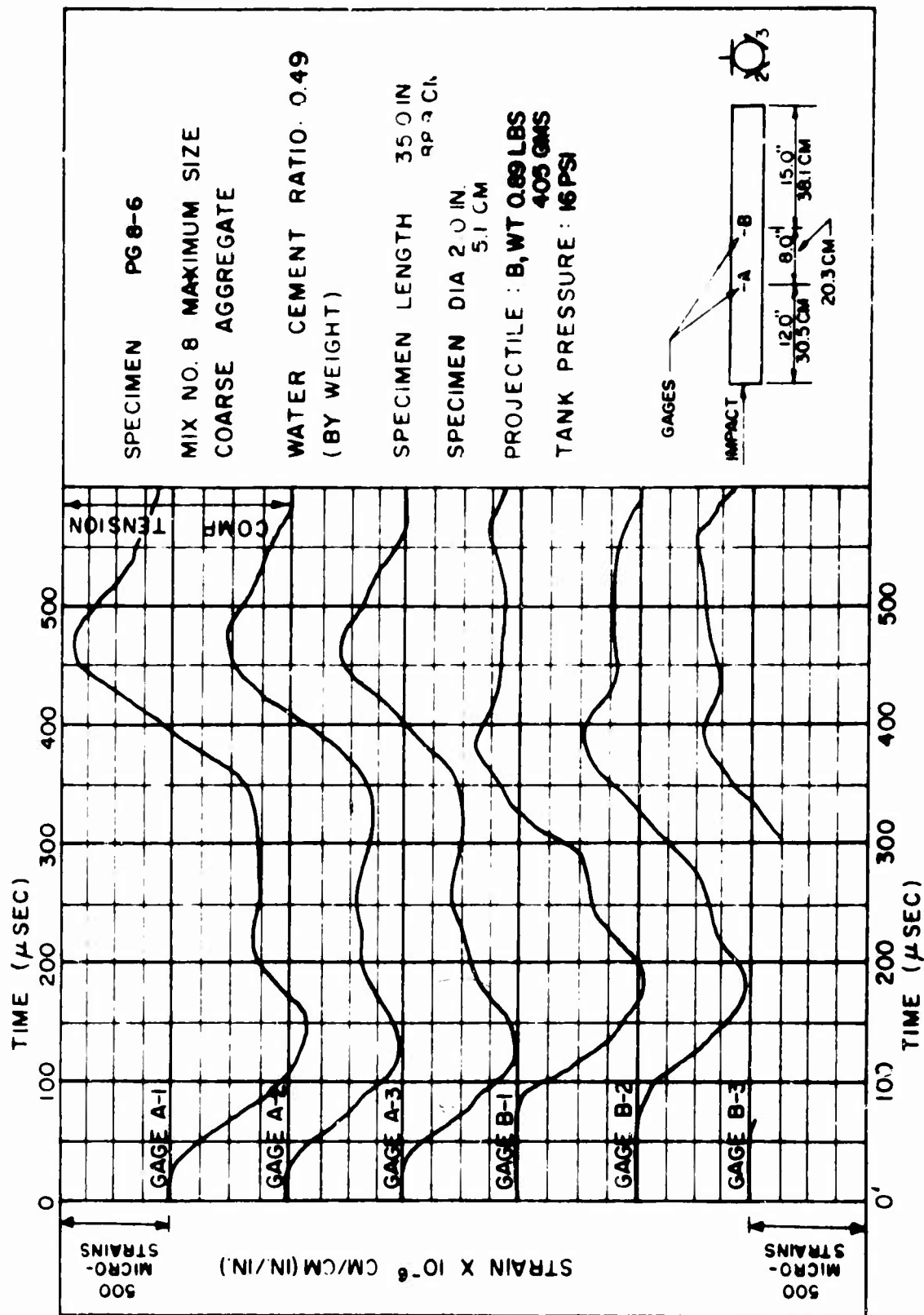
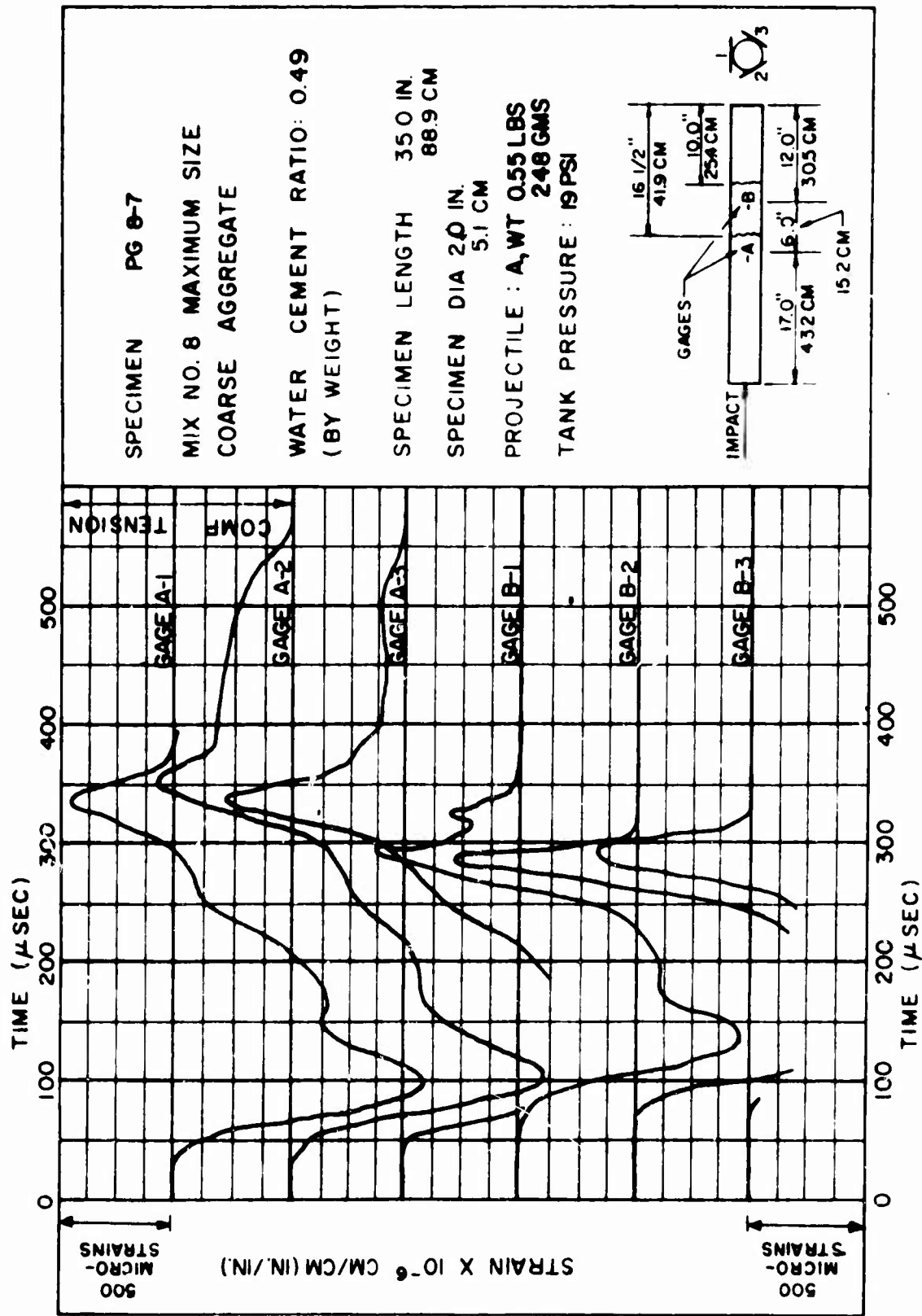
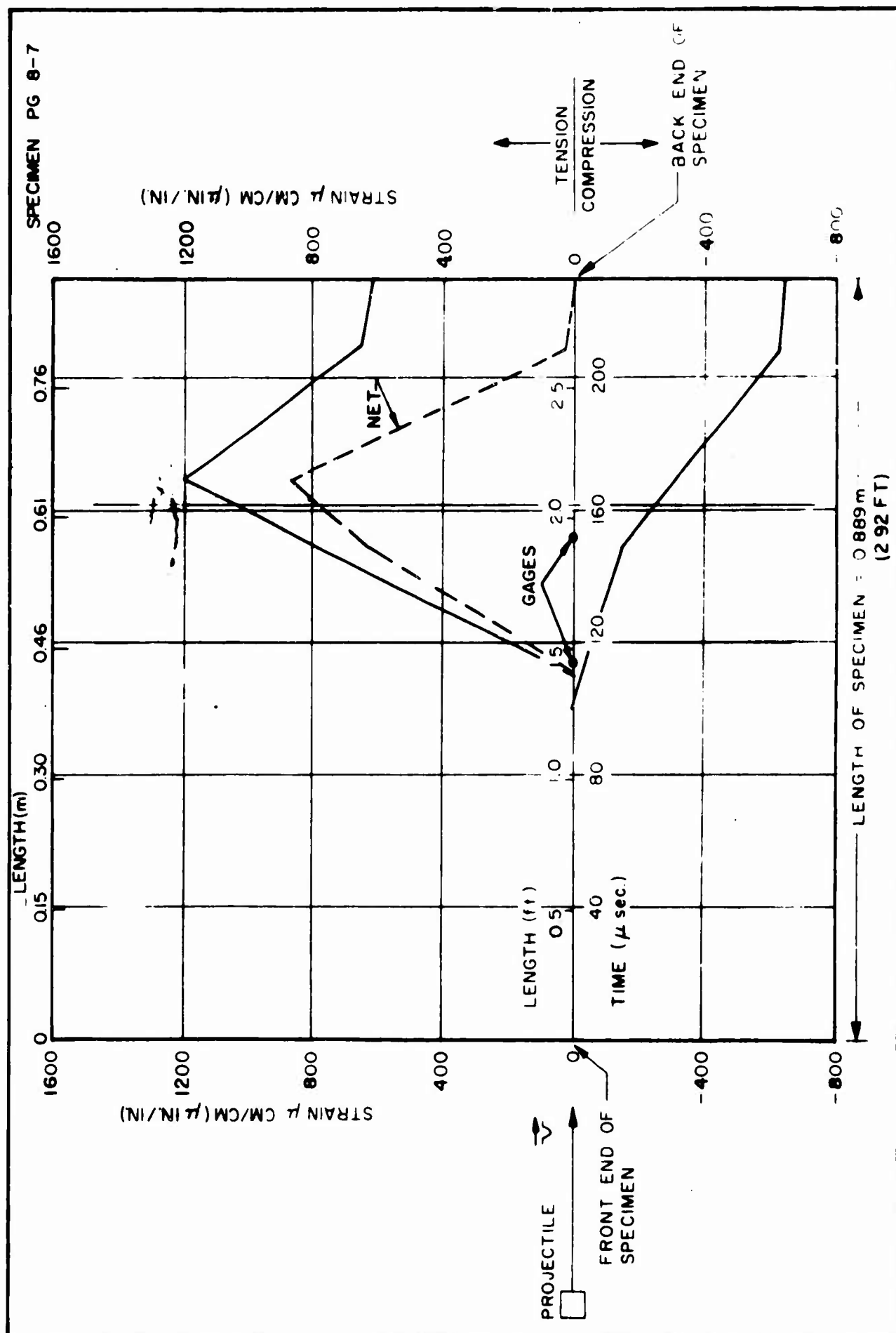


FIGURE 109









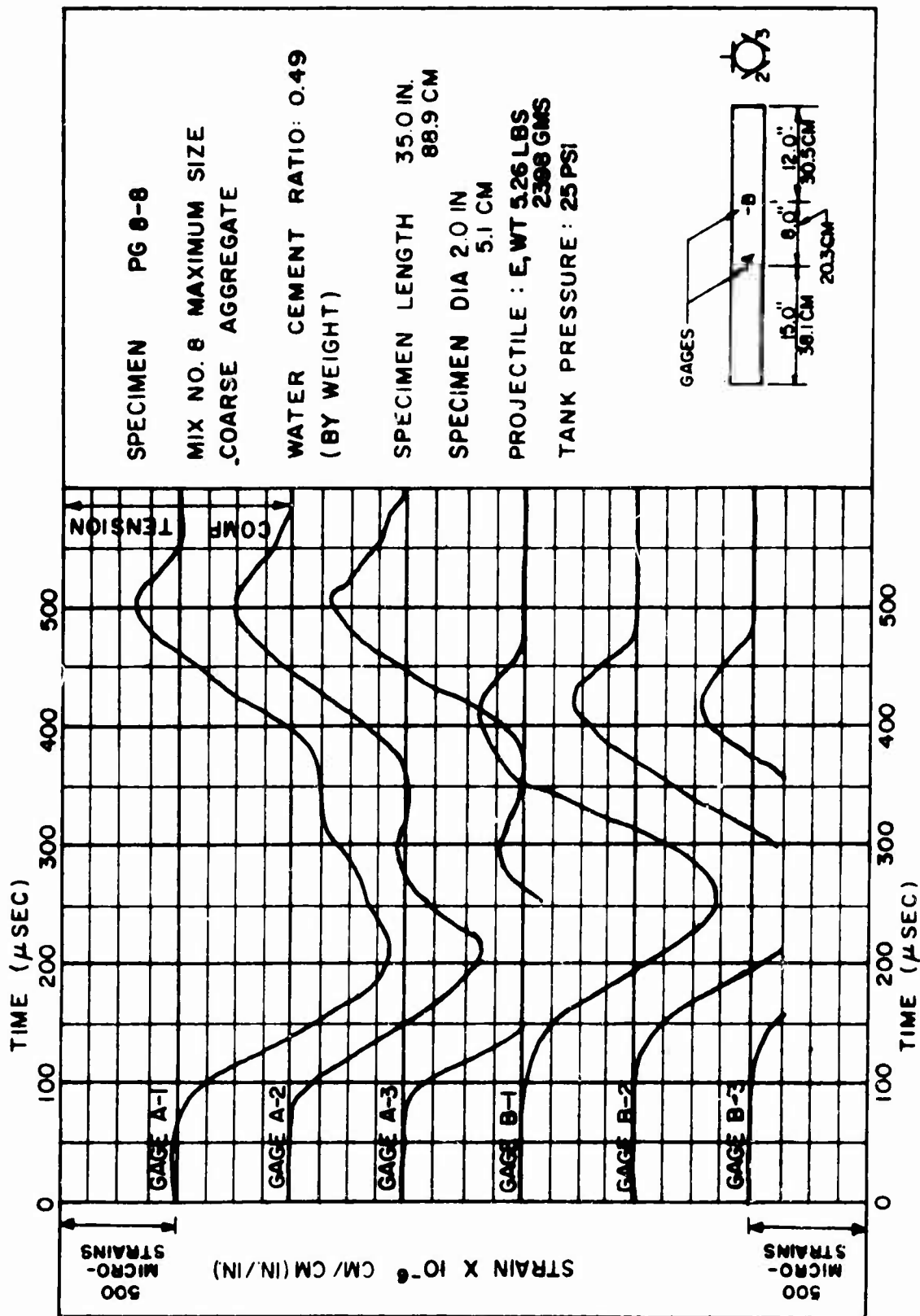
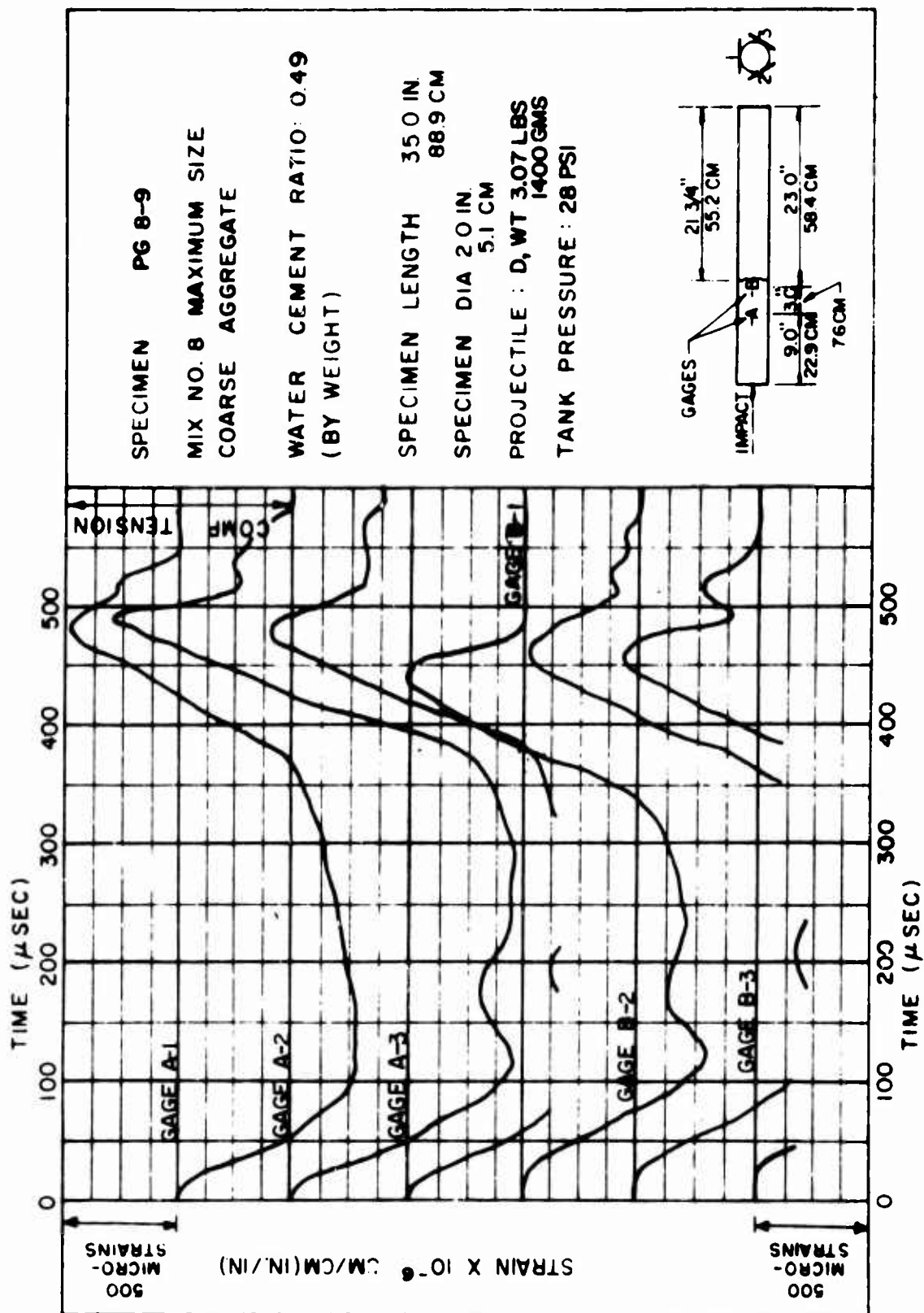
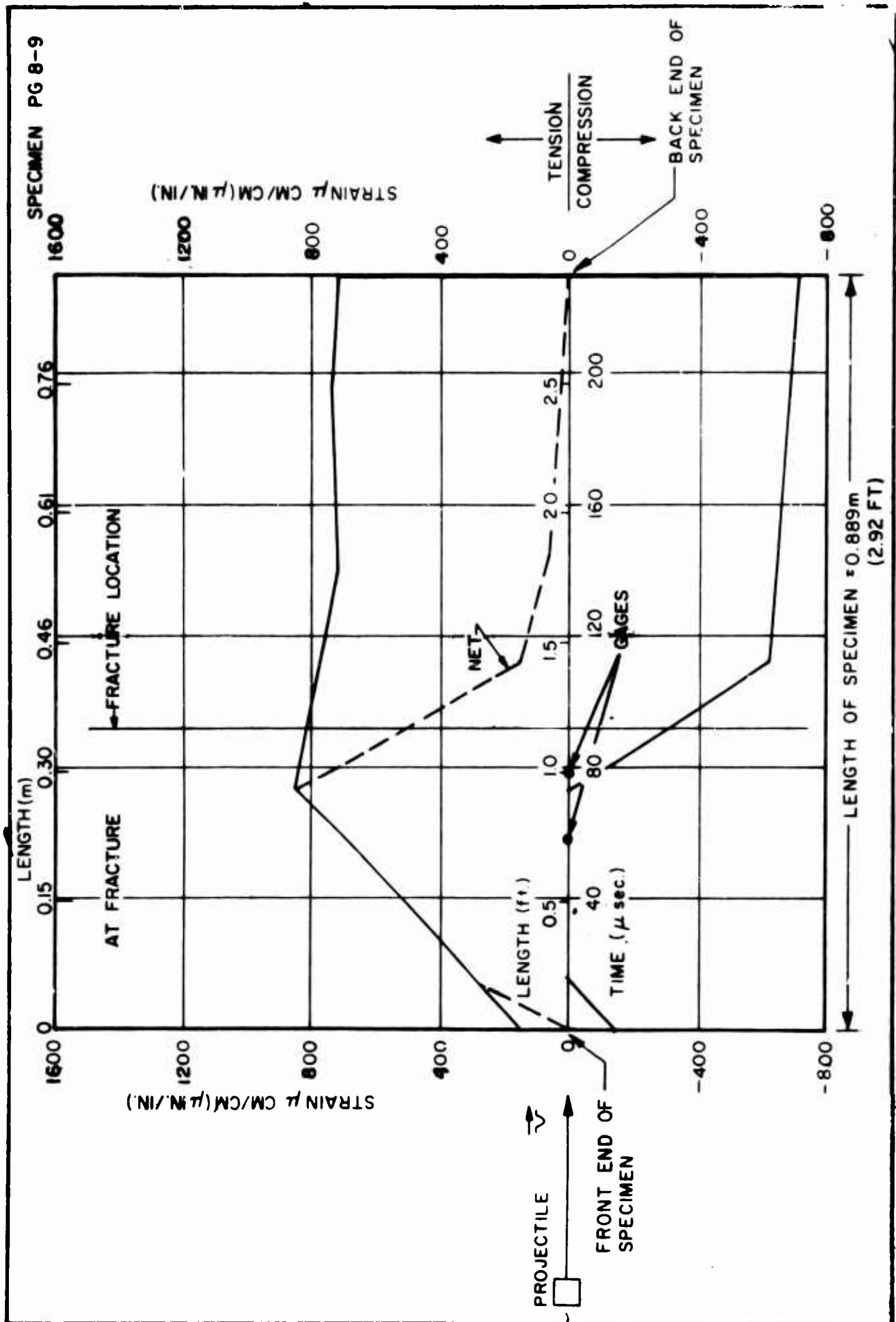
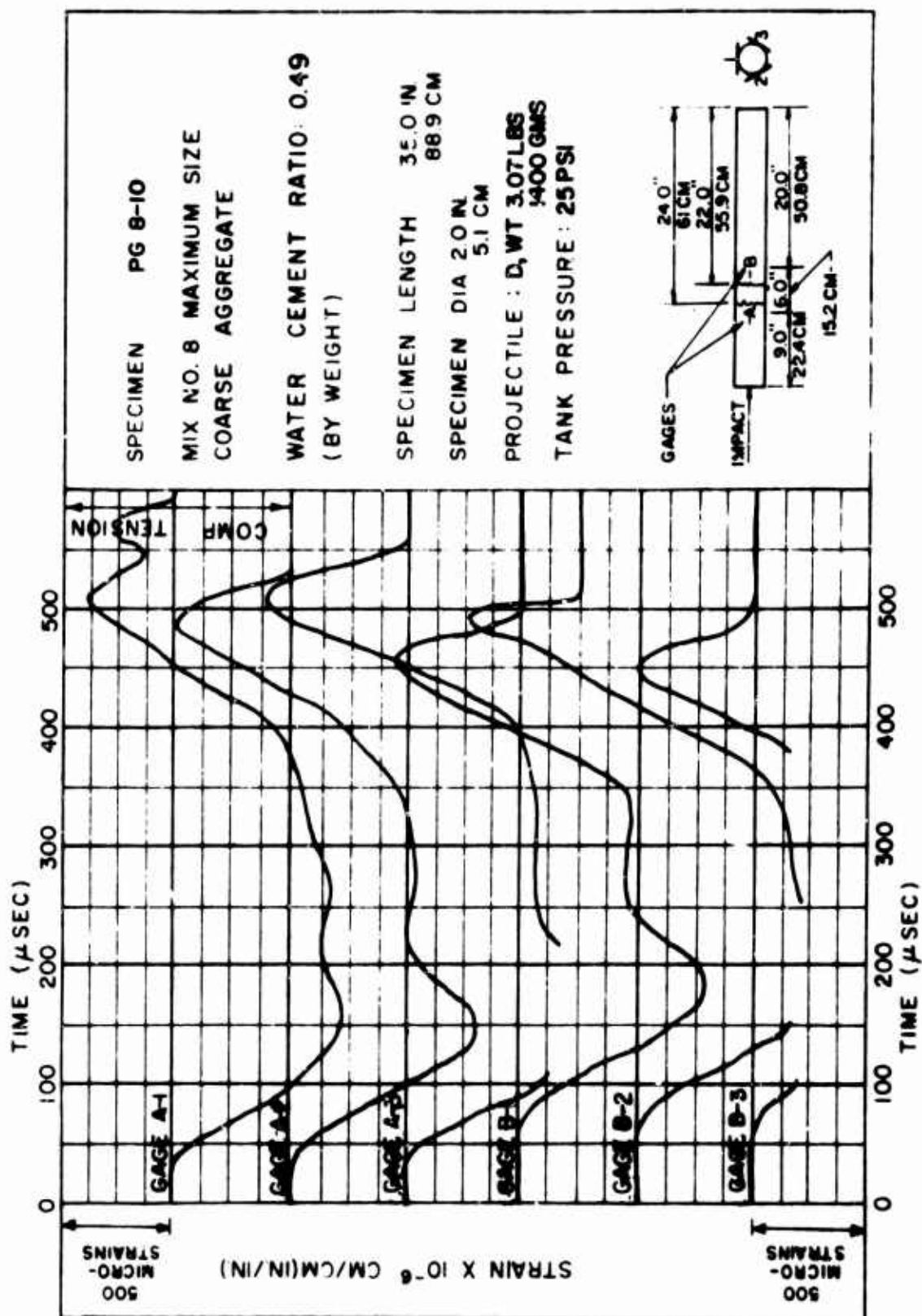
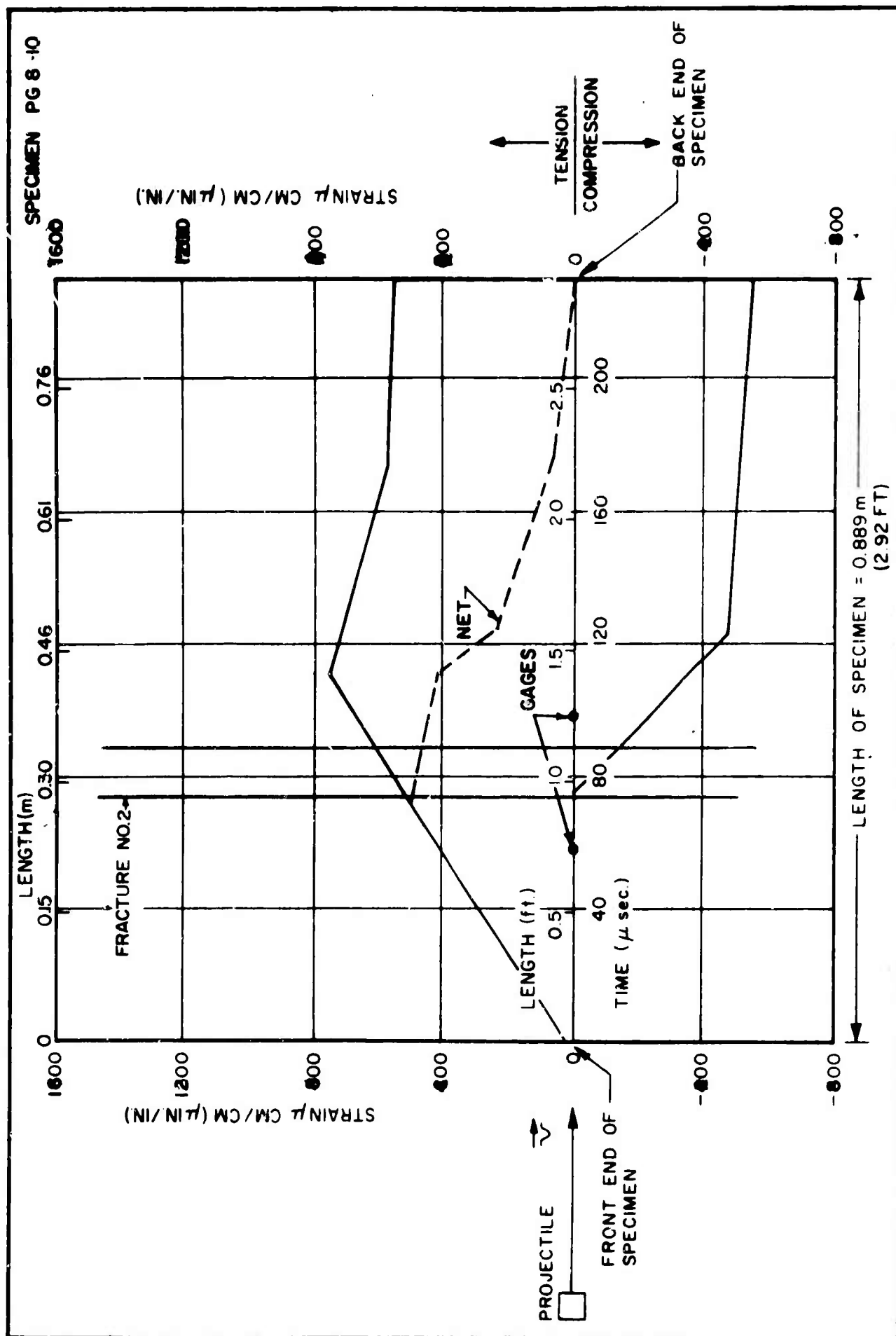


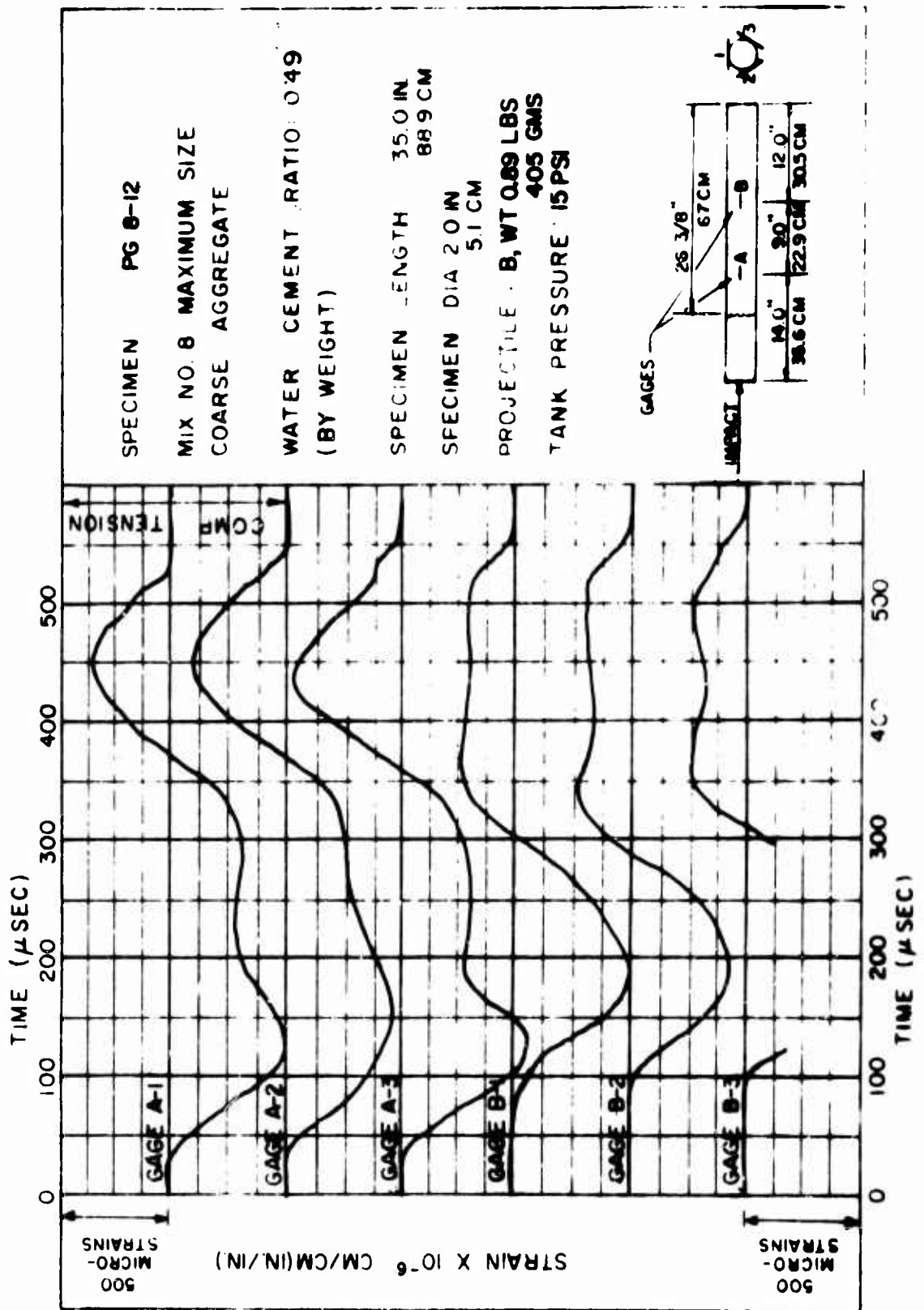
FIGURE 114

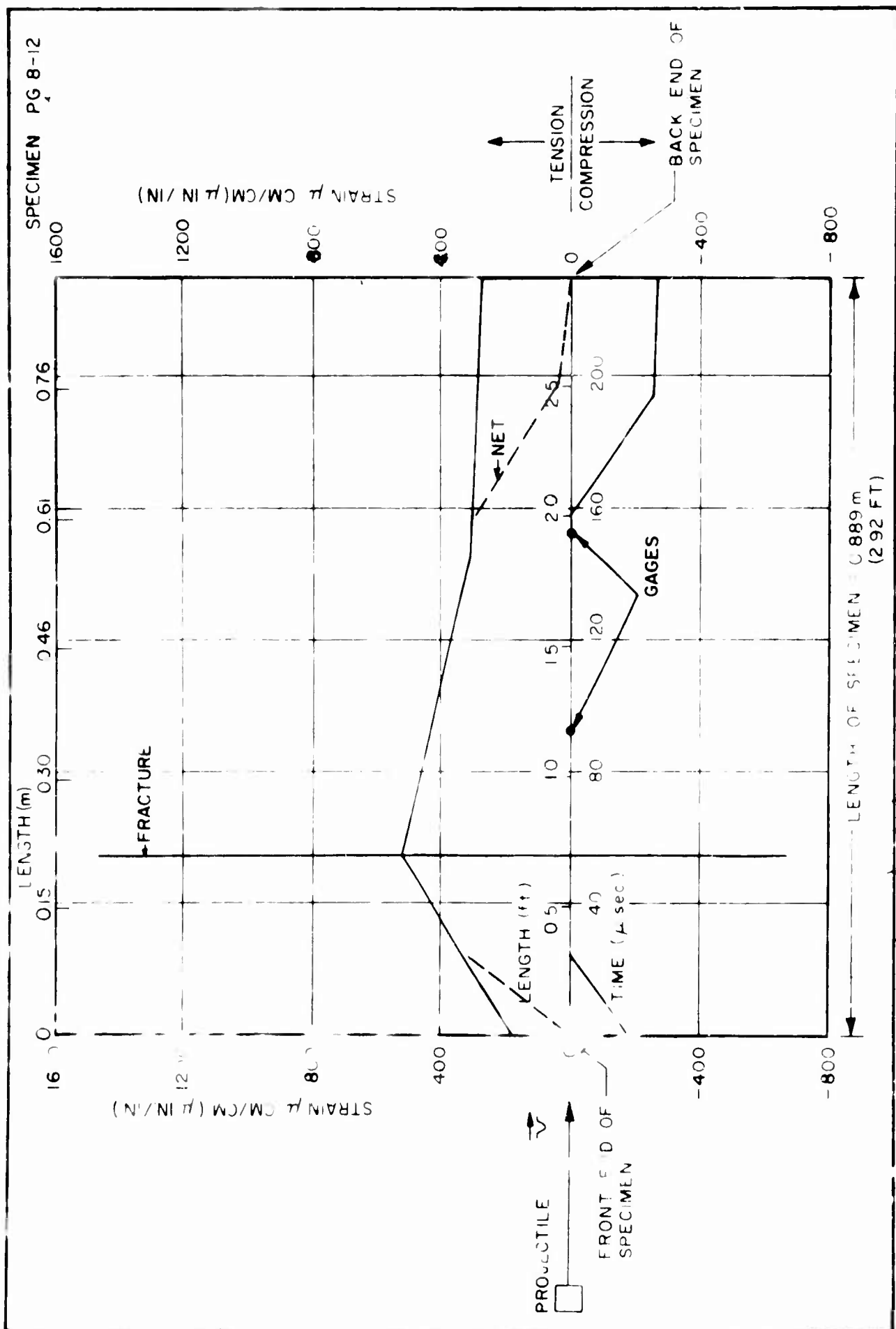












APPENDIX A

IMPACT LOADING DEVICE

BLANK PAGE

APPENDIX A

Impact Loading Device

1. The loader used to propel the projectile for impact is a cold gas-fired projectile impact loader. The equipment consists of a lucite tube, 6.4 cm (2.5 in.) in diameter and 91 cm (36 in.) long, coupled to a diaphragm housing and an air storage tank. An electromechanical pointed plunger is housed within the storage tank for rupturing the diaphragms. The diaphragm material is a repolish film base. The air is supplied through a rubber hose to the storage tank. A pressure gage with an 11.25-kg/cm^2 (160-psi) capacity is used to control the tank pressure and is calibrated so that interpolation to the nearest 0.07 kg/cm^2 (1 psi) can be made. This facilitates control of the projectile velocity as well as the projectile momentum at the end of the tube. The relations between pressure and the projectile velocity as well as the projectile momentum at the end of the tube are given by Figures 1A through 5A. The air-fired projectile impact loader and recording equipment are shown in Plate 1Aa.

2. Five basic projectile configurations were used. These projectiles are designated and described as follows:

Projectile A: This projectile is made of two pieces of aluminum 5.72 cm (2.25 in.) in diameter, and separated by a piece of hardwood 2.5 cm (1.0 in.) in diameter and two pieces of fiberboard 6.4 cm (2.5 in.) in diameter. The sections of the projectile are joined by a metal bolt running from the posterior into the aluminum head. A typical wave form produced by this projectile in the plain concrete tested is shown by Figure 6A. The secondary peak is produced by the projectile impacting the specimen a second time. The effect is caused by the flutter of the end pieces of this projectile. The actual overall length of the projectile is 10 cm (4 in.) and the total weight is 248.1 gm (0.547 lb). The impact end of this projectile is rounded to a smooth curve. This projectile is shown by Plate 1Ab.

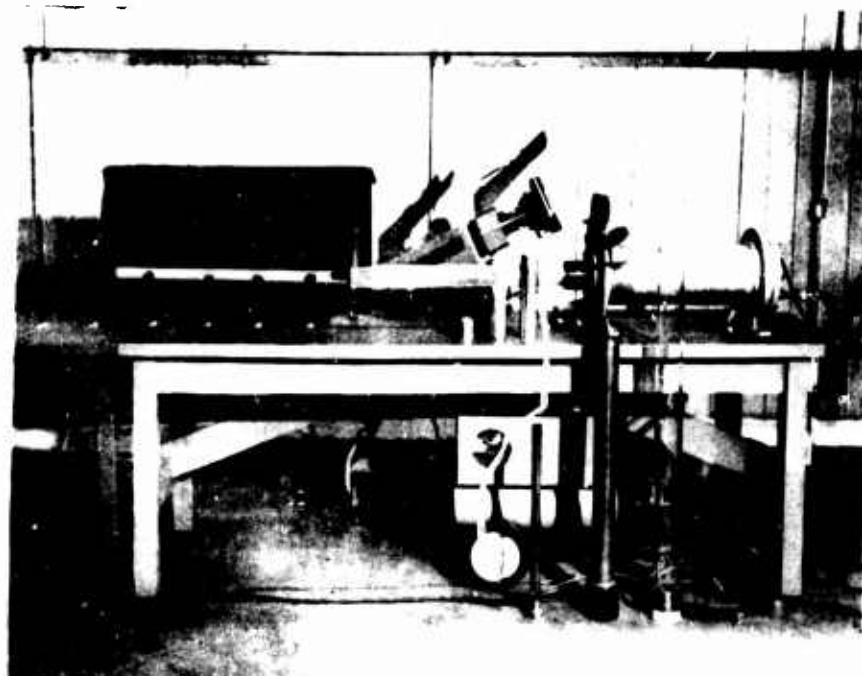
Projectile B: This projectile is made of two pieces of aluminum 6.269 cm (2.468 in.) in diameter, and separated by a piece of hardwood 2.5 cm (1.0 in.) in diameter and two pieces of fiberboard 6.4 cm (2.5 in.) in diameter. The 3.8-cm (1.5-in.) long aluminum head is connected to the fiberboard only by Eastman 910 adhesive. The remaining sections of the projectile are connected by a metal bolt running from the posterior end into the fiberboard. This configuration makes the rise time of the wave roughly the same as it would be for the 3.8-cm (1.5-in.) aluminum piece alone. The weight of this projectile is 405.1 gm (0.893 lb) and it is shown in Plate 2Aa. A typical wave form produced by this projectile in the concrete tested is shown by Figure 7A.

Projectile C: This projectile consists of a solid piece of aluminum 6.032 cm (2.375 in.) in diameter and 7.6 cm (3.0 in.) in length. This projectile has a rounded head and is shown in Plate 2Ab. The total weight of this projectile is 556.1 gm (1.226 lb). A typical wave form produced by this projectile in the concrete tested is shown by Figure 8A.

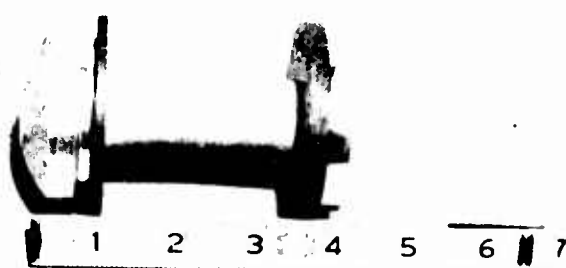
Projectile D: This projectile consists of a solid piece of aluminum which is 6.032 cm (2.375 in.) in diameter and 17.8 cm (7.0 in.) in length. This projectile has a rounded head and is shown in Plate 3Aa. The total weight of this projectile is 1399.8 gm (3.086 lb). A typical wave form produced by this projectile in the concrete tested is shown by Figure 9A.

Projectile E: This projectile consists of a solid piece of aluminum which is 6.032 cm (2.375 in.) in diameter by 30 cm (12 in.) in length. This projectile has a rounded head and is shown in Plate 3Ab. The total weight of this projectile is 2397.7 gm (5.286 lb). A typical wave form produced by this projectile in the concrete tested is shown by Figure 10A.

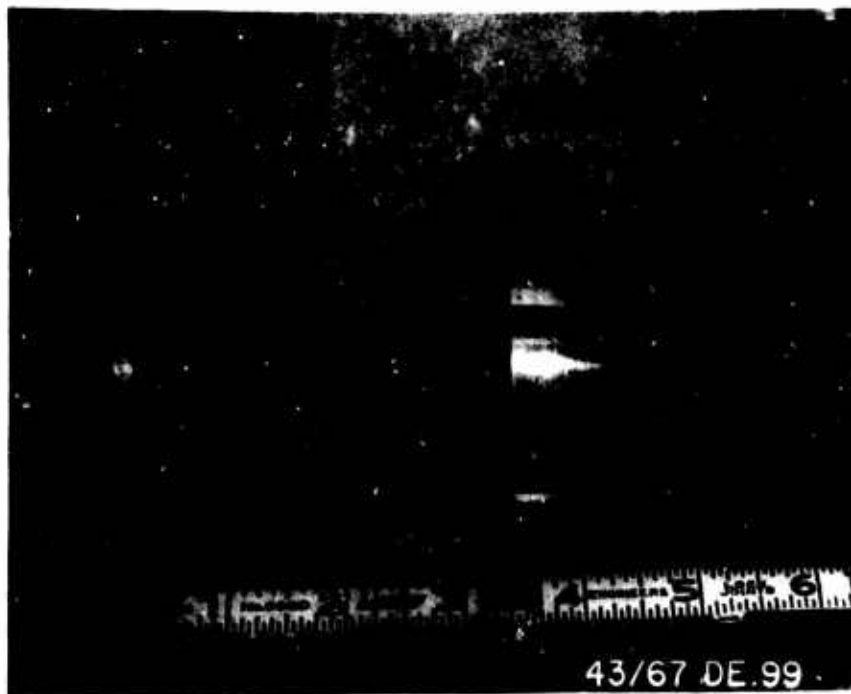
3. The specimen support system consisted of simple supports placed 20 cm (8 in.) on center in a longitudinal line. The support system is shown in Plate 4A. The specimens rested on felt pads placed between the specimen and the support.



a. ORDL Impact Loader



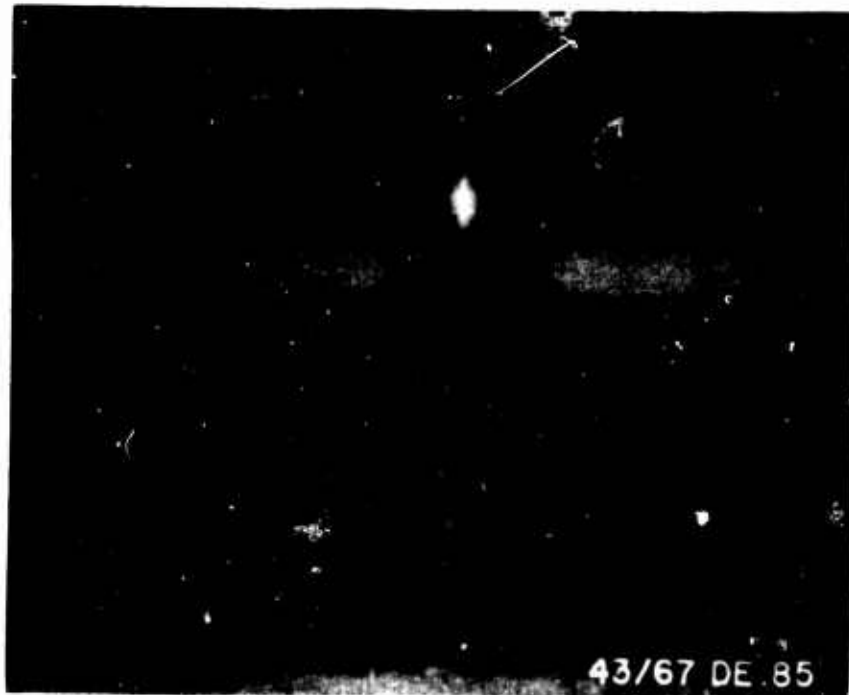
b. Projectile A



a. Projectile B



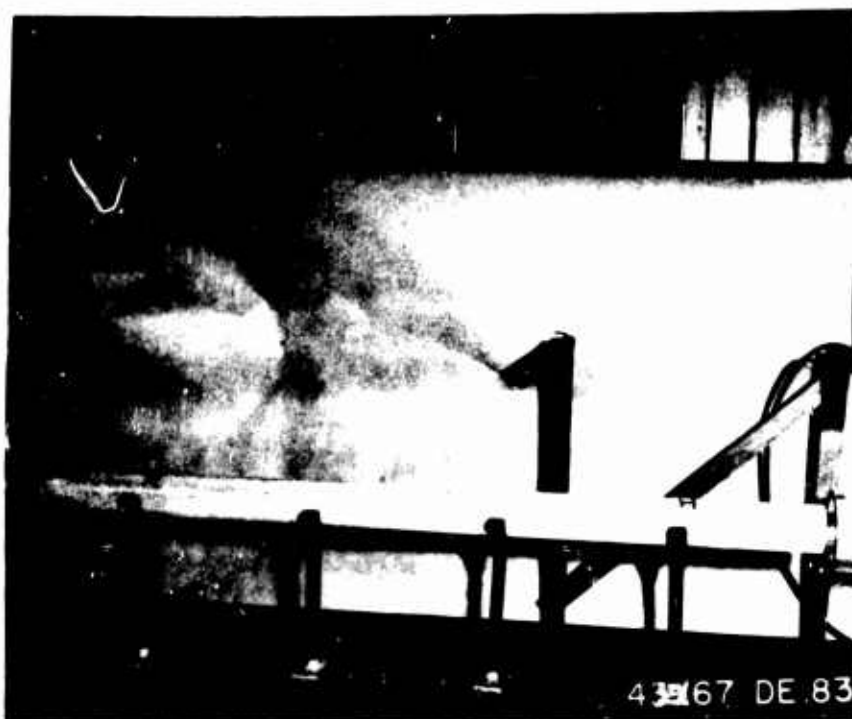
b. Projectile C



a. Projectile D



b. Projectile E



Specimen Support System

VELOCITY OF PROJECTILE (MOMENTUM) VS PRESSURE

PROJECTILE A

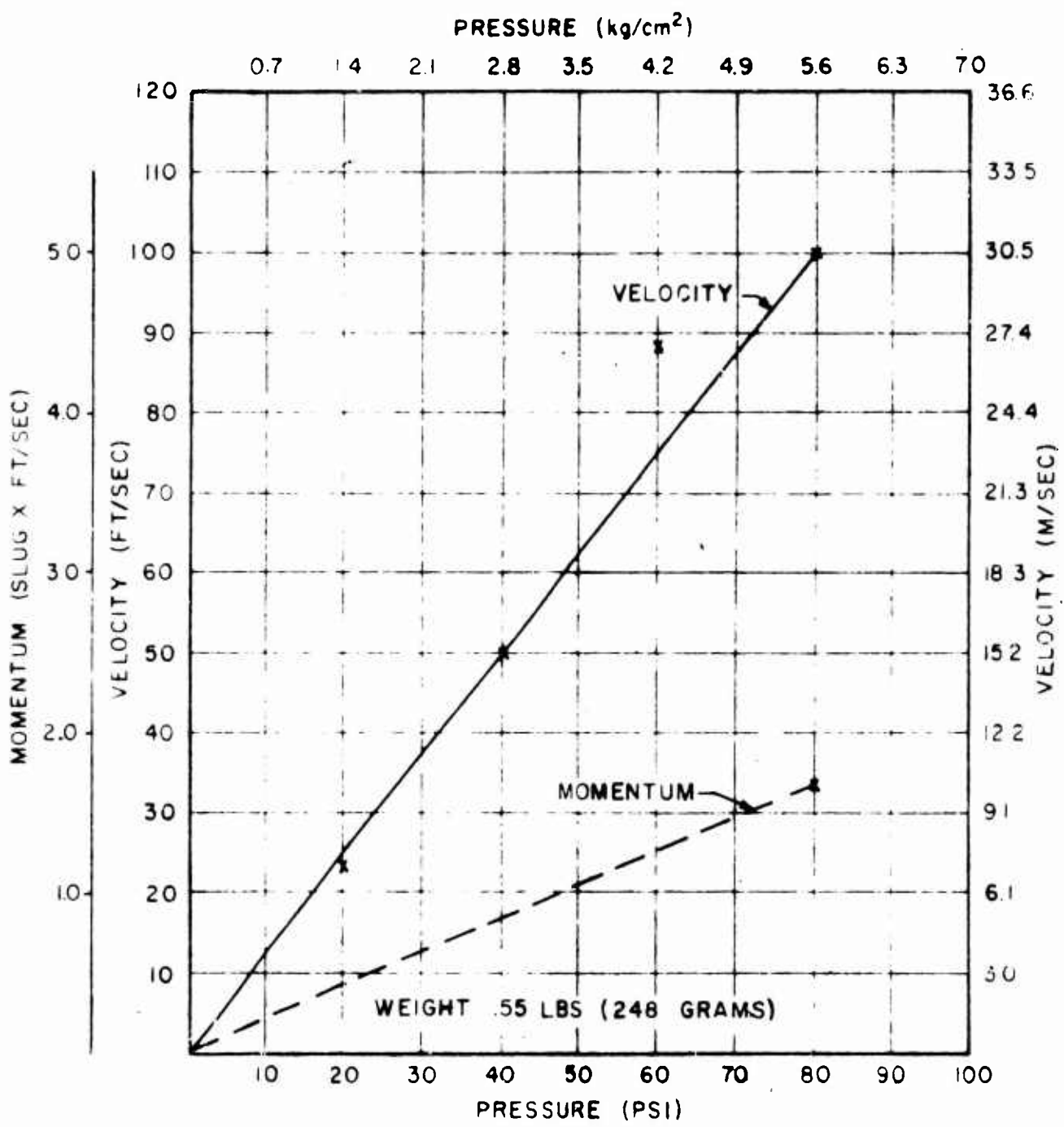


FIGURE 1A

VELOCITY OF PROJECTILE (MOMENTUM) VS PRESSURE

PROJECTILE B

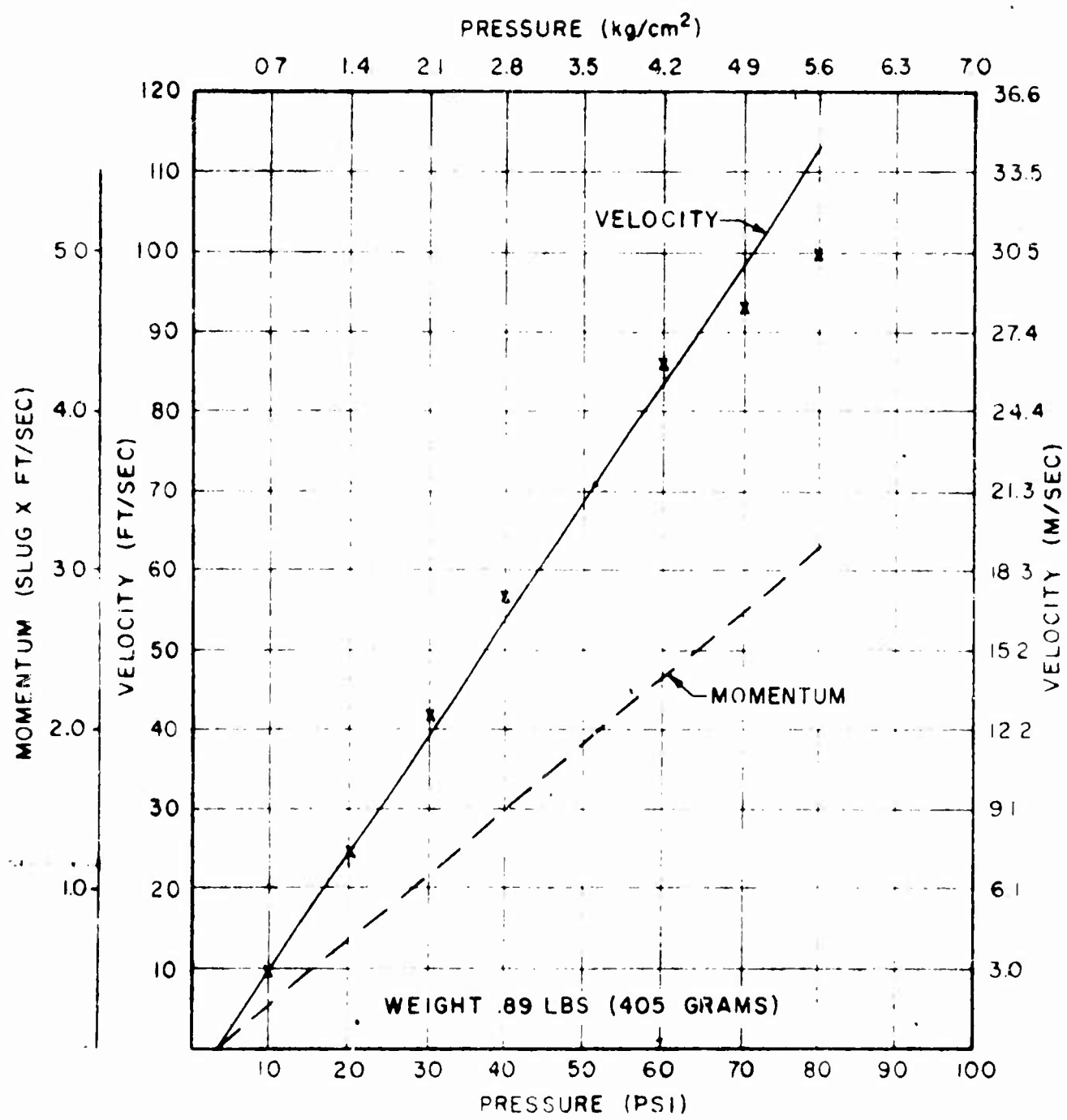
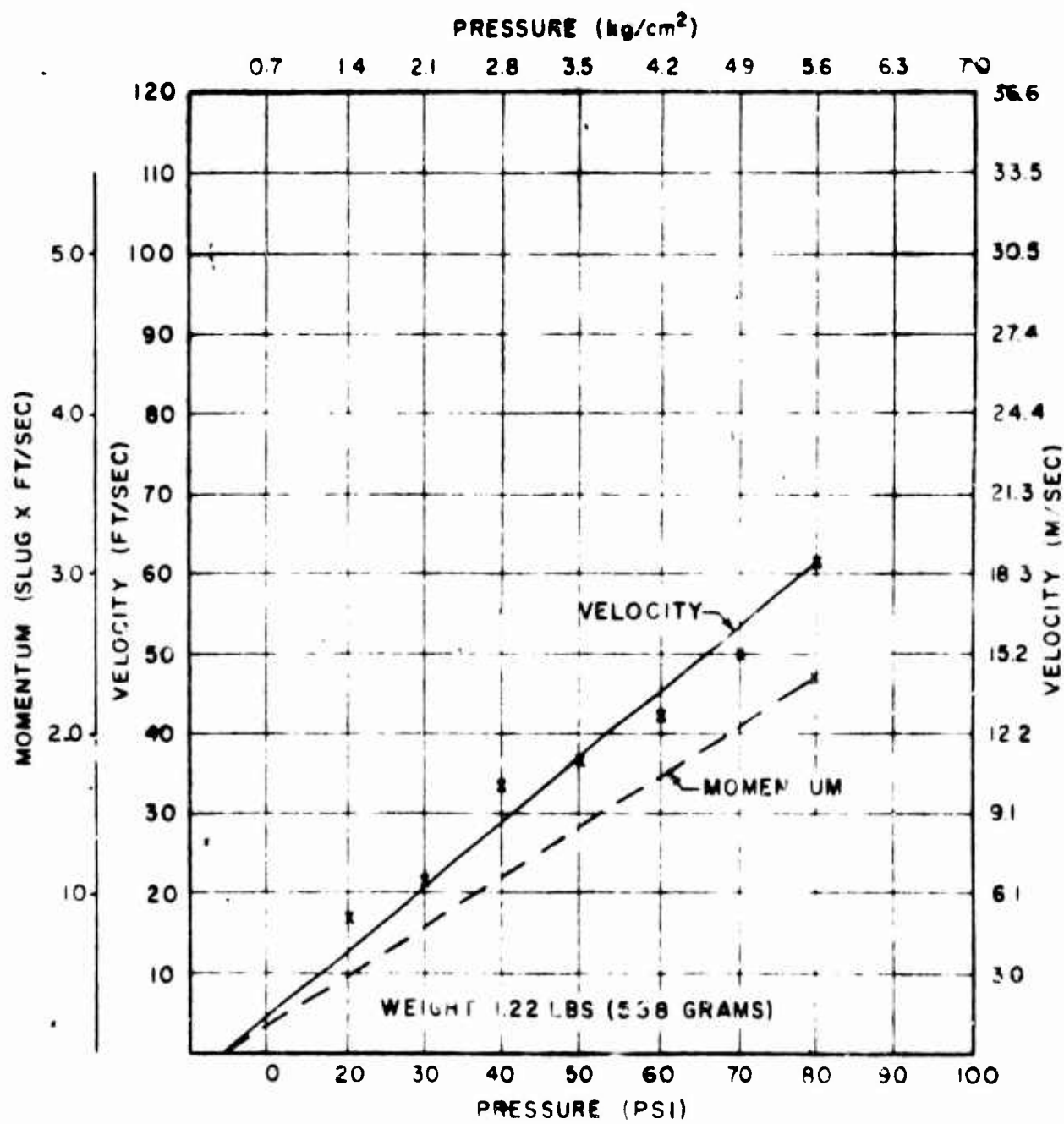


FIGURE 2A

VELOCITY OF PROJECTILE (MOMENTUM) VS PRESSURE

PROJECTILE C



VELOCITY OF PROJECTILE (MOMENTUM) VS PRESSURE

PROJECTILE D

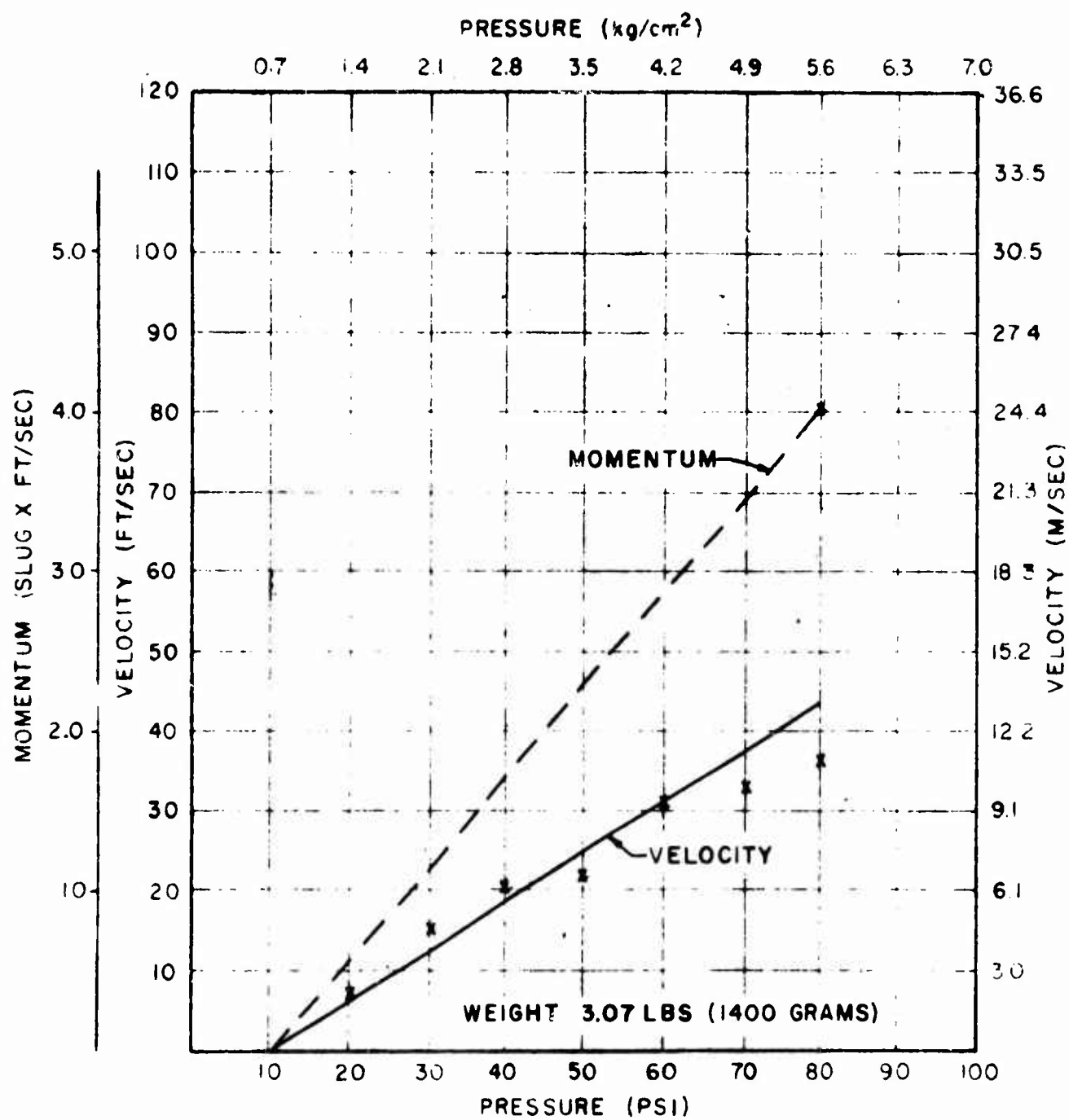
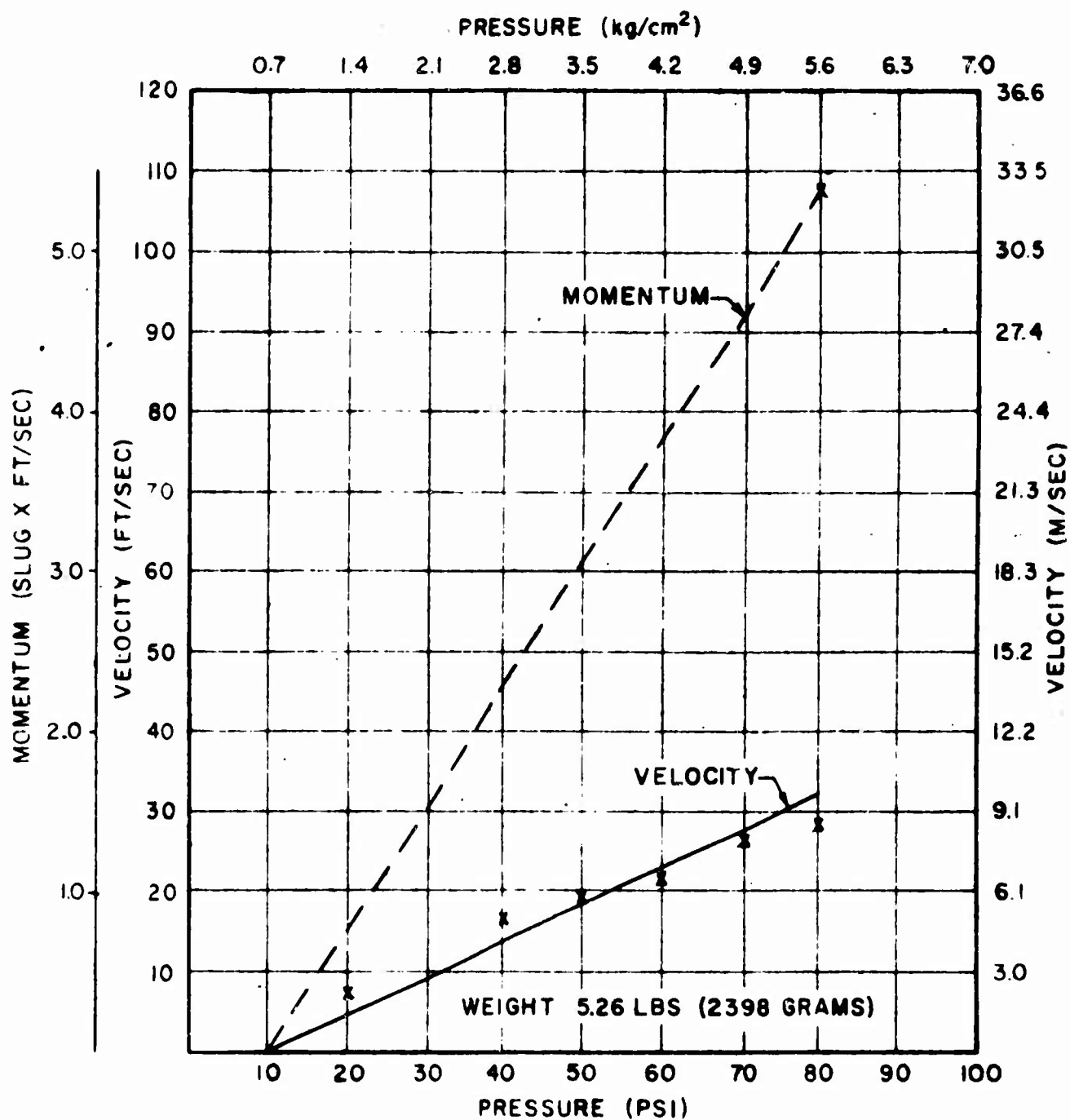


FIGURE 4A

VELOCITY OF PROJECTILE (MOMENTUM) VS PRESSURE

PROJECTILE E



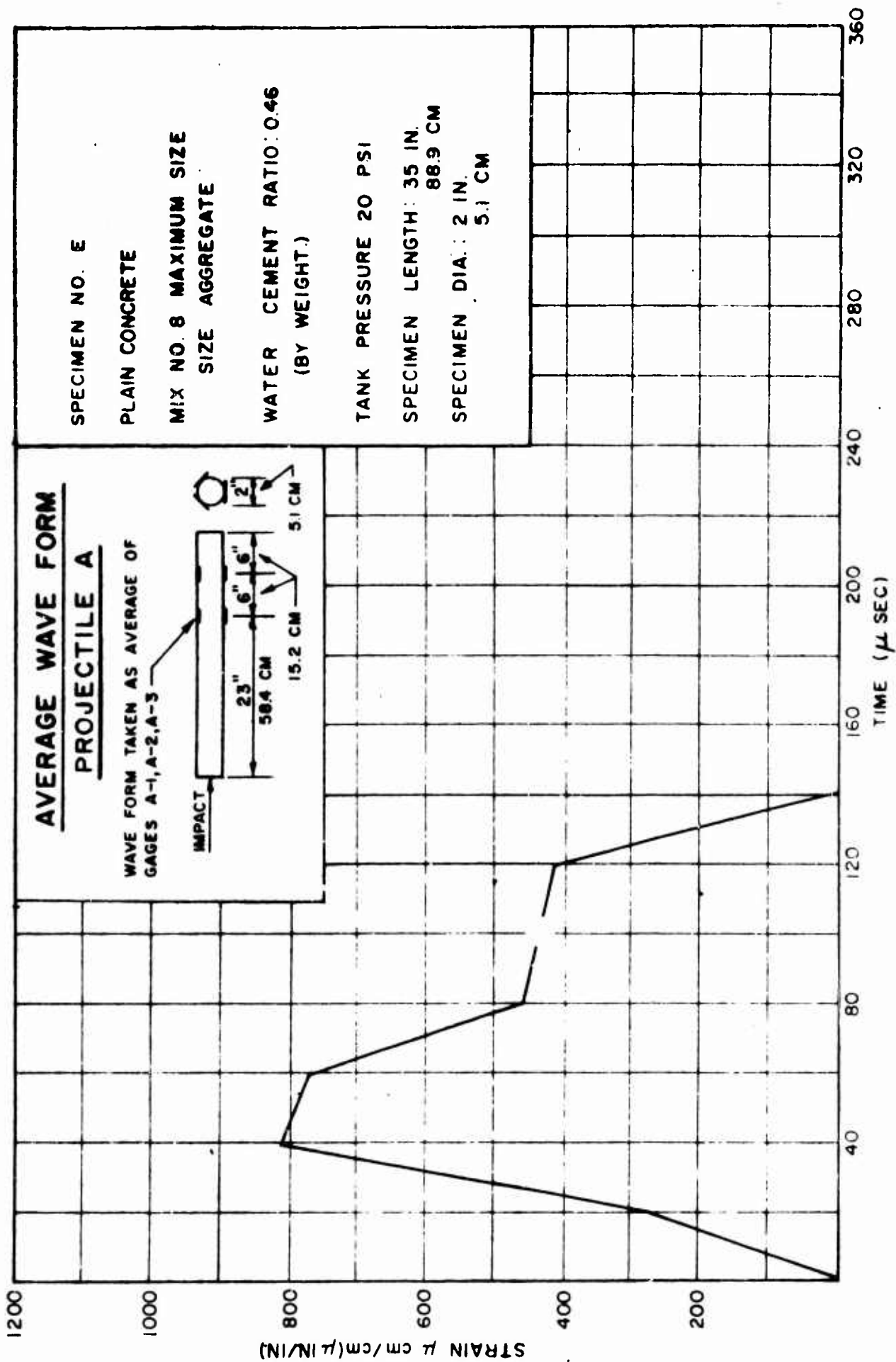


FIGURE 6A

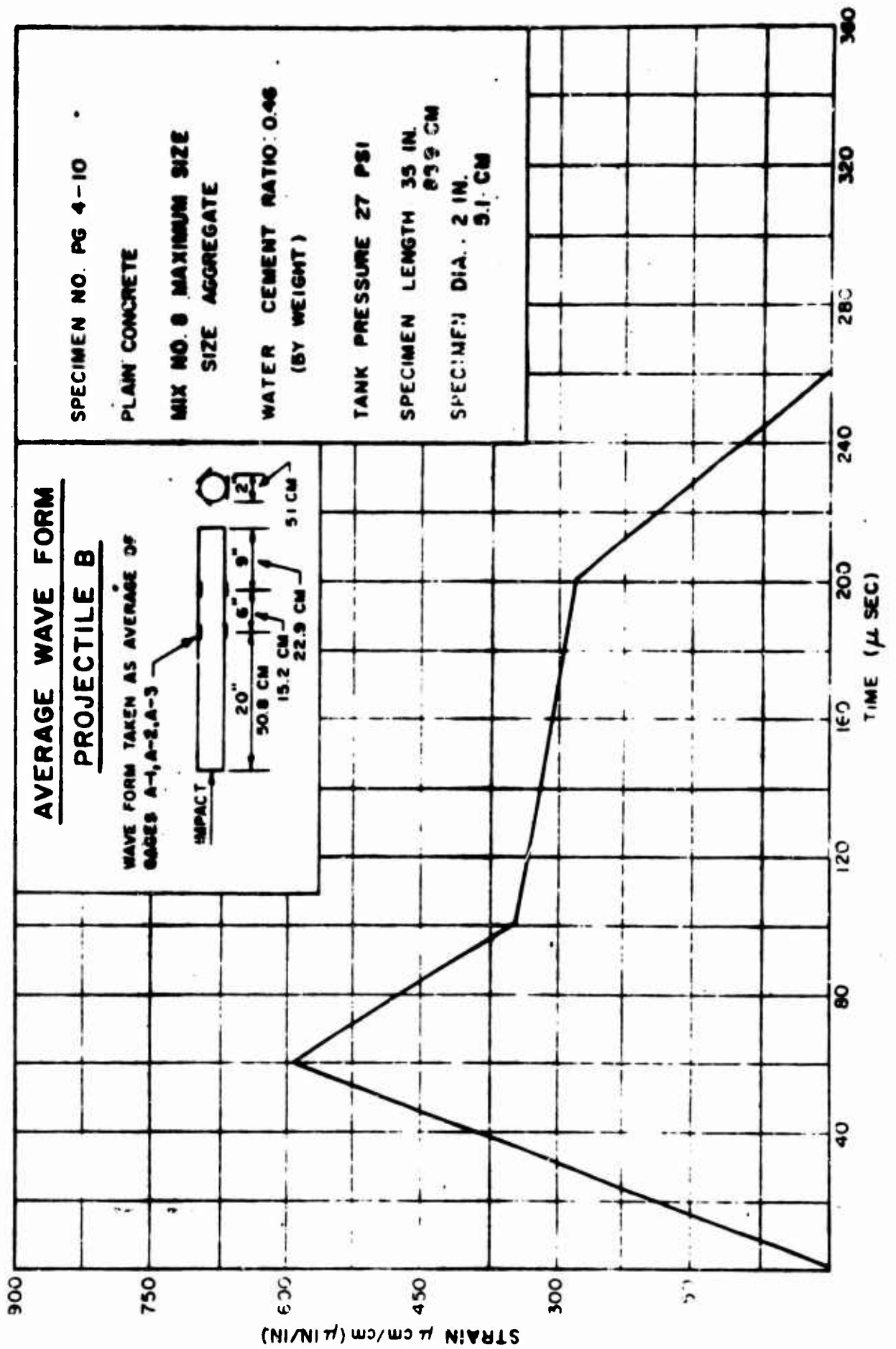


FIGURE 7A

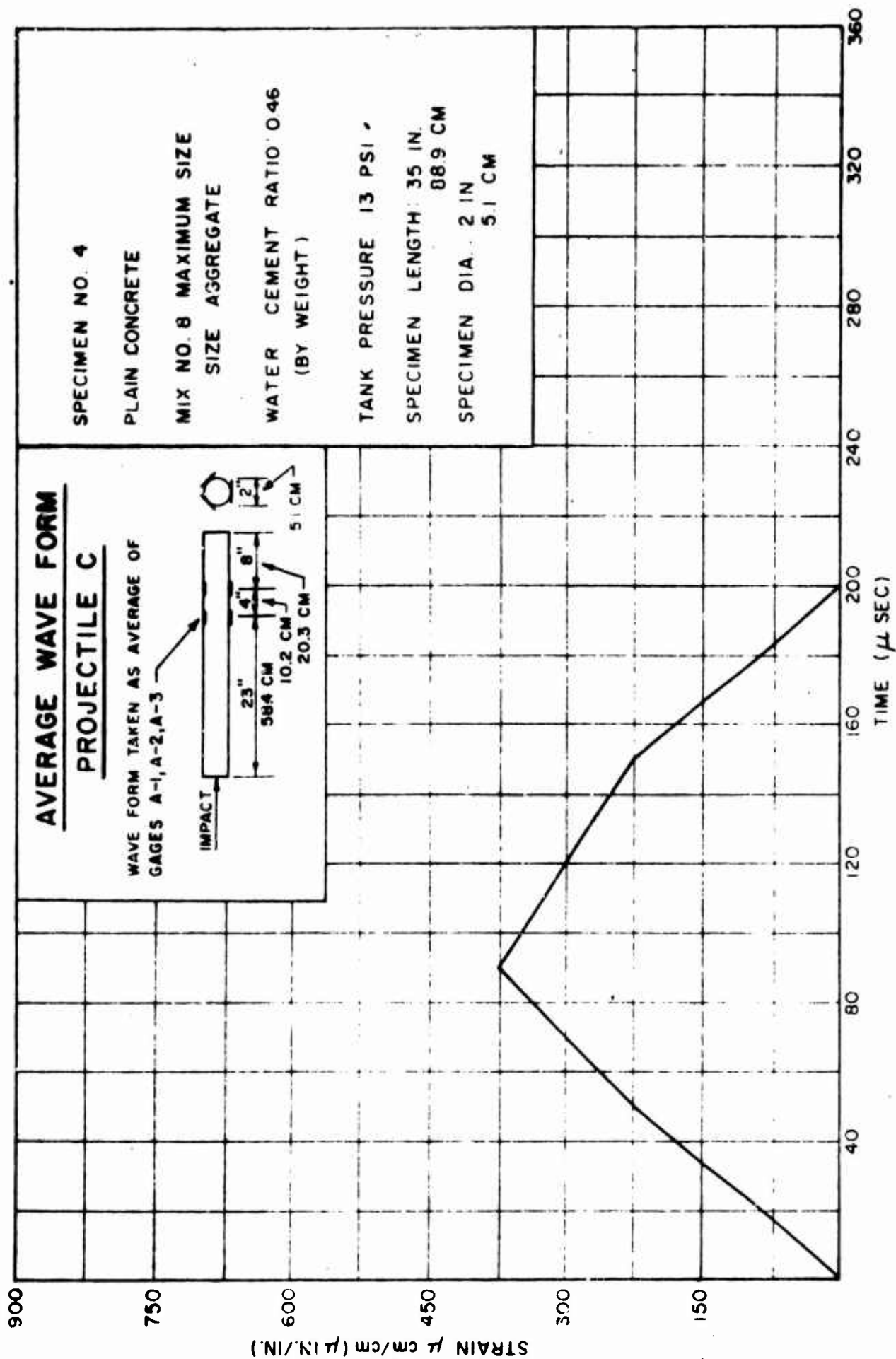
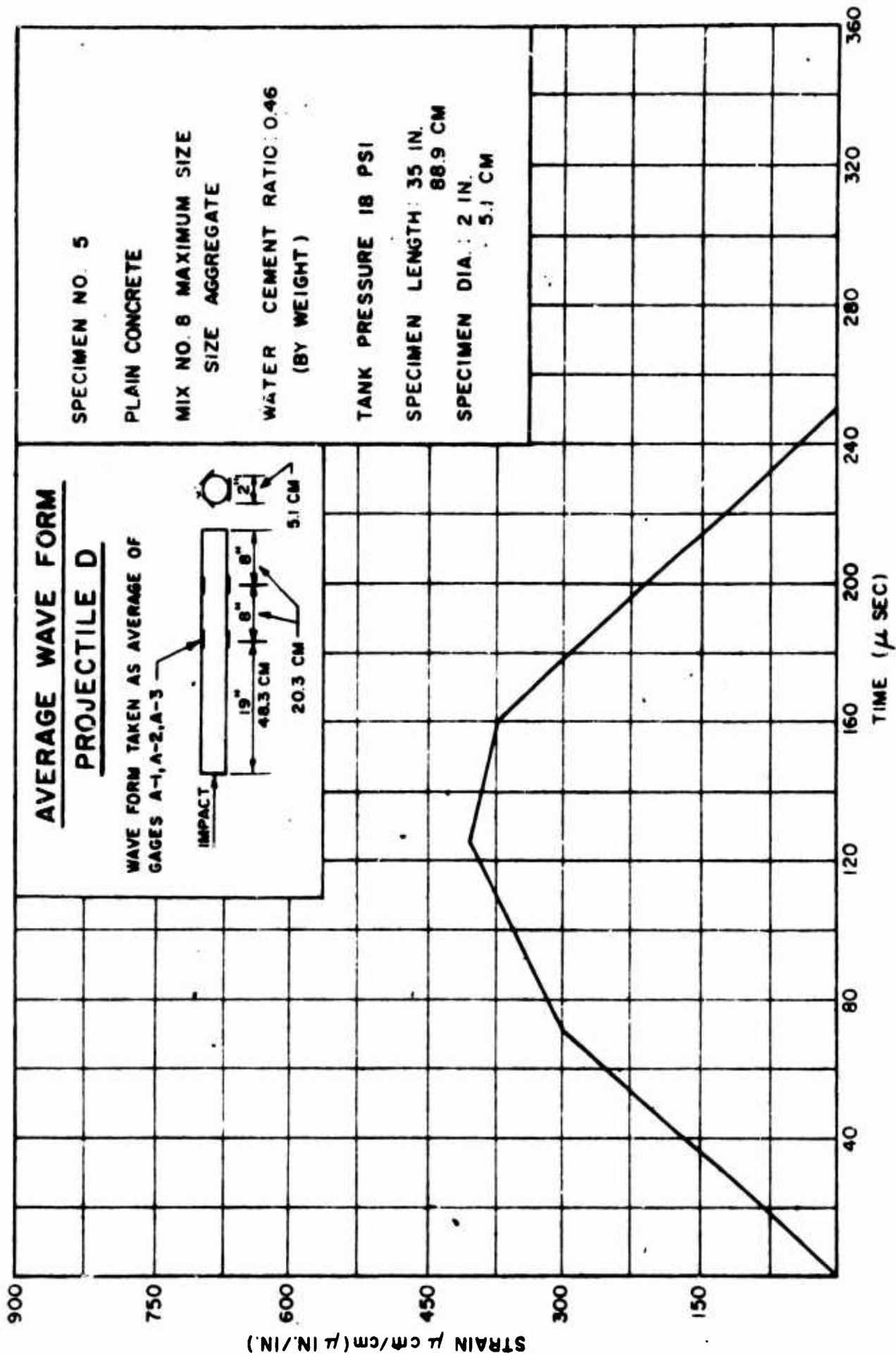


FIGURE 8A



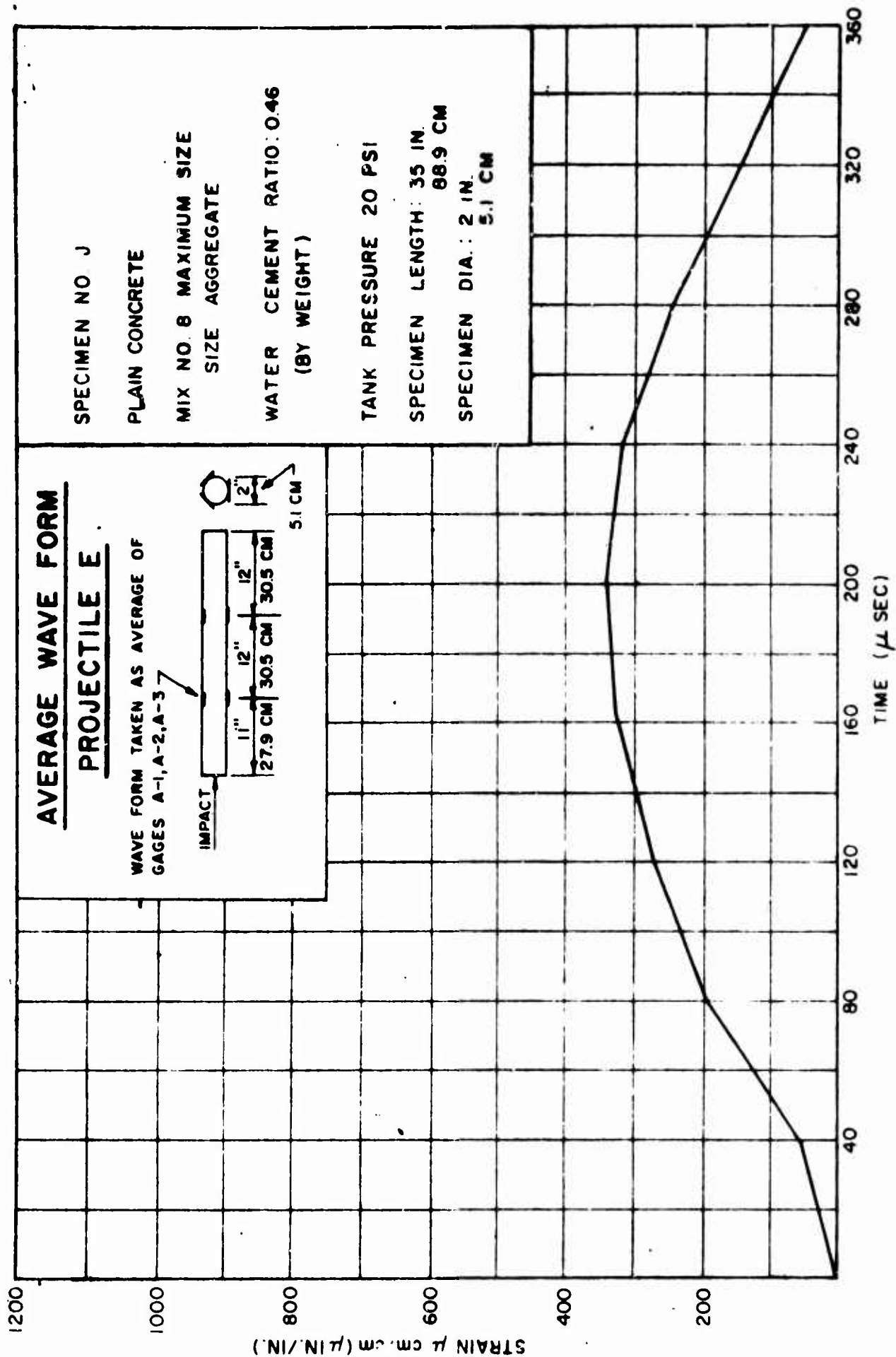


FIGURE 10A

APPENDIX B

STRAIN MEASURING APPARATUS

APPENDIX B

Strain Measuring Apparatus

1. Electronic measurements of strains on the surface of the test specimens under impact loading were made using a strain gage system. The basic elements of this system consist of foil type strain gage transducers, bridge balance circuits, power supplies, high gain DC amplifiers, a fast rise-time oscilloscope, and an oscilloscope recording camera. Plate 1B is a photograph of this apparatus. A block diagram of the overall system is shown by Figure 1B. The maximum number of recording data channels used was six.

2. The strain gages used for this application were W. T. Beam's "Micro Measurements," gage type EA-13-250BB-120, which are temperature compensated to 13 parts per million. This is reasonably close to the coefficient of thermal expansion of the material being tested. The gage is constructed of a foil-grid mounted on a flexible epoxy carrier. The physical dimensions of the gage were 1.24 cm (0.49 in.) overall length, 0.64 cm (0.25 in.) actual gage length, 0.444 cm (0.175 in.) overall width, and 0.444 cm (0.175 in.) grid width. The overall gage thickness was 0.0030 cm + 0.0005 cm (0.0012 + 0.0002 in.). The epoxy carrier is capable of elongation of up to 25 % while the gage element will measure strains up to 5 % (50,000 microstrains) with an accuracy of $\pm 3\%$ of the induced strain. Extreme care was exercised in preparing the surface of the specimen for the transducer. A standard gage resistance of 120 ohms was used for compatibility with the bridge calibration system.

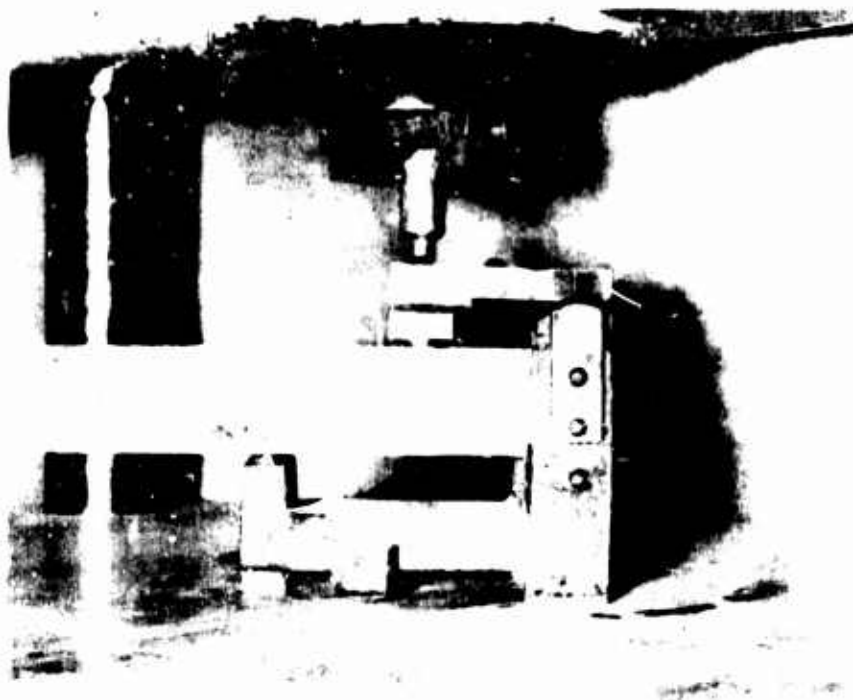
3. The bridge balance system was a standard Wheatstone bridge with three internal arms to complete the bridge. The balance system contained the balance circuit, a built-in shunt calibration, and gage span control. The bridge excitation voltages were provided by a regulated DC power supply.

4. Amplification of the strain gage signal was accomplished by the use of high-gain differential DC amplifiers. The amplifiers used had the following applicable specifications:

Linearity: $\pm 0.01\%$
Gain : x 10 to x 1000
Bandwidth: ± 1 db; 0-20,000 cycles/sec.

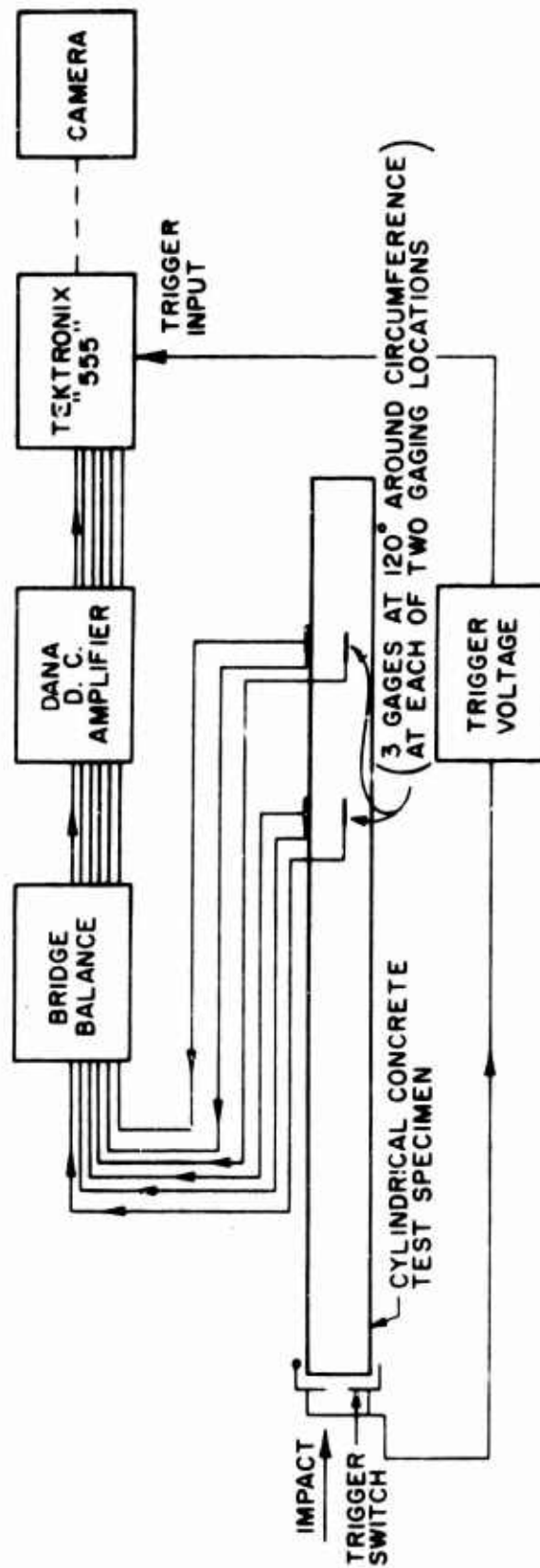
5. The strain signals from the amplifiers were displayed on a Tektronix 555 oscilloscope, using a type "L" fast rise-time plug-in preamplifier. This unit is capable of displaying transient signals with a rise-time of 15 nanoseconds, and a frequency rate of up to 30 megacycles. A "one-shot" triggering device enables one to couple the scope to an outside event in order to display the information in one trace. A Polaroid camera attached to the oscilloscope was used to record the output.

6. Using this equipment, the strains existing at all transducer locations were measured with respect to time. This gave an indication of the rise time of the actual wave as well as the shape of the strain pulse.



Strain Gage System

ARRANGEMENT OF APPARATUS
FOR MEASURING LONGITUDINAL STRAIN IN A CYLINDRICAL
TEST SPECIMEN UNDER IMPACT LOADING



INSTRUMENTATION BLOCK DIAGRAM

Unclassified
Security Classification

DOCUMENT CONTROL DATA - R&D		
(Security classification of title, body of abstract and indexing annotation must be entered when the overall report is classified)		
1 ORIGINATING ACTIVITY (Corporate author) Department of the Army Construction Engineering Research Laboratory		2a REPORT SECURITY CLASSIFICATION Unclassified
		2b GROUP
3 REPORT TITLE CRITICAL NORMAL FRACTURE STRAIN OF PLAIN AND STEEL WIRE FIBROUS-REINFORCED CONCRETE		
4 DESCRIPTIVE NOTES (Type of report and inclusive dates) Final Report		
5 AUTHOR(S) (Last name, first name, initial) Birkimer, Donald L.		
6 REPORT DATE October 1969	7a TOTAL NO OF PAGES 220	7b NO OF REFS 14
8a CONTRACT OR GRANT NO	9a ORIGINATOR'S REPORT NUMBER(S) M-1	
b PROJECT NO		
c Subtask R13B193	9b OTHER REPORT NO(S) (Any other numbers that may be assigned this report) Defense Documentation Center: AD number on cover	
d		
10 AVAILABILITY/LIMITATION NOTICES This document has been approved for public release and sale; its distribution is unlimited.		
11 SUPPLEMENTARY NOTES Public Release copies obtainable from: Clearinghouse (CFSTI), Springfield, Va. 22151 (order by AD number on cover)		12 SPONSORING MILITARY ACTIVITY Defense Atomic Support Agency Nuclear Weapons Effects Research
13 ABSTRACT <p>This report presents the results of a series of eighty-one impact tests performed on 5.1 x 88.9-cm (2.0 x 35.0-in.) cylindrical test specimens. The cylinders consisted of either plain or steel wire fibrous-reinforced concrete.</p> <p>Basic properties relating to the concrete test specimens used were quantitatively evaluated: static ultimate tensile strength and the corresponding ultimate tensile strain; static initial Young's modulus of elasticity; static ultimate unconfined compressive strength, specific gravity, mass density; seismic velocity; dynamic Young's modulus of elasticity. Histograms for the frequency distributions of basic material properties show variations of these properties within the experiment.</p> <p>The results revealed that the critical normal fracture strain (critical value of tensile strain which causes fracture of the material) of the materials tested is functionally dependent on the rise times of the straining pulse. The results also showed that the critical normal fracture strain of plain concrete can be increased by the inclusion of the randomly placed steel wire fibre of the type tested.</p> <p>Consideration of the variation of the critical normal fracture strain (or the corresponding calculated dynamic tensile strength) with rise times reveals that a minimum dynamic tensile strength should be used for design. Standard testing procedures should be developed based on this consideration.</p>		

DD FORM 1473
1 JAN 64

Unclassified
Security Classification

14 KEY WORDS	LINK A		LINK B		LINK C	
	ROLE	WT	ROLE	WT	ROLE	WT
Critical Normal Fracture Strain Rise Time Test Specimens: Plain Concrete, Steel Wire Fibrous-Reinforced Concrete Ultimate Tensile Strength Ultimate Tensile Strain Young's Modulus of Elasticity: Static / Dynamic						

INSTRUCTIONS

1. **ORIGINATING ACTIVITY:** Enter the name and address of the contractor, subcontractor, grantee, Department of Defense activity or other organization (*corporate author*) issuing the report.

2a. **REPORT SECURITY CLASSIFICATION:** Enter the overall security classification of the report. Indicate whether "Restricted Data" is included. Marking is to be in accordance with appropriate security regulations.

2b. **GROUP:** Automatic downgrading is specified in DoD Directive 5200.10 and Armed Forces Industrial Manual. Enter the group number. Also, when applicable, show that optional markings have been used for Group 3 and Group 4 as authorized.

3. **REPORT TITLE:** Enter the complete report title in all capital letters. Titles in all cases should be unclassified. If a meaningful title cannot be selected without classification, show title classification in all capitals in parenthesis immediately following the title.

4. **DESCRIPTIVE NOTES:** If appropriate, enter the type of report, e.g., interim, progress, summary, annual, or final. Give the inclusive dates when a specific reporting period is covered.

5. **AUTHOR(S):** Enter the name(s) of author(s) as shown on or in the report. Enter last name, first name, middle initial. If military, show rank and branch of service. The name of the principal author is an absolute minimum requirement.

6. **REPORT DATE:** Enter the date of the report as day, month, year, or month, year. If more than one date appears on the report, use date of publication.

7a. **TOTAL NUMBER OF PAGES:** The total page count should follow normal pagination procedures, i.e., enter the number of pages containing information.

7b. **NUMBER OF REFERENCES:** Enter the total number of references cited in the report.

8a. **CONTRACT OR GRANT NUMBER:** If appropriate, enter the applicable number of the contract or grant under which the report was written.

8b, 8c, & 8d. **PROJECT NUMBER:** Enter the appropriate military department identification, such as project number, subproject number, system numbers, task number, etc.

9a. **ORIGINATOR'S REPORT NUMBER(S):** Enter the official report number by which the document will be identified and controlled by the originating activity. This number must be unique to this report.

9b. **OTHER REPORT NUMBER(S):** If the report has been assigned any other report numbers (*either by the originator or by the sponsor*), also enter this number(s).

10. **AVAILABILITY/LIMITATION NOTICES:** Enter any limitations on further dissemination of the report, other than those imposed by security classification, using **standard statements** such as:

(1) "Qualified requesters may obtain copies of this report from DDC."

(2) "Foreign announcement and dissemination of this report by DDC is not authorized."

(3) "U. S. Government agencies may obtain copies of this report directly from DDC. Other qualified DDC users shall request through _____."

(4) "U. S. military agencies may obtain copies of this report directly from DDC. Other qualified users shall request through _____."

(5) "All distribution of this report is controlled. Qualified DDC users shall request through _____."

If the report has been furnished to the Office of Technical Services, Department of Commerce, for sale to the public, indicate this fact and enter the price, if known.

11. **SUPPLEMENTARY NOTES:** Use for additional explanatory notes.

12. **SPONSORING MILITARY ACTIVITY:** Enter the name of the departmental project office or laboratory sponsoring (*paying for*) the research and development. Include address.

13. **ABSTRACT:** Enter an abstract giving a brief and factual summary of the document indicative of the report, even though it may also appear elsewhere in the body of the technical report. If additional space is required, a continuation sheet shall be attached.

It is highly desirable that the abstract of classified reports be unclassified. Each paragraph of the abstract shall end with an indication of the military security classification of the information in the paragraph, represented as (TS), (S), (C), or (U).

There is no limitation on the length of the abstract. However, the suggested length is from 150 to 225 words.

14. **KEY WORDS:** Key words are technically meaningful terms or short phrases that characterize a report and may be used as index entries for cataloging the report. Key words must be selected so that no security classification is required. Identifiers, such as equipment model designation, trade name, military project code name, geographic location, may be used as key words but will be followed by an indication of technical context. The assignment of links, rules, and weights is optional.